UNIVERSITÉ DE STRASBOURG

ÉCOLE DOCTORALE DES SCIENCES DE LA VIE ET DE LA SANTÉ

INSERM UMR_S1255 Biologie et pharmacologie des plaquettes sanguines : hémostase, thrombose, transfusion

THÈSE

Présentée par

Alexandra YAKUSHEVA

Soutenue le 20 Septembre 2022

Pour obtenir le grade de : Docteur de l'université de Strasbourg
Discipline/Spécialité : Hématologie et physiopathologie vasculaire

Le rôle des plaquettes, de la fibrine et de l'hémodynamique dans l'hémostase et la thrombose artérielle

THÈSE DIRIGÉE PAR :

M Pierre MANGIN — DR1, INSERM, Université de Strasbourg

M Mikhail PANTELEEV — DR, Center for Theoretical Problems of Physicochemical Pharmacology

RAPPORTEURS :

M Christophe DUBOIS — PU-PH, AMU INSERM UMR-S1076

Mme Hind HAMZEH-COGNASSE — IR, Université Jean Monnet

EXAMINATEUR :

Mme Florence TOTI — PU-PH, Université de Strasbourg

INSERM UMR_S1255

« Biologie et pharmacologie des plaquettes sanguines : hémostase, thrombose, transfusion »

Directeur : Docteur Pierre H. MANGIN

Etablissement Français du Sang (EFS) – Grand Est

10, rue Spielmann, BP 36, F-67065 Strasbourg Cedex, France

Tel : +33 3 88 21 25 25, Fax : +33 3 88 21 25 21

Directeur de thèse :

Docteur Pierre H. MANGIN

E-mail : pierre.mangin@efs.sante.fr

Оставляю мечту, может кто-то захочет,
Три тетради сомнений моим неровным почерком,
Деньги в банке и многих себе подобных…

Песня “Итоги”
Земфира

I leave my dream - maybe someone will want it,
Three notebooks of doubts in my uneven handwriting,
Money in the bank, and many people just like me…

Adapted from Song “Results”
By Zemfira

Acknowledgements

First and foremost, I am really really grateful to my teacher, supervisor, boss and my French "uncle" ***Pierre Mangin*** *for advising me, showing me how "a big scientific machine" works, helping in realizing my ideas and explaining how present them to the World in a right way. Thank you for tolerating my horrible English and French, my harsh assessments in each sphere of life, my infinity rides home and the millions of my emails each minute of your life. You helped me to integrate into a grown-up life and to see the wider world. Thank you for helping with all my stuff during relocations, for family diners, for all tickets to football games, for your advices and chatting and for all this care during my time in France!*

I would like to express my special thanks of gratitude to my teacher and boss ***Mikhail Panteleev*** *who gave me the opportunity to work in real science. You sparked my interest in science and supported it during long period of time. You believed in me and entrusted the project which has changed my life. You have even been believing in me when I didn't believe in myself. Thank you for allowing me to make my own decisions and for giving me a lot of freedom.*

I would like to earnestly acknowledge the sincere efforts and valuable time given by our scientific "grandpa" of Russian team ***Fazly Ataullakhanov****. Thank you for giving me a chance, for all your criticisms and comments, for confidence in me and for forgiveness of all my stunts.*

My thanks to ***Christian Gachet*** *who allowed me to become a part of this laboratory in the beginning of my way.*

My thanks to ***Christophe Dubois****,* ***Hind Hamzeh-Cognasse*** *and* ***Florence Toti*** *for your interest in this subject by accepting to judge this work.*

I would like to thank ***Campus France****, especially* ***Sophie Bussinger****,* ***Pierre Blouin-Hulin*** *and* ***Pauline Kracher****, and* ***Embassy of France****, especially* ***Olivier Dubert, Abdo Malac*** *and* ***Anaëlle Durand****, for granting me a scholarship.*

I am grateful to ***François Lanza*** *for reading my thesis, providing important corrections and discussions not only on my thesis, but also on my scientific projects.*

Many many thanks to ***Catherine Bourdon*** *who has been teaching me, working with me and supporting me during all these 6 years in France. You are the person I really could count on! Thank you for family diners, weekend hiking, tasting food from your garden, chatting on many subjects and all this care and attention to me!*

I am really grateful to our "laboratory guru" ***Nicolas Receveur****. Thank you for your criticism, music, chatting at any time, practicing English with me and teaching it during my first year in France! And of course thank you for your incredible cuisines! You have shown me the World of French cheeses and wine☺ I have shed a lot of tears because of your comments, but thank you for that, it made me better and stronger!*

And, of course, I would like to thank all other members of Pierre's team: ***Emily****,* ***Usman****,* ***Clarisse****,* ***Axelle****,* ***Luc****,* ***Kevin****,* ***Marianne****,* ***Marion*** *and* ***Margot****, -- for our meetings, your help in realization of projects, the jokes during working time and a lot of conversations.*

Thanks a lot to ***Valentin****,* ***Quentin****,* ***Lea*** *and* ***Cyril*** *for your help in my integrating into life outside the laboratory. Thank you for diners, weekends together, saving my life and the life of my cat, and huge amount of conversations!*

My many thanks to ***Monique, Catherine Z, Ketty, Nolwenn*** *and* ***Lauriane*** *for teaching me, helping in my projects and, especially, to Monique who forgave all my stunts ☺*

*I would like to thank **Anita**, **Jean-Yves** and **Fabienne** who taught me and helped me with doing electron microscopy. Thank you for your time and patience!*

*I am thankful to **Veronique**, **Patricia** and **Sylvie** for their working advices and also for conversations, support and jokes during this time.*

*Many thanks to **Valerie** who helped me with document preparation, tickets and laboratory's purchases. Thank you for your emotional involvement and concern about me.*

*I would like to thank **Nathalie Brouard, Blandine Maitre, Catherine Strassel, Beatrice Hechler, Catherine Leon, Catherine Angenieux, Stephanie Benoit, Josiane Weber, Henri de la Salle, Catherine Ravanat, Yotis Senis** and **Alexandra Mazharian** for their help in improving my work, for all comments and advices.*

*Thanks a lot to **Elmina**, **Adele, Julie, Alicia, Thao, Marie-Belle, Camille, Yannick, Inès, Anaïs, Desline, Floriane, David, Gabriel, Sébastien** and **Morgane** for this time in the laboratory! Your help, jokes and advices made this time more colorful!*

*I am thankful to my first scientific tutor **Nikita Gudimchuk** for teaching me how to read scientific papers, analyze data and write my first computational model (sorry that I failed in the latter!).*

*I would like to express my special thanks to my first supervisor, my "micro-shef" **Vladimir Kolyadko**! Thank you for your time, enthusiasm and efforts which you have spent to improve my skills and for teaching me to work hard.*

*I would like to thank my teachers **Anna Nozdracheva, Svetlana Ishenko, Galina Shipareva, Simon Shnoll**, **Anastasia Sveshnikova**, **Ekaterina Simonenko, Larisa***

Menshinina, Vsevolod Tverdislov, Enno Ruuge, Alexander Tikhonov, Valentin Lobyshev, Leonid Yakovenko, Yuruj Nechipurenko, Mariya Popzova *and* ***Sergey Yakovenko*** *for teaching me, for their help in improving my skills and for all comments and advices!*

I would like to thank my classmates ***Vasya, Dima G, Sasha M*** *and* ***Anton*** *who helped me to survive during my first two years in France. Thank you a lot for your visits, food, chatting and presents!*

Thanks to the team of the Institute of Immunology ***Ravshan Ataullakhanov, Alexei Pichugin, Marina****,* ***Katya*** *and* ***Natasha*** *for allowing me to work with you, for your support, comments and advices and thanks a lot for overcoming with me the refurbishment and microscope's relocations!*

Thanks to my Russian team ***Galya, Dmitry N, Nadya M, Andrey U, Taya, Andrey M, Sergey O, Fedya, Zhenya B, Anya Z (****you will always be Zadorozhnaya for me ☺****), Sasha R, Soslan, Polina, Nastya I, Lena A, Lena L, Nadya P, Anya G, Masha S, Tanya, Katya K, Sonya K, Olga F, Inna, Zhenya P, Vadim*** *and* ***Alexei B*** *for their help, support, jokes, motivation, inspiration and criticism!*

Thanks to my partners in crime ***Kirill, Lesha*** *and* ***Lera****. A long and difficult road together, I love you guys!*

Of course, many many thanks to ***Oxana*** *and* ***Filya (Sasha F****)! Girls, you are more than my friends, you are my family! There is not enough time to tell what you have done for me… Thanks for your support, faith, our quarrels and reconciliations, all our night chattings, your help and advices and many other things!*

A lot of thanks to my man, my love and my husband ***Andrey G*** *for your patience, understanding and care. You turned the distance between us to seem nothing! Thank you for*

being with me all the time, even if we were in different countries, for your arrivals, for our calls, for finding the words in any situations, for trying to create a sense of security and to support my career ambitions.

Thanks to very important people in my life: ***my grandparents****! I know how it is important for you and I hope that I worthily present our family and that I became a good successor of family's knowledge.*

Finally, a lot of thanks to ***my mum*** *and* ***dad****. I love you so much! Thank you for your infinity support, belief that I can rise to the life challenges, your provocations which made me stronger and, I hope, better, deep conversations, trust in me, the opportunity to make my own errors and to have frustrations. I hope you are proud of which person I became!*

Thanks to ***all people*** *who I forgot to mention and with whom I have shared working time during these years!*

Table of contents

List of figures

List of tables

Abbreviations

AA	arachidonic acid
AC	adenylate cyclase
ADAMTS13	A Desintegrin and Metalloproteinase with ThromboSpondin type 1 repeat 13
ADP	adenosine diphosphate
Akt	protein kinase B alpha
APC	activated protein C
AT	antithrombin
ATIII	antithrombin
ATP	adenosine triphosphate
Btk	Bruton tyrosine kinase
CalDAG-GEFI	calcium and DAG-regulated guanine-nucleotide-exchange factor
cAMP	cyclic adenosine monophosphate
CDM	cell-derived extracellular matrix
CLEC-2	C-type lectin-like type II transmembrane receptor
COX-1	cyclooxygenase-1
CTLD	carbohydrate-recognizing domain
DAG	diacylglycerol
Erk	extracellular signal-regulated kinase
F	factor
FAK	focal adhesion kinase

Fgn	fibrinogen
FN	fibronectin
FpA	fibrinopeptide A
FpB	fibrinopeptide B
Fyn	tyrosine-protein kinase
Gads	Grb2-related adapter dowstream of Shc
GDP	guanosine diphosphate
G protein	guanine nucleotide binding protein
GP	glycoprotein complex
GPCR	G protein–coupled receptor
Grb	growth factor receptor-bound protein
GTP	guanosine triphosphate
HIT	heparin-induced thrombocytopenia
HTPR	high on-treatment residual platelet reactivity
ILK	integrin linked kinase
IP3	inositol 1,4,5-triphosphate
ITAM	immunoreceptor tyrosine-based activation motif
LAT	linker for activation of T cells
LDL	low-density lipoprotein
LM	laminin
LMWH	low molecular weight heparin
MLC	myosin light chain
PAR	protease-activated receptor
PF4	platelet factor 4
PGH2	prostaglandin H2

PI3K	phosphoinositide 3-kinase
PIP2	phosphatidylinositol 4',5'-bisphosphate
PKA	protein kinase A
PKC	protein kinase C
PKG	protein kinase G
PLA2	phospholipase A2
PLC	phospholipase
PLCβ	phospholipase Cβ
PLCγ	phospholipase Cγ
PLCγ2	phospholipase Cγ2
PM	membrane phospholipids
P130C	p130 Crk-associated substrate
Rac	Ras-related C3 botulinum toxin substrate
Rap1b	Ras-related protein 1b
RBC	red blood cell
RGD	sequence of Arg-Gly-Asp
RhoA	Ras homolog family memeber A
Rho-GEF	Guanine nucleotide exchange factor for Rho
ROCK	Rho-associated protein kinase
SFK	Src family kinase
SLP76	Scr homology 2 domain-containing leukocyte phosphoprotein of 76 kDa adapter protein
SMC	smooth muscle cell
Syk	spleen tyrosine kinase
TA	thromboxane A2 synthase

TAFI	thrombin-activated fibrinolysis inhibitor
TF	tissue factor
TM	thrombomodulin
TP	thromboxane receptor
tPA	Tissue plasminogen activator
TRAP	thrombin receptor activating peptide
TxA2	thromboxane A2
uPA	urokinase plasminogen activator
vWF	von Willebrand factor
WBC	white blood cells
WSR	wall shear rate

General introduction

Platelets are small discoid-shaped anucleated cells derived from megakaryocytes in the bone marrow and circulating freely in the bloodstream. Their main role is to ensure hemostasis, which represents the physiological process leading to the arrest of bleeding. After vessel lesion, under high flow conditions, von Willebrand factor (vWF) bound to subendothelial collagen recruits platelets through its interaction with the glycoprotein complex (GP) Ib-IX-V. Stable adhesion of platelets is then ensured by the interaction of integrins α2β1, α5β1 and α6β1 with their respective ligands namely collagen, fibronectin and laminins. Integrin αIIbβ3 is also involved in stable platelet adhesion through the binding to vWF and fibronectin. This adhesion step leads to the interaction between subendothelial collagen and GPVI, which initiates strong platelet activation, notably through the release of ADP and TxA2. These soluble agonists, via their receptors, amplify platelet activation by increasing the affinity of integrin αIIbβ3 for its main plasma ligand, soluble fibrinogen, which ensures aggregation and the formation of the hemostatic plug. Some activated platelets expose negatively charged phospholipids on their surface allowing the recruitment of coagulation factors and the generation of thrombin. This serine protease is then able to cleave fibrinogen within the clot into an insoluble fibrin network which stabilizes the aggregate and stops bleeding under physiological conditions.

A similar process can occur in a pathological context, after erosion or rupture of an evolved atherosclerotic plaque in a diseased artery. This leads to the exposure of tissue factor and highly reactive proteins such as fibrillar collagen, initiating the coagulation cascade and the recruitment and aggregation of flowing platelets. The forming thrombus can become occlusive and block the bloodstream which leads to necrosis of surrounding tissue responsible for a high rate of mortality.

Rheology plays a central role in the regulation of hemostasis and arterial thrombosis. First of all, it regulates receptor-ligand bond formation during the initial step of platelet adhesion at the site of injury. Once platelets have adhered, hemodynamic forces can stimulate

their mechano-receptors to activate them. In addition, the amplification of platelet activation by soluble agonists is finely tuned by the flow which carries them away from the place of injury.

While the importance of blood flow in the regulation of platelet activation, thrombus growth and stability has been defined, the precise rheological conditions occurring after lesion of a healthy vessel remain undetermined. Moreover, while the molecular mechanism that occurs during hemostasis and arterial thrombosis is well established, and the role of the main adhesion receptors has been characterized, the importance of integrin α5β1 remains elusive. Finally, the process by which the platelet plug stops his growth to limit unwanted vessel occlusion at site of lesion of healthy vessels is also unclear.

The main objective of my thesis project consists in: i) the characterization of flow conditions occurring after lesion of a healthy vessel; ii), define the importance of platelet integrin α5β1 in hemostasis and arterial thrombosis; iii) evaluate the role of fibrin in the termination of the hemostatic response.

Review of Literature

I. Hemostasis

Hemostasis is the physiological process leading to the arrest of bleeding (Sang et al., 2021). It includes primary hemostasis, coagulation and fibrinolysis. Primary hemostasis is mainly ensured by platelets which adhere, activate and aggregate at the injured site (Broos et al., 2011). Coagulation is a cascade of enzymatic reactions leading to generation of thrombin which cleaves fibrinogen within the clot to form an insoluble fibrin network leading to stabilization of the platelet aggregate (Palta et al., 2014). Finally, at the end of the process, fibrinolysis is initiated and generates locally plasmin, which degrades fibrin to dissolve the clot and restore normal blood flow (Gale, 2011).

A. Primary hemostasis: the major role of platelets

Primary hemostasis relies on the ability of platelets to form the hemostatic plug at the site of vascular injury to limit bleeding.

1. Platelet morphology and ultrastructure

Platelets are anucleate fragments derived from the cortical cytoplasm of bone marrow megakaryocytes (**Figure 1**) (Gremmel et al., 2016). In man they have a mean diameter of 3.1 ± 0.3 μm, an average thickness of 1.0 ± 0.2 μm and a volume of approximately 7 fm^3 (David-Ferreira, 1964). After being released from the megakaryocytes, platelets circulate in the blood

in a discoid shape for about 7 to 10 days. A normal human platelet count is ranging from 150,000 up to 450,000 platelets per microliter.

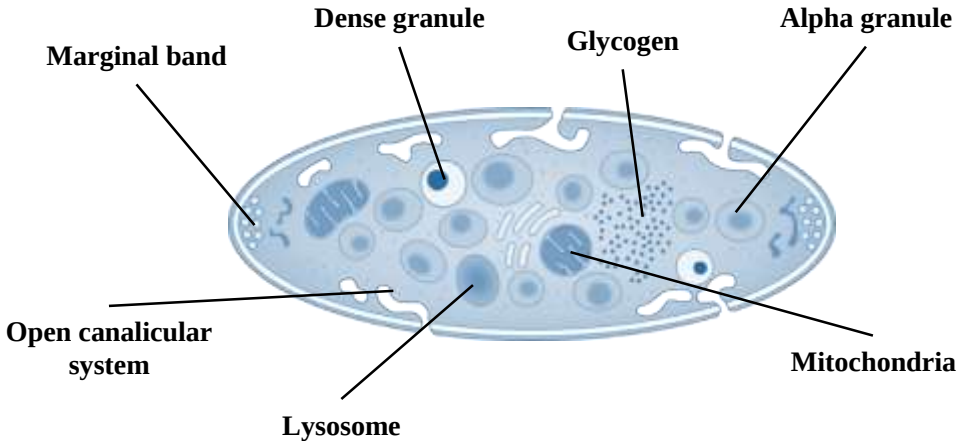

Figure 1: Schematic representation of platelet ultrastructure (Adapted from (Brisson et al., 1997)).

The platelet cytoskeleton is responsible for the discoid shape of platelets. It is mainly composed of microtubules forming a circumferential network under the plasma membrane and acto-myosin filaments located under the plasma membrane and in the cytosol (White, 1969). Upon activation, platelets change their shape which is regulated by rapid and dramatic actin filament de- and re-polymerization (Bearer et al., 2002). Platelets contain on average seven times more actin by cell volume than non-muscle cells (Hartwig et al., 1999). Inside platelets, actin exists in a dynamic equilibrium between the monomeric or globular form (G-actin) and the polymeric filamentous form (F-actin). The actin dynamics underlying shape changes of platelets depend on a large number of actin-binding proteins. For example, VASP inhibits filament disassembly and Arp2/3 is required to polymerize new filaments (Bearer et al., 2002).

Platelets have a complete set of organelles: mitochondria, endoplasmic reticulum, glycogen grains, dense tubular system, and granules. Platelets contain three types of granules—

α-granules, dense granules and lysosomes — which carry distinct cargos and vary in biogenesis, trafficking, and exocytosis (Heijnen and van der Sluijs, 2015).

The α-granules count is 40–80 per platelet with a diameter of 200–500 nm and they account for about 10-16% of the platelet volume (Eckly et al., 2016; Frojmovic and Milton, 1982; White, 1998). The content of α-granules comes either from its biosynthesis in megakaryocytes or endocytosis from the plasma (**Table 1**) (Fitch-Tewfik and Flaumenhaft, 2013; Mumford et al., 2015). Defects of α–granule formation lead to a severe bleeding disorder named gray platelet syndrome, which highlights the importance of these organelles in platelet function (Buchanan and Handin, 1976; Costa et al., 1976).

The dense granules count is 3–8 per platelet and their diameter is about 150 nm (White, 1998). These granules contain small non-protein molecules such as ADP, ATP, serotonin, pyrophosphates, calcium and polyphosphates (**Table 1**) (Holmsen, 1989; Smith and Morrissey, 2008). The role of dense granules in hemostasis is evidenced by the bleeding tendency in patients with inherited dense granule deficiency, such as Hermansky-Pudlak syndrome (Ambrosio and Di Pietro, 2017; Toro et al., 1993) and by increasing bleeding times in mice with dense granule defects (Ren et al., 2010).

The lysosomes count is lower than 3 per platelet and their diameter is about 200–250 nm. Platelet lysosomes contain β-hexosaminidase, acid glycohydrolases, membrane bound proteins such as LAMP-1, LAMP-2 and LAMP-3 (**Table 1**) (Holmsen and Dangelmaier, 1989). Secretion of the lysosomal content has important extracellular functions, such as supporting receptor cleavage, fibrinolysis and degradation of extracellular matrix components, and remodeling of the vasculature (Heijnen and van der Sluijs, 2015).

Table 1. Platelet granules components

Type of granules	Type of granule components	Components
α–granules	Adhesive proteins	Fibrinogen, fibronectin, vWF, vitronectin
	Membrane glycoproteins	GPIb, αIIbβ3, GPVI
	Coagulation factors	FV, FXI, FXIII, TF, kininogens
	Coagulation inhibitors	TFPI, protein S, protease nexin-2
	Fibrinolysis components	PAI-1, TAFI, α2-antiplasmin, plasminogen, uPA
	Inflammatory, pro-atherogenic, wound healing and antimicrobial proteins	P-selectin, PSLGP-1, thrombospondin, chemokines and cytokines, TLT-1, osteonectin, complement components, VEGF
Dense granules	Small molecules	ATP, ADP, serotonin (5-HT), calcium, polyphosphates, pyrophosphate
Lysosomes	Enzymes	Hydrolases, metalloproteases

2. The molecular mechanisms of primary hemostasis

The molecular mechanisms of primary hemostasis have been widely described. After vessel lesion, under high flow conditions, von Willebrand factor (vWF) bound to subendothelial collagen recruits platelets through its interaction with the glycoprotein complex Ib-IX-V (Savage et al., 1996). Stable adhesion of platelets is then ensured by the interaction of integrins notably, α2β1, α5β1 and α6β1 which bind to their respective ligands namely collagen, fibronectin and laminins (Bergmeier and Hynes, 2012). Integrin αIIbβ3 is also involved in stable platelet adhesion through the binding to vWF and fibronectin (Giuliano et al., 2003; Maurer et al., 2015). This adhesion step leads to the interaction of collagen with GPVI, which initiates strong platelet activation, that is amplified through the release of the soluble agonists, ADP, ATP and TxA2 (Zahid et al., 2012). These soluble agonists via their receptors, P2Y1 and P2Y12 for ADP, P2X1 for ATP and the thromboxane receptor (TP) for TxA2, amplify platelet activation by increasing the affinity of integrin αIIbβ3 for its main plasma ligand, soluble

fibrinogen, which ensures aggregation and the formation of the hemostatic plug (**Figure 2**) (Versteeg et al., 2013).

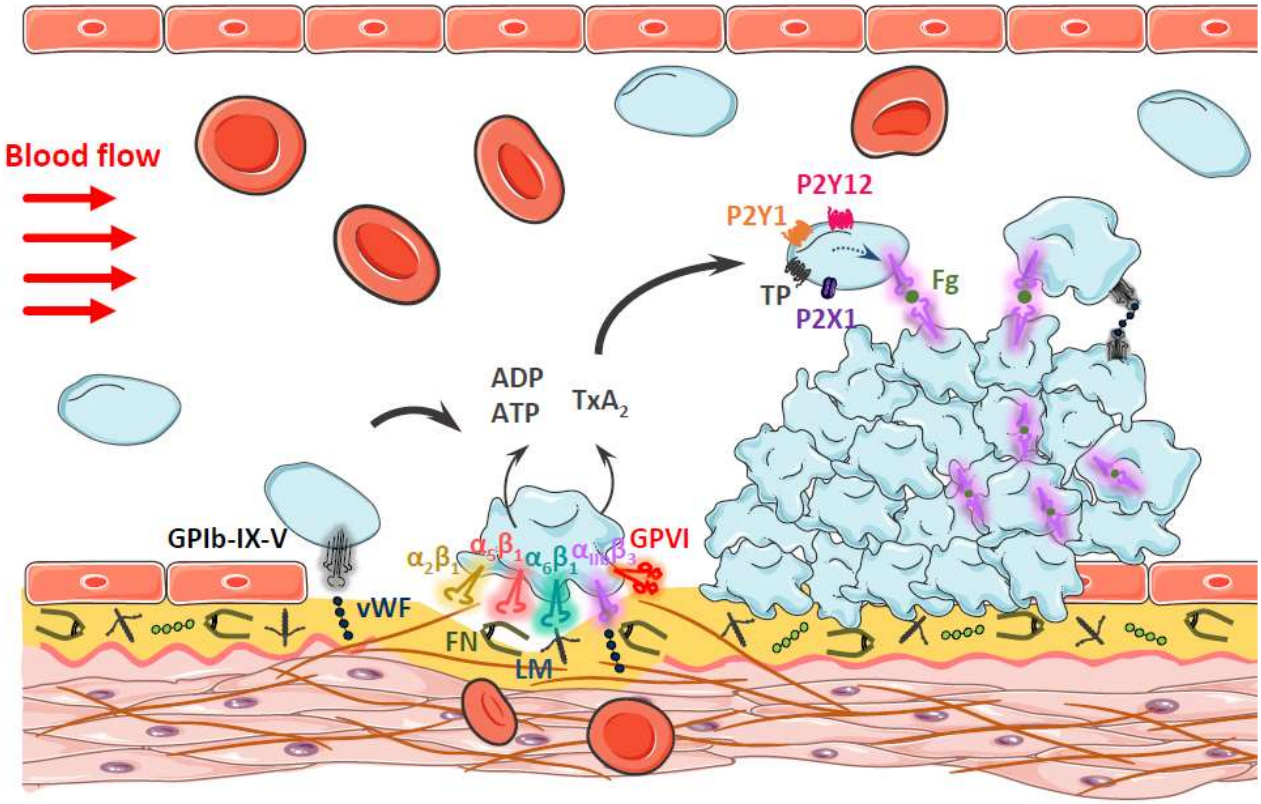

Figure 2: The molecular mechanisms of primary hemostasis. ADP, adenosine diphosphate; ATP, adenosine triphosphate; Fgn, fibrinogen; FN, fibronectin; vWF, von Willebrand factor; GP, glycoprotein complex; LM, laminin; PAR, protease-activated receptor; TP, thromboxane receptor; TxA2, thromboxane A2.

3. Platelet receptors involved in primary hemostasis

Primary hemostasis is mediated by receptors that allow platelet adhesion, activation and aggregation.

3.1. Activation and adhesion receptors

3.1.1. The GPIb-IX-V Complex

The GPIb-IX-V complex is expressed only in megakaryocytes and platelets. It belongs to the leucine-rich repeat protein family (Hickey et al., 1989; Lopez et al., 1988). GPIb-IX-V contains 4 types of subunits: 1 GPIbα molecule linked to 2 GPIbβ subunits via disulfide bridges to form the GPIb; the latter is non-covalently associated with 1 GPIX subunit to form the GPIb-IX complex. GPIb-IX complex is weakly linked to one GPV subunit (Luo et al., 2007b; Mo et al., 2012; Modderman et al., 1992; Phillips and Agin, 1977). There are about 25,000 copies of GPIb-IX and 12,500 copies of GPV per platelet which was measured by antibody binding (Modderman et al., 1992).

The main ligand of GPIbα is vWF, which becomes instrumental in platelet recruitment at elevated shear (>900 s^{-1}) at site of vessel injury or to a growing thrombus. *In vitro*, this interaction induces platelet rolling on immobilized vWF which is explained by the fact that GPIbα-vWF bonds have fast association and dissociation rates (Fressinaud et al., 1988). GPIbα also binds to additional ligands including thrombin, P-selectin, thrombospondin-1, factor XI, factor XII and high-molecular weight kininogen, which all bind to the 45-kDa globular N-terminal extracellular domain of the receptor (Andrews et al., 2003; Bradford et al., 1997; Bradford et al., 2000; Jurk et al., 2003; Simon et al., 2000). At the intracytoplasmic level, GPIbα interacts with the actin binding protein filamin A, phosphoinositide 3-kinase and the adapter 14-3-3ζ through its cytoplasmic tail domain (Bryckaert et al., 2015).

Ligation of vWF to the GPIbα subunit induces an intracellular signal involving a member of the Src-kinase family, which leads to phospholipase Cγ2 activation, and subsequent Ca^{2+} release from internal stores generating oscillations (Ozaki et al., 2005). This signal is

relatively weak, but is nevertheless proposed to contribute to αIIbβ3 activation and filopodia extension (**Figure 3**) (Fredrickson et al., 1998; Mangin et al., 2003).

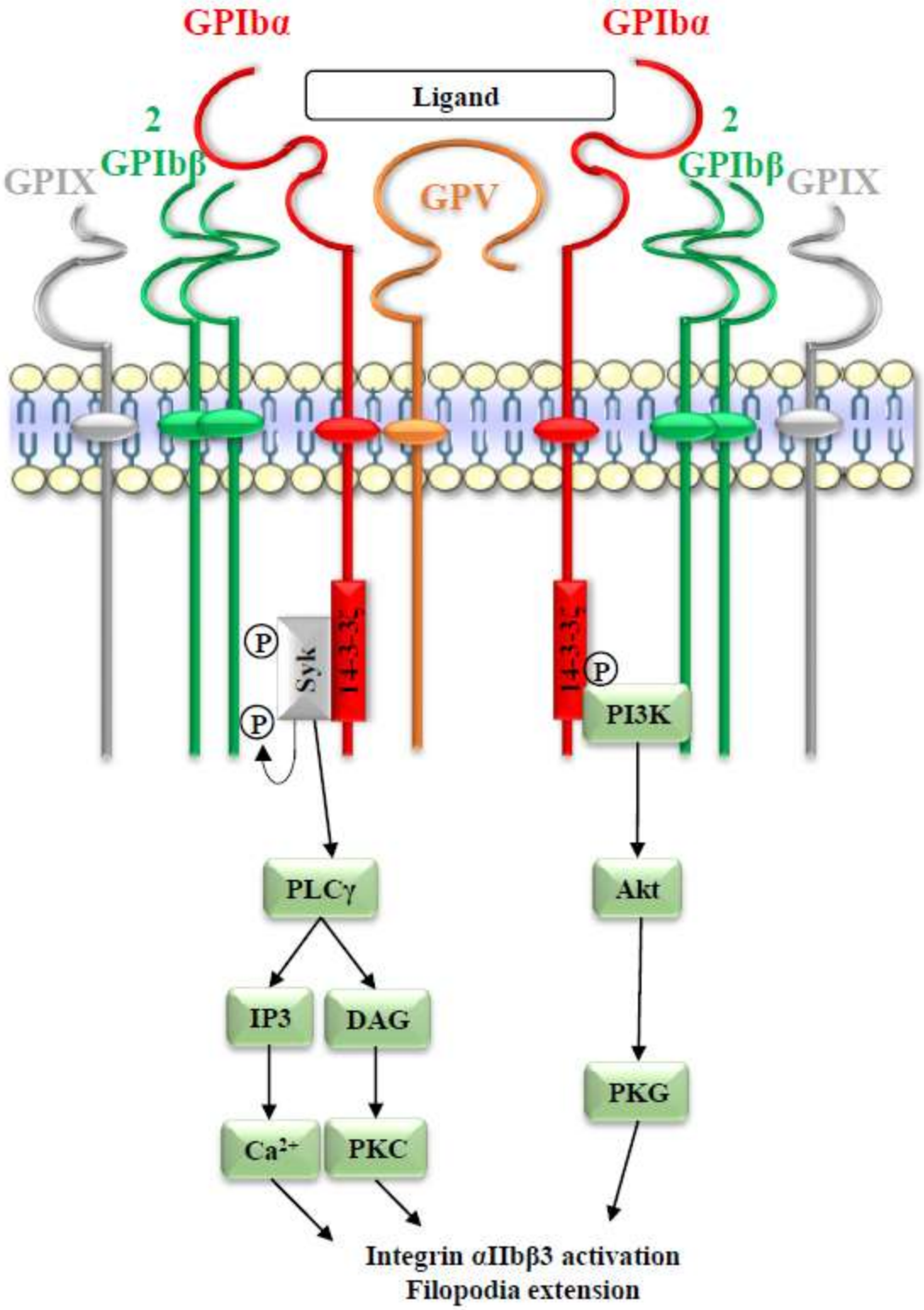

Figure 3: The signaling pathway triggered by the GPIb–IX–V complex. Akt, protein kinase B alpha; DAG, diacylglycerol; GP, glycoprotein; IP3, inositol 1,4,5-triphosphate; PI3K, phosphoinositide 3-kinase; PKC, protein kinase C; PKG, protein kinase G; PLCγ, phospholipase Cγ; Syk, spleen tyrosine kinase (Adapted from (Andrews et al., 2003)).

Defects of one of the members of the GPIb-IX complex leads to a rare bleeding disorder named Bernard-Soulier syndrome, which is characterized by a macrothrombocytopenia, highlighting the importance of this receptor in hemostasis (Buchanan and Handin, 1976; Costa et al., 1976; Liang et al., 2005; Strassel et al., 2009). Numerous *in vitro* and *in vivo* studies have shown that absence of the GPIb-IX complex or blockade of the vWF-GPIb interaction reduces experimental thrombosis, indicating the importance of the GPIb-IX complex in thrombus formation (Bergmeier et al., 2006; Konstantinides et al., 2006; Maurer et al., 2013). In contrast, this receptor does not appear to play a major role in thrombus stability (Ni et al., 2000). Targeting GPIb-IX complex is recognized as a potential efficient antithrombotic strategy, however, the function blocking antibodies could have an impact on the bleeding risk and need therefore to be further investigated.

3.1.2. Glycoprotein VI

GPVI is a 62 kDa glycoprotein expressed only on platelets and megakaryocytes (Nieswandt and Watson, 2003; Zahid et al., 2012). It is best known as the main platelet activating receptor for collagen. It belongs to the Ig receptor superfamily and has: i) two extracellular Ig domains (D1 and D2), to which ligands are binding, ii) a mucin-like stalk rich in serine and threonine with sites of O-glycosylation, iii) a single transmembrane helix and iv) a cytoplasmic tail. There are 3,000 to 4,000 copies of GPVI per platelet (Best et al., 2003). GPVI is mainly expressed as a monomer on resting platelets, but 30% of it is expressed as a

dimer and this proportion increases upon activation up to 44% (Jung et al., 2012). GPVI is associated with two FcRγ-chains through a salt bridge (Feng et al., 2005). The FcRγ-chain contains an immunoreceptor tyrosine-based activation motif (ITAM) which initiates a signaling cascade following GPVI – ligand interaction. The coupling to the FcRγ-chain with GPVI is necessary for the surface expression of GPVI, and to initiate its signaling (Zheng et al., 2001).

Ligand binding to GPVI promotes its clustering and brings into close proximity the Src family kinases, Fyn and Lyn, bound to the proline-rich region of the cytoplasmic tail of GPVI and the ITAM domain of the FcRγ-chain, promoting its phosphorylation (Ezumi et al., 1998; Quek et al., 2000; Suzuki-Inoue et al., 2002). This leads to the recruitment and phosphorylation of the tyrosine kinase Syk which initiates a downstream signaling cascade leading to the formation of a LAT-based signaling complex located at the cell membrane (Pasquet et al., 1999). Formation of this complex allows effector proteins such as the tyrosine kinases Btk and Tec to come into contact with their substrate resulting in the activation of phospholipase Cγ2 (Watson et al., 2005). Phospholipase Cγ2 hydrolyzes phospho-inositol-4,5-bisphosphate into DAG and inositol-1,4,5-triphosphate, which leads to the release of Ca^{2+} from internal stores into the cytosol. Post-calcium events are then initiated which ultimately increase the affinity of αIIbβ3 for its main ligand, fibrinogen, promoting platelet aggregation. The GPVI signaling pathway is particularly efficient in releasing soluble agonists such as ADP and TxA2, which enhance platelet activation (**Figure 4**) (Ahmed et al., 2020).

Fibrillar collagen is the first identified, best known and most potent ligand of GPVI (Nieswandt et al., 2001). The glycine-proline-hydroxyproline (GPO) sequences of type I and type III collagens are instrumental to bind GPVI (Jarvis et al., 2008). Additional ligands have been identified including the adhesive proteins fibrinogen (Induruwa et al., 2018; Mangin et al., 2018), fibrin (Alshehri et al., 2015; Mammadova-Bach et al., 2015) and laminins (Inoue et al., 2006). A family of snake venom toxins – the C-type lectins (convulxin, ophioluxin,

alboagregin-A and alboluxin) – have been shown to activate GPVI (Dormann et al., 2001; Du et al., 2002a; Du et al., 2002b; Murakami et al., 2003).

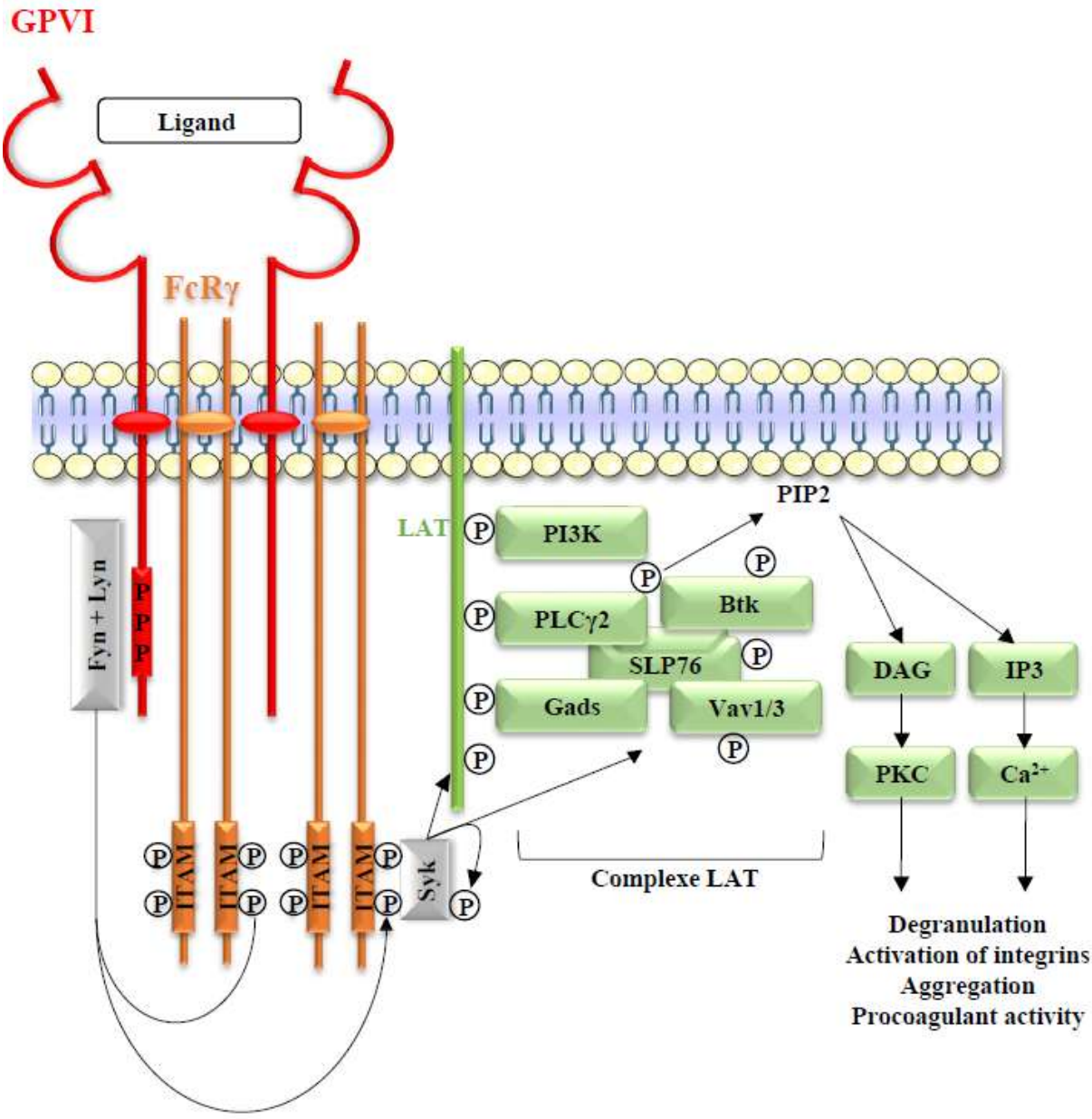

Figure 4: The signaling pathway triggered by the GPVI/FcRγ complex. DAG, diacylglycerol; Fyn, tyrosine-protein kinase Fyn; Gads, Grb2-related adapter dowstream of Shc; GP, glycoprotein; IP3, inositol 1,4,5-triphosphate; ITAM immunoreceptor tyrosine-based activation motif; LAT, linker for activation of T cells; PI3K, phosphoinositide 3-kinase; PIP2, phosphatidylinositol 4',5'-bisphosphate; PKC, protein kinase C; PLCγ2, phospholipase Cγ2;

SLP76, Scr homology 2 domain-containing leukocyte phosphoprotein of 76 kDa adapter protein; Syk, spleen tyrosine kinase (Adapted from (Rayes et al., 2019)).

GPVI is not considered as a key platelet receptor for hemostasis as patients presenting a defect in GPVI only present minor bleedings such as purpura or epistaxis (Jandrot-Perrus et al., 2019). In addition, mice deficient or immuno-depleted for GPVI do not present a prolongation in tail-bleeding time (Kato et al., 2003; Lockyer et al., 2006; Mangin et al., 2012). In contrast, numerous studies based on *in vitro, ex vivo* and *in vivo* models have identified a role of these receptor in some experimental models of thrombosis (Andrews et al., 2014; Bender et al., 2011; Hechler et al., 2010; Munnix et al., 2005). Ultrasound or mechanical injuries of atherosclerotic plaque in aged $ApoE^{-/-}$ mice, which are proposed to better mimic pathological conditions of atherothrombosis, further highlighted an important role of GPVI in arterial thrombosis (Cosemans et al., 2005; Hechler and Gachet, 2011a; Kuijpers et al., 2009; Mangin et al., 2006; Massberg et al., 2003). Together, these observations suggest that GPVI represents an attractive anti-thrombotic target with a potential minor effect on bleedings.

3.1.3. C-type lectin-like type II transmembrane receptor

C-type lectin-like type II transmembrane receptor (CLEC-2) is a 30 kDa protein expressed on platelets and megakaryocytes, and at low levels on dendritic cells and myeloid cells (Lowe et al., 2015; Suzuki-Inoue et al., 2006). Its extracellular domain consists of a stem and a carbohydrate-recognizing domain (CTLD) (Watson et al., 2009) and its cytoplasmic domain is composed of a short cytosolic tail harboring a single YxxL sequence termed hemITAM (Watson et al., 2007; Watson et al., 2010). There are 2,000 to 4,000 copies of CLEC-2 per platelet (Gitz et al., 2014). On non-activated platelets, CLEC-2 is mainly expressed as a monomer with only about a third of the receptors being in a dimerized state, but after ligand

binding with CLEC-2, most molecules pass into an oligomerized state, which contributes to the receptor clustering to induce signals (Hughes et al., 2010; Martin et al., 2021; Martyanov et al., 2020; Martyanov et al., 2018).

CLEC-2 was identified by affinity chromatography as a receptor for rhodocytin, the snake C type lectin toxin, which activates platelets through a Src kinase-regulated pathway (Suzuki-Inoue et al., 2006). In contrast to the GPVI pathway, CLEC-2 activates Syk through a dimerization mechanism *via* a hemITAM, while downstream signaling is similar to the one induced by GPVI, with phosphorylation of Syk, LAT, SLP-76, Btk and PLCγ2 (Fuller et al., 2007; Spalton et al., 2009; Suzuki-Inoue et al., 2006) ultimately leading to Ca^{2+} release and platelet activation events (**Figure 5**) (Lombard et al., 2018).

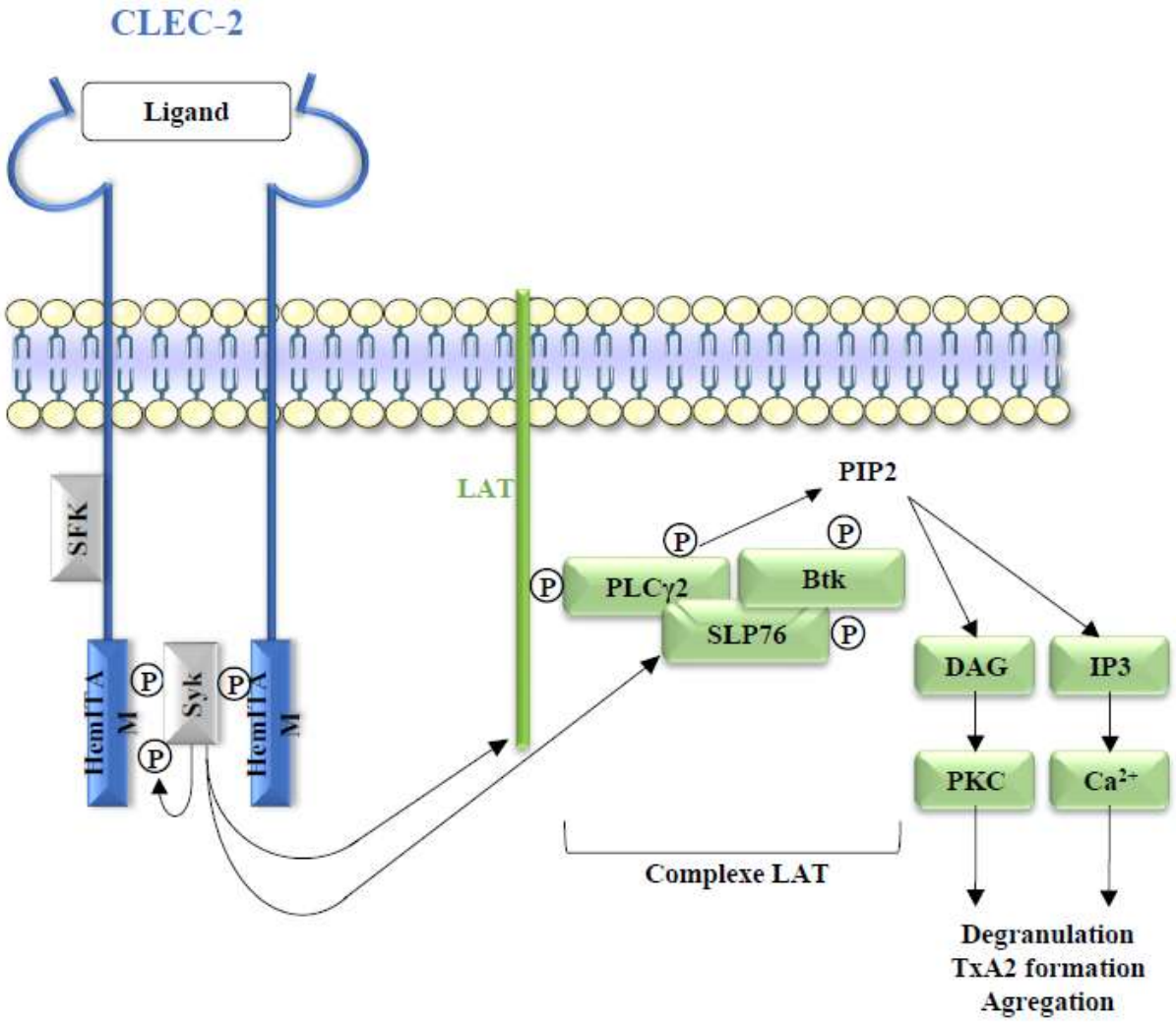

Figure 5: The signaling pathway triggered by the CLEC-2 receptor. Btk, Bruton tyrosine kinase; CLEC-2, C-type lectin-like receptor-2; DAG, diacylglycerol; IP3, inositol 1,4,5-triphosphate; ITAM immunoreceptor tyrosine-based activation motif; LAT, linker for activation of T cells; PIP2, phosphatidylinositol 4',5'-bisphosphate; PKC, protein kinase C; PLCγ2, phospholipase Cγ2; SFK, Src family kinase; SLP76, Scr homology 2 domain-containing leukocyte phosphoprotein of 76 kDa adapter protein; Syk, spleen tyrosine kinase; TxA2, thromboxane A2 (Adapted from (Rayes et al., 2019)).

Podoplanin is the first identified endogenous ligand of CLEC-2. It is a type I transmembrane glycoprotein, which is present on the surface of endothelial cells of lympho-capillaries, type I alveolocytes, kidney podocytes, cardiomyocytes, and reticular fibroblasts (Astarita et al., 2012). Under pathological conditions it was found on the surface of malignant tumors (squamous cell carcinomas, melanomas, gliomas) (Sekiguchi et al., 2016; Shirai et al., 2017), macrophages during macro-inflammation process (Hitchcock et al., 2015) and inside atherosclerotic plaques (Inoue et al., 2015).

CLEC-2 does not appear to play a key role in hemostasis, since bleeding time in mice with CLEC-2 deficiency is not prolonged (Shirai et al., 2017). However, mice deficient in CLEC-2 or treated with a depleting anti-podoplanin antibody have been reported to experience reduced experimental thrombosis (Bender et al., 2013; Inoue et al., 2015; May et al., 2009; Suzuki-Inoue et al., 2010). Podoplanin is unlikely to be the ligand explaining the potential role of CLEC-2 in thrombosis models as it is not found on the healthy vessel wall. Of note, the role of CLEC-2 in experimental thrombosis could not be confirmed in our laboratory with GPIbCre-CLEC-2-deficent mice which presented a normal thrombus formation after mechanical injury of the aorta and $FeCl_3$ of the carotid artery (unpublished data). CLEC-2 has also been shown to be involved in arterial thrombosis independently of hemITAM signaling. Indeed, mice

presenting the CLEC-2 receptor with a mutation impairing hemITAM signaling, have defects in thrombus formation only with an anti–CLEC-2 antibody (Haining et al., 2017).

CLEC-2/podoplanin interaction has been proposed to play a role beyond hemostasis. As podoplanin is present on the surface of endothelial cells of lympho-capillaries, CLEC-2-mediated platelet activation appears important during vessel development to block blood effusion and to prevent blood filling of the lymphatic system, a process potentially restricted to chronic vascular remodeling (Haining et al., 2021; Suzuki-Inoue et al., 2010; Zhang et al., 2018). In addition, a role for the CLEC-2-podoplanin interaction has been shown to contribute to tumor progression notably through the ability of podoplanin expressed on tumor cells to promote platelet aggregation (Christofori, 2007). In agreement with this study, anti-podoplanin antibody has been reported to suppress lung colonization of colon adenocarcinoma intestines revealing that CLEC-2-mediated platelet activation is a potential trigger of tumor metastasis (Sugimoto et al., 1991; Suzuki-Inoue, 2019).

3.1.4. Integrins

Integrins are a family of transmembrane glycoproteins functioning as cell adhesion and signaling molecules. They are heterodimers composed of α and β subunits which associate non-covalently (Burke, 1999). Each subunit consists of 3 domains: a large extracellular domain that is responsible for ligand binding, a single-pass transmembrane domain and a smaller cytoplasmic tail (Hynes, 2002). In mammals, 24 integrins have been described which consist of the association of 18 different α-chains with 8 β subunits (Humphries et al., 2006; Kinashi, 2005; Luo et al., 2007a). Integrins are regulating many biological functions, such as cell migration, proliferation, differentiation, survival and apoptosis (Nieswandt et al., 2009). Two subgroups of integrins are present on human platelets: β1 and β3 families, which account for a

total of five human platelet integrins: α2β1, α5β1, α6β1, αvβ3 and αIIbβ3 (Piotrowicz et al., 1988; Sonnenberg et al., 1988; Staatz et al., 1989).

Integrins can adopt three different conformational states as identified by electronic microscopy (Takagi et al., 2002): i) on resting platelets, integrins are mostly inactive with low affinity for extracellular ligands. The integrin ectodomain is folded forming an inverted V which presents a closed binding side; ii) after platelet activation which generates an inside-out signal, integrins switch to an intermediate state in which the molecule expands, but contains a closed globular head. In this conformation, integrins have an intermediate affinity for their ligands (Huang et al., 2019); and iii) in case of stronger signals integrins expand and the globular head opens allowing a high affinity for ligands (Chen et al., 2019). Besides these conformational changes, integrins can cluster into oligomers to increase avidity for their ligands (Carman and Springer, 2003).

Inside-out signaling of integrins, which has been mainly studied for αIIbβ3, is initiated upon ligand binding of agonists such as collagen, ADP, TxA2 or thrombin to their receptors (**Figures 6**). Most of the signaling pathways stimulated by these agonists lead to phospholipase C (PLC) β or PLCγ activation. PLC generates diacylglycerol (DAG) and inositol-1,4,5-triphosphate (IP3), activating protein kinase C (PKC) and mobilizing intracellular Ca^{2+}, respectively. This promotes activation of a small GTPase Rap1 which is a common downstream activator in this signaling pathway (Boettner and Van Aelst, 2009; Bos, 2005; Katagiri and Kinashi, 2012). Activated Rap1b forms a complex with the integrin activator talin through Rap1-GTP-interacting adaptor molecule (Han et al., 2006) and thus facilitates talin interaction with the cytoplasmic tail of the β subunit (Bromberger et al., 2018) resulting in conformational change and increase in the affinity of integrins for their ligands (Lefort et al., 2012). Kindlin-3 cooperates with talin to facilitate talin binding to the β subunit (Haydari et al., 2020).

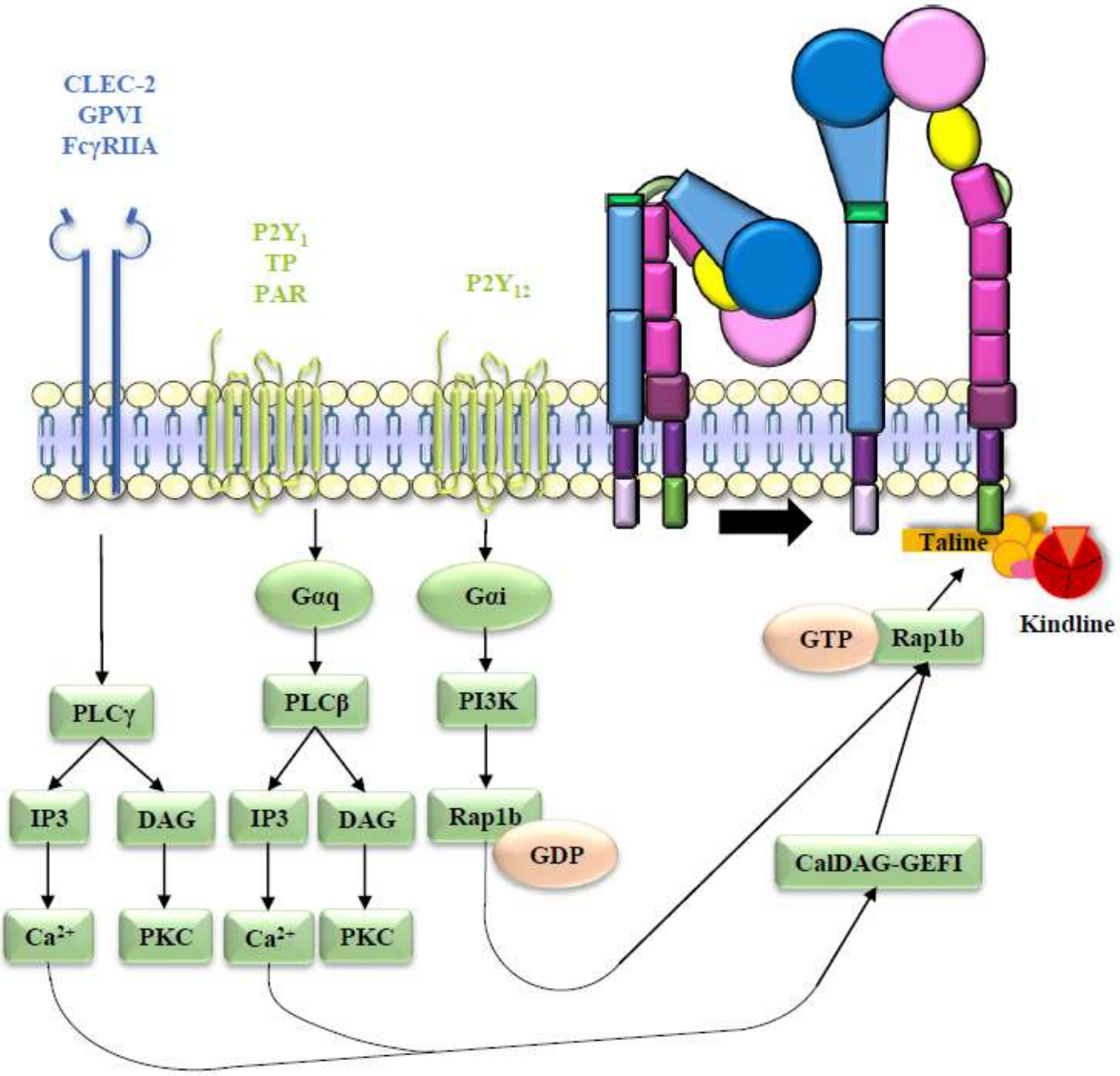

Figure 6: Molecular mechanisms of platelet integrin activation (inside-out signalling). CalDAG-GEFI, calcium and DAG-regulated guanine-nucleotide-exchange factor; CLEC-2, C-type lectin-like receptor-2; DAG, diacylglycerol; GDP, guanosine diphosphate; GP, glycoprotein; GTP, guanosine triphosphate; IP3, inositol 1,4,5-triphosphate; PAR, protease-activated receptor; PI3K, phosphoinositide 3-kinase; PKC, protein kinase C; PLCβ, phospholipase Cβ; PLCγ, phospholipase Cγ; Rap1b, Ras-related protein 1b; TP, thromboxane receptor (Adapted from (Stefanini et al., 2015)).

The ligand binding to integrins initiates an outside-in signal, which has also been mainly studied for αIIbβ3 (Luo et al., 2007a). This process initiates focal adhesion kinase (FAK) and Src recruitment to the β integrin cytoplasmic tail. They phosphorylate paxillin and P130C, leading to Rac activation. This Rac pathway promotes formation of lamellipodial protrusion (Kurokawa et al., 2005; Machacek et al., 2009). In parallel, integrin linked kinase (ILK) is recruited to the β integrin cytoplasmic domain and together with Src promote Akt activity. This Akt pathway regulates sensitivity to thrombin receptor activating peptide (TRAP)-dependent fibrinogen binding and secretion of dense and α-granule contents (Woulfe et al., 2004). Activated Src also initiates Ras–Erk pathway which regulates store-mediated Ca^{2+} entry in human platelets (**Figure 7**) (Hu and Luo, 2013; Rosado and Sage, 2001).

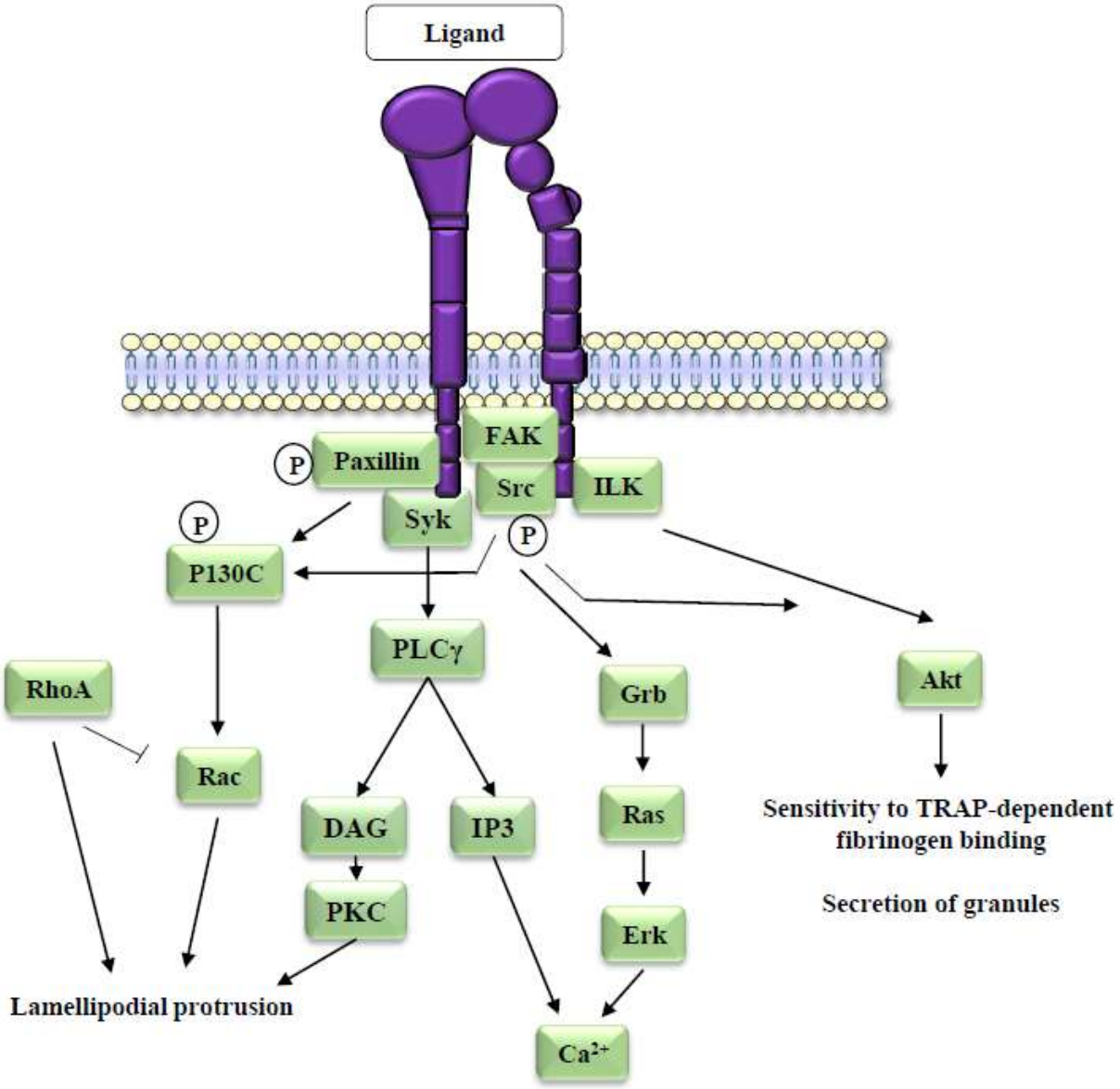

Figure 7: The outside-in signaling of integrin αIIbβ3. Akt, protein kinase B alpha; DAG, diacylglycerol; Erk, extracellular signal-regulated kinase; FAK, focal adhesion kinase; Grb, growth factor receptor-bound protein; ILK, integrin linked kinase; IP3, inositol 1,4,5-triphosphate; PKC, protein kinase C; PLCγ, phospholipase Cγ; P130C, p130 Crk-associated substrate; Rac, Ras-related C3 botulinum toxin substrate, RhoA, Ras homolog family memeber A; Syk, spleen tyrosine kinase; TRAP, thrombin receptor activated peptide (Adapted from (Hu and Luo, 2013)).

3.1.4.1. Integrin α2β1

Integrin α2β1 is expressed on the surface of platelets, fibroblasts, epithelial, and endothelial cells (Ojalill et al., 2018; Zutter and Santoro, 1990). Two polymorphisms in the α2 gene are associated with the cell-surface density of integrin α2β1 (Corral et al., 1999; Kritzik et al., 1998). The expression of this receptor varies between 2,000 and 8,000 copies per platelet (Di Paola et al., 2005). The α2β1 integrin is the first collagen receptor identified on platelets (Santoro et al., 1988) and mainly supports stable adhesion (Sarratt et al., 2005). It recognizes type I fibrillar collagen with high affinity (Knight et al., 2000), but can also bind type IV subendothelial collagen (Vandenberg et al., 1991). Integrin α2β1 has also a large number of additional ligands, such as tenascin C, laminins, proteoglycans endorepellin/ perlecan and decorin (Bix et al., 2004; Chan and Hemler, 1993; Guidetti et al., 2002; Sriramarao et al., 1993). The outside-in signaling pathway of this receptor results in shape change, filopodia extension, lamellipodia formation and platelet spreading (Inoue et al., 2003).

Integrin α2β1 does not seem to play a critical role in hemostasis. Two patients with α2β1 genetic defects presented only a moderate bleeding phenotype (Kehrel et al., 1988; Nieuwenhuis et al., 1985). This result is in agreement with the normal tail-bleeding time in mice with a deficiency of the α2 chain (Chen et al., 2002; Habart et al., 2013; Holtkotter et al., 2002; Nieswandt et al., 2001). In humans with overexpression of α2β1, an increased risk of myocardial infarction, diabetic retinopathy and stroke has been reported, pointing out to a role of this integrin in arterial thrombosis (Matsubara et al., 2000; Santoso et al., 1999). The role of integrin α2β1 in thrombus formation and stability has been demonstrated in a flow-based assay consisting in blood perfusion over collagen (He et al., 2003; Kuijpers et al., 2007). The role of this integrin has also been shown in experimental thrombosis in *in vivo* mouse models based on chemical injuries ($FeCl_3$; Rose Bengal) but appears dispensable after intravascular injection of collagen, a model mimicking thromboembolism (He et al., 2003; Kuijpers et al., 2007).

3.1.4.2. Integrin α5β1

Integrin α5β1 is expressed on the surface of platelets, endothelial cells, fibroblasts, lymphocytes, monocytes and cancer cells (Kita et al., 2001; Wayner et al., 1988). The expression of this receptor varies between 2,000 and 4,000 copies per platelet (Ni and Freedman, 2003). The main ligand for the α5β1 integrin is fibronectin, which is present in plasma, in the subendothelium of the vessel wall and stored in platelet α-granules (Magnusson and Mosher, 1998), but this receptor also interacts with other proteins presenting an Arg-Gly-Asp (RGD) sequence (Rocha et al., 2018). α5β1 binding to fibronectin supports platelet adhesion under static and low flow conditions resulting in outside-in signaling which promotes platelet shape change and filopodia formation (Beumer et al., 1994; Maurer et al., 2015; McCarty et al., 2004).

Integrin α5β1 is involved in cell migration and differentiation, therefore, its absence leads to embryonic lethality due to a lack of development of blood vessels (Francis et al., 2002; Yang et al., 1993). For this reason, the investigation of its role in thrombus formation *in vivo* was precluded for a while. During my PhD studies, we generated a mouse for which the gene of α5β1 was deleted specifically in the megakaryocyte lineage, allowing to study the importance of integrin α5β1 specifically in hemostasis and thrombosis (see ***Publication 2***).

3.1.4.3. Integrin α6β1

Integrin α6β1 is expressed on the surface of platelets, endothelial cells, pericytes, eosinophils, neutrophils and cancer cells (Bohnsack, 1992; Georas et al., 1993; Larrieu-Lahargue et al., 2011; Wewer et al., 1997). The expression of this receptor varies between 4,000 and 12,000 copies per platelet (Burkhart et al., 2012; Ni and Freedman, 2003). The main ligands for the α6β1 integrin are laminins, which are present in various cell types of both developing

and adult tissues, including vascular endothelial and smooth muscle cells (Magnusson and Mosher, 1998). Integrin α6β1 can also interact with TSP-1 as proposed after observation of a reduction in adhesion to TSP-1 of platelets deficient for α6 (Schaff et al., 2013). The integrin binding to its ligands supports platelet adhesion under static and flow conditions (Geberhiwot et al., 1999; Hindriks et al., 1992; Inoue et al., 2006; Nigatu et al., 2006; Schaff et al., 2013; Sonnenberg et al., 1988) and promotes outside-in signaling resulting in an increase in intracellular Ca^{2+} concentrations, shape change and filopodia extension (Inoue et al., 2006; Schaff et al., 2013).

Integrin α6β1 does not seem to play a critical role in hemostasis as bleeding time in mice with an α6 deficiency is not increased (Schaff et al., 2013). In contrast, this integrin plays a role in thrombus formation both *in vitro* under shear flow and *in vivo* in 3 experimental thrombosis animal models based on mechanical-injury of the aorta, laser-injury of the mesenteric arteriole and guide wire-injury of the carotid artery (Schaff et al., 2013).

3.1.4.4. Integrin αIIbβ3

Integrin αIIbβ3 is a heterodimer of 230 kDa composed of an αIIb subunit and a β3 subunit (Jennings and Phillips, 1982). Integrin αIIbβ3 is specifically expressed on platelets, even though it has been proposed to also be expressed by tumor cells (Boukerche et al., 1989; Grossi et al., 1988; Honn et al., 1992a; Timar et al., 1998). This receptor is present at 80,000 copies on the surface of a resting platelet and 30,000 additional copies are found on the membrane of the open canalicular system and α granules which are exposed after platelet activation (Wagner et al., 1996). Fibrinogen is the main ligand of integrin αIIbβ3. This receptor recognizes both the RGD peptide-binding sequence of the α chain of fibrinogen and the KQAGDV sequence of the γ chain. This interaction allows the bridging of adjacent platelets resulting in their aggregation, which represents the main function of αIIbβ3 (Marguerie et al.,

1979; Springer et al., 2008). This integrin also recognizes additional adhesive proteins with an RGD motif including vWF, fibronectin and vitronectin. Its interaction with collagen-bound vWF and fibronectin is involved in stable platelet adhesion (Giuliano et al., 2003; Maurer et al., 2015) and could also participate in the formation of aggregates under low shear (<1,000 s^{-1}) (Moake et al., 1988; Moake et al., 1986). Following ligand binding the outside-in signaling pathway of this receptor results in the change of the shape of platelets, promotes secretion of the granule content and the retraction of the fibrin clot (Huang et al., 2019).

Defects or deficiency of one subunit of integrin αIIbβ3 leads to a rare and severe bleeding disorder named Glanzmann's thrombasthenia, which is characterized by a decreased ability of platelets to adhere, spread and aggregate, despite a normal platelet count (Nurden, 2006; Solh et al., 2015). On the other hand, integrin αIIbβ3 plays a crucial role in arterial thrombosis through its ability to ensure platelet aggregation and therefore the growth and stability of the thrombus (Akuta et al., 2020; Goschnick et al., 2006; Hodivala-Dilke et al., 1999; Tronik-Le Roux et al., 2000). The inhibition of this integrin results in prevention of thrombus growth in experimental models (Schaff et al., 2013). Its importance in arterial thrombosis is attested by the clinical use of a class of anti-platelet agents targeting this integrin, and named: abciximab, eptifibatide and tirofiban. These drugs are restricted to acute settings as their use is accompanied by a significant hemorrhagic risk.

3.1.4.5. Integrin αvβ3

Integrin αvβ3 is expressed on the surface of platelets, smooth muscle cells, fibroblasts, neutrophils, osteoclasts and tumor cells (Honn et al., 1992b; Kappert et al., 2001; Nesbitt et al., 1993; Rainger et al., 1999). The expression level of this receptor reaches only a couple of hundred copies per platelet (Poujol et al., 1997). Similarly to αIIbβ3, this receptor recognizes

an RGD peptide-binding sequence, and its ligands were proposed to be vitronectin, vWF, osteopontin, fibrinogen and fibronectin (Adair et al., 2005; Bennett et al., 1997). At the functional level, αvβ3 supports platelet adhesion to fibronectin, vitronectin and osteopontin which are present in the vessel wall (McCarty et al., 2004; Paul et al., 2003). This integrin has also been proposed to participate in clot retraction (Mor-Cohen, 2016).

The importance of the αvβ3 integrin in hemostasis and arterial thrombosis has not yet been reported. In humans, no αv integrin mutation has been described to induce hemorrhagic disease. Unpublished data of our group indicate that mice deficient for αv specifically in the platelet lineage have a normal tail bleeding time and an unaltered response in models of experimental thrombosis (unpublished, Mangin P. and Léon C. 2016).

3.2. Receptors for soluble agonists

Soluble agonists such as ADP, ATP, thrombin or TxA2 play an instrumental role in amplifying platelet activation to ensure thrombus growth and stability. They act through ion channel receptors (P2X1 receptor) and G protein–coupled receptors (P2Y1, P2Y12, TP and PARs receptors) (**Figure 8**) (Gurbel et al., 2015).

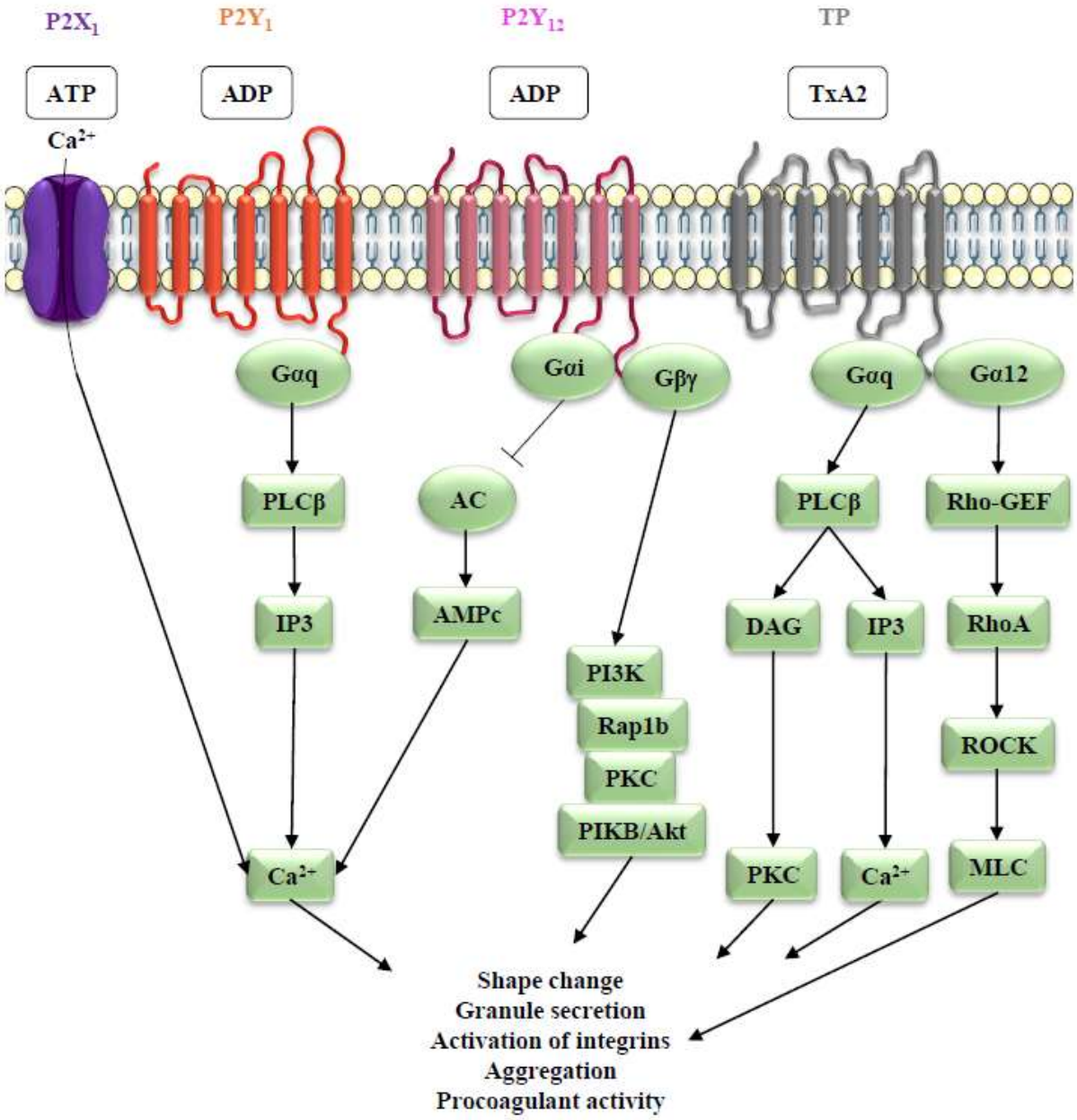

Figure 8: Signaling pathways triggered by soluble agonist receptors P2Y1, P2Y12, P2X1 and TP. AC, adenylate cyclase; ADP, adenosine diphosphate; Akt, protein kinase B alpha; cAMP, cyclic adenosine monophosphate; ATP, adenosine triphosphate; DAG, diacylglycerol; IP3, inositol 1,4,5-triphosphate; MLC, myosin light chain; PI3K, phosphoinositide 3-kinase; PKC, protein kinase C; PLCβ, phospholipase β; Rap1b, Ras-related protein 1b; Rho-GEF, Guanine nucleotide exchange factor for Rho; ROCK, Rho-associated protein kinase; TP,

thromboxane receptor; TxA2, thromboxane A2 (Adapted from (Mahaut-Smith, 2012; Offermanns, 2006).

3.2.1. The P2X1 receptor

P2X1 belongs to the ion channel family that is activated by ATP and inhibited by ADP (Sun et al., 1998). This receptor is expressed on the surface of platelets, smooth muscle cells, neutrophils, macrophages (Hinze et al., 2013; Lecut et al., 2009; Sim et al., 2007). The expression of this receptor ranges from 100 to 150 copies per platelet (MacKenzie et al., 1996; Vial et al., 1997). The activation of P2X1 results in a rapid intracellular calcium influx into platelets and, further, myosin light chain phosphorylation that leads to platelet activation evidenced by platelet shape change, pseudopodia formation and degranulation (Mahaut-Smith, 2012; Rolf et al., 2001; Toth-Zsamboki et al., 2003). Stimulation of the P2X1 receptor does not induce platelet aggregation, but it amplifies aggregation under high shear conditions or in response to various agonists (Erhardt et al., 2006; Fung et al., 2007; Gachet et al., 2006; Ilkan et al., 2018; Jones et al., 2014; Oury et al., 2004; Oury et al., 2001; Vial et al., 2002).

The P2X1 receptor is rapidly desensitized after interaction with ATP, which has complicated the *in vitro* study of its role in platelet function (Gachet et al., 2006). Experiments with P2X1-deficient mice identified a reduced ability of platelets to adhere and form aggregates on collagen, particularly under high shear stress (Hechler et al., 2003). Deletion or inhibition of P2X1 in mice does not modify bleeding time, but reduces thrombus size in a laser-induced thrombosis model (Erhardt et al., 2006; Hechler et al., 2003; Hechler et al., 2005). In agreement, genetically modified mice overexpressing P2X1 have a prothrombotic phenotype (Oury et al., 2003).

3.2.2. G protein–coupled receptors

G protein–coupled receptors (GPCRs) account for the largest family of proteins in the human genome (Fredriksson et al., 2003; Pierce et al., 2002; Vassilatis et al., 2003). GPCRs consist of 7 transmembrane α-helices connected to 3 extracellular loops containing ligand binding sites and to 3 intracellular loops associated with guanine nucleotide binding proteins (G proteins). A GPCR can be associated with different G proteins which determine its specific intracellular responses to agonists. G proteins are heterodimers with α, β, and γ subunits. In their inactive state Gα subunit is bound to GDP and tightly associated with Gβ-Gγ unit. After agonist binding, GDP becomes phosphorylated and induces Gα subunit dissociation allowing interaction with downstream effectors (Offermanns, 2006; Smyth et al., 2009).

3.2.2.1. The P2Y1 receptor

The P2Y1 receptor is a GPCRs coupled to the Gαq protein. This receptor is widely expressed in human tissues and is found in particular on endothelial cells, smooth muscle cells, immune cells including macrophages, eosinophils and lymphocytes (Abbracchio et al., 2006). The expression of this receptor is estimated to be around 150 copies per platelet (Gurbel et al., 2015; Leon et al., 1997). The binding of ADP to P2Y1 results in the interaction of Gαq subunit with PLCβ leading to the generation of IP3 and subsequent mobilization of intracellular Ca^{2+} stores (Cattaneo, 2007; Hechler and Gachet, 2011b; Offermanns, 2006). P2Y1 signaling results in platelet shape change, integrin activation and subsequent platelet aggregation (Fabre et al., 1999; Gachet, 2008; Hechler et al., 1998; Leon et al., 1999). P2Y1 also participates in the procoagulant function of platelets (Leon et al., 2004; Leon et al., 2003).

Bleeding time in mice deficient in P2Y1 or treated by its inhibitor MRS 2500 is slightly increased suggesting a minor role of this receptor in hemostasis (Fabre et al., 1999; Hechler et al., 2006; Leon et al., 1999; Wong et al., 2016). In contrast, deletion or inhibition of P2Y1 in mice leads to protection from collagen-, ADP- or TF-induced thromboembolism (Fabre et al., 1999; Leon et al., 1999) and reduction of thrombus formation after laser-induced injury of the mesenteric arterioles or $FeCl_3$ injury of the carotid artery (Gachet, 2006; Hechler et al., 2006; Lenain et al., 2003; Leon et al., 2001). These results indicate an important role of P2Y1 in arterial thrombosis.

3.2.2.2. The P2Y12 receptor

The P2Y12 receptor is a GPCR coupled to the Gαi protein. This receptor is mainly expressed in platelets (Gurbel et al., 2015), but is also found in particular in brain tissue, smooth muscle cells, dendritic cells and some leukocytes (Ben Addi et al., 2010; Wang et al., 2004; Wihlborg et al., 2004). The expression of this receptor is estimated to be around 600 copies per platelet (Gurbel et al., 2015; Ohlmann et al., 2013). The binding of ADP to P2Y12 results in the Gαi-associated inhibition of adenylyl cyclase leading to the reduction of cAMP (Cattaneo, 2007; Hechler and Gachet, 2011b; Hollopeter et al., 2001). Since cAMP levels control protein kinase A activation and by consequence the inhibition of IP3 receptor, which itself mediates Ca^{2+} levels, a decrease in cAMP leads to an increase of intracellular Ca^{2+} (Quinton and Dean, 1992; Tertyshnikova and Fein, 1998). In parallel, ADP-binding to the P2Y12 receptor results in a downstream signaling through the Gβγ which activates PI3K, and then Akt and Rap1b, resulting in activation of αIIbβ3 and subsequent platelet aggregation (Cosemans et al., 2006; Guidetti et al., 2008; Kim et al., 2004; Schoenwaelder et al., 2007; Stefanini and Bergmeier,

2018; Woulfe et al., 2002). P2Y12 also participates in the procoagulant function of platelets (Leon et al., 2003).

Absence of P2Y12 in humans results in an increased bleeding time and mild signs of hemorrhages (Cattaneo et al., 2003; Conley and Delaney, 2003; Lecchi et al., 2015; Nurden et al., 1995; Remijn et al., 2007; Shiraga et al., 2005). In agreement, bleeding times in mice deficient in P2Y12 were shown to be increased (Andre et al., 2003). The importance of P2Y12 receptor in arterial thrombosis is attested by the clinical use of antithrombotic drugs targeting this receptor. One finds irreversible antagonists of P2Y12, such as clopidogrel, prasugrel and ticlopidine, and reversible antagonists, such as ticagrelor and cangrelor (Gachet, 2006). In agreement, deletion or inhibition of P2Y12 in mice leads to reduction of thrombus formation after $FeCl_3$ injury of the mesenteric arterioles or after photochemical injury of the carotid artery (Andre et al., 2003; Conley and Delaney, 2003; Reiner et al., 2017).

3.2.2.3. The TP receptor

The thromboxane A2 receptor is a GPCR coupled to Gαq and Gα12/13 proteins. This receptor is mainly expressed in platelets (Gurbel et al., 2015), but is also found on endothelial cells, smooth muscle cells, monocytes and macrophages (Davi et al., 2012). The expression of this receptor is around 1,500 copies per platelet (Halushka et al., 1986). The main ligand of this receptor is TxA2 whose action is locally restricted because of its short half-life (Hamberg et al., 1975; Offermanns, 2006). As mentioned above, platelet activation leads to production of TxA2 through synthesis of arachidonic acid which is further metabolized to unstable PGH2 by cyclooxygenase-1 and then to TxA2 by TxA2 synthase (O'Donnell et al., 2014). The binding of TxA2 to its receptor results in the interaction of Gαq subunit with PLCβ leading to the generation of IP3 and subsequent mobilization of intracellular Ca^{2+} stores (Cattaneo, 2007;

Hechler and Gachet, 2011b; Offermanns, 2006). In parallel, ligand binding to the TP receptor results in a downstream signaling through the Gα12 subunit that activates Rho-associated protein kinase pathway leading to phosphorylation of the myosin light chain (Klages et al., 1999). TP signaling results in platelet shape change, granule secretion, integrin activation and subsequent platelet aggregation (Bauer et al., 1999; Getz et al., 2010).

Genetic defects of TP in humans result in a modest bleeding, highlighting the role of this receptor in hemostasis (Defreyn et al., 1981; Lages et al., 1981; Samama et al., 1981; Wu et al., 1981). This is further supported by the increased bleeding time in mice deficient in TP receptor (Cathcart et al., 2008; Thomas et al., 1998; Yu et al., 2004). Moreover, deletion or inhibition of TP receptor in mice leads to a reduction of thrombus formation after catheter-induced injury of the carotid artery or after photochemical injury of the femoral artery indicating an important role of this receptor in arterial thrombosis (Capra et al., 2014; Cheng et al., 2002; Grad et al., 2012). The importance of TP receptor in arterial thrombosis is further attested by the clinical trials of antithrombotic drugs targeting this receptor: terutroban, terbogrel (Capra et al., 2014; Gurbel et al., 2015).

3.2.2.4. The protease-activated receptors

The protease-activated receptors (PARs) are GPCRs coupled to Gαq, Gα12/13 and Gαi (Klages et al., 1999; Offermanns et al., 1994). These receptors are expressed in platelets (Gurbel et al., 2015), but are also found in endothelial cells, smooth muscle cells, monocytes and astrocytes (Ossovskaya and Bunnett, 2004). Human platelets express PAR1 and PAR4 at around 1,000 to 2,000 copies per platelet, while mouse platelets express PAR3 and PAR4 at 1,500 to 5,000 copies per platelet (Kahn et al., 1999; Zeiler et al., 2014). The main ligand of these receptors is thrombin (Coughlin, 2005) which cleaves the extracellular N-terminal end of

the receptor between residues Arg41 and Ser42, in order to expose a new N-terminal end which can then bind and activate the PAR receptors (Vu et al., 1991). PAR1 and PAR3 have additionally a hirudin-like sequence close to the C-terminal thrombin cleavage site which facilitates the binding to thrombin and is not present on PAR4 (Kahn et al., 1998; Xu et al., 1998). After ligand binding to the PARs, a signaling is initiated through Gαq which activates PLCβ leading to mobilization of intracellular Ca^{2+} stores, while Gα12–mediated activation of the Rho-associated protein kinase pathway leads to phosphorylation of the myosin light chain and actin remodeling (Voss et al., 2007; Woulfe, 2005). The Gαi subunit-mediated signaling leads to the inhibition of adenylyl cyclase inducing the reduction of cAMP (Kim et al., 2002). PAR1 and PAR3 are activated by a low concentration of thrombin (order of 1 nM), while PAR4 is activated by higher concentrations (order of 50 nM) (Kahn et al., 1999). Due to this unique mechanism of action, these two receptors signaling pathways complete each other: the signal from PAR1 is fast, but it is quickly switched off, while, PAR4 signals are slow but prolonged (Leger et al., 2006). PAR signaling results in platelet shape change, TxA2 release, granule secretion, integrin activation and subsequent platelet aggregation (Bauer et al., 1999; Henriksen and Hanks, 2002; Kahn et al., 1999). These receptors are also involved in the procoagulant activity of platelets (**Figure 9**) (Andersen et al., 1999).

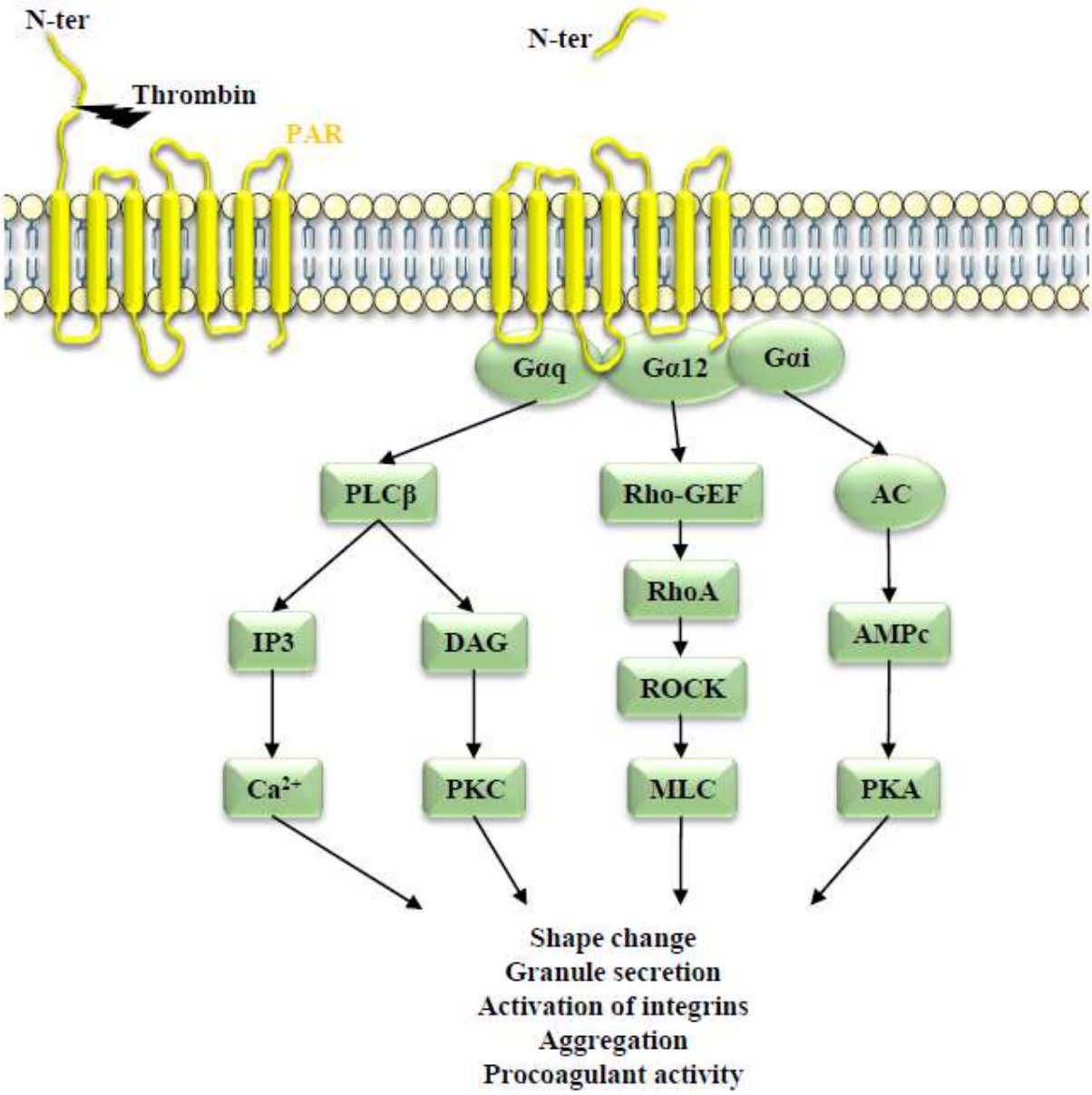

Figure 9: The signaling pathway triggered by PAR receptors. AC, adenylate cyclase; cAMP, cyclic adenosine monophosphate; DAG, diacylglycerol; IP3, inositol 1,4,5-triphosphate; MLC, myosin light chain; PAR, protease-activated receptor; PKA, protein kinase A; PLCβ, phospholipase β; Rho-GEF, Guanine nucleotide exchange factor for Rho; ROCK, Rho-associated protein kinase.

The importance of PAR receptors in arterial thrombosis is attested by the clinical use of the vorapaxar which inhibits PAR1 and is recommended in the prevention of ischemic events (Gupta et al., 2021; Kraft et al., 2016). These results were in line with pre-clinical data indicating that the deletion of PAR3 or PAR4 in mice leads to a reduction in thrombus formation after $FeCl_3$ injury of the mesenteric arteriole or the carotid artery, after laser injury of the cremaster arteriole or after thromboplastin-induced pulmonary embolism (Cornelissen et al., 2010; Hamilton et al., 2004; Sambrano et al., 2001; Vandendries et al., 2007; Weiss et al., 2002). Interestingly, vorapaxar does not prolong bleeding time suggesting that PAR1 does not play a major role in hemostasis (Kraft et al., 2016). In agreement, bleeding time in cynomolgus monkeys inhibited of PAR1 receptor was not modified (Chintala et al., 2010; Coughlin, 2005). In contrast, mice deficient in PAR3 or PAR4 receptors have a prolonged bleeding time (Hamilton et al., 2004; Sambrano et al., 2001; Weiss et al., 2002).

B. Coagulation

La coagulation sanguine est une cascade de réactions enzymatiques aboutissant à la génération de thrombine qui clive le fibrinogène plasmatique en fibrine pour former un réseau insoluble consolidant l'agrégat plaquettaire (Norris, 2003). Ce processus est subdivisé en deux voies : la voie extrinsèque et la voie intrinsèque, qui conduisent toutes deux à la génération de facteur X (**Figure 10**). L'activation du facteur X via ces deux voies marque le début de la voie commune, menant à la génération de thrombine (Palta et al., 2014).

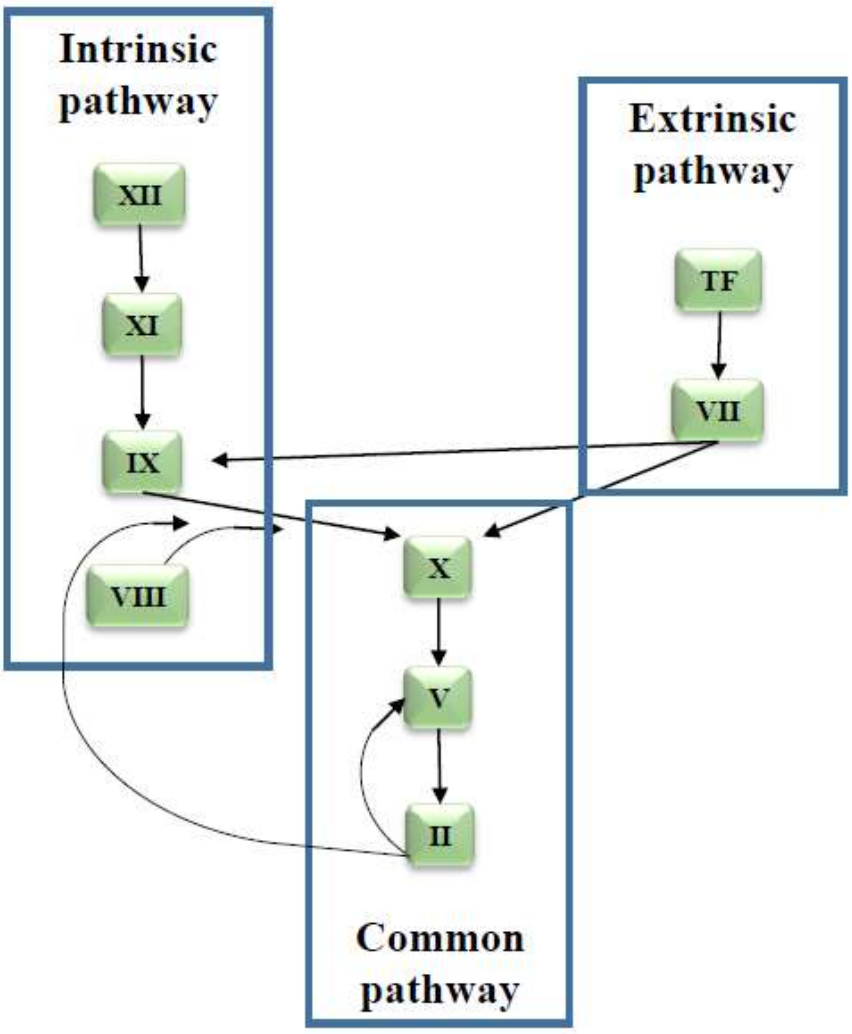

Figure 10: Cascade de coagulation schématique. TF, facteur tissulaire (Adapté de (Palta et al., 2014))**.**

1. La voie extrinsèque

L'activateur principal de la voie extrinsèque est le facteur tissulaire, qui est une glycoprotéine transmembranaire (TF) (Williams et Mackman, 2012). Cette glycoprotéine de 47kD contient un domaine extracellulaire composé de 2 fibronectine de type III qui se lient à deux endroits différents du facteur VII : l'un à sa partie transmembranaire, l'autre à une courte partie intracellulaire. (Banner et al., 1996 ; Butenas, 2012). TF est exprimé à la surface des cellules périvasculaires et des cellules épithéliales entourant les vaisseaux sanguins et dans le

placenta, le cœur, les poumons et le cerveau (Drake et al., 1989 ; Fleck et al., 1990 ; Grover et Mackman, 2018 ; Hoffman et al., 2007). Lors d'une lésion vasculaire, le facteur tissulaire est exposé au flux sanguin, ce qui permet la liaison du facteur VII et conduit à son activation (VIIa) (Owens et Mackman, 2010). Le complexe TF-VIIa permet alors la liaison calcium-dépendante des facteurs de coagulation plasmatiques (F), à savoir le facteur IX et le facteur X (Zeerleder, 2018).

2. La voie intrinsèque

La voie intrinsèque est initiée par le contact du facteur XII avec une surface chargée négativement, entraînant son activation (van der Graaf et al., 1982). Le FXIIa active la prékallikréine en α-kallikréine qui va alors activer le FXII 30 fois plus efficacement qu'une surface chargée négativement et sert de rétroaction positive (Wiggins et Cochrane, 1979). Le FXIIa conduit à l'activation ultérieure du facteur XI et du facteur IX (Mackman et al., 2007). Le facteur IX agit avec son cofacteur VIII pour former un complexe ténase pour transformer/cliver les facteurs X en facteur Xa (Chaudhry et al., 2022).

3. La voie commune

Le facteur Xa produit par les voies extrinsèques et intrinsèques clive la prothrombine pour générer de la thrombine (Smith et al., 2015). Quelques secondes après le début du processus de coagulation, seules de très petites quantités de thrombine (<<1 nM) sont générées, mais elles sont suffisantes pour activer les facteurs V et VIII, ces deux derniers étant des cofacteurs de protéases actives (Wolberg, 2007). Le facteur Va se lie au facteur Xa et à la prothrombine sur la membrane chargée négativement des microparticules ou des plaquettes activées, pour former le complexe prothrombinase qui accélère la réaction de formation de thrombine de 10^5 fois (Mann et al., 1990 ; Podoplevova et al., 2016). À la suite de cette réaction, la thrombine est générée à des concentrations très élevées explosives atteignant de l'ordre 100

nM (Cawthern et al., 1998). La thrombine catalyse la conversion du fibrinogène en filaments de fibrine et active également le facteur XIII, qui réticule et renforce les polymères de fibrine conduisant à la formation d'un caillot de fibrine qui stabilise les agrégats plaquettaires (Wolberg, 2007).

4. Régulation spatio-temporelle des voies extrinsèques et intrinsèques

La coagulation est un processus complexe, strictement régulé dans l'espace et dans le temps, qui conduit à la formation d'un caillot de fibrine à un endroit donné. Ce processus est subdivisé en trois phases : initiation, amplification et propagation. L'initiation de la cascade de coagulation et son amplification commencent au niveau de la paroi vasculaire endommagée. A ce stade, la voie extrinsèque a un fort impact car elle permet de produire localement de la thrombine (Palta et al., 2014). Cependant, la voie extrinsèque ne peut pas assurer la propagation de la génération de thrombine conduisant à la croissance linéaire d'un caillot de fibrine dans l'espace car la distance de diffusion de la thrombine et du FXa est limitée **:** ils sont rapidement et irréversiblement inactivés par des inhibiteurs plasmatiques (Travis et Salvesen, 1983). Par conséquent, l'étape de la voie intrinsèque concernant l'activation du facteur IX par la thrombine a un impact important sur l'étape de propagation (**Figure 11**). Le taux d'inactivation du facteur IXa est d'un ordre de grandeur inférieur à celui du facteur Xa et de la thrombine (Afosah et al., 2022). Cette caractéristique permet au facteur IXa de diffuser efficacement, assurant la polymérisation de la fibrine à de plus grandes distances du site initial d'activation de la coagulation (Dashkevich et al., 2012). La propagation par diffusion du facteur IXa peut entraîner une propagation d'onde auto-entretenue de la thrombine dans l'espace et une augmentation linéaire de la taille du caillot de fibrine à une vitesse d'environ 1 μm/sec (Ataullakhanov et Guriia, 1994).

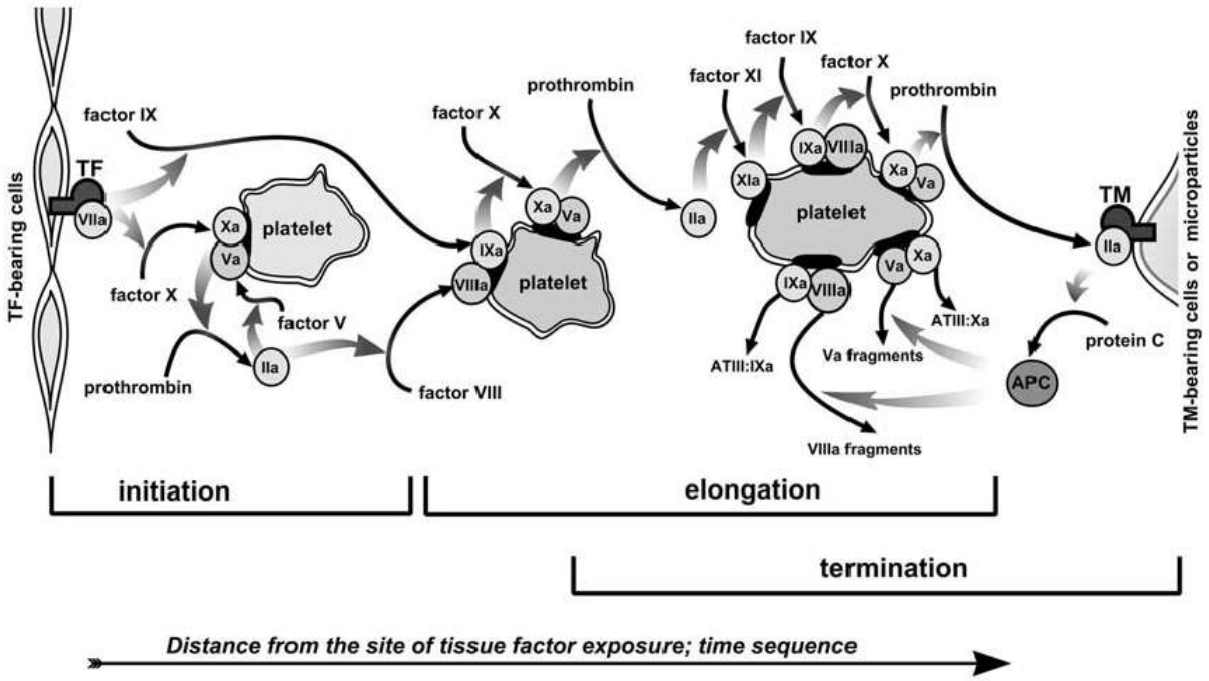

Figure 11: Régulation spatio-temporelle des voies extrinsèques et intrinsèques. APC, protéine C activée; ATIII, antithrombine; TF, facteur tissulaire ; TM, thrombomoduline (Adapté de (Panteleev et al., 2006)).

5. Régulation négative de la coagulation

Pour éviter l'activation incontrôlée du processus telle que la coagulation intravasculaire disséminée, plusieurs régulateurs négatifs de la cascade de coagulation existent, notamment la protéine C, l'antithrombine, la α2-macroglobuline et d'autres (Travis et Salvesen, 1983). Ces inhibiteurs régulent l'activité des protéases de coagulation et peuvent réduire à zéro la concentration locale de thrombine au site de la lésion en un temps caractéristique d'environ 100 s. La protéine C est activée par la thrombine et dégrade les facteurs Va et VIIIa (Panteleev et al., 2006). L'activation de la protéine C par la thrombine est accélérée par un cofacteur de la thrombine, la thrombomoduline, présente à la surface de l'endothélium vasculaire intact (Esmon et Esmon, 1988). L'antithrombine est un inhibiteur de sérine protéase, qui inactive la thrombine

et les facteurs IXa, Xa, XIa et XIIa. Son activité est renforcée en présence d'héparine (Opal et al., 2002).

6. Défauts de la cascade de coagulation

Les défauts génétiques du système de coagulation chez l'homme peuvent entraîner des saignements massifs (Bolton-Maggs, 1996 ; Martin-Salces et al., 2010 ; Perry, 2003). L'une des maladies les plus courantes de la coagulation sanguine est l'hémophilie A et B associée à un déficit en facteurs de coagulation sanguine VIII et IX, respectivement (Kurian et al., 2020). Ces pathologies se traduisent par un défaut majeur de génération de thrombine, et se manifestent par des hémorragies survenant au niveau des articulations, des muscles et des organes internes, spontanément ou à la suite d'un traumatisme ou d'une intervention chirurgicale (Kulkarni et Soucie, 2011). Une autre thrombophilie héréditaire est une mutation du facteur V Leiden, dans laquelle le site de clivage de la protéine C dans le polypeptide du facteur V est muté et son inactivation ne se produit pas. Cette maladie se manifeste par un risque accru de thrombose veineuse mésentérique et de thromboembolie veineuse (Kujovich, 2011 ; van Langevelde et al., 2012 ; Zheng et al., 2021).

7. Contribution de la fibrine et du fibrinogène à la formation de thrombus

7.1. La structure et la fonction de la fibrine et du fibrinogène

Le fibrinogène est une glycoprotéine hexamérique soluble synthétisée par les hépatocytes (Drury et McMaster, 1929). Sa concentration dans le plasma varie entre 2 et 4 mg/mL (Lowe et al., 1997). Le fibrinogène est également stocké dans les granules plaquettaires α (Harrison et al., 1990 ; Wencel-Drake et al., 1985). Cette glycoprotéine est composée de 2 ensembles de 3 chaînes polypeptidiques, Aα, Bβ et γ, délimitées par des ponts disulfure (Kattula et al., 2017). La partie centrale du fibrinogène est constituée des extrémités N-terminales des

six chaînes présentant les sites de clivage des fibrinopeptides A et B (Mosesson, 2005). Le clivage par la thrombine du fibrinopeptide A entraîne la formation de monomérique de fibrine, ce qui, ensuite, initie la polymérisation de la fibrine en présence d'une transglutaminase (facteur XIIIa), entraînant la formation d'un caillot de fibrine stable (**Figure 12**) (Litvinov et al., 2005; Weisel et Litvinov, 2013).

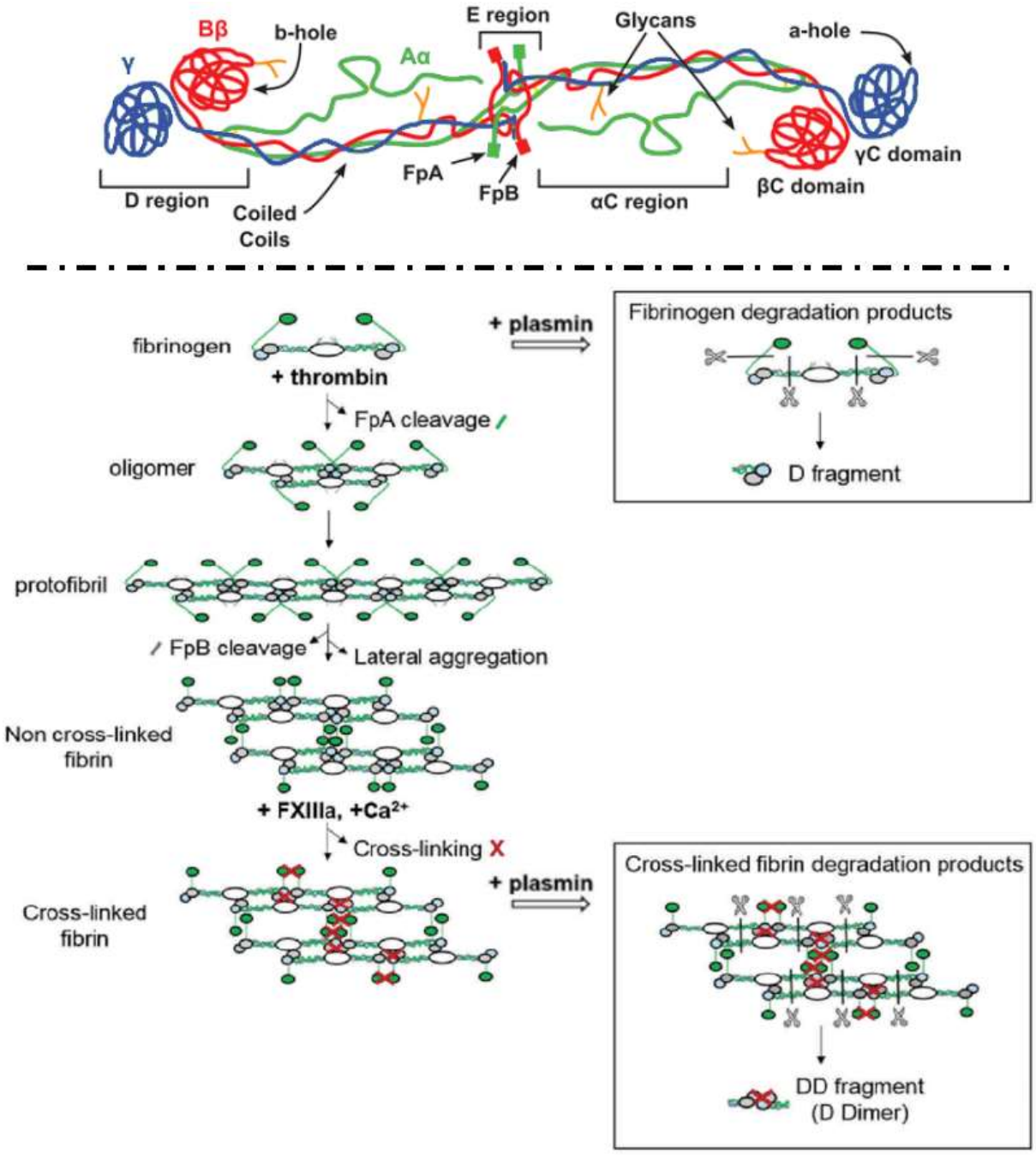

Figure 12: Fibrinogène, fibrine, fibrinolyse. FpA, fibrinopeptide A; FpB ; fibrinopeptide B (Adapté de (Kohler et al., 2015; Slater et al., 2019)).

Le fibrinogène et la fibrine participent tous les deux à la formation d'un thrombus stable. La liaison du fibrinogène à αIIbβ3 permet l'agrégation plaquettaire (Isenberg et al., 1987 ; Mangin et al., 2018). La fibrine forme une structure insoluble. Cela facilite à son tour la liaison des facteurs de coagulation ce qui conduit à une stimulation supplémentaire de la formation de thrombus et de sa stabilisation (Sang et al., 2021 ; van Geffen et al., 2016). Les patients afibrinogénémiques ont des complications avec des événements thromboemboliques artériels et veineux qui démontrent l'importance de la fibrine et du fibrinogène dans la formation de thrombus (de Moerloose et al., 2010 ; Dupuy et al., 2001 ; Girolami et al., 2006 ; Lak et al., 1999).

7.2. La structure du caillot de fibrine

La structure du caillot de fibrine peut avoir différentes architectures en fonction des variations génétiques des chaînes polypeptidiques, de la concentration locale de thrombine et du débit à travers le thrombus nécessaire pour un accès optimal aux régulateurs négatifs de la coagulation (Stalker et al., 2014 ; Weisel, 2007). Le caillot peut être composé de fibres de fibrine épaisses et lâches conduisant à une porosité élevée ou de fibres fines et serrées induisant à une faible porosité (Gu et Lentz, 2018). Dans des études cliniques, il a été démontré que le plasma des patients hémophiles forme des caillots de fibrine lâches anormaux, tandis que le plasma des patients atteints d'anévrisme de l'aorte abdominale, d'accident vasculaire cérébral ischémique, de thromboembolie veineuse ou chez les fumeurs forme des caillots de fibrine denses (Brummel-Ziedins et al. , 2009 ; Laurens et al., 2006 ; Parastatidis et al., 2008 ; Scott et

al., 2011 ; Undas et al., 2009a ; Undas et al., 2009c). Étant donné que le réseau / maillage de fibrine est reconnu comme une caractéristique spécifique de la formation stable du thrombus, le ciblage de la polymérisation de la fibrine avec des peptides synthétiques qui bloquent les interactions entre les monomères de fibrine tels que les peptides avec des séquences de boutons de fibrine A ou B attachés à l'albumine, a été proposé comme une stratégie innovante pour bloquer la thrombose (Risser et al., 2022 ; Stabenfeldt et al., 2012 ; Watson et Doolittle, 2011).

7.3. Le rôle respectif du fibrinogène et de la fibrine dans la formation du thrombus

Malgré des études de longue date sur la contribution de la fibrine et du fibrinogène dans la formation du thrombus, il est encore difficile de distinguer leur rôle respectif car ce sont les ligands des récepteurs plaquettaires αIIbβ3 et GPVI, et ils dérivent l'un de l'autre (Inoue et al., 2006; Mammadova -Bach et al., 2015). Pour ces raisons, le groupe de M. Flick a généré des souris exprimant le gène FibAEK n'ayant pas la capacité de former un réseau de fibrine, mais avec des quantités normales de fibrinogène (Prasad et al., 2015). Dans les modèles hémostatiques, certaines de ces souris ont pu arrêter la perte de sang après la coupe du bout de la queue contrairement aux souris déficientes en fibrinogène qui ne parviennent pas à arrêter le saignement, confirmant le rôle clé du fibrinogène. Dans un modèle de thrombose après application de FeCl3, les souris FibAEK forment un thrombus, mais la formation de fibrine était nécessaire pour une occlusion complète du vaisseau. Ces résultats laissent une certaine incertitude sur le rôle du réseau de fibrine par rapport au fibrinogène soluble dans la formation du thrombus. Au cours de mes études doctorales, nous avons utilisé ces souris FibAEK dans des modèles d'hémostase et de thrombose pour étudier l'importance de la formation de fibrine dans la dynamique de croissance du thrombus et dans la limitation de la thrombose, au-delà de son rôle dans la stabilisation du caillot (voir **Publication 3**).

C. Fibrinolyse

La fibrinolyse est le processus physiologique conduisant à la dégradation de la fibrine (Chapin et Hajjar, 2015 ; Gale, 2011 ; Mackie et Bull, 1989). Les principaux activateurs de ce processus sont les activateurs du plasminogène tissulaire (tPA) et de l'urokinase (uPA). Le tPA est sécrété dans la circulation sanguine par l'endothélium vasculaire au cours d'un processus d'inflammation, d'une stase sanguine et d'états pathologiques supplémentaires. L'uPA est sécrétée par les monocytes, les macrophages et l'épithélium urinaire (Chapin et Hajjar, 2015). Les deux activateurs du plasminogène ont de courtes demi-vies de 4 à 8 minutes dans la circulation en raison d'une concentration élevée d'inhibiteurs présents dans le plasma, notamment la α2-antiplasmine, la α1-antitrypsine et l'inhibiteur de l'activateur du plasminogène-1 (Rijken et Lijnen, 2009). Le tPA et uPA forment un complexe avec le plasminogène à la surface de la fibrine (Ilich et al., 2017) induisant son clivage pour générer la plasmine, qui est l'acteur majeur de la fibrinolyse (Cesarman-Maus et Hajjar, 2005). Le plasminogène est une protéine de 92 kDa qui circule dans le sang à une concentration de 200 mg/L (2 μM) (Keragala et Medcalf, 2021). Le plasminogène s'associe au fibrinogène, par conséquent, lorsqu'un caillot riche en fibrine se forme, le plasminogène est déjà présent à l'intérieur du caillot où il est nécessaire pour former la plasmine (Mosesson, 2005). La plasmine est régulée positivement par le FXIIa de la voie de coagulation par contact et régulée négativement par l'inhibiteur de fibrinolyse activé par la thrombine (TAFI) (**Figure 13**). TAFI est une protéase qui est activée par la thrombine et élimine les résidus de lysine et d'arginine C-terminaux sur la fibrine, entraînant une diminution du nombre de sites de liaison au plasminogène (Sillen et Declerck, 2021). La plasmine clive les polymères de fibrine aux deux extrémités de la chaîne α, libérant ainsi des fragments αC qui forment le fragment X - un produit de dégradation de poids moléculaire élevé (Mutch et al., 2003). Ce fragment peut être à nouveau polymérisé par la thrombine ou dégradé en fragments D et E qui sont inhibiteurs de la

polymérisation du monomère de fibrine (Lane et al., 1978). Le fragment D de deux molécules de fibrine liées l'une à l'autre est appelé D-dimères et est un indicateur de la coagulation intravasculaire en cours (Bailey et al., 1951 ; Tripodi, 2011).

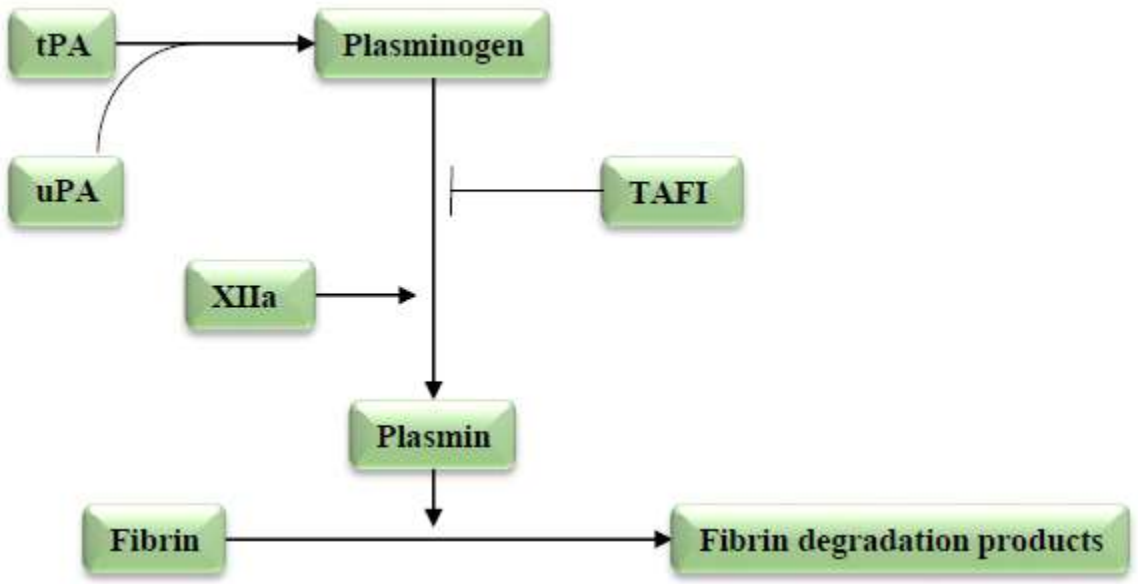

Figure 13: Cascade fibrinolytique schématique. Les flèches indiquent la stimulation et l'activation, et la barre à la fin d'une ligne indique un inhibiteur. TAFI, inhibiteur de fibrinolyse activable par la thrombine ; t-PA, activateur du plasminogène de type tissulaire ; u-PA, activateur du plasminogène de l'urokinase (Adapté de (Meltzer et al., 2009)).

II. Arterial thrombosis

Arterial thrombosis is a pathological process taking place in a diseased vessel after erosion or rupture of an evolved atherosclerotic plaque (Lippi et al., 2011). The thrombus forming on the injured plaque is mainly composed of platelets and fibrin and can lead to the obstruction of a vessel resulting in a reduction in blood supply for downstream tissues (Kurihara et al., 2021), and as a consequence tissue necrosis and a high mortality rate (Leadley et al., 2000). According to statistics, Cardiovascular Diseases are the most common underlying cause of death in the world. In 2018, they accounted for an estimated 30.9% (95% uncertainty interval, 30.3%–32.9%) of all global deaths (Virani et al., 2021).

Arterial thrombosis is the final complication of a chronic vascular disease named atherosclerosis (**Figure 14**).

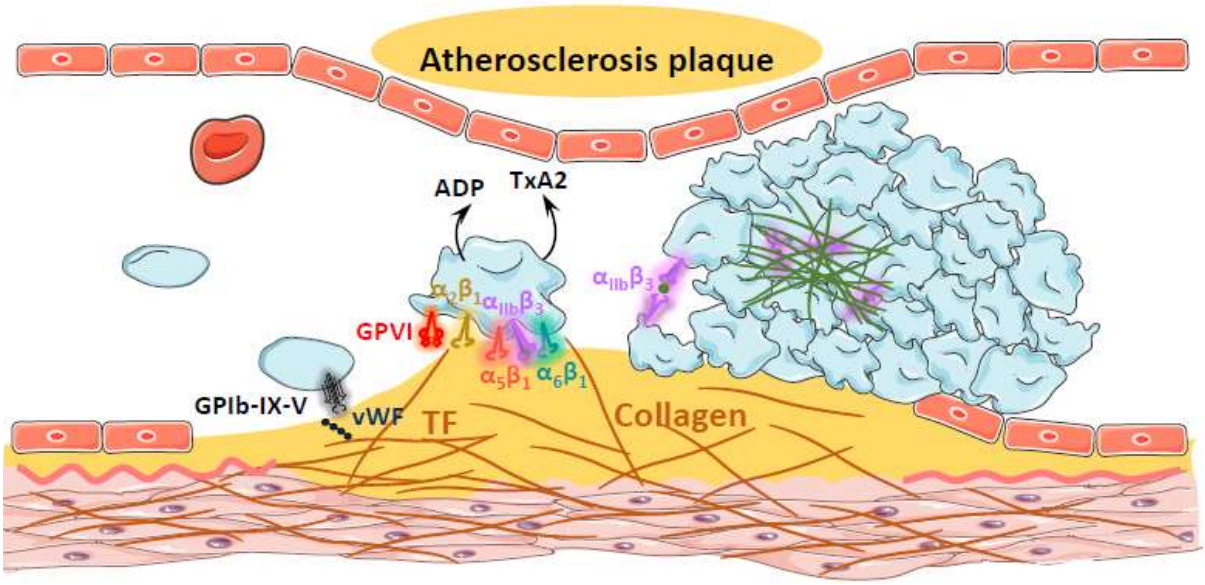

Figure 14: The molecular mechanisms of atherothrombosis. ADP, adenosine diphosphate; vWF, von Willebrand factor; GP, glycoprotein complex; TF, tissue factor; TxA2, thromboxane A2.

1. Pathophysiology of atherothrombosis

1.1. From atherosclerosis to atherothrombosis

Atherosclerosis is a progressive vascular inflammatory disease resulting in the accumulation of lipids in the arterial vessel wall and the formation of an atherosclerotic plaque narrowing the blood vessel lumen (Mackman, 2008). In humans, atherosclerotic plaques are usually found in the aorta, coronary, carotid and cerebral arteries (Lusis, 2000). An evolved plaque can be stable for a long time, and suddenly rupture under the effect of blood flow forces thereby precipitating thrombus formation (Emini Veseli et al., 2017). Ruptured plaque exposes to the blood stream a highly thrombogenic surface containing TF and collagen that initiates thrombus growth (Toschi et al., 1997; van Zanten et al., 1994).

1.2.The process of atherosclerosis

The process of atherosclerotic plaque formation is initiated by high plasma levels of low-density lipoprotein (LDL) (Gimbrone and Garcia-Cardena, 2016). LDLs accumulate in the sub-endothelial space of the arterial wall through endocytosis (Libby et al., 2011). There, they are oxidized and initiate an inflammatory response of the endothelial cells which starts to express chemotactic proteins such as monocyte chemoattractant protein-1 (MCP-1), vascular cell adhesion molecule-1 (VCAM-1), E- selectin and P-selectin (Fuster et al., 2012; Tabas et al., 2015). These proteins recruit circulating immune and pro-inflammatory cells, especially monocytes into arterial vessel wall (Galkina and Ley, 2007; Sakakura et al., 2013). Within the vessel wall, the monocytes differentiate into macrophages capable of cholesterol phagocytosis leading to formation of foam cells secreting inflammatory mediators (Libby et al., 2011;

Sakakura et al., 2013). This is followed by the migration of vascular smooth muscle cells (SMCs) from the tunica media to the tunica intima where they proliferate and synthesize components of the extracellular matrix such as collagen and elastin that form the fibrous cap covering and stabilizing the plaque (Fuster et al., 2012). Foam cells and SMCs in the center of the plaque undergo apoptosis and necrosis inducing the release of oxidized LDL and generating a cholesterol-rich area called the lipid core or necrotic core plaque (Libby et al., 2011). If the plaque contains a limited amount of lipids and is covered by a thick fibrous cap, it represents a "stable plaque" and its probability to rupture is low (Finn et al., 2010). In contrast, if the plaque has a lipid-reach core covered by a weakened fibrous cap, it is considered as a "vulnerable plaque" and its probability to erode or rupture is very high (**Figure 15**) (Tomaniak et al., 2020).

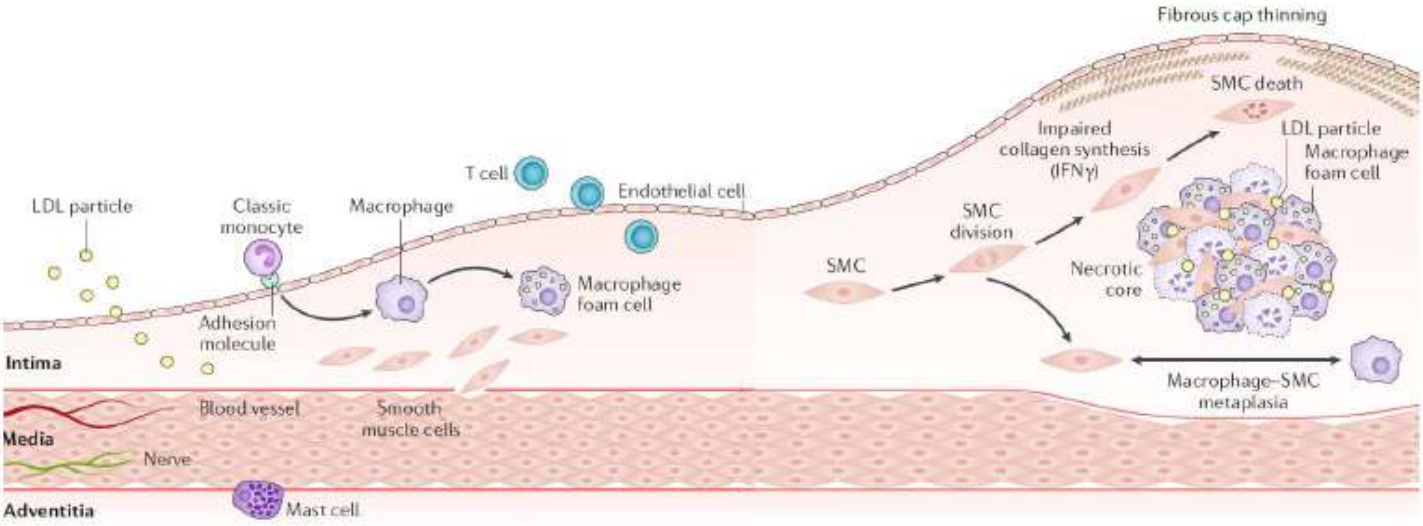

Figure 15: The mechanism of atherothrombosis. LDL, low density lipoprotein; SMC, smooth muscle cells (Adapted from (Libby et al., 2019)).

2. Treatment of arterial thrombosis

The management of arterial thrombosis depends on its severity and the affected artery. The therapy usually consists in pharmacological treatment which can be combined to an endovascular approach with the aim to restore normal circulation and prevent thrombus regrowth. The endovascular approach is usually an angioplasty consisting in the introduction of a catheter in an artery of the arm or a leg which is guided to the blocked artery (Kerzmann et al., 2018; Sorini Dini et al., 2019). This catheter has a small balloon on its tip whose inflation dilates the artery, crushing the atherosclerotic plaque. This procedure can be accompanied by the placement of a stent that keeps the vessel open and helps restore normal blood flow (Mehta et al., 2016).

Concerning the pharmacological treatment, it mainly relies on antiplatelet agents, anticoagulants or fibrinolytic agents (**Figure 16**).

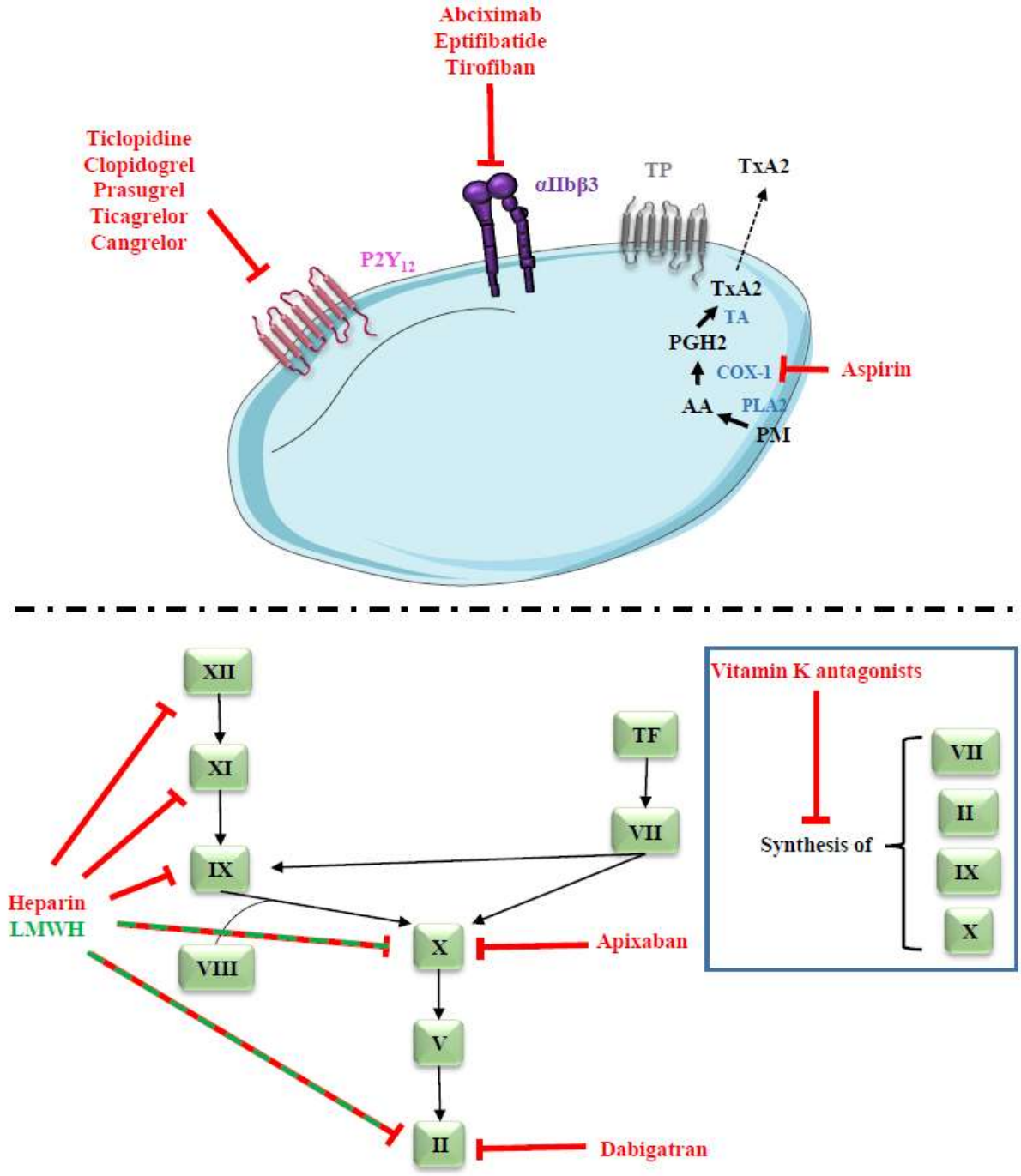

Figure 16: Pharmacological treatment of arterial thrombosis. AA, arachidonic acid; COX-1, cyclooxygenase-1; LMWH, low molecular weight heparin; PGH2, prostaglandin H2; PLA2, phospholipase A2; PM, membrane phospholipids; TA, thromboxane A2 synthase; TF, tissue factor; TP, thromboxane receptor; TxA2, thromboxane A2.

2.1. Pharmacological treatment of arterial thrombosis

2.1.1. Aspirin

The first anti-platelet agent identified and still widely used in clinics is aspirin. It irreversibly inhibits cyclooxygenase-1 (COX-1) in platelets by acetylation of a serine residue within its catalytic pocket (Finamore et al., 2019). This leads to prevention of the arachidonic acid transformation to prostaglandins impairing/limiting TxA2 formation and the subsequent platelet activation through TP receptors (Awtry and Loscalzo, 2000). Aspirin is generally used orally at a dose of 75-100 mg per day in the treatment and secondary prevention of thrombotic cardiovascular diseases such as myocardial infarction and stroke (Johnston et al., 2020). The half-life of aspirin in the bloodstream is 13–19 min after its single oral administration (Ornelas et al., 2017). Aspirin treatment is accompanied by adverse effects including bleeding, which occurs notably at the gastrointestinal level (Lanas et al., 2018).

2.1.2. P2Y12 receptor antagonists

A second class of antiplatelet drugs widely used in arterial thrombosis targets the P2Y12 receptor (Gachet, 2015). Antagonists of this receptor can be divided into two groups based on their mechanism of action: i) prodrugs whose active metabolites inhibit irreversibly the P2Y12 receptor, such as ticlopidine, clopidogrel and prasugrel; ii) direct and reversible inhibitors of the P2Y12 receptor, such as ticagrelor and cangrelor (Secco et al., 2013) (**Table 2**). These antithrombotics are used in the prevention and treatment of thrombotic events such as acute coronary syndrome, stent thrombosis and ischemic stroke (Baqi and Muller, 2019; Lasica et al., 2022; Verheugt et al., 2021). The main limitation of targeting P2Y12 is the risk of bleeding, which increases with the degree of inhibition of the receptor, explaining that the doses used in

the clinic only promote 50–60% inhibition of ADP-induced platelet aggregation (Gachet, 2006; Wallentin, 2009).

Table 2. ADP-P2Y12 inhibitors (Patti et al., 2020; Schneider et al., 2015; Secco et al., 2013)

Title	Structure	Mechanism of action	Administration	Side effects
Ticlopidine	thienopyridine	prodrug, irreversible	the use is discouraged	neutropenia, aplastic anemia, thrombotic thrombocytopenic purpura and gastrointestinal distress
Clopidogrel	thienopyridine	prodrug, irreversible	oral, once daily	dark purple bruise, itching, pain, redness, or swelling
Prasugrel	thienopyridine	prodrug, irreversible	oral, once daily	increased risk of major and life-threatening bleedings
Ticagrelor	cyclo-pentyltriazolopyrimidine	noncompetitive, reversible	oral, twice daily	high rate of major bleedings, bleeding gums, blurred vision, chest pain, tightness, or discomfort, confusion *etc*
Cangrelor	adenosine triphosphate analogue	competitive, reversible	IV, continuous infusion	abdominal or stomach pain, back pain, blood in the eyes, blood in the urine

2.1.3. Dual-antiplatelet therapy

The treatment recommended for secondary prevention of arterial thrombosis and stent thrombosis is based on dual-antiplatelet therapy combining aspirin and a P2Y12 inhibitor (Sharma et al., 2020; Sinnaeve and Adriaenssens, 2021). This dual therapy consisting of aspirin and clopidogrel at 12 months has been reported in the CURE study to reduce cardiovascular events (cardiovascular death, non-fatal myocardial infarction or stroke) more than aspirin alone. It is however, accompanied with an increased risk of major bleeding in patients with acute coronary syndrome (Roberto et al., 2021; Sharma et al., 2020). In the CHARISMA trial the combination of aspirin with clopidogrel is also more effective than clopidogrel alone by reducing the risk of cardiovascular events (Bhatt et al., 2006).

Current recommendations suggest to use the newest P2Y12 inhibitors, prasugrel and ticagrelor. These inhibitors act faster than clopidogrel (30 min vs 2 hours) and lead to lesser high on-treatment residual platelet reactivity (HTPR) (3% vs 30%) (Kamran et al., 2021). In patients with risk of acute coronary syndrome after coronary intervention, the combination of aspirin with prasugrel has been reported to reduce cardiovascular risk further than clopidogrel, with, nevertheless, an increased risk of bleeding (Wiviott et al., 2007). The same result was observed in a study comparing the rate of cardiovascular risk in patients with acute coronary syndrome after a therapy combining ticagrelor and aspirin or clopidogrel and aspirin (Wallentin et al., 2009).

Dual-antiplatelet therapy is not recommended following an ischemic stroke because of the high risk of bleeding (Kamran et al., 2021). In this situation, the combination of platelet aggregation inhibitors amplifies the risk of hemorrhagic transformation which can be fatal for the patient.

2.1.4. Integrin αIIbβ3 blockers

A third class of antiplatelet drugs used in arterial thrombosis targets integrin αIIbβ3 (Huang et al., 2019). There are only three agents inhibiting this integrin approved for clinical use: abciximab, eptifibatide and tirofiban (Giordano et al., 2016). Abciximab (ReoPro) is a Fab fragment of a chimeric monoclonal antibody inhibiting the interaction of αIIbβ3 with fibrinogen (Giordano et al., 2016). Eptifibatide (Integrilin) is a cyclic heptapeptide containing a KGD sequence (Scarborough et al., 1993). Finally, tirofiban (Aggrastat) is a non-peptide antagonist structurally mimicking a RGD sequence (Hartman et al., 1992). These therapeutic agents are administered intravenously in emergency situations such as myocardial infarction or during percutaneous coronary interventions (Jamasbi et al., 2017). The main limitation of anti-αIIbβ3

agents is the risk of bleeding which is higher than for P2Y12 receptor antagonists (Gammie et al., 1998; Junghans et al., 2001; Rasty et al., 2002; Tigen et al., 2021). A new strategy to inhibit αIIbβ3 with a potential lower risk of bleeding is to only target the activated form of αIIbβ3. These agents are promising in pre-clinical studies but have not yet been evaluated in clinic (Hohmann et al., 2013; Huang et al., 2015; Li et al., 2014).

2.1.5. Anticoagulant therapy

Another class of agents targeting arterial thrombosis are anticoagulants which can be divided on their mode of action in: i) heparin and low molecular weight heparins (LMWHs); ii) vitamin K antagonists; iii) direct factor Xa inhibitors and iv) direct thrombin inhibitors (DeWald et al., 2018).

Heparin and LMWHs interact with antithrombin (AT) and catalyze AT-mediated inhibition of thrombin, and factors IXa, Xa, XIa, and XIIa (Garcia et al., 2012). At high doses, heparin catalyzes thrombin inactivation by heparin cofactor II and binds to IXa leading to inhibition of Xa (Hirsh et al., 1995). Heparin equally inhibits the activity of thrombin and Xa while LMWHs efficiently inhibits the activity of Xa compared to thrombin whose inhibition requires the presence of the high affinity pentasaccharide sequence and an oligosaccharide chain with at least 18 units length that is absent in LMWH due to its shortened chain length (Garcia et al., 2012; Lam et al., 1976; Petitou et al., 1999). A potential major side effect of heparin treatment is heparin-induced thrombocytopenia (HIT) which is triggered by the ability of heparin to bind platelet factor 4 (PF4) which is released after platelets activation (Onishi et al., 2016). The heparin/PF4 complex can activate the immune system producing antibodies against the complex activating platelets and monocytes. This leads to TF and procoagulant microparticles releases resulting in facilitating of platelets activation and formation of

aggregates (Marcucci et al., 2021). LMWHs have weaker protein binding capacities and therefore led to a lower rate of HIT (Cosmi et al., 1997). Heparin and LMWHs are used to treat pulmonary embolism, but can also be combined to aspirin in the setting of complications of acute coronary syndrome (myocardial infarction and unstable angina) (Amane and Burte, 2011; Cohen et al., 2014; Undas et al., 2009b).

Another anticoagulant family comprises the vitamin K antagonists. Vitamin K participates in the biosynthesis of several key coagulation factors as a cofactor for their carboxylation in the liver (Dowd et al., 1995). Warfarin, is one of the member of the vitamin K antagonists, and inhibits the C1 subunit of vitamin K leading to distortions of its function in the synthesis of thrombin and factors VII, IX, and X (Stirling, 1995). Therefore, warfarin blocks the generation of coagulation factors but has no impact on circulating factors or pre-existing thrombi. This anticoagulant is used to reduce the risk of recurrent myocardial infarction, systemic embolism after it and stroke (Jones et al., 2021; Mant et al., 2007). The main disadvantage of this agent is its interaction with numerous drugs and food which influences its anticoagulant response (Wells et al., 1994).

Another type of anticoagulants is inhibitors of factor Xa. Apixaban is a direct reversible inhibitor that binds to free and clot-bound factor Xa leading to decrease of thrombin generation (Byon et al., 2019). This anticoagulant is used in the prevention and treatment of thrombotic events such as pulmonary embolism and stroke in patients with non-valvular atrial fibrillation (Cirincione et al., 2018; Halvorsen et al., 2014). Its main limitation is the risk of hemorrhage and thrombocytopenia (Gresham et al., 2009; Harter et al., 2015).

Finally, one of the member of anticoagulants which directly inhibit thrombin is dabigatran. It binds to free and fibrin-bound thrombin (Antonijevic et al., 2017). This anticoagulant is used in the prevention of embolic events in patients with non-valvular atrial fibrillation and with non-hemorrhagic stroke (Connolly et al., 2009; Gomez-Outes et al., 2013).

Possible side effects of dabigatran are gastrointestinal bleeding and intracranial hemorrhage (Eikelboom et al., 2011).

2.1.6. Thrombolytic therapy

The thrombolytic therapy consists in transforming plasminogen into plasmin to promote the degradation of the fibrin clot and restore vessel patency. The clinically used thrombolytic agents includes recombinant forms of tPA (rtPA) and urokinase (Simpson et al., 2006). rtPA is the most widely used pharmacologically approved treatment for acute ischemic stroke (Tsivgoulis et al., 2020). It is used alone or combined with thrombectomy to promote the dissolution of a clot which occludes a cerebral artery (Alberts et al., 2015; Anfray et al., 2021; Frey, 2005). Due to the risk of intracerebral haemorrhage associated with rtPA-mediated thrombolysis, a strict treatment window of up to 4.5 hours post-stroke onset has been applied as a threshold for administration of rtPA (Shobha et al., 2011; Su et al., 2008; Yepes and Lawrence, 2004). rtPA-treated patients have a low recanalization rate of 17% and 38% depending on the vessel (Nichols et al., 2008; Rohan et al., 2014). Side effect rtPA is its ability to induce seizure and excitotoxicity through promoting the activation of N-Methyl-D-Aspartate receptors (NMDAR) (Alvarez et al., 2013; Nicole et al., 2001; Tsirka et al., 1995). Taken together, only a small fraction of stroke patients benefit from thrombolysis with no side effects (National Institute of Neurological and Stroke rt, 1995; Vivien, 2017).

3. Murine models of experimental thrombosis

Models of experimental thrombosis represent unique tools to study the mechanism of thrombus formation *in vivo*, allowing to dissect cellular and molecular events of this complex process. This section is focusing on the *in vivo* models which were used during my PhD studies.

Mouse models are extensively used because of numerous advantages including their high fertility, low cost of breeding and small size (Kohnken et al., 2017). The use of mouse models also allows to study thrombus formation in transgenic mice which were instrumental to better characterize the function of numerous receptors or signaling molecules (Whinna, 2008). A very common approach to induce thrombosis in murine healthy vessels consists in damaging the vessel wall chemically, mechanically, with electricity or a laser (Cooley, 2012; Westrick et al., 2007). Besides their advantages, mouse models have limitations, notably the absence of correlation to any clinical situation as the lesion are performed on healthy vessels in young mice which do not mimic a clinical setting in patients.

3.1. The $FeCl_3$-induced injury model

$FeCl_3$-induced injury is realized by putting a drop or the application of the filter paper with this chemical to the external part of the mouse vessel (**Figure 17**) (Grambow et al., 2020; Zhou et al., 2015). $FeCl_3$ in small vesicles has been shown to cross the endothelium by an endocytic-exocytic pathway and to generate reactive oxygen species which initiates thrombus formation (Kurz et al., 1990; Tseng et al., 2006). Although this thrombosis model is widely used the exact mechanism by which it triggers thrombosis is still not fully understood. In some studies, the generation of reactive oxygen species triggers the denudation of endothelial cells and the exposure of the subendothelium matrix (Dubois et al., 2006; Westrick et al., 2007; Woollard et al., 2009). In other studies, $FeCl_3$ damages the vessel wall but the endothelial denudation is absent (Barr et al., 2013; Eckly et al., 2011). In this case the mechanism initiating the thrombus formation is unclear. One hypothesis is that RBC-derived structures recruit platelets and this process initiates thrombus formation. Another hypothesis is that $FeCl_3$ bodies exposed on the injured vessel wall to the blood flow contain large amounts of tissue factor on

their surface that could support thrombus formation by generating thrombin (Eckly et al., 2011). These different outcomes probably depend on the vessel type to which $FeCl_3$ is applied (Chauhan et al., 2007; Konstantinides et al., 2006).

The technical simplicity of this model allows to target any mouse vessel (especially, the mesenteric, cremaster or carotid vessels), and resulted in a broad use in our research field. The level of thrombus formation depends on the concentration of $FeCl_3$, application time and the injury size which could result in the formation of occlusive or non-occlusive thrombi (Eckly et al., 2011; Kurz et al., 1990). The recording of thrombus formation can be done in real time by visualizing platelet accumulation with fluorescent microscopy (and another thrombus components if it is necessary) or by measuring the blood flow with a Doppler probe (Denis et al., 1998; Fay et al., 1999).

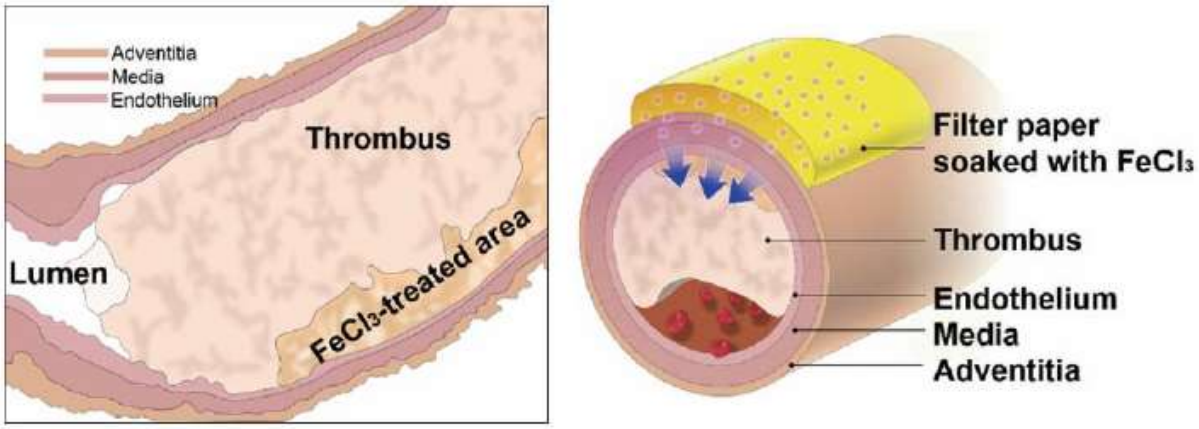

Figure 17: $FeCl_3$-induced model of arterial thrombosis. (Figure from (Shim et al., 2021)).

3.2. The laser-induced injury model

Laser-induced injury is realized with the pulsed, high power laser focused on a small tissue volume with minimum damaging of surrounding tissue due to the microscope optics

(**Figure 18**) (Stalker, 2020). This type of injury includes thermal and mechanical damages. The laser beam superheats the tissue or cells which are further destroyed by mechanical forces created by cavitation bubble formation (Dubois et al., 2007; Falati et al., 2002; Rau et al., 2006; Vogel and Venugopalan, 2003). As a result, laser injury is a mechanical injury, but subsequent physical rupture of cells or tissue has additional biochemical effects. The level of laser injury depends on its wavelength, pulse duration, pulse energy and beam diameter (Ando et al., 2011; Larsson et al., 2022). In our laboratory we showed that minimal laser ablation induces endothelial cell denudation, while strong laser ablation leads to the disruption of all vessel wall layers (Hechler et al., 2010). However, depending on the laser intensity and studied vessel different levels of injury could be induced: endothelial cell denudation when thrombus formation is induced by subendothelium matrix and activation of endothelial cells without denudation (Atkinson et al., 2010). Because of the thickness of many vessel walls and the presence of fat in surrounding tissue which absorbed laser energy, a main limitation of this murine thrombosis model is that not every vessel can be targeted. This model is currently mainly used in small murine vessels: mesenteric arterioles, ear microcirculation and the cremaster muscle microcirculation (Dubois et al., 2006; Falati et al., 2002; Falati et al., 2004; Hechler et al., 2003; Nonne et al., 2005; Stalker, 2020). The thrombus formation in laser-induced model is studied in real time by using brightfield and/or fluorescence imaging (Dubois et al., 2007; Stalker et al., 2013).

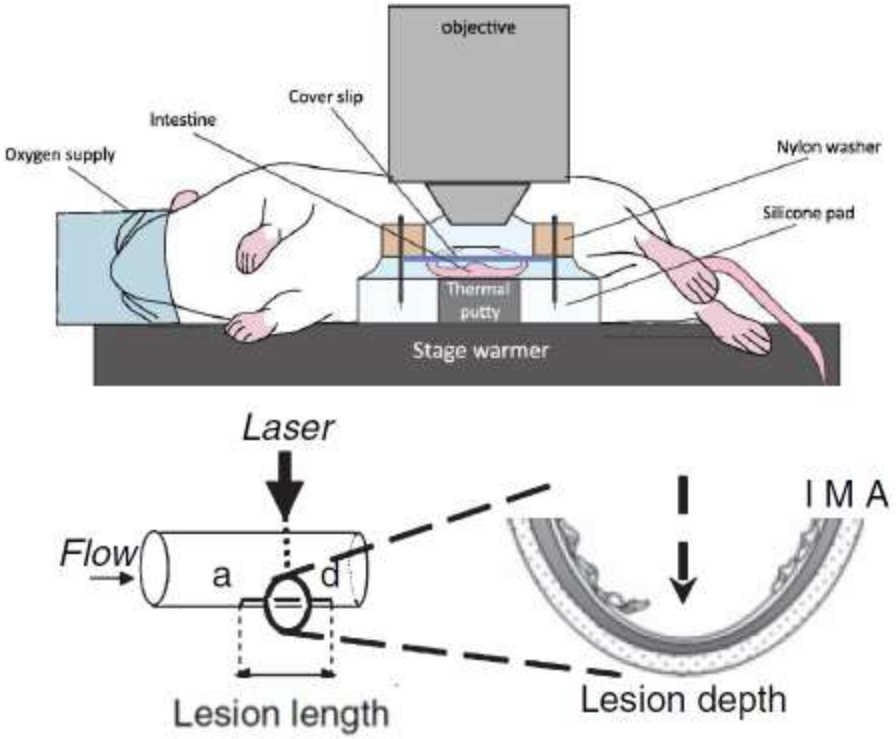

Figure 18: Laser-induced model of arterial thrombosis. (Figure from (Hechler et al., 2010; Kolesnikov et al., 2015)).

3.3. The electrolytic injury model

Electrolytic injury is generated by an electrical current delivery through a probe to the vessel that is often also subjected to a stasis mediated with a hemostatic clamp (**Figure 19**) (Sturgeon et al., 2006). This type of injury leads to a damage of the intima, the extent of which appears to be controlled by regulation of the voltage of the stimulation current and by application time. This model is currently used in carotid artery and results mostly in occlusive thrombus formation (Aleman et al., 2013; Hughan et al., 2014; Schoenwaelder et al., 2017). The electrolytic injury model is not widely used to study the mechanism of arterial thrombosis because the level of damage is extremely high. Thrombus formation in electrolytic injury models is studied in real time by using brightfield imaging or by measuring the flow with a Doppler probe (Kusada et al., 2007; Mangin et al., 2006).

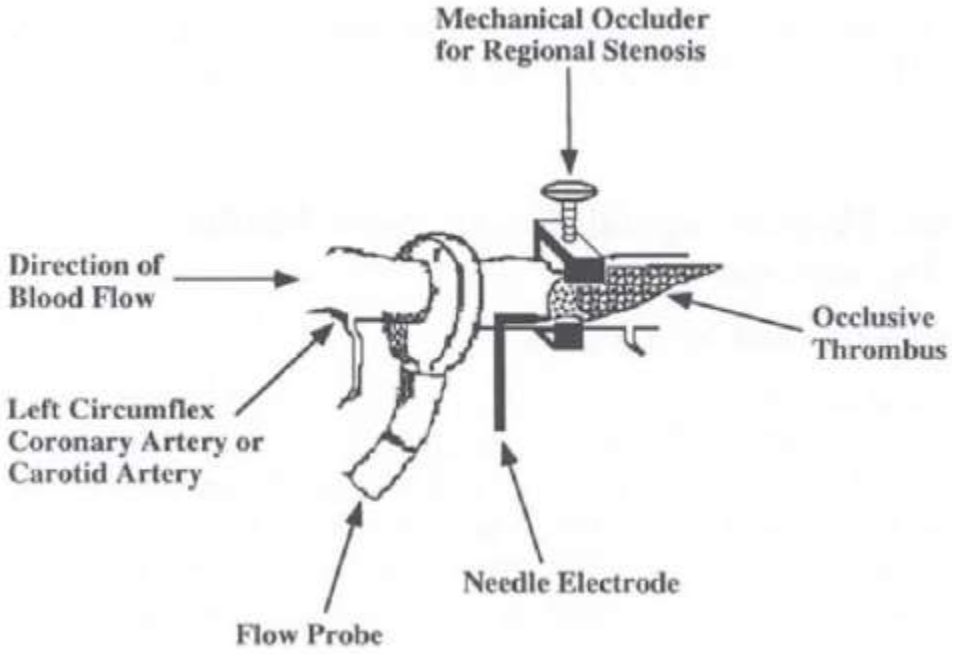

Figure 19: Electrolytic model of arterial thrombosis. (Figure from (Huang et al., 2000)).

3.4. The mechanical injury model

Mechanical injury is generated by forceps compression of the vessel which can sometimes be coupled to concentric vessel stenosis (Folts-like method) (**Figure 20**) (Westrick et al., 2007). This type of injury leads to the deformation or detachment of the endothelium depending on compression by the forceps jaws or application time (Tang et al., 2016). Two levels of injuries were reported with a moderate injury corresponding to the deformation of the endothelium but not a complete detachment, while the severe injury promotes denudation and breakage of the internal elastic lamina (Tang et al., 2016). This model is used in the carotid artery, aorta and femoral vein (Gruner et al., 2005; Pierangeli et al., 1995; Pozgajova et al., 2006). Thrombus formation in mechanical injury models is studied in real time by using fluorescent imaging or by measuring the flow with a Doppler probe (Mangin et al., 2006;

Mangin et al., 2012). The main limitation of this model is that it is operator-dependent and requires skills and a lot of practice (Tang et al., 2016).

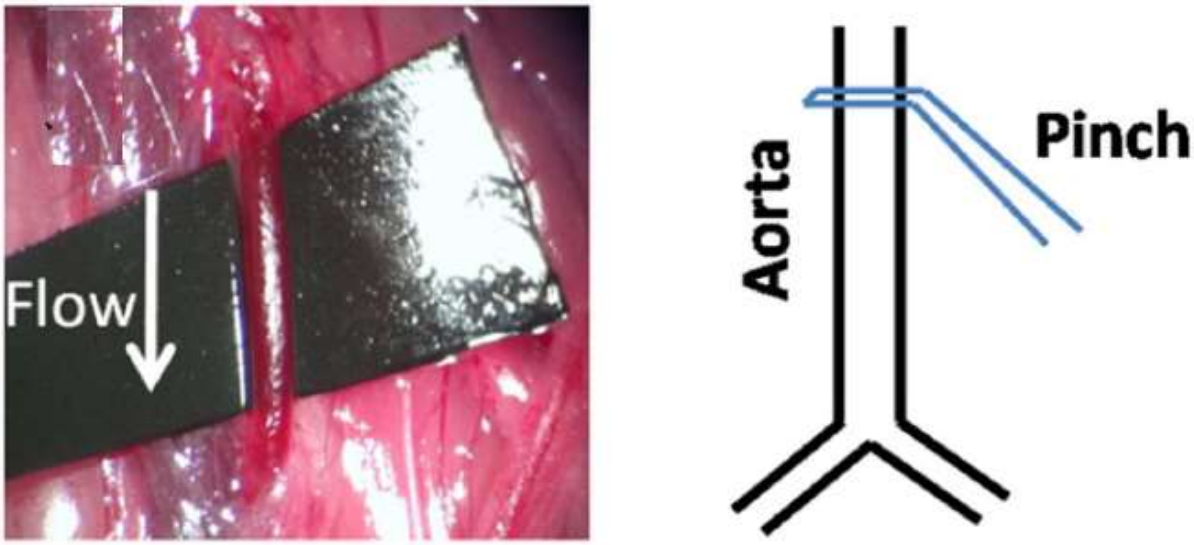

Figure 20: Mechanical model of arterial thrombosis. The injury was induced by using the forceps to pinch the aorta (Figure from (Tang et al., 2016)).

III. The role of blood flow in hemostasis and arterial thrombosis

In the 1,800s the physician Rudolf Virchow described three key features of intravascular venous thrombosis, which later became known as Virchow's Triad: stagnant flow, hypercoagulability and endothelial injury (Bagot and Arya, 2008). Later, this concept was expanded to recognize the importance of blood flow in the regulation of hemostasis and arterial thrombosis (Sakariassen et al., 2015; Storch et al., 2018). The importance of flow in thrombosis is notably evidenced by the impact of the flow regime on thrombus composition. Indeed, arterial thrombi formed under high flow velocities are rich in platelets and fibrin, while venous thrombi formed under lower flow velocities and are rich in RBC and fibrin (Baumgartner, 1973).

1. Rheology applicable to blood flow

Blood is a viscous fluid which consists of a liquid fraction – plasma – and a cellular fraction – cells: platelets, red blood cells (RBCs) and leukocytes (Sweeney, 2008). Blood cells tend to move towards the streamlines of higher velocities, *i.e.* towards the center of the lumen with gravity having only a negligible effect on their motion in bloodstream. RBC are the dominant part of blood cellular mass and are usually localized in the center of bloodstream where they push other cells towards the walls, a process called margination (Basmadjian, 1990; Goldsmith and Turitto, 1986). This lateral migration creates a layer of platelets and white blood cells (WBC) near the vessel wall in the so-called cell-free layer (Aarts et al., 1988; Czaja et al., 2020; Eckstein et al., 1988).

1.1. Concept of blood flow motion

For simplification blood is usually considered as an incompressible fluid with a constant viscosity, named Newtonian fluid. The blood movement through a cylindrical tube is considered as a Poiseuille flow, which means that it relies on a pressure difference created by the heart. Blood flowing through a cylindrical tube has a parabolic velocity profile with a maximal velocity in the center that decreases towards the wall (**Figure 21**) (Ruggeri, 2009). Therefore, blood flow is modelled as a series of adjacent layers sliding smoothly one over another, which creates a friction called shear. Due to the parabolic profile of velocities the flow near the vessel wall being close to zero, it facilitates the initiation of coagulation reaction as well as platelet adhesion (Hathcock, 2006).

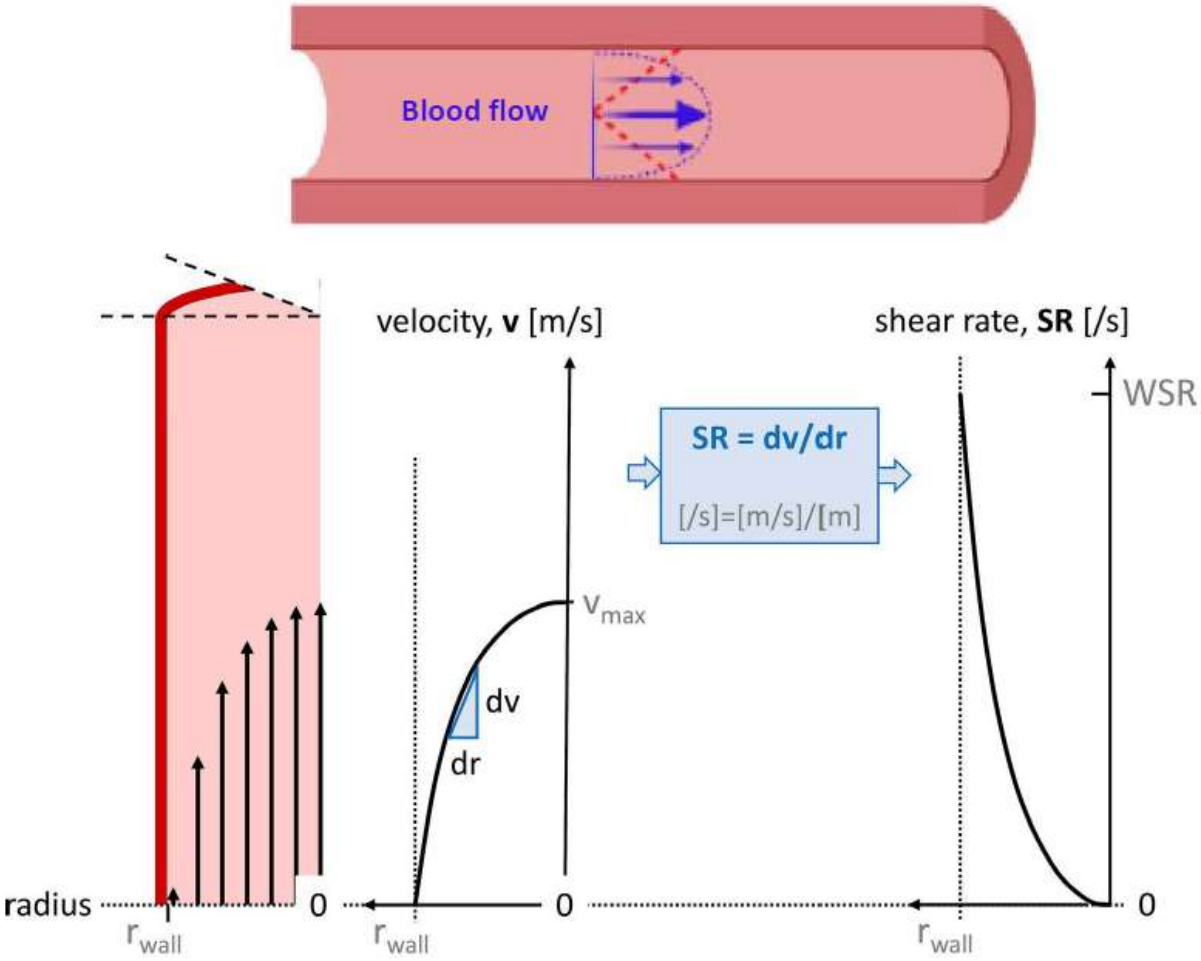

Figure 21: Blood flow rheology. The blood vessel section illustrates a typical flow profile through a vessel. The arrows indicate blood velocity along the radius. (Figure from (Panteleev et al., 2021)).

Although, blood is usually described as a Newtonian fluid, in reality, it is non-Newtonian because under low flow its viscosity depends on the hematocrit which decreases exponentially with increasing blood flow (Goldsmith and Turitto, 1986; Schmid-Schonbein et al., 1981). As a consequence, blood exhibits non-Newtonian behaviors such as shear thinning, yield stress and viscoelasticity (Fisher and Rossmann, 2009; Gijsen et al., 1999; Merrill et al., 1963; Thurston, 1972). These properties affect the blood movement inside the vessel, fluid transport and blood force acting on vessel walls and surrounding tissues especially in paths with irregular lumen geometry or stenosed arteries (Liu and Tang, 2011; Lou and Yang, 1993). Another important parameter to consider is the pulsatile nature of arterial flow which ranges from 0 (or even reversed flow) up to two times the average velocity during each cyclic period (Rhode et al., 2005). Taking into account the pulsatility, the peak blood flow parameters exceed the values of blood flow regimes calculated for non-Newtonian fluid (Lutz et al., 1983).

1.2.Shear rate and shear stress as major hemodynamic parameters

A key parameter to define blood flowing in different vessels is the shear rate (γ). It is used to characterize the rate at which one fluid layer passes over another. For a Poiseuille flow, the wall shear rate increases linearly with a volume velocity (Q) and decreases as the inverse cube of tube radius (R) (1):

$$\gamma = \frac{4Q}{\pi R^3} \quad (1)$$

For healthy human vessels the mean wall shear rates are 450–2,000 s^{-1} in the microcirculation and in arterioles, 300–800 s^{-1} in the large arteries and 15–200 s^{-1} in veins (**Table 3**) (Goldsmith and Turitto, 1986; Nader et al., 2019; Panteleev et al., 2021). Of note, these values are mean wall shear rates and they can vary in arteries due to pulsatile flow.

Table 3. Time-average values of shear rate within the human vasculature vessel (Hathcock, 2006)

Vessel	Diameter, mm	Shear rate, s^{-1}
Ascending aorta	23-45	50-300
Femoral artery	5	300
Common carotid artery	5.9	250
Left main coronary artery	4	460
Small arteries	0.3	1,500
Arterioles	0.03	1,900
Large veins	5-10	200
Inferior vena cava	20	40-60

Blood flow is creating a tangential force between fluid layers called shear stress (τ) which linearly depends on shear rate with a proportionality constant called viscosity (η) (2) (Benis et al., 1971):

$$\tau = \eta \cdot \gamma \quad (2)$$

Shear stress and shear rate regulate receptor-ligand bond formation during the initial step of platelet adhesion at the site of injury.

2. Role of blood flow in thrombus formation

The process of platelet aggregate formation in thrombosis and hemostasis shows a high degree of similarity. Following vascular injury, platelets carried by flow adhere, become activated and aggregate. In parallel, the coagulation cascade becomes activated leading to the generation of thrombin and to the formation of fibrin insoluble network. Blood flow affects

every step of this process (Savage et al., 1998; Weiss et al., 1978). First, the flow has an impact on the ability of platelet receptors to engage their ligands immobilized at site of injury. While under relatively low shear (< 900 s^{-1}) almost all the adhesive receptors can bind their ligands to ensure the capture of flowing platelets, under high shear only the GPIb-IX complex has the potential to sustain platelet attachment through its interaction with vWF (Maxwell et al., 2007; Turitto et al., 1984). Once platelets have adhered, hemodynamic forces can stimulate mechano-sensors, such as the GPIb-IX complex and integrin αIIbβ3, mechano-receptor Piezo1 and mechano-sensitive ion channels TRPV2 and TRPV4, to initiate signal transduction and subsequent platelet activation (Abbonante et al., 2017; Chen et al., 2019; Li et al., 2021; Mazzucato et al., 2002; Shen et al., 2013; Zhao et al., 2021). Moreover, once the aggregate is formed, the shear forces tend to disrupt the receptor/ligand and/or receptor/receptor bonds and thereby promote thrombus instability and platelet disaggregation. Finally, the amplification of platelet activation by soluble agonists, such as ADP, TxA2 or thrombin, is finely tuned by the flow which carries away those released by activated platelets at site of thrombus formation to avoid excessive thrombus growth at site of vascular injury.

2.1. vWF, a shear sensitive molecule

vWF is a multimeric plasma glycoprotein which is synthesized by endothelial cells and megakaryocytes (Jaffe et al., 1974; Sporn et al., 1985). It is also stored in the platelet α granules and becomes released after platelet activation (Mumford et al., 2015). vWF is composed of several domains: i) the A1 domain which binds GPIbα and type IV collagen, ii) the A2 domain, site of cleavage of the vWF by A Desintegrin and Metalloproteinase with ThromboSpondin type 1 repeat 13 (ADAMTS13) which reduces the size and reactivity of circulating multimers,

iii) the A3 domain binding site of type I and III subendothelial collagen, iv) the C4 domain which binds the integrin αIIbβ3 and v) the D3 domain which binds FVIII (Brehm, 2017).

Under low shear rates, this protein has a closed globular conformation hiding a cryptic binding site in the A1 domain, and therefore preventing its accessibility to the GPIb-IX complex (De Luca et al., 2000; Di Stasio and De Cristofaro, 2010; Ulrichts et al., 2005). Under high shear rates (> 5,000 s^{-1}) or when immobilized on a surface in the presence of low shear, vWF stretches due to the hydrodynamic force and exposes the A1 domain allowing platelet adhesion through the GPIb-IX complex (Alexander-Katz et al., 2006; Li et al., 2008; Shankaran et al., 2003; Springer, 2014).

2.2. Platelet aggregation under pathological conditions

In diseased arteries with a thickening of the wall due to an evolved atherosclerotic plaque or a pre-existing thrombus, the irregular vessel geometry leads to generation of flow perturbations (**Figure 22**) (Glagov et al., 1988; Young and Tsai, 1973). For example, blood flowing through a stenosed vessel generates i) flow acceleration in the pre-stenotic area, ii) high shear exceeding 45,000 s^{-1} in the stenosis throat and iii) regions of flow recirculation in the post-stenotic zone (Bark and Ku, 2010). In the pre-stenotic region, acceleration of the blood flow generates elongational flows and shear gradients which facilitate vWF unfolding that exposes the A1 domain and can promote platelet aggregation (Sing and Alexander-Katz, 2010). Concerning the apex of the stenosis, the shear exceeds threshold values of 5,000 s^{-1} and can also unfold circulating vWF (Kroll et al., 1996). Finally, in the post-stenotic zone, the recirculation flows have been shown to be highly prothrombotic in *in vitro* and *in vivo* models. This effect is likely explained by the accumulation of soluble activators and platelets which are not washed away and can more easily accumulate (Jackson et al., 2009).

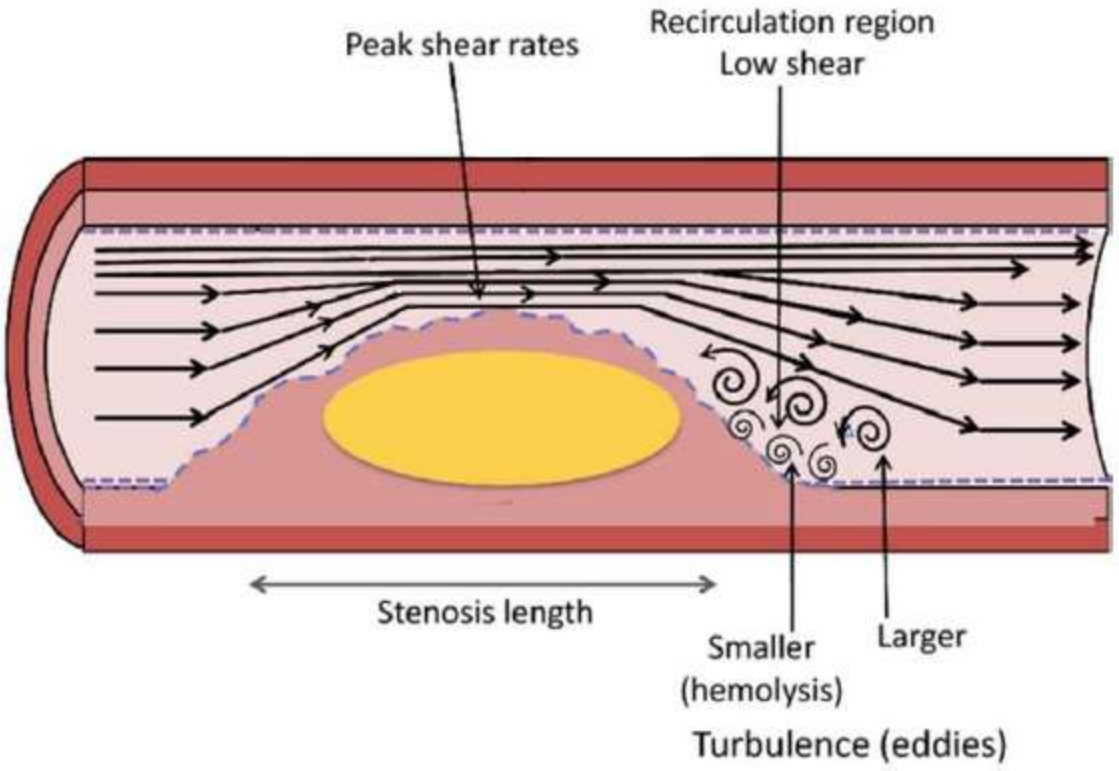

Figure 22: Pathological blood flow condition. The blood vessel section illustrates a typical flow profile through a diseased vessel. The arrows indicate blood velocity along the radius. (Figure from (Gorog and Jeong, 2015)).

3. Shear-selective therapy

Shear-selective anti-platelet therapies have been proposed as an innovative treatment to prevent pathological thrombus formation while only modestly increasing the risk of bleeding. Two approaches to block high shear-mediated thrombosis were proposed. One is focusing on inhibition of the shear-driven interaction between the vWF A1 domain and GPIbα (a single-chain antibody scFv-A1) (Hoefer et al., 2021). The second approach is based on shear-sensitive vehicles or nanoparticles aggregates with anti-thrombotic agents which release their contents

only under high shear rates (Holme et al., 2012; Korin et al., 2012; Marosfoi et al., 2015; Molloy et al., 2017).

Results

Blood flow conditions taking place at the edge of the wound after traumatic injury of the vessel

Publication 1:

« Traumatic vessel injuries initiating hemostasis generate high shear conditions»

Alexandra Yakusheva[1-3], Kirill Butov[2-4], Georgii Bykov[2], Gábor Závodszky[6], Anita Eckly[1], Fazly Ataullakhanov[2,3,5], Christian Gachet[1], Mikhail Panteleev[#2,3,5], Pierre H Mangin[#1]

[1]Université de Strasbourg, INSERM, EFS Grand-Est, BPPS UMR-S1255, FMTS, F-67065 Strasbourg, France;
[2]Center for Theoretical Problems of Physicochemical Pharmacology, Moscow 119991, Russia;
[3]Federal Research and Clinical Centre of Pediatric Hematology, Oncology and Immunology, Moscow 117198, Russia;
[4]Molecular Biology and Biotechnology Department, Pirogov Russian National Research Medical University, Ministry of Healthcare of the Russian Federation, Moscow 117997, Russia;
[5]Faculty of Physics, Moscow State University, Moscow 119991, Russia;
[6]Computational Science Lab, Faculty of Science, Institute for Informatics, University of Amsterdam, Amsterdam, The Netherlands.

[#]These authors contributed equally to this work.

Blood Adv. 2022 Jun 21. doi: 10.1182/bloodadvances.2022007550

Introduction

The parameter most commonly used to characterize blood flow is the shear rate, which describes the rate at which one fluid layer passes over another and estimates the velocity change in the direction perpendicular to the flow. The current view is that low and intermediate flows (50 s^{-1}, 500 s^{-1}) occur in intact healthy vessels, while high shear levels (>2,000 s^{-1}) are reached in stenosed arteries, notably during thrombosis (Goldsmith and Turitto, 1986; Panteleev et al., 2021). High shear found at the apex of a plaque believed to be a specific feature of thrombosis. It has been proposed that targeting high shear through the inhibition of the shear gradient specific conformation of VWF or by shear-sensitive vehicles of anti-thrombotic agents represents an innovative strategy to selectively block thrombosis with a minor impact on hemostasis, thereby potentially avoiding bleeding complications (Hoefer et al., 2021; Korin et al., 2012). While the range of physiological wall shear rates values is well established in intact vessels, the shear rates occurring at the edge of a lesion in a healthy vessel remain unknown.

The objective of my first project was to measure the blood flow occurring in wounds after different types of vessel injuries in a context relevant to hemostasis in human and mice. For this purpose, we developed two novel mouse models of hemostasis in distinct vessels (carotid artery, aorta, saphenous vein and spermatic artery) which represent the two basic scenarios of traumatic injury, *i.e.* vessel puncture or vessel transection. The lesions and the plugs forming in these models were characterized by fluorescence and scanning electron microscopies. Combining Doppler probe measurements and computations, we determined the variation of blood flow over time after vessel damage. On the basis of the flows and the size of the injury measured experimentally, the shear rate at the edge of the wound was calculated using Navier-Stokes equations and ComSol Multiphysics software. An original model was also developed in humans, based on measurement of the blood loss after injury of the median cubital vein. A puncture was created by inserting a catheter into the cubital vein of healthy human

volunteers and the blood loss was measured every minute after injury to calculate the shear levels by applying Poiseuille's equation with volumetric rates of blood loss. This work has been published in *Blood Advances* in June 2022.

REGULAR ARTICLE

blood advances

Traumatic vessel injuries initiating hemostasis generate high shear conditions

Alexandra A. Yakusheva,[1-3] Kirill R. Butov,[2-4] Georgii A. Bykov,[2,5] Gábor Závodszky,[6] Anita Eckly,[1] Fazly I. Ataullakhanov,[2,3,5] Christian Gachet,[1] Mikhail A. Panteleev,[2,3,5,*] and Pierre H. Mangin[1,*]

[1]Université de Strasbourg, INSERM, EFS Grand-Est, BPPS UMR-S1255, FMTS, Strasbourg, France; [2]Center for Theoretical Problems of Physicochemical Pharmacology, Moscow, Russia; [3]Federal Research and Clinical Centre of Pediatric Hematology, Oncology and Immunology, Moscow, Russia; [4]Molecular Biology and Biotechnology Department, Pirogov Russian National Research Medical University, Ministry of Healthcare of the Russian Federation, Moscow, Russia; [5]Faculty of Physics, Moscow State University, Moscow, Russia; and [6]Computational Science Laboratory, Faculty of Science, Institute for Informatics, University of Amsterdam, Amsterdam, The Netherlands

Key Points

- Various types of lesions in small and large mouse and human vessels result in high shear rates and elongational flows.
- The relative hydrodynamic resistance of the vessel and wound explains a decrease in shear rate with increase in injury size.

Blood flow is a major regulator of hemostasis and arterial thrombosis. The current view is that low and intermediate flows occur in intact healthy vessels, whereas high shear levels (>2000 s^{-1}) are reached in stenosed arteries, notably during thrombosis. To date, the shear rates occurring at the edge of a lesion in an otherwise healthy vessel are nevertheless unknown. The aim of this work was to measure the shear rates prevailing in wounds in a context relevant to hemostasis. Three models of vessel puncture and transection were developed and characterized for a study that was implemented in mice and humans. Doppler probe measurements supplemented by a computational model revealed that shear rates at the edge of a wound reached high values, with medians of 22 000 s^{-1}, 25 000 s^{-1}, and 7000 s^{-1} after puncture of the murine carotid artery, aorta, or saphenous vein, respectively. Similar shear levels were observed after transection of the mouse spermatic artery. These results were confirmed in a human venous puncture model, where shear rates in a catheter implanted in the cubital vein reached 2000 to 27 000 s^{-1}. In all models, the high shear conditions were accompanied by elevated levels of elongational flow exceeding 1000 s^{-1}. In the puncture model, the shear rates decreased steeply with increasing injury size. This phenomenon could be explained by the low hydrodynamic resistance of the injuries as compared with that of the downstream vessel network. These findings show that high shear rates (>3000 s^{-1}) are relevant to hemostasis and not exclusive to arterial thrombosis.

Introduction

Rheology plays a central role in the regulation of the cellular and molecular processes of hemostasis. First of all, it regulates receptor-ligand bond formation during the initial step of platelet adhesion at the site of injury.[1] Once platelets have adhered, hemodynamic forces stimulate their mechano-receptors to activate them.[2-4] The activation is strengthened by soluble agonists released by the platelets,[5,6] such as ADP, ATP and TxA2, and also by thrombin, the end-product of coagulation. This amplification of platelet activation is crucial in hemostasis, and it is finely tuned by the flow, which carries away the soluble agonists.[7,8]

Submitted 11 March 2022; accepted 10 June 2022; prepublished online on *Blood Advances* First Edition 21 June 2022; final version published online 18 August 2022. DOI 10.1182/bloodadvances.2022007550.

*M.A.P. and P.H.M. are joint senior authors.

The full-text version of this article contains a data supplement.

Contact the corresponding author for data sharing: mapanteleev@yandex.ru.

The parameter most commonly used to characterize blood flow is the shear rate, which describes the rate at which one fluid layer passes over another and estimates the velocity change in the direction perpendicular to the flow. Modification of the geometry of a vessel results in elongational flow, which represents the rate of velocity change in the direction parallel to the flow. Both shear rate and elongational flow influence hemostasis when they reach critical levels, notably by activating von Willebrand factor (vWF). Indeed, elongational flow above 300 s^{-1} or shear rates exceeding 5000 s^{-1} can unfold circulating vWF to expose cryptic sites and allow its adhesion to platelets through their membrane GPIb-IX-V complex.[9-11]

Disturbed flow has long been recognized as a major mediator of arterial thrombosis. The presence of an evolved atherosclerotic plaque profoundly modifies the local geometry and generates prothrombogenic flows,[12] including (i) flow acceleration with elongational flows in the prestenotic area,[13] (ii) high shear exceeding 45 000 s^{-1} in the stenosis throat,[14] and (iii) regions of flow recirculation in the poststenotic zone.[15-17] Because the high shear found at the apex of a plaque is recognized as a specific feature of thrombosis, targeting high shear has been proposed as an innovative strategy to selectively block thrombosis[18] with a minor impact on hemostasis, thereby potentially avoiding bleeding complications.[19]

A major blind spot in our current knowledge, however, concerns the flow conditions prevailing during hemostasis. Although homeostatic flow conditions (ie, flows in intact vessels) are well known and involve relatively low shear forces (<2000 s^{-1}), the shear flow occurring after lesion of a vessel has never been measured experimentally.[20,21] The aim of this study was to evaluate the shear rates and elongational flows occurring in wounds after vessel damage.

Three novel models were developed and applied to various murine vessels, with the aim of mimicking the main scenarios of vessel injury (ie, puncture or transection). The lesions and the plugs forming in these models were characterized by fluorescence and electron microscopy. An original model was also developed in humans, based on measurement of the blood loss after injury of the cubital vein. Using our experimental data, a computational fluid dynamics model was employed to calculate the magnitudes of the shear rate and elongational flow occurring after vessel injury. Evidence is provided that both the shear rate and the elongational flow generated at the edge of a wound reach extremely high levels, similar to those previously thought to prevail only in stenosed arteries during thrombotic events.

Materials and methods

Mouse model of hemostasis based on vessel puncture

Wild-type mice with a pure C57BL/6 background were maintained in the animal facilities of the EFS Grand-Est. Ethical approval for the experiments was obtained from the French Ministry of Research. The fluorescent agent 3,3 -dihexyloxacarbocyanine iodide ($DIOC_6$; Thermo Fisher Scientific, MA) was injected into the jugular vein of 7- to 28-week-old mice, 5 minutes before the experiment, to label platelets. Before puncture of the vessel (carotid artery, aorta, or saphenous vein), an ultrasound Doppler probe with PS-Series Nanoprobe (Transonic Systems Inc) was used to measure the uninjured flow velocity. The ultrasonic window of the probe has the same flow sensitivity, so that the vessel can be positioned anywhere within the probe lumen. Afterward, 2 laser Doppler probes were placed at the up- and downstream sides of the site of injury to measure the velocity of the blood flow relative to each other. The vessel was then punctured with a 25- or 30-gauge needle. The relative flow velocities were recorded continuously and normalized to absolute values using the uninjured mean flow velocity (detailed in supplemental materials; supplemental Figure 1A-B). The time to cessation of bleeding after the injury was determined. To measure the blood loss, the blood was collected on a tissue compress in a tube containing 10 mL of lysis buffer (NH_4Cl 150 mM, $KHCO_3$ 1 mM, EDTA 0.1 mM, pH 7.2) and then centrifuged at 550*g*, and the optical density was read at 540 nm. At the end of the experiment, the thrombus was fixed and processed for electron microscopy.[22]

Mouse model of hemostasis based on vessel puncture using a catheter

The left common carotid artery of adult mice was exposed, and the blood flow was stopped by placing 2 ligatures at the top and bottom of the vessel. A catheter with an inner diameter of 127 μm was inserted into the vessel and fixed with a drop of optical matching gel (Moor Instruments Ltd, Devon, UK). At the end of the procedure, the blood flow was restored. Blood was collected into a tube, which was weighed to determine the volume of blood lost.

Mouse model of hemostasis based on vessel transection

$DIOC_6$ was injected into the jugular vein of adult mice, 5 minutes before starting the experiment, to label platelets. Two sites on the spermatic artery were exposed: one to place a Doppler probe and the other to perform transection. The Doppler probe was used to measure the blood flow before and after disruption of the vessel with microscissors (15000-08; Fine Science Tools, Heidelberg, Germany). The measured flow velocities were normalized to absolute values using the mean velocity in the intact vessel (detailed in supplemental materials; supplemental Figure 1C-F). The time to cessation of bleeding was recorded.

Human model of hemostasis based on vessel puncture

The investigations were performed in accordance with the Declaration of Helsinki and with the approval of the Center for Theoretical Problems of Physicochemical Pharmacology, Russian Academy of Sciences (CTPPCP RAS) Ethical Committee, and written informed consent was obtained from all donors. The median cubital vein of healthy donors (6 male and 3 female) was punctured with a 22-gauge (diameter = 0.41 mm) or 24-gauge needle (diameter = 0.31 mm) connected to a peripheral venous catheter. After placement of the catheter and removal of the stiletto, blood was collected into a tube for 2 minutes by gravity, and the volume of blood lost was determined by weighing the tube.

Computational model to calculate the flow parameters after puncture or transection of murine or human vessels

To calculate the shear rate and elongational flow in murine and human vessels, a computational fluid dynamics model of blood flow was applied to the injury region. The damaged vessel was modeled as a tube representing the vessel wall with an outer diameter based

on experimental measurements and a thickness derived from the literature,[23-25] in which a hole represented the injury. The size of the injury was determined by using experimental fluorescent microscopy data, and the measurements were confirmed by scanning electron microscopy (supplemental Figure 2A-G). The blood was considered to be a non-Newtonian fluid (supplemental Figure 2H), and the time-dependent incompressible Navier-Stokes equation was solved in 3 dimensions (3D) to calculate the flow field. For the boundary conditions of the flow up- and downstream of the hole, we used the experimental flows measured with Doppler probes. The vessel wall was taken to be nondeformable, and the wound led to a larger tank with an upper lid at constant pressure. Further details of the simulation setup can be found in the supplemental materials (supplemental Figure 3).

Hybrid computational model of the blood flow in the intact and injured venous network of the human arm

To analyze the hemodynamic conditions in the human venipuncture experiments, not only near the wound but also in the adjacent vessels, we developed a simulation of the blood circulation in the human arm. The first superficial and deep vein branches of the brachiocephalic vein were modeled as rigid pipes with diameters and lengths based on literature values,[26,27] while the redistribution of the blood flow and pressure was calculated by the method of electronic-hydraulic analogy (MEHA).[28] The damaged median cubital vein was modeled as a pipe with a round hole on the top where stationary numerical solutions of the Navier-Stokes equation were obtained in 3D. The blood was considered to be a non-Newtonian[29] (detailed in the supplemental materials; supplemental Figure 4A). The boundary conditions at both ends of the median cubital vein were obtained from the 2-way coupled method of electronic-hydraulic analogy simulation of the venous network (detailed in the supplemental materials).

Statistical analyses

All statistical analyses were performed using a GraphPad Prism program, version 6.0 (Prism, GraphPad, La Jolla, CA). All values are reported as the mean ± SEM for a normal distribution, or median for a nonnormal distribution. The data of 2 groups were compared by the 2-tailed paired Student *t* test.

Results

Development and characterization of 2 novel models of hemostasis in mice

To determine the blood flow conditions occurring at the edge of a wound, 2 novel mouse models of hemostasis were developed. In the first model, a 25-gauge needle was used to puncture the murine carotid artery (Figure 1A). Intravital microscopy showed the formation of an initial small, reversible platelet plug reaching a maximum size 30 seconds after vessel puncture, which remained mainly located in the extravascular space (Figure 1B-C; supplemental Figure 2A,C,E). SEM imaging indicated that the residual plug was largely composed of tightly packed platelets, indicative of their elevated degree of activation (Figure 1D, supplemental Figure 2B,D,F). The thrombus surface was covered with fibrous strands, whose ultrastructure resembles fibrin and contained erythrocytes. The mean time to arrest of bleeding was 41 seconds (25% to 75% percentile: 25 to 48 seconds; n = 6) (Figure 1E). In the second model, the spermatic artery was sectioned with microscissors to mimic vessel disruption (Figure 1F). Intravital microscopy indicated that an occlusive, platelet-rich plug formed at the vessel outlet and stopped blood loss after 43 seconds (25% to 75% percentile: 27.5 to 97 seconds; n = 9) (Figure 1G-H). These 2 models represent the main scenarios of vascular injury and were used to measure the average velocity of the blood flow in the vessel experimentally, in order to reconstruct the flow field at the edge of the wound.

Puncture of a mouse carotid artery generates high shear at the edge of the wound

To determine the flow conditions prevailing during hemostasis, we first employed the murine carotid puncture model (Figure 1A). Measurements with an ultrasound Doppler probe indicated a mean blood flow velocity of 5 ± 0.2 cm/s in the intact carotid (Figure 2A). Two laser Doppler probes recorded the variations in blood flow throughout the hemostatic process (Figure 2B; supplemental Figure 4B). The upstream velocity profile showed a rapid rise to a maximal value reached 11 ± 2 seconds after injury, which stabilized after 23 ± 2 seconds at 7 ± 1 cm/s (supplemental Figure 4C,D). The simulation indicated that the shear rate at the edge of the wound attained a maximal value of ~16 000 s^{-1} for a wound area of 40 × 10^3 μm^2 (Figure 2C-D). Further simulations with the numerical model revealed that the shear rate was only modestly influenced by the shape of the injury, because a circular form and an ellipsoidal one led to variations of < 20% (Figure 2E; supplemental Table 1). The presence of ruptured borders of the injury inside the vessel lumen likewise had a modest impact (<21%) (Figure 2E). The median maximum shear rate at the edge of wounds in the carotid artery having a surface area ranging from 9 × 10^3 to 6 × 10^4 μm^2 was 22 000 s^{-1} (Figure 2F; Table 1). Concerning the importance of the wound area, we observed that the shear rate decreased with increasing wound area, but a wide range of areas, from 9 × 10^3 to 61 × 10^3 μm^2, all generated high shear levels far above those encountered in intact vessels (Figure 2G). The presence of high shear levels was confirmed using another approach, based on applying Poiseuille's equation to the volumetric rates of blood loss, which resulted in values ranging from 3 000 to 31 000 s^{-1} (supplemental Figure 4E,F). Calculation of the elongational flow from the simulated data also showed strongly elevated values reaching 3000 ± 1000 s^{-1} in a broad region in front of the injury and 5000 ± 2000 s^{-1} at the edge of the wound, significantly exceeding the threshold levels required for unfolding of vWF (Figure 2H). In summary, both the shear rate and the elongational flow reached extremely high levels following puncture of the murine common carotid artery.

Puncture of large or small mouse vessels generates high shear at the edge of the wound

To determine whether high shear in the wound is a general feature occurring after puncture of a vessel, blood flow velocities were measured following injury of 2 additional vessels, the aorta and the saphenous vein, which present distinct features with respect to the carotid in terms of diameter, pressure, and vessel wall composition. Ultrasound Doppler measurements in the intact aorta and saphenous vein indicated mean flow velocities of 2.9 ± 0.6 and 1.9 ± 0.1 cm/s, respectively (Figure 3A). The blood flow dynamics during hemostasis were similar to those in the carotid artery in both vessels, with maximal velocities of 4.1 ± 0.4 cm/s (Figure 3B) and

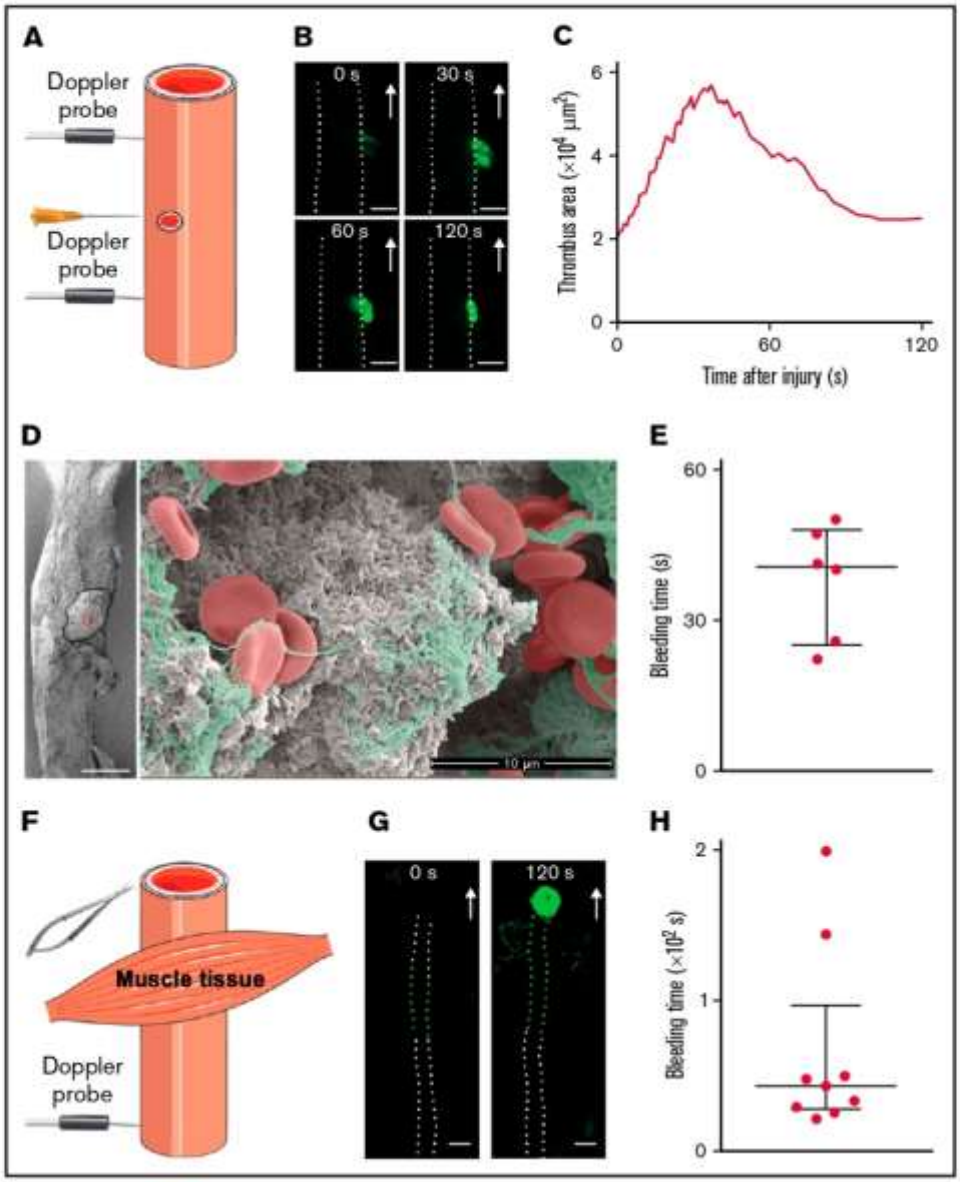

Figure 1. Two novel models of hemostasis in mice. (A) Schema of the murine vessel puncture model with 2 laser Doppler probes. (B-E) Thrombus formation was induced by needle puncture of the left common carotid artery of wild-type mice. (B) Representative fluorescence images of the thrombus (platelets labeled with $DIOC_6$ in green) at the indicated time points after injury with a 25-gauge needle. Scale bar: 250 μm. The arrows represent the direction of blood flow, and the dotted lines represent the borders of the vessel. (C) The curve shows the area of the hemostatic thrombus as a function of the time after injury. (D) Representative scanning electron microscopy images of the external thrombus 3 minutes after vessel puncture. The black solid line represents the border of the thrombus. Scale bar: 250 μm (left), 10 μm (right). The thrombus is composed of tightly packed platelets, fibrous strands whose ultrastructure resembles fibrin, and RBCs, colored on the enlarged image of the area in the red square in gray, green, and red, respectively. (E) The dot plot shows the bleeding times of the wounds after vessel puncture. Data are presented as the mean ± the standard error of the mean (SEM) and individual symbols represent individual mice. (F) Schema of the murine vessel transection model with a laser Doppler probe. (G-H) Thrombus formation was induced by transection of the spermatic artery of wild-type mice with microscissors. (G) Representative fluorescence images of the thrombus (platelets labeled with $DIOC_6$ in green) at the indicated time points after injury. Scale bar: 250 μm. The arrows indicate the direction of blood flow. The white dotted lines represent the borders of the exposed vessel, and the green dotted lines represent the borders of the vessel under muscle tissue. (H) The dot plot shows the bleeding times of the wounds after vessel transection. Data are presented as the mean ± SEM, and individual symbols represent individual mice.

3.6 ± 0.5 cm/s (Figure 3C) resulting in maximal shear rates of 25 000 s^{-1} (Figure 3D) and 7000 s^{-1} (Figure 3E), in the aorta (injury area of 1 × 10^3 to 47 × 10^3 μm^2) and the saphenous vein (injury area of 3 × 10^3 to 24 × 10^3 μm^2), respectively (Figure 3F; Table 1; supplemental Table 3). These shear levels were 28 and 7 times higher in the aorta and the saphenous vein, respectively, as compared with the steady conditions in the intact vessels. The maximum shear rate in both types of vessels decreased with increasing wound area, in line with the results obtained in the carotid artery (Figure 3G). The rates of elongational flow were also highly

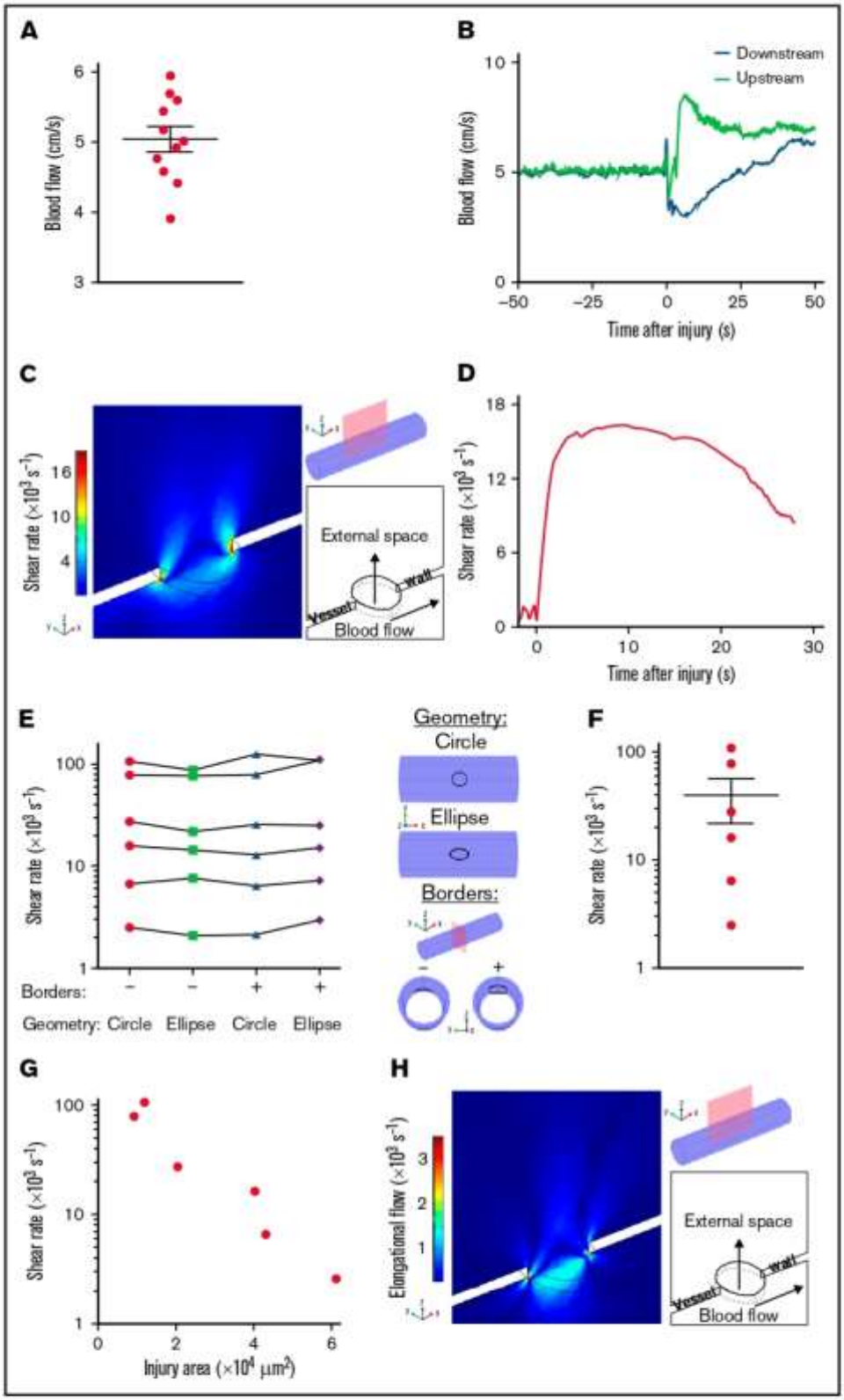

Figure 2. Shear rates after puncture of a mouse carotid artery. (A) The dot plot shows the mean blood flow velocities in the intact left carotid artery. Data are presented as the mean ± SEM, and individual symbols represent individual mice. (B-H) Injury was induced by needle puncture of the left common carotid artery of wild-type mice. (B) The curves show the blood flow velocities upstream and downstream of the site of injury, as a function of the time after injury. (C) Representative image obtained with the model, whose 3D geometry is presented in the upper right corner. The red rectangle defines the zx-section of observation, and the injury appears at the top of the

Table 1. Table of the shear rates calculated for different scenarios

Vessel	Species	Type of vessel injury	Diameter of the injury, μm	SR at the wound, s^{-1}		SR in the intact vessel, s^{-1}
				Median	25%-75% percentile	
Carotid artery	Mouse	Puncture	108-280	22 000	5 600-85 000	950
Aorta	Mouse	Puncture	40-240	25 000	6 000-138 000	900
Saphenous vein	Mouse	Puncture	66-173	7 000	3 000-31 000	1 000
Spermatic artery	Mouse	Disruption	215	14 500	11 000-20 000	900
Median cubital vein	Man	Puncture	310	7 400	5 400-27 300	250
			410	3 500	2 300-5 400	250

SR, shear rate.

elevated, reaching 8000 ± 5000 s^{-1} and 1500 ± 600 s^{-1} in a broad region in front of the wound, and 13 000 ± 8000 s^{-1} and 3000 ± 1000 s^{-1} at the edge of the injury in the aorta and saphenous vein, respectively (Figure 3H). These results indicate that in 2 additional mouse vessels, puncture of small and large veins or arteries leads to extremely high shear rates and elongational flows at the edge of the wound.

Transection of the mouse spermatic artery generates high shear at the edge of the wound

To determine the flow conditions occurring during the other scenario of vessel injury, we applied the transection model to sectioning of the murine spermatic artery with microscissors (Figure 1F). Because of the small size of this vessel, which precludes the use of an ultrasound Doppler probe, the absolute blood flow velocities for normalization were derived from larger vessels (detailed in the supplemental methods) (Figure 4A). The dynamics of blood flow after transection of the spermatic artery presented a rapid rise to a maximal value of 7 ± 1 cm/s reached 11 ± 4 seconds after injury (Figure 4B-D). Calculation of the shear rates with the computational model indicated the presence of elevated shear levels attaining 15 000 ± 2000 s^{-1}, 17-fold higher than under homeostatic conditions (Figure 4E-G; Table 1). The elongational flow rates were also significantly elevated both in front of the outlet (1000 ± 300 s^{-1}) and at the edge of the wound (1700 ± 500 s^{-1}), exceeding the threshold levels for unfolding of vWF (Figure 4H). These results indicate that after vessel rupture, as following vessel puncture, the shear rate and elongational flow can reach very high levels.

Puncture of the human cubital vein results in high shear rates at the edge of the wound

We next investigated whether shear rates were also dramatically increased after injury of a human vessel, using a puncture model in the human cubital vein (Figure 5A). For ethical reasons, an open wound was not induced with a needle. Instead, a 22- or 24-gauge needle coupled to a 25-mm-long catheter was inserted into the cubital vein of healthy volunteers. The mean velocity of the outflow, measured by weighing the tubes into which the blood was collected, was calculated to be 0.6 ± 0.2 and 0.19 ± 0.04 m/s for wound surface areas of 75 × 10^3 and 132 × 10^3 μm^2, respectively, corresponding to the outer circumference of the needle (Figure 5B). Poiseuille's equation led to estimated shear rates of 14 500 ± 5000 and 3700 ± 800 s^{-1}, respectively, for these injury sizes (Figure 5C; Table 1). In control experiments, we used a numerical and an experimental approach to obtain evidence that use of a catheter did not cause overestimation of the shear rates. First, a hybrid model of median cubital vein puncture (Figure 5D) predicted maximum shear rates of 47 000 and 2400 s^{-1} at the edge of the wound and in the catheter, respectively, for an injury size of 132 × 10^3 μm^2 (Figure 5E). Second, an experimental model of murine carotid artery puncture using a catheter indicated shear rates of 2000 ± 300 s^{-1} at the edge of the injury, 70 times lower than in the experiment without a catheter, confirming that the presence of a catheter in fact underestimates the shear levels in the wound (Figure 5F-G). Thus, in humans as in mice, the level of shear at the edge of a wound was found to be strongly increased after vessel damage.

Figure 2 (continued) cylinder mimicking the carotid artery. At the side, the colors indicate the shear rates 8.75 seconds after puncture in the zx-section. The schema in the lower right corner depicts the positions of the external space and vessel lumen with arrows indicating the direction of blood flow. (D) The curve shows the shear rate at the edge of the wound calculated with the model, as a function of the time after injury. (E), The graph shows the maximum shear rates at the edge of the wound calculated with the model for 2 different shapes of the lesion (circle and ellipse), whose 3D geometry is presented in the upper right corner. The presence or absence (+ or –) of the vessel borders rolled inside the lumen was used to mimic the presence or absence of the ruptured ends of the carotid artery, whose 3D geometry is presented in the lower right corner. Individual symbols in the columns represent individual mice, and symbols pertaining to the same mouse are joined by a line. (F) The dot plot shows the maximum shear rates at the edge of the wound calculated with the model. Data are presented as the mean ± SEM, and individual symbols represent individual mice. (G) The graph shows the maximum shear rates at the edge of the wound calculated with the model, as a function of the area of the injury. Individual symbols represent individual mice. (H) Representative image obtained with the model, whose 3D geometry is presented in the upper right corner. The red rectangle defines the zx-section of observation, and the injury appears at the top of the cylinder mimicking the carotid artery. At the side, the colors indicate the elongational flows 8.75 seconds after puncture in the zx-section. The schema in the lower right corner depicts the positions of the external space and vessel lumen with arrows indicating the direction of blood flow.

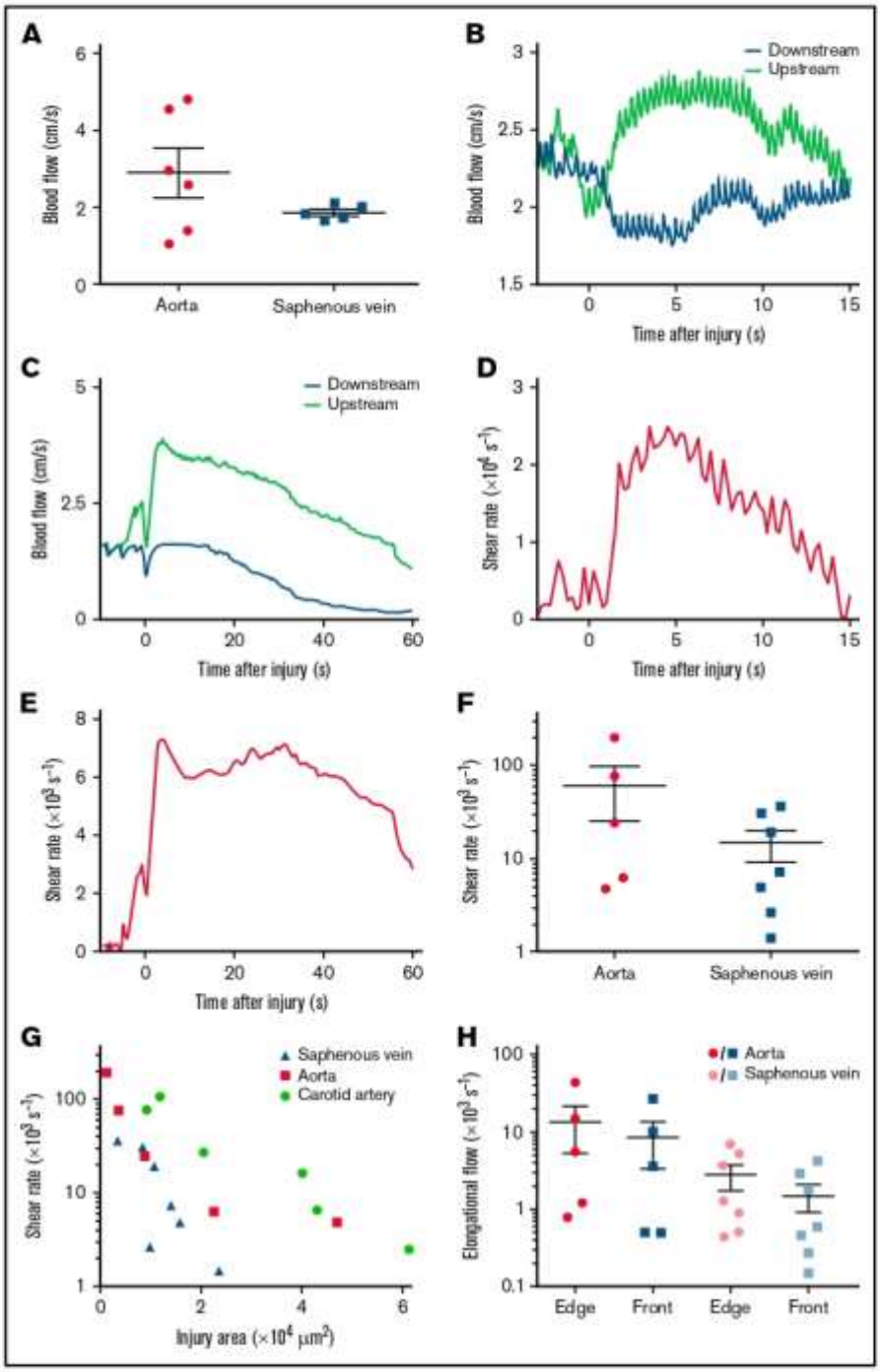

Figure 3. Shear rates after puncture of the mouse aorta or saphenous vein. (A) The dot plots show the mean blood flow velocities in the intact aorta and saphenous vein. Data are presented as the mean ± SEM, and individual symbols represent individual mice. (B) The curves show the blood flow velocities upstream and downstream of the site of injury after puncture of the aorta, as a function of the time after injury. (C) The curves show the blood flow velocities upstream and downstream of the site of injury after puncture of the saphenous vein, as a function of the time after injury. (D) The curve shows the shear rate at the edge of the wound in the aorta, calculated with the model as a function of the time after injury. (E) The curve shows the shear rate at the edge of the wound in the saphenous vein, calculated with the model as a function of the time after injury. (F) The dot plot shows the maximum shear rates at the edge of the wound in the aorta or saphenous vein calculated with the model. Data are presented as the mean ± SEM, and individual symbols represent individual mice. (G) The graph shows the maximum shear rates at the edge of the wound in the carotid artery, aorta, or saphenous vein, calculated with the model as a function of the area of the injury. Individual symbols represent individual mice. (H) The dot plots show the maximum elongational flows at the edge of the wound (edge) and the mean elongational flows in a broad area in front of the wound (front), calculated with the model for puncture of the aorta or saphenous vein. Data are presented as the mean ± SEM, and individual symbols represent individual mice.

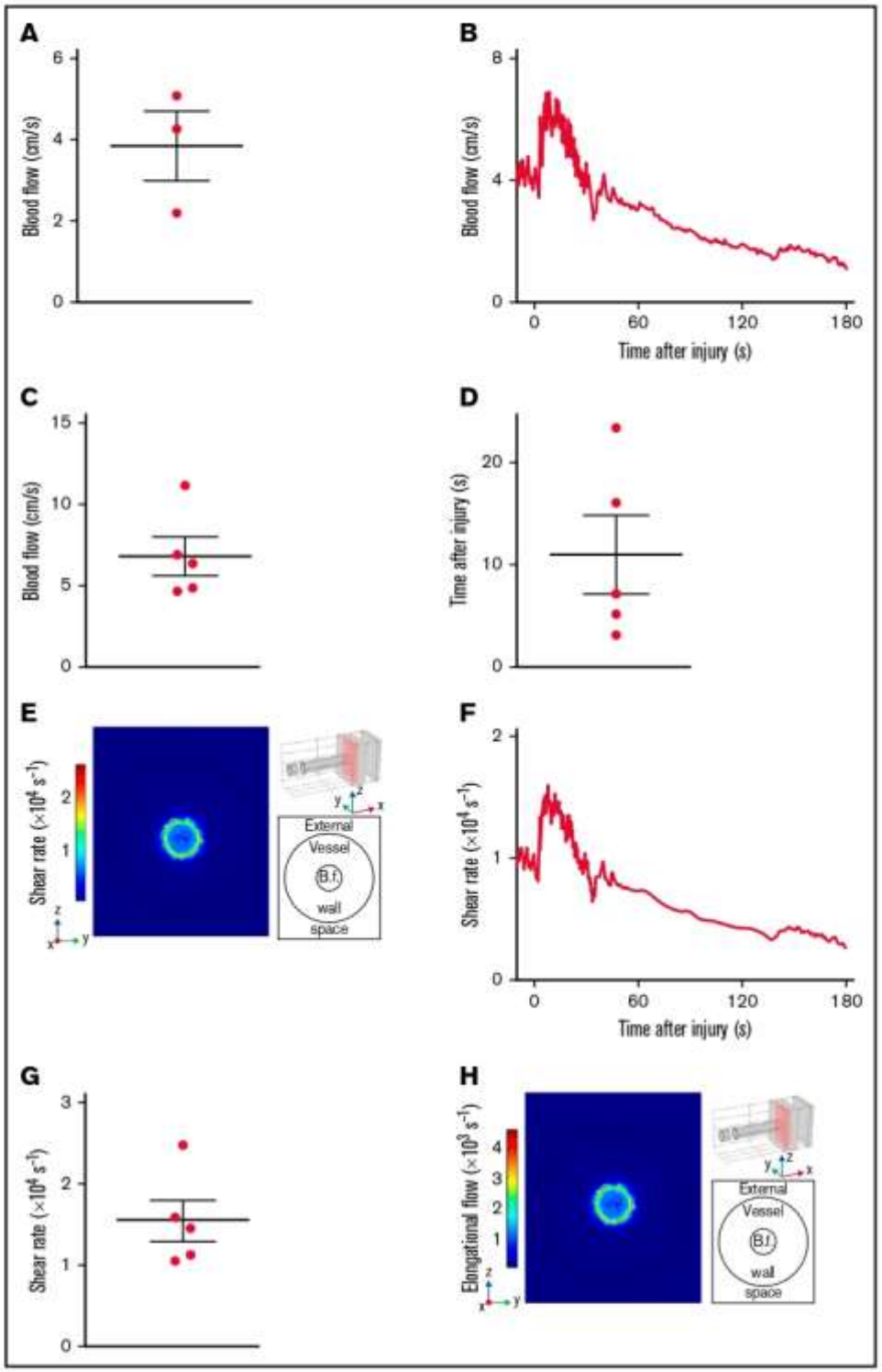

Figure 4. Shear rates after transection of the mouse spermatic artery. (A) The dot plot shows the mean blood flow velocities in the intact spermatic artery. Data are presented as the mean ± SEM, and individual symbols represent individual mice. (B-H) Injury was induced by transection of the spermatic artery of wild-type mice with microscissors. (B) The curve shows the blood flow velocities upstream of the site of injury, as a function of the time after injury. (C) The dot plot shows the maximum blood flow velocities upstream of the site of injury. Data are presented as the mean ± SEM, and individual symbols represent individual mice. (D) The dot plot shows the times after injury at which the maximum upstream blood flow velocities were reached. Data are presented as the mean ± SEM, and individual symbols represent individual mice. (E) Representative image obtained with the model, whose 3D geometry is presented in the upper right corner. The red rectangle defines the zy-section of observation, and the injury appears at the top of the cylinder mimicking the spermatic artery. At the side, the colors indicate the shear rates 8.5 seconds after transection in the zx-section. The schema in the lower right corner depicts the positions of the external space and vessel lumen with the blood flow (B.f.) in the middle. (F) The curve shows the shear rate at the edge of the wound calculated with the model, as a function of the time after injury. (G) The dot plot shows the maximum shear rates at the edge of the

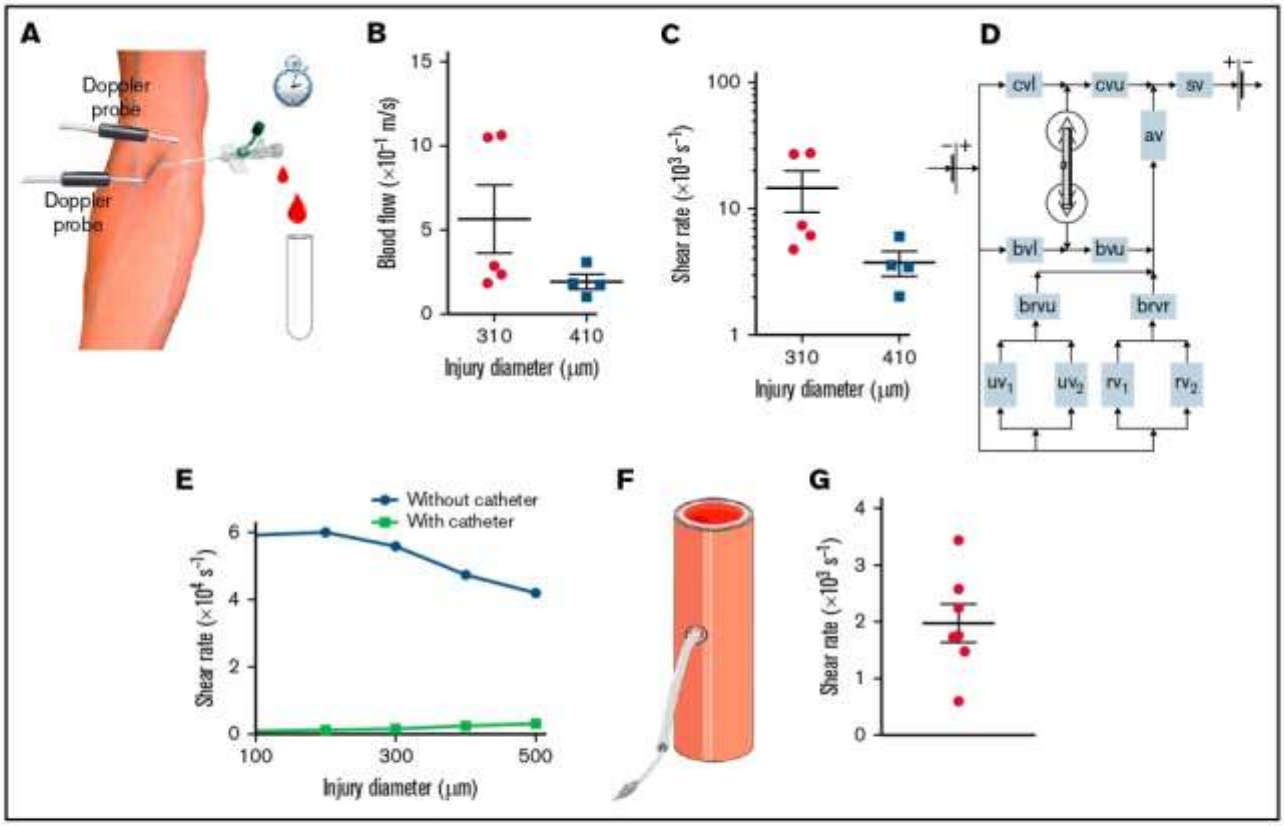

Figure 5. Shear rates after puncture of a human median cubital vein. (A) Schema of the human vessel puncture model using a catheter. (B) The dot plots show the mean blood flow velocities through the catheter after puncture of the median cubital vein with a 22-gauge (diameter = 0.41 mm) or 24-gauge (diameter = 0.31 mm) needle. Data are presented as the mean ± SEM, and individual symbols represent individual donors. (C) The dot plots show the shear rates at the edge of the wound calculated with Poiseuille's equation for puncture of the median cubital vein with a 22- or 24-gauge needle. Data are presented as the mean ± SEM, and individual symbols represent individual donors. (D) Schema of the hybrid computational model of blood flow in the intact and injured venous network of the human arm. The intact vessels are represented as rectangles with the following abbreviations: av, axillary vein; brvr, brachial vein divided into 2 radial veins; brvu, brachial vein divided into 2 ulnar veins; bvl, lower part of the basilic vein; bvu, upper part of the basilic vein; cvl, lower part of the cephalic vein; cvu, upper part of the cephalic vein; rv_1, radial vein 1; rv_2, radial vein 2; sv, subclavian vein; uv_1, ulnar vein 1; uv_2, ulnar vein 2. The damaged median cubital vein is represented in 3D geometry. (E) The curves show the maximum shear rate at the edge of the wound calculated with the hybrid model for experiments with and without a catheter, as a function of the diameter of the injury. Individual symbols represent individual simulations. (F) Schema of the murine carotid artery puncture model with a catheter. (G) The dot plot shows the shear rates at the edge of the wound calculated with Poiseuille's equation. Data are presented as the mean ± SEM, and individual symbols represent individual mice.

Possible mechanisms governing the decrease in shear rate with increasing wound size

The experimental values measured in different mouse or human injuries, ranging from 50 to 410 μm in size, displayed an unexpected inverse relationship between the shear rate and the size of the wound (Figure 6A). In an attempt to explain this result, we first considered the simple analytical case of Poiseuille flow in a cylinder, which showed that the wall shear rate increased linearly as a function of the radius for a constant pressure drop and decreased as the inverse cube of the radius for a constant flow velocity (detailed in the supplemental materials; supplemental Figure 5A). To explore this finding in the more realistic setting of wound hemodynamics, we used the in silico model of the median cubital vein injury described above (Figure 5D). The shear rates in the wound displayed a linear dependence on size for injury radii <30 μm, and an inverse cube dependence for radii >150 μm (Figure 6B red dots), in agreement with the results for a Poiseuille flow dictated by a "constant pressure regime" and a "constant flow regime," respectively (Figure 6B lines). Evaluation of the blood flow rate through the wound showed that it was much lower than the flow through the downstream vessel network for very small injuries (<50 μm). For large injuries (>200 μm), it was comparable to the inflowing bloodstream, corresponding to essentially constant flow conditions (Figure 6C). To gain insight into the causes of the transition between these 2 fluid regimes, the threshold of hydrodynamic

Figure 4 (continued) wound calculated with the model. Data are presented as the mean ± SEM, and individual symbols represent individual mice. (H) Representative image obtained with the model, whose 3D geometry is presented in the upper right corner. The red rectangle defines the zy-section of observation, and the injury appears at the top of the cylinder mimicking the spermatic artery. At the side, the colors indicate the elongational flows 8.5 seconds after transection in the zx-section. The schema in the lower right corner depicts the positions of the external space and vessel lumen with the blood flow in the middle.

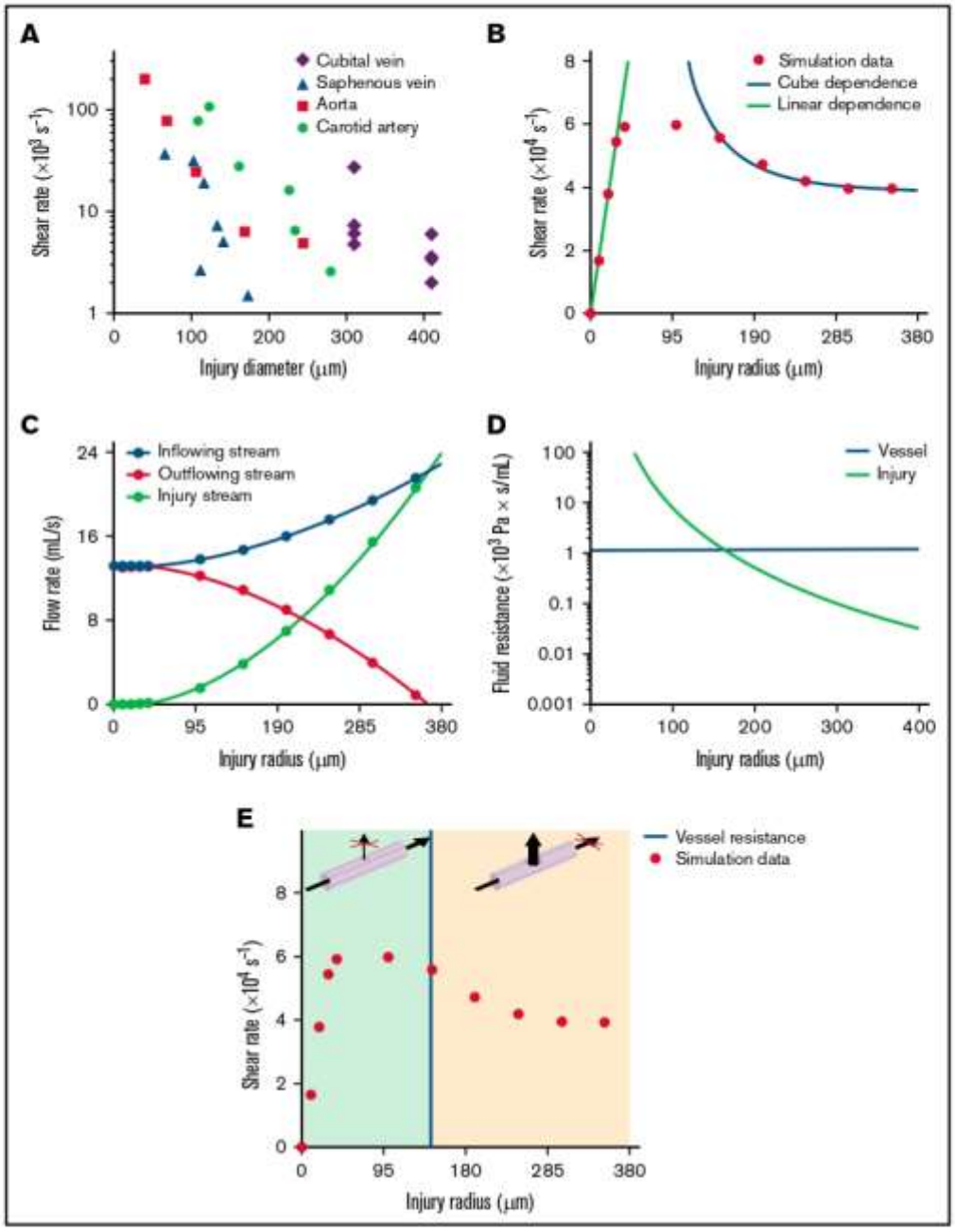

Figure 6. Mechanism governing the decrease in shear rate with increasing wound size. (A) The graph shows the maximum shear rates at the edge of the wound after puncture of the carotid artery, aorta, saphenous vein, or median cubital vein, as a function of the diameter of the injury. Individual symbols represent individual mice or donors. (B-E) Simulations of puncture of the median cubital vein without a catheter. (B) The dot plot shows the maximum shear rates at the edge of the wound calculated with the hybrid model, as a function of the radius of the injury. Individual symbols represent individual simulations. The dots are approximated by linear (linear dependence) and inverse cube (cube dependence) functions for injury radii of 0 to 30 μm and 150 to 350 μm, with adjusted R^2 values of 0.99 and 0.98, respectively. (C) The curves show the blood flow rate upstream (inflowing stream) and downstream (outflowing stream) of the site of injury and through the wound (injury stream) calculated with the hybrid model, as a function of the radius of the injury. Individual symbols represent individual simulations. (D) The green curve represents the hydrodynamic resistance of the wound, as a function of the radius of the injury. The horizontal blue line represents the hydrodynamic resistance of the median cubital vein. (E) The dot plot shows the maximum shear rates at the edge of the wound calculated with the hybrid model, as a function of the radius of the injury. Individual symbols represent individual simulations. The vertical blue line represents the threshold value of the radius of the injury at which the hydrodynamic resistance of the median cubital vein is equal to that of the wound. The green and orange areas indicate the ranges of injury radii for which the blood flow passes mostly through the downstream vessel network or through the injury, respectively, as shown in the 3D schemas above.

resistance in the wound was determined and found to be 1, 16, 32, and 22 × 10^3 Pa*s/mL for the cubital vein, carotid artery, aorta, and saphenous vein, respectively. Above these values, the blood flow through the injury is determined by the capacity of the vessel supplying it, while below them only a fraction of the blood flow passes through the injury (Figure 6D-E; supplemental Figure 5B-E). This shift in the relative vessel-wound resistance determines the redistribution of the blood flow between the wound and the downstream vessel, the blood passing mostly through the downstream vessel network for small injuries and through the wound for large injuries. Altogether, these results indicate that all our experimental data for injuries in human and mouse vessels were obtained under constant flow conditions, which explains the inverse relationship between shear rate and injury size.

Discussion

The main finding of this study is that various types of lesions in small and large mouse and human blood vessels result in extremely high shear rates at the edge of the wound where hemostasis occurs. Such shear levels far exceed those observed in healthy vessels under homeostatic conditions and are even more elevated than those found in pathological arteries with evolved atherosclerotic plaques, in which very high shear rates appear at the apex of a stenosis. Our results indicate that high shear is not restricted to pathological conditions and can also occur in healthy vessels following an injury. We also demonstrate the presence of elevated levels of elongational flow in the wound with values far >1000 s^{-1}, known to efficiently unfold circulating vWF. This further highlights the notion that such rheological conditions are not specific to arterial thrombosis.

Our study indicates that upon vessel puncture, the shear rate reaches elevated values ranging from 10^3 to 10^6 s^{-1}. These levels might seem surprisingly high but are in general agreement with a numerical study predicting that shear in a wound could be higher than in intact vessels.[21] Our results are also concordant with work based on an in vitro device mimicking vessel injury, which indicated that shear rates in the wound could reach 10 000 s^{-1}.[30] The 2 latter studies nevertheless propose lower shear levels in the wound as compared with our in vivo measurements, which could be due to the fact that their calculations were based on a model of pressure difference between the circulation system and the outside. Another explanation might be that both studies focused on small arteries of capillary size, unlike in our work.

Our findings indicate that the blood flow after a puncture injury occurs under a "constant flow regime" for wounds with a radius well above that of the threshold fluid resistance (determined by the relative hydrodynamic resistance of the wound and the vessel) and under a "constant pressure regime" for wounds with a radius well below that of the threshold resistance. It is known that occlusive thrombus formation can occur only under a flow regime with a constant pressure drop, which correlates with our prediction that large wounds are less likely to close. This also explains why the disruption model led to smaller increases in shear rate. However, in our study it was technically impossible to realize injuries with a smaller diameter resulting in a "constant pressure regime." Other studies also faced such technical limitations, notably a publication using an experimental hemostasis model based on laser injury of the saphenous vein where the injury diameter reached 48 μm.[31]

The approaches employed in this study present some limitations, notably the fact that we used smooth borders in the in silico model, and that vessel contraction was considered to be negligible because it was not detected by intravital microscopy. The model also does not take into account the thrombus formation in the wound, which does not change our main message, as a reduction in injury size would increase the shear as for a constant flow system. In addition, the blood flow was simulated as a laminar fluid, and its pulsatility was not taken into account. These assumptions were legitimate because the Reynold numbers were lower than the critical values (Re < 4 for all vessels) and the shear rates were high. As the order of magnitude of the shear rates after vessel injury being elevated (>10^3 s^{-1}), one may postulate that these limitations did not affect the main results.

The nature of thrombus formation in our hemostasis model is in agreement with studies of other groups. We have the same dynamic of reversible platelet plug formation and comparable bleeding time for the same type of injury (for saphenous vein bleeding time was 4 to 20 seconds for 48 μm of injury diameter[31] vs 37 seconds for 66 μm of injury diameter [A.A.Y., K.R.B., G.A.B., G.Z., A.E., F.I.A., C.G., M.A.P. and P.H.M., unpublished data]). The composition of thrombus was also similar, and the plug was composed mostly of tightly packed platelets with a small proportion of RBC and fibrin detected on the surface. Compared with work of Tomaiuolo et al, thrombi have the same composition, but although ours remained mainly located in the extravascular space, theirs were mainly located on the intraluminal side of the vessel wall.[32]

The high shear occurring at the edge of a wound is consistent with our knowledge of the molecular mechanisms of hemostasis. Indeed, platelet aggregation is strongly dependent on the GPIb-IX/vWF axis at high shear rates. Despite that our study was performed mostly in large vessels and not in the microvasculature, it may be considered that high shear rates also take place there because the bleeding phenotype observed in patients deficient in the high shear sensitive molecules GPIb-IX or vWF occur generally in the microvasculature.

Recently, shear-selective antiplatelet therapies have been proposed as an innovative treatment to prevent pathological thrombus formation while only modestly increasing the risk of bleeding. Two approaches to block high shear-mediated thrombosis were proposed, one focusing on inhibition of the shear-driven interaction between the vWF A1 domain and GPIbα, and the second based on shear-sensitive vehicles of antithrombotic agents, which release their contents only under high shear rates.[18,19] As our study shows that elevated shear also occurs at the edge of a wound in healthy vessels, one may speculate that targeting high shear will probably not be devoid of bleeding complications after traumatic injuries (falls, trauma, surgery, etc).

In conclusion, we report that various types of lesions in small and large mouse and human blood vessels can result in extremely high shear rates and elongational flows. Such rheological conditions are therefore relevant to the physiological process of hemostasis and cannot be considered to be exclusively pathological.

Acknowledgments

The authors thank J.N. Mulvihill for reviewing the English of the manuscript and J.Y. Rinckel and F. Proamer for help in preparing the samples for SEM.

This work was supported by the Ministry of Education and Science of Russia grant 075-15-2022-242.

Authorship

Contribution: A.A.Y. acquired and analyzed the data; K.R.B. performed the human experiments; A.A.Y., G.A.B., and G.Z. carried out the computational experiments; A.A.Y., M.A.P., and P.H.M. interpreted the data and wrote the manuscript; A.E. and A.A.Y. performed the SEM experiments and analyzed the data; C.G. and F.I.A. handled funding; and M.A.P. and P.H.M. conceived and designed the research and handled funding and supervision.

Conflict-of-interest disclosure: The authors declare no competing financial interests.

ORCID profiles: A.A.Y., 0000-0001-5292-2312; K.R.B., 0000-0002-4664-6953; G.A.B., 0000-0002-5623-723X; G.Z., 0000-0003-0150-0229; A.E., 0000-0001-9620-4961; F.I.A., 0000-0002-6668-0948; C.G., 0000-0003-1303-4210; M.A.P., 0000-0002-8128-7757; P.H.M., 0000-0001-9522-6261.

Correspondence: Pierre H. Mangin, Université de Strasbourg, INSERM, EFS Grand-Est, BPPS UMR-S1255, FMTS, 10 rue Spielmann, F-67065 Strasbourg, France; e-mail: pierre.mangin@efs.sante.fr; and Mikhail A. Panteleev, Center for Theoretical Problems of Physicochemical Pharmacology, Russian Academy of Sciences, Moscow 119991, Russia; e-mail: mapanteleev@yandex.ru.

References

1. Dopheide SM, Maxwell MJ, Jackson SP. Shear-dependent tether formation during platelet translocation on von Willebrand factor. *Blood*. 2002; 99(1):159-167.
2. Savage B, Sixma JJ, Ruggeri ZM. Functional self-association of von Willebrand factor during platelet adhesion under flow. *Proc Natl Acad Sci USA*. 2002;99(1):425-430.
3. Goncalves I, Nesbitt WS, Yuan Y, Jackson SP. Importance of temporal flow gradients and integrin alphaIIbbeta3 mechanotransduction for shear activation of platelets. *J Biol Chem*. 2005;280(15):15430-15437.
4. Hechler B, Lenain N, Marchese P, et al. A role of the fast ATP-gated P2X1 cation channel in thrombosis of small arteries in vivo. *J Exp Med*. 2003; 198(4):661-667.
5. Diamond SL. Systems analysis of thrombus formation. *Circ Res*. 2016;118(9):1348-1362.
6. Gachet C. Regulation of platelet functions by P2 receptors. *Annu Rev Pharmacol Toxicol*. 2006;46(1):277-300.
7. Zhu S, Tomaiuolo M, Diamond SL. Minimum wound size for clotting: flowing blood coagulates on a single collagen fiber presenting tissue factor and von Willebrand factor. *Integr Biol*. 2016;8(8):813-820.
8. Shibeko AM, Lobanova ES, Panteleev MA, Ataullakhanov FI. Blood flow controls coagulation onset via the positive feedback of factor VII activation by factor Xa. *BMC Syst Biol*. 2010;4(1):5.
9. Receveur N, Nechipurenko D, Knapp Y, et al. Shear rate gradients promote a bi-phasic thrombus formation on weak adhesive proteins, such as fibrinogen in a VWF-dependent manner. *Haematologica*. 2020;105(10):2471-2483.
10. Casa LD, Deaton DH, Ku DN. Role of high shear rate in thrombosis. *J Vasc Surg*. 2015;61(4):1068-1080.
11. Sing CE, Alexander-Katz A. Elongational flow induces the unfolding of von Willebrand factor at physiological flow rates. *Biophys J*. 2010;98(9): L35-L37.
12. Bark DL Jr, Ku DN. Wall shear over high degree stenoses pertinent to atherothrombosis. *J Biomech*. 2010;43(15):2970-2977.
13. Bortot M, Sharifi A, Ashworth K, et al. Pathologic shear and elongation rates do not cause cleavage of von Willebrand factor by ADAMTS13 in a purified system. *Cell Mol Bioeng*. 2020;13(4):379-390.
14. Coenen DM, Mastenbroek TG, Cosemans JMEM. Platelet interaction with activated endothelium: mechanistic insights from microfluidics. *Blood*. 2017;130(26):2819-2828.
15. Nesbitt WS, Westein E, Tovar-Lopez FJ, et al. A shear gradient-dependent platelet aggregation mechanism drives thrombus formation. *Nat Med*. 2009;15(6):665-673.
16. Kroll MH, Hellums JD, McIntire LV, Schafer AI, Moake JL. Platelets and shear stress. *Blood*. 1996;88(5):1525-1541.
17. Goto S, Handa S. Coronary thrombosis. Effects of blood flow on the mechanism of thrombus formation. *Jpn Heart J*. 1998;39(5):579-596.
18. Korin N, Kanapathipillai M, Matthews BD, et al. Shear-activated nanotherapeutics for drug targeting to obstructed blood vessels. *Science*. 2012; 337(6095):738-742.
19. Rana A, Westein E, Niego B, Hagemeyer CE. Shear-dependent platelet aggregation: mechanisms and therapeutic opportunities. *Front Cardiovasc Med*. 2019;6:141.
20. Mangin PH, Gardiner EE, Nesbitt WS, et al; Subcommittee on Biorheology. In vitro flow based systems to study platelet function and thrombus formation: recommendations for standardization: communication from the SSC on Biorheology of the ISTH. *J Thromb Haemost*. 2020; 18(3):748-752.
21. Tsiklidis EJ, Sinno T, Diamond SL. Coagulopathy implications using a multiscale model of traumatic bleeding matching macro- and microcirculation. *Am J Physiol Heart Circ Physiol*. 2019;317(1):H73-H86.
22. Eckly A, Hechler B, Freund M, et al. Mechanisms underlying FeCl3-induced arterial thrombosis. *J Thromb Haemost*. 2011;9(4):779-789.
23. Bas CE, Cwykiel J, Siemionow M. A new supermicrosurgery training model of saphenous artery and great saphenous vein anastomosis for development of advanced microsurgical skills. *J Reconstr Microsurg*. 2017;33(6):426-434.

24. Korshunov VA, Wang H, Ahmed R, et al. Model-based vascular elastography improves the detection of flow-induced carotid artery remodeling in mice. *Sci Rep.* 2017;7(1):12081.

25. Liu G, Jia W, Sun V, Choi B, Chen Z. High-resolution imaging of microvasculature in human skin in-vivo with optical coherence tomography. *Opt Express.* 2012;20(7):7694-7705.

26. Shima H, Ohno K, Michi K, Egawa K, Takiguchi R. An anatomical study on the forearm vascular system. *J Craniomaxillofac Surg.* 1996; 24(5):293-299.

27. He Y, Liu H, Himeno R. A one-dimensional thermo-fluid model of blood circulation in the human upper limb. *Int J Heat Mass Transf.* 2004; 47(12-13):2735-2745.

28. Olufsen MS, Nadim A. On deriving lumped models for blood flow and pressure in the systemic arteries. *Math Biosci Eng.* 2004;1(1):61-80.

29. Johnston BM, Johnston PR, Corney S, Kilpatrick D. Non-Newtonian blood flow in human right coronary arteries: steady state simulations. *J Biomech.* 2004;37(5):709-720.

30. Schoeman RM, Rana K, Danes N, et al. A microfluidic model of hemostasis sensitive to platelet function and coagulation. *Cell Mol Bioeng.* 2017; 10(1):3-15.

31. Getz TM, Piatt R, Petrich BG, Monroe D, Mackman N, Bergmeier W. Novel mouse hemostasis model for real-time determination of bleeding time and hemostatic plug composition. *J Thromb Haemost.* 2015;13(3):417-425.

32. Tomaiuolo M, Matzko CN, Poventud-Fuentes I, Weisel JW, Brass LF, Stalker TJ. Interrelationships between structure and function during the hemostatic response to injury. *Proc Natl Acad Sci USA.* 2019;116(6):2243-2252.

Supplementary Material

Traumatic vessel injuries initiating hemostasis generate high shear conditions

Alexandra A Yakusheva[1-3], Kirill R Butov[2-4], Georgii A Bykov[2], Gábor Závodszky[6], Anita Eckly[1], Fazly I Ataullakhanov[2,3,5], Christian Gachet[1], Mikhail A Panteleev[2,3,5*] and Pierre H Mangin[1*]

[1]Université de Strasbourg, INSERM, EFS Grand-Est, BPPS UMR-S1255, FMTS, F-67065 Strasbourg, France; [2]Center for Theoretical Problems of Physicochemical Pharmacology, Moscow 119991, Russia; [3]Federal Research and Clinical Centre of Pediatric Hematology, Oncology and Immunology, Moscow 117198, Russia; [4]Molecular Biology and Biotechnology Department, Pirogov Russian National Research Medical University, Ministry of Healthcare of the Russian Federation, Moscow 117997, Russia; [5]Faculty of Physics, Moscow State University, Moscow 119991, Russia; [6]Computational Science Lab, Faculty of Science, Institute for Informatics, University of Amsterdam, Amsterdam, The Netherlands.

* Equal contribution

Corresponding authors: Pierre H Mangin, Université de Strasbourg, INSERM, EFS Grand-Est, BPPS UMR-S1255, FMTS, 10 rue Spielmann, F-67065 Strasbourg, France; Phone: (+33) 3 88 21 25 25; Fax: (+33) 3 88 21 25 21; E-mail: pierre.mangin@efs.sante.fr; Mikhail A Panteleev, Center for Theoretical Problems of Physicochemical Pharmacology, Russian Academy of Sciences, Moscow, Russia; E-mail: mapanteleev@yandex.ru.

Supplementary Materials and Methods

Measurement of the blood flow after vessel puncture

An ultrasound Doppler probe was used to measure the absolute blood flow in a vessel of interest: carotid artery, aorta or saphenous vein. Ultrasound Doppler measurements in the intact carotid artery, aorta and saphenous vein indicated mean blood flow velocities of 5±0.2, 2.9±0.6 and 1.9±0.1 cm/s, respectively (**Figure 2A, 3A**). Before vessel puncture, two laser Doppler probes were placed on both sides of the site of injury to measure the blood flow continuously relative to that in the intact vessel. The laser Doppler probes were placed perpendicular to the vessel. Based on the company's recommendations (Moor instruments), the angle of insonation has no major impact on the measure, as the Doppler signal is broadened and rather has a random scatter. The mean relative blood flow velocity in the intact vessel was calculated for each probe in each experiment. The time resolution of the Doppler probes does not allow to take into account the pulsatility of the flow. We collected the mean value during a constant time interval, and we did not modify this parameter because this adds an excessive noise to the recording. The accuracy of our data is +/- 10% of the measured value, and the precision is +/- 3% in accordance with the technical specifications. The vessel was then punctured and the blood flows were converted into absolute values by multiplying by the normalizing coefficient, which was calculated by dividing the mean blood flow velocity in the intact vessel by the mean relative blood flow velocity in the same vessel (**Supplementary Figure 1A**). To test the validity of our measurements, we checked the consistency of our probes by constructing a correlation curve (**Supplementary Figure 1B**). We found that the values obtained with the two probes in the carotid artery and the aorta agreed well. In contrast, the measurements performed in the saphenous vein did not agree, which may be explained by the fact that the downstream signal during baseline measurements was strongly elevated (**Supplementary Figure 1C, Figure 3C**). This could result in an underestimation of the shear rate at the edge of the wound, but would not change the main finding, which was that high shear rates occur.

Measurement of the blood flow after transection of the spermatic artery

Two regions of the spermatic artery were exposed: one site to place the Doppler probe and the other to perform transection. One laser Doppler probe was used to measure

the blood flow before (baseline signal) and after disruption of the vessel with micro-scissors. The flows were converted into absolute values by multiplying by the normalizing coefficient, which was calculated by dividing the mean blood flow velocity in the intact vessel by the mean relative blood flow velocity in the same vessel. Due to the small diameter of the spermatic artery, it was not possible to measure the absolute blood flow velocity in the intact vessel using an ultrasound Doppler probe. To circumvent this problem, we determined the blood flow velocity in the intact spermatic artery using the laser Doppler probe and compared the measurements in this vessel with those in the intact aorta and carotid artery. Firstly, the relative blood flow velocities were measured sequentially in the intact carotid artery, aorta and spermatic artery using one laser Doppler probe for each mouse (**Supplementary Figure 1D**). The normalizing coefficient was calculated by dividing the mean blood flow velocity in the intact carotid artery by the mean relative blood flow velocity in this vessel as described above, and this coefficient was used to convert the blood flow velocities in all vessels into absolute values (**Supplementary Figure 1E**). In these experiments, the mean blood flow velocities in the intact aorta and spermatic artery were found to be 2.6±0.6 and 3.8±1.5 cm/s, respectively. It was shown that there was no significant difference between the mean blood flow velocities in the intact aorta determined using this method or using an ultrasound Doppler probe (**Supplementary Fig. 1F**).

Computational model to calculate the flow parameters after puncture or transection of murine or human vessels

To calculate the shear rate and elongational flow in murine and human vessels, we developed a computational fluid dynamics model of blood flow in the injury region. To model the time-dependent blood flow and pressure distribution in 3D, we employed standard methods of computational hydrodynamics. The blood was treated as a continuous incompressible non-Newtonian fluid in a Carreau-Yasuda model [1] (1), with parameters (**Supplementary Table 2**) derived from experimental data for the viscosity of murine blood [2] (**Supplementary Figure 2H**):

$$\mu = \mu_{inf} + (\mu_0 - \mu_{inf})[1 + (\lambda\dot{\gamma})^2]^{\frac{n-1}{2}}$$
$$\dot{\gamma} = max(\sqrt{D:D}, \dot{\gamma}_{min}) \quad (1)$$
$$D = \frac{1}{2}[\nabla u + (\nabla u)^T]$$

Comsol Multiphysics software (COMSOL Inc., Burlington, MA, USA) was employed for computations, using the finite element method to study time-dependent numerical solutions of the Navier-Stokes equations in 3D. The vessel was modeled as a tube representing the vessel wall with an outer diameter based on experimental measurements and a thickness on literature values [3-5] (**Supplementary Table 4**). A wound was represented as a hole in the wall of the tube (**Supplementary Table 1, 3**). The simulation involved calculation of the non-stationary flow field using numerical solutions of the Navier-Stokes equations (with a laminar flow approximation) (2):

$$\rho\frac{\partial u}{\partial t} + \rho(u\cdot\nabla)u = \nabla\cdot[-\rho I + \mu(\nabla u + (\nabla u)^T)] + F$$
$$\rho\nabla\cdot(u) = 0 \qquad (2)$$

where p is the pressure and I the unity tensor, u represents the velocity vector and F is a volumetric force. No-slip boundary conditions (u=0) were chosen for the solid interfaces of the system, while for the boundary conditions of the flow upstream and downstream in the vessel, we used the experimental flows measured with Doppler probes. The vessel wall was considered to be non-deformable and the wound led to a larger tank with an upper lid at constant pressure. The outlet and inlet of the vessel were represented as abrupt ends with a uniform velocity profile. The length of the simulated part of the vessel was chosen to be sufficient for a fully developed flow to reach the stationary velocity profile. Atmospheric pressure conditions were chosen for the hole outlet and gradual tetrahedral extremely fine mesh refining was performed to check that the results were independent of this parameter (**Supplementary Table 5, Supplementary Figure 3**). The information about conditions where this model was used is in the **Supplementary Table 7**. Our results demonstrate that these types of injuries generate high shear rates at which blood is known to behave like a Newtonian fluid. To double check this, we calculated the shear rate distribution using a non-Newtonian fluid, and found no significant difference (**Supplementary Figure 4A**).

Hybrid computational model of the blood flow in the intact and injured venous network of the human arm

The model describes the distributions of blood flow and pressure in the venous system of the human arm in the normal state and following injury. The venous system is divided

into two compartments. The first simulates the network of undamaged vessels in a simplified 1D approximation. In our work, we considered the following vessels: cephalic vein, basilic vein, subclavian vein, axillary vein, brachial veins, ulnar veins and radial veins. The model of each vein assumes that the pressure difference Δp measured between the ends of the vessel is proportional to the blood flow q propagating through the vessel with a coefficient of resistance R (3, 4):

$$\Delta p = qR \tag{3}$$

$$R = \frac{8\mu l}{\pi r^4} \tag{4}$$

where μ is the dynamic viscosity of blood, l is the length of the vessel and r is its radius. The influence of gravity and the tissues adjacent to the vessel which deform it were not taken into account.

The electronic-hydraulic analogy (EHA) was employed to model vessels of the first compartment. This analogy establishes the compliance between physical quantities in the theory of electrical circuits and in hydrodynamics. Each vessel is characterized by a resistance, which can be calculated with equation (4) using the geometric parameters of the vessel [6,7] (**Supplementary Table 6**), and is a coefficient of proportionality between the pressure difference at the ends of the vessel and the flow through the vessel according to Poiseuille's equation (3). Each vessel is designated by a rectangle, similarly to the resistance in an electrical circuit schema (**Figure 5D**). The pressure conditions used as boundary conditions are designated as sources of constant "voltage". The boundary conditions linking two compartments are described as direct current sources, which have the dimensions of a flux. This allows one to write a system of equations for the vascular network using laws analogous to Kirchhoff 's laws (5-17):

$$\epsilon_{in} - \epsilon_{out} = I_{RaV2}R_{RaV2} + I_{BrVr}R_{BrVr} + I_{AV}R_{AV} + I_{SV}R_{SV} \tag{5}$$

$$0 = I_{UV2}R_{UV2} + I_{BrVu}R_{BrVu} - R_{BrVr} - I_{RaV1}R_{RaV1} \tag{6}$$

$$0 = I_{BVl}R_{BVl} + I_{BVu}R_{BVu} - I_{BrVu}R_{BrVu} - I_{UV1}R_{UV1} \tag{7}$$

$$0 = I_{UV1}R_{UV1} - I_{UV2}R_{UV2} \tag{8}$$

$$0 = I_{CVl}R_{CVl} + I_{CVu}R_{CVu} - I_{AV}R_{AV} - I_{BrVr}R_{BrVr} - I_{RaV2}R_{RaV2} \tag{9}$$

$$\epsilon_{in} - \epsilon_{out} = I_{CVl}R_{CVl} + I_{CVu}R_{CVu} + I_{SV}R_{SV} \tag{10}$$

$$I_{SV} = I_1 + J_1 + J_2 \tag{11}$$

$$I_1 = I_{RaV1} + I_{RaV2} + I_{UV1} + I_{UV2} + I_{BVl} + I_{CVl} \tag{12}$$

$$I_{BrVr} = I_{RaV1} + I_{RaV2} \tag{13}$$

$$I_{BrVu} = I_{UV1} + I_{UV2} \quad (14)$$

$$I_{BVu} = I_{BVl} + J_2 \quad (15)$$

$$I_{AV} = I_{BrVr} + I_{BrVu} + I_{BVu} \quad (16)$$

$$I_{SV} = I_{CVu} + I_{AV} \quad (17)$$

where ϵ_{in} and ϵ_{out} are the pressures at the inlet and outlet of the system, J_1 is the blood flow at the inlet of the median cubital vein, J_2 is the blood flow at the outlet of the median cubital vein, I is the blood flow through a vessel with its abbreviation in the subscript and R is the resistance of a vessel with its abbreviation in the subscript. SV is the subclavian vein, CVu the upper part of the cephalic vein, CVl the lower part of the cephalic vein, BVu the upper part of the basilic vein, BVl the lower part of the basilic vein, AV the axillary vein, BrVU the brachial vein (which divides into two ulnar veins), BrVR the brachial vein (which divides into two radial veins), UV1 the ulnar vein 1, UV2 the ulnar vein 2, RV1 the radial vein 1 and RV2 the radial vein 2.

The second compartment simulates the damaged vessel, the median cubital vein, in explicit 3D form as a straight rigid pipe with blood flowing in it. At the wall of the vessel, another pipe representing a catheter or vessel wall (in the case of puncture) joins it at an angle. It has a smaller radius than the vessel and the pipes form a T-shaped junction. The blood was treated as a continuous incompressible non-Newtonian fluid in a Carreau-Yasuda model (1), with parameters derived from the literature[8] (**Supplementary Table 2**). The stationary Navier-Stokes equation is solved in the 3D compartment (18):

$$\rho(u \cdot \nabla)u = -\nabla p + \mu \nabla u$$

$$\rho \nabla \cdot (u) = 0 \quad (18)$$

where u is the fluid velocity, p the pressure and ρ the density of the fluid.

The model allowed us to calculate the distributions of flow velocity, shear rate and pressure in the region of the injury. No-slip boundary conditions (u=0) were chosen for the solid interfaces of the system, while a pressure condition was used for the outlet of the injury (p=0). The boundary conditions at the inlet and outlet of the damaged vessel connected the first compartment with the second. The pressures calculated at the connection points of the current sources in the vascular network of the first compartment were transferred to the second compartment as the boundary conditions at the inlet and outlet of the vessel. Similarly, we equated the blood flows at the inlet

and outlet of the vessel in the second compartment with the currents of the first compartment.

Comsol Multiphysics software (COMSOL Inc., Burlington, MA, USA) was employed for computations. Each compartment was simulated sequentially at each iteration of the numerical method using an individual solver. The MUMPS (Multifrontal Massively Parallel Solver) direct solver was used to solve the system of equations of the first compartment. An iterative solver for sparse matrices based on the GMRES (Generalized Minimal Residual) method, with the AMG (Algebraic Multigrid) method of setting preconditions, was used to solve the system of equations of the second compartment. The information about conditions where this model was used is indicated in the **Supplementary Table 7**.

Supplementary Results

Possible mechanisms governing the decrease in shear rate with increasing wound size

To investigate the mechanisms of the variations in shear rate with injury size, we firstly considered the simple analytically solvable case of the Poiseuille flow of a stationary Newtonian fluid in a cylinder (19):

$$\begin{cases} v = \dfrac{1}{4\mu}\dfrac{\Delta p}{L}(R^2 - r^2) \\ \Delta p = \dfrac{8\mu L}{\pi R^4} Q \end{cases} \tag{19}$$

where v is the flow velocity at a distance r from the center of the cylinder of radius R, Δp the pressure difference between the ends of the cylinder, L the length of the cylinder, Q the blood flow through the cylinder and μ the dynamic viscosity of blood.

As a function of the radius, the wall shear rate γ increases linearly for a constant pressure drop and decreases as the inverse cube for a constant flow velocity (20):

$$\begin{cases} \gamma = \dfrac{dv}{dR} = \dfrac{1}{2\mu}\dfrac{\Delta p}{L} R, & \Delta p - const \\ \gamma = \dfrac{dv}{dR} = \dfrac{4Q}{\pi R^3}, & \Delta Q - const \end{cases} \tag{20}$$

This suggests that our experiments, where the shear rate decreased with increasing hole size, were performed under "constant flow" conditions. Indeed, evaluation of the flow through the wound in the model showed that the major part of the incoming blood flowed through the injury, which corresponds to essentially constant flow conditions. This agrees with our experimental data for the fraction of the blood flowing through the wound in the carotid artery and aorta (**Supplementary Figure 5B**).

To gain insight into the causes of the transition between these two fluid regimes, we calculated the hydrodynamic resistance of the wound as a function of its radius in each murine vessel (4). Thus, using the thickness of the vessel wall (**Supplementary Table 4**) as the parameter l, we determined a threshold above which the blood flow through the injury is governed by the capacity of the vessel supplying it, and below which only a fraction of the blood flow passes through the injury (**Supplementary Figure 5C-F**). This shift in the relative vessel-wound resistance determines the redistribution of the blood flow, which passes mostly into the downstream vessel network for small injuries and through the wound for large injuries.

References

1. Gijsen FJ, Allanic E, van de Vosse FN, Janssen JD. The influence of the non-Newtonian properties of blood on the flow in large arteries: unsteady flow in a 90 degrees curved tube. *J Biomech*. 1999;32(7):705-713.
2. Windberger U, Bartholovitsch A, Plasenzotti R, Korak KJ, Heinze G. Whole blood viscosity, plasma viscosity and erythrocyte aggregation in nine mammalian species: reference values and comparison of data. *Exp Physiol*. 2003;88(3):431-440.
3. Bas CE, Cwykiel J, Siemionow M. A New Supermicrosurgery Training Model of Saphenous Artery and Great Saphenous Vein Anastomosis for Development of Advanced Microsurgical Skills. *J Reconstr Microsurg*. 2017;33(6):426-434.
4. Korshunov VA, Wang H, Ahmed R, et al. Model-based vascular elastography improves the detection of flow-induced carotid artery remodeling in mice. *Sci Rep*. 2017;7(1):12081.
5. Liu G, Jia W, Sun V, Choi B, Chen Z. High-resolution imaging of microvasculature in human skin in-vivo with optical coherence tomography. *Opt Express*. 2012;20(7):7694-7705.

6. He Y, Liu H, Himeno R. A one-dimensional thermo-fluid model of blood circulation in the human upper limb. *International Journal of Heat and Mass Transfer*. 2004;47(12-13):2735-2745.

7. Shima H, Ohno K, Michi K, Egawa K, Takiguchi R. An anatomical study on the forearm vascular system. *J Craniomaxillofac Surg*. 1996;24(5):293-299.

8. Johnston BM, Johnston PR, Corney S, Kilpatrick D. Non-Newtonian blood flow in human right coronary arteries: steady state simulations. *J Biomech*. 2004;37(5):709-720.

9. Go YM, Son DJ, Park H, et al. Disturbed flow enhances inflammatory signaling and atherogenesis by increasing thioredoxin-1 level in endothelial cell nuclei. *PLoS One*. 2014;9(9):e108346.

10. Crouch AC, Cao AA, Scheven UM, Greve JM. In Vivo MRI Assessment of Blood Flow in Arteries and Veins from Head-to-Toe Across Age and Sex in C57BL/6 Mice. *Ann Biomed Eng*. 2020;48(1):329-341.

11. Stock SR, Müller B, Lang S, et al. High-resolution tomographic imaging of microvessels. 2008;7078:70780B.

12. Cwykiel J, Bas C, Siemionow M. A New Supermicrosurgery Training Model of Saphenous Artery and Great Saphenous Vein Anastomosis for Development of Advanced Microsurgical Skills. *Journal of Reconstructive Microsurgery*. 2017;33(06):426-434.

13. Schulz C, Kessinger CW, Kim JW, et al. Statins Improve the Resolution of Established Murine Venous Thrombosis: Reductions in Thrombus Burden and Vein Wall Scarring. *Plos One*. 2015;10(2):e0116621.

Supplementary Table 1. Geometric parameters of wounds in the carotid artery

Experiment	Circle	Ellipse	
	Radius, μm	a-semiaxis, μm	b-semiaxis, μm
Mouse 1	81	102	64
Mouse 2	113	141	91
Mouse 3	140	191	102
Mouse 4	117	134	102
Mouse 5	61	67	56

Mouse 6	54	57	51

Supplementary Table 2. Fluid properties of murine blood

Parameter	Symbol	Murine value	Human value	Units
Zero shear rate viscosity	μ_0	13.88999e-3	0.056	Pa*s
Infinite shear rate viscosity	μ_{inf}	3.5e-3	3.5e-3	Pa*s
Model parameter #1	λ	0.82644	3.313	s
Model parameter #2	n	0.52988	0.3568	1
Density	ρ	1060	1060	kg/m^3

Supplementary Table 3. Geometric parameters of wounds in the aorta, saphenous vein

Vessel	Experiment	Radius, μm
Aorta	Mouse 1	85
	Mouse 2	34
	Mouse 3	20
	Mouse 4	122
	Mouse 5	53
Saphenous vein	Mouse 1	71
	Mouse 2	86
	Mouse 3	56
	Mouse 4	58
	Mouse 5	67
	Mouse 6	51
	Mouse 7	33

Supplementary Table 4. Geometric parameters of murine vessels

Vessel	Parameter	Value, μm	Reference
Carotid artery	Outer diameter	235	Go Y.M. et al., 2014[9]
	Wall thickness	17	Go Y.M. et al., 2014[9]
	Inner diameter	218	–
Aorta	Outer diameter	350	Colleen Crouch A. et al., 2019[10]

	Wall thickness	55	Müller B. et al., 2008[11]
	Inner diameter	295	–
Saphenous vein	Outer diameter	145	Bas C. E., 2017[12]
	Wall thickness	17	Kessinger C. W. et al., 2015[13]
	Inner diameter	128	–
Spermatic artery	Outer diameter	66	experimentally measured (max: 72 μm; min: 53 μm)
	Wall thickness	50	Müller B. et al., 2008[11]
	Inner diameter	16	–

Supplementary Table 5. Element size parameters of the mesh in the model

Parameter	Normal mesh	Fine mesh	Finer mesh	Extra fine mesh	Extremely fine mesh
Maximum element size	1000	800	550	350	200
Minimum element size	180	100	40	15	2
Maximum element growth rate	1.5	1.45	1.4	1.35	1.3
Curvature factor	0.6	0.5	0.4	0.3	0.2
Resolution of narrow regions	0.5	0.6	0.7	0.85	1

Supplementary Table 6. Geometric parameters of human vessels

Vessel	Length, cm	Radius, μm	Resistance, $\frac{Pa \cdot s}{ml}$
Subclavian vein	20	5,300	2.1
Cephalic vein (upper part)	33	950	3,368
Cephalic vein (lower part)	17		1,735
Medial cubital vein	9	900	1,140
Basilic vein (upper part)	17	950	1,735

Basilic vein (lower part)	33		3,368

Supplementary Table 7. Models for shear rate calculation

Type of injury	Vessel	Figures	Model	Data-in	Source of data-in
Puncture	Carotid Artery	Fig. 2C-H, 3G, 6A; Sup. Fig. 2B, 2F, 2G, 3A, 3E	Comsol model based on Navier-Stokes equation (NSe)	Velocity profile measured by combination of laser and ultrasound Doppler probes	Individual curve for each mice such as Fig. 2B
				Size of the wound	Sup. Table 1
				Size of the vessel	Sup. Table 4
		Fig. 5G; Sup. Fig. 2F, 2G	Poiseuille's equation	Blood loss volume	Experimental data
				Size of the wound	Sup. Table 1
	Aorta	Fig. 3D, 3F-H, 6A; Sup. Fig. 3A, 3E	Comsol model based on NSe	Velocity profile measured by combination of laser and ultrasound Doppler probes	Individual curve for each mice such as Fig. 3B
	Saphenous vein	Fig. 3E-H, 6A; Sup. Fig. 3E		Size of the wound	Sup. Table 3
				Size of the vessel	Sup. Table 4
	Median cubital vein	Fig. 5E, 6A-C, 6E; Sup. Fig. 3E	Hybrid COMSOL model based on NSe and MEHA method	Parameters of vessels	Sup. Table 6
				Pressure values	
		Fig. 5B-C	Poiseuille's equation	Blood loss volume	Experimental data
				Size of the catheter	-

Transection	Spermatic artery	Fig. 4E-H	Comsol model based on NSe	Velocity profile measured by combination of laser and ultrasound Doppler probes	Individual curve for each mice such as Fig. 4B
				Size of the vessel	Sup. Table 4

Supplementary Figure Legends

Supplementary Figure 1. Measurement of the mean blood flow velocities in intact murine vessels. A, The dot plots show the normalization coefficients for top and bottom (b-m) laser Doppler probes in the intact carotid artery, aorta and saphenous vein. Data are presented as the mean ± the standard error of the mean (SEM) and individual symbols represent individual mice. **B,** The graph shows the normalization coefficients for bottom laser Doppler probes (D.p.) in the intact carotid artery, aorta and saphenous vein, as a function of the normalization coefficients for top laser Doppler probes in these vessels. Individual symbols represent individual mice. **C,** The curves show the blood flow velocities in relative units upstream and downstream of the site of injury after puncture of the saphenous vein, as a function of the time after injury. **D,** The curves show the blood flow velocities in relative units in the intact spermatic artery, aorta and carotid artery, as a function of time. **E,** The curves show the blood flow velocities in absolute units in the intact spermatic artery, aorta and carotid artery, as a function of time. **F,** The dot plots show the mean blood flow velocities in the intact aorta calculated using ultrasound Doppler probe measurements, or laser Doppler probe measurements with a normalizing coefficient. Data are presented as the mean ± SEM and individual symbols represent individual mice.

Supplementary Figure 2. Model of the puncture of a mouse carotid artery. A-G, Thrombus formation was induced by needle puncture of the left common carotid artery of wild-type mice. **A, C, E,** Representative fluorescence images of the thrombus (platelets labeled with $DIOC_6$ in green) at the indicated time points after injury with a 25G needle. Scale bar: 500 µm. The arrows represent the direction of blood flow and the dotted lines represent the borders of the vessel. **B, D, F,** Representative scanning

electron microscopy images of the external thrombus obtained at 81 s (**B**), 26 s (**D**) and 27 s (**F**) after vessel puncture. The black solid line represents the border of the thrombus. Scale bar: 1 mm (**B**), 250 µm (left **D, F**), 5 µm (right **D, F**). **G,** The dot plots show the injury diameter calculated using data from fluorescent and scanning electron microscopies. Individual symbols represent individual mice. The symbols pertaining to the same mouse are joined by a line. Result was compared by paired t-test. Ns $p > 0.05$. **H,** The dot plot shows the median viscosity of murine whole blood (40% Hct), as a function of the shear rate. The dots are approximated by a Carreau-Yasuda equation.

Supplementary Figure 3. Comparison of different meshes in the model of the puncture of a mouse carotid artery. A-E, Representative image obtained with the model, whose 3D geometry is presented in the top middle. The red rectangle defines the zx-section of observation and the injury appears at the top of the cylinder mimicking the carotid artery. At the side, the colors indicate the shear rates 10.75 s after puncture in the zx-section. The scheme in the bottom middle depicts the positions of the external space and vessel lumen with arrows indicating the direction of blood flow in the colored shear rate figure. In the middle, the big figure shows the mesh conditions of the calculation domain (blue). The scheme in the lower right corner depicts the positions of the external space and vessel lumen with arrows indicating the direction of blood flow. The mesh types are normal (**A**), fine (**B**), finer (**C**), extra fine (**D**), extremely fine (**E**). **F,** The curve shows the shear rate at the edge of the wound calculated using the model with five different meshes (normal, fine, finer, extra fine and extremely fine), as a function of the time after injury.

Supplementary Figure 4. Measurement of the shear rates in the model of the puncture of a mouse carotid artery. A, The curve shows the shear rate at the edge of the wound calculated using the model with non-Newtonian and Newtonian fluids, as a function of the time after injury. **B-F,** Injury was induced by needle puncture of the left common carotid artery of wild-type mice. **B,** The curves show the blood flow velocities in relative units upstream and downstream of the site of injury, as a function of the time after injury. **C,** The dot plots show the times after injury at which the maximum blood flow velocities upstream of the injury were reached, or the blood flow velocities upstream of the injury stabilized. Data are presented as the mean ± SEM and individual symbols represent individual mice. **D,** The dot plot shows the mean

stable blood flow velocities upstream of the injury. Data are presented as the mean ± SEM and individual symbols represent individual mice. **E,** The dot plots show the maximum shear rates at the edge of the wound calculated using Navier-Stokes equation and those calculated using Poiseuille's equation. Individual symbols represent individual mice. The symbols pertaining to the same mouse are joined by a line. Result was compared by paired t-test. Ns $p > 0.05$. **F,** The dot plots show the mean blood flow velocities through the injury calculated using ultrasound Doppler probe measurements, or blood loss measurements. Individual symbols represent individual mice. The symbols pertaining to the same mouse are joined by a line. Result was compared by paired t-test. * – $p \leq 0.05$.

Supplementary Figure 5. Mechanism governing the decrease in shear rate with increasing wound size. A, The graph shows the maximum blood flows through the wound as the percentage of the blood flows upstream of the injury at the same time point after vessel puncture, as a function of the diameter of the injury. Individual symbols represent individual mice. **B-D,** The green curves show the hydrodynamic resistance of the wound as a function of the radius of the injury for the carotid artery (**B**), aorta (**C**) and spermatic artery (**D**). The horizontal blue lines represent the hydrodynamic resistance of the carotid artery (**B**), aorta (**C**) and spermatic artery (**D**). **E,** The dot plot shows the maximum shear rates at the edge of the wound after puncture of the carotid artery, aorta, saphenous vein or median cubital vein, as a function of the radius of the injury. Individual symbols represent individual mice or donors. The vertical lines represent the threshold values of the injury radius at which the hydrodynamic resistances of the carotid artery (green), aorta (blue), saphenous vein (orange) and median cubital vein (purple) are equal to the hydrodynamic resistance of the wound.

Supplementary figure 1

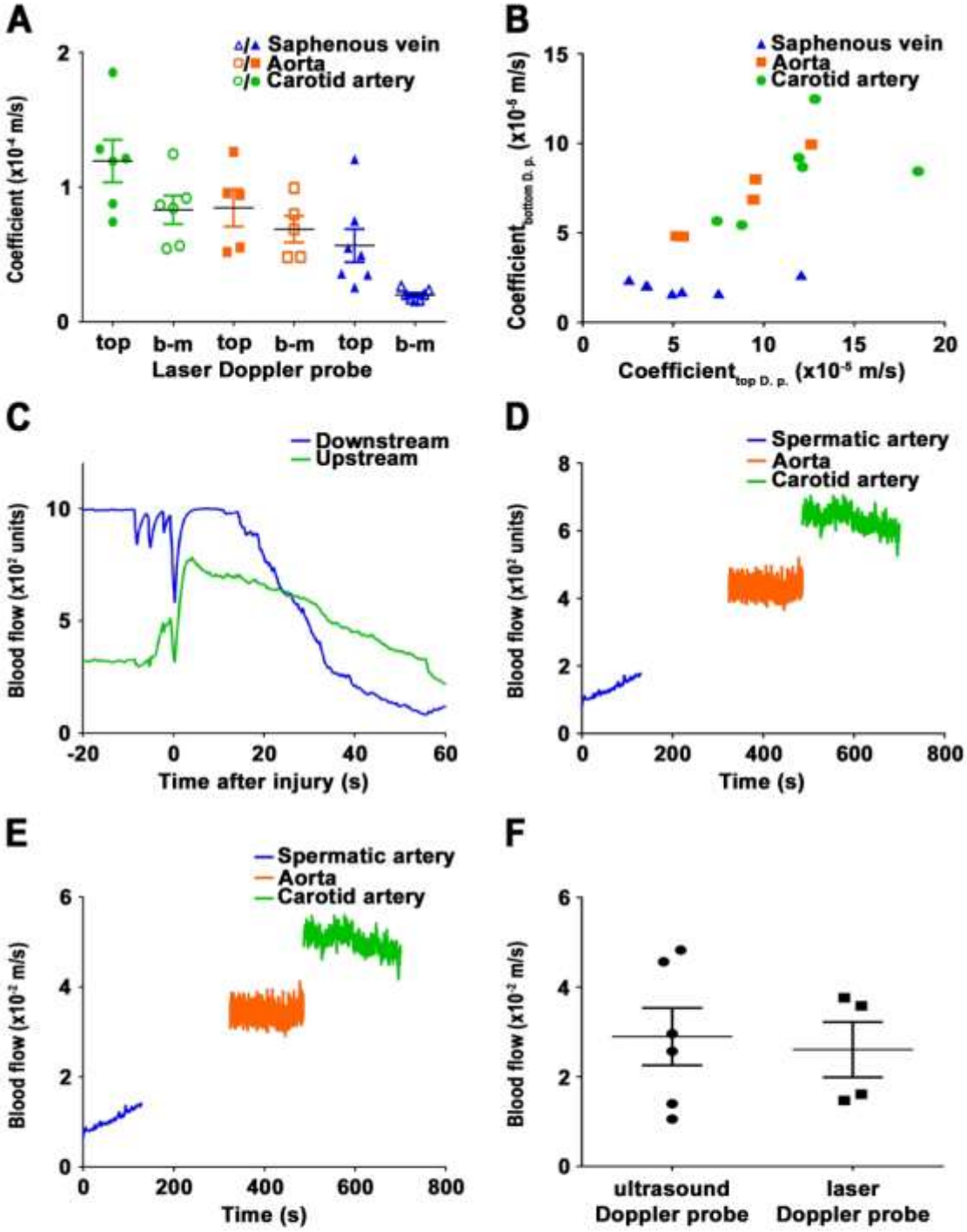

Supplementary figure 2

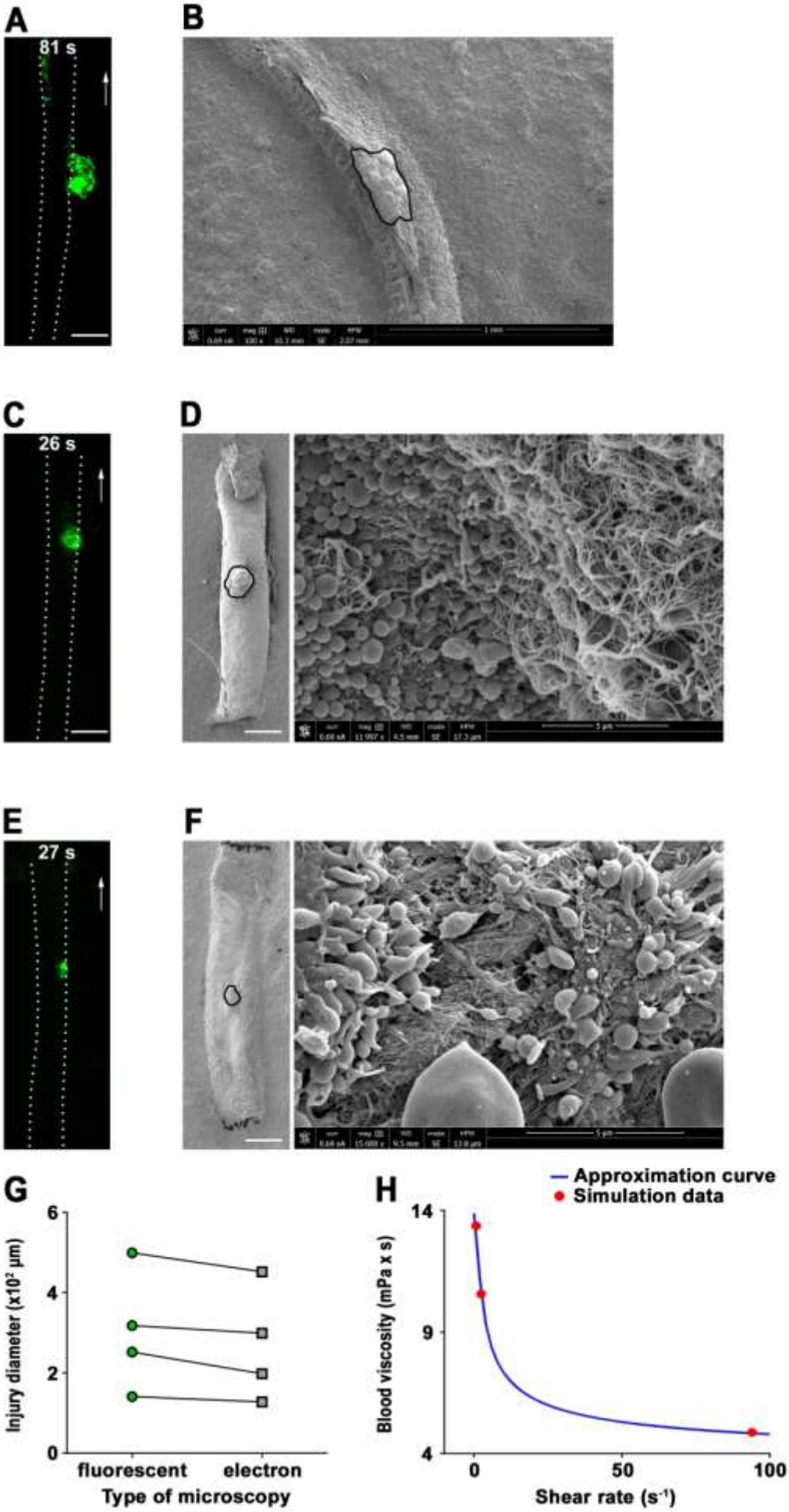

Supplementary figure 3

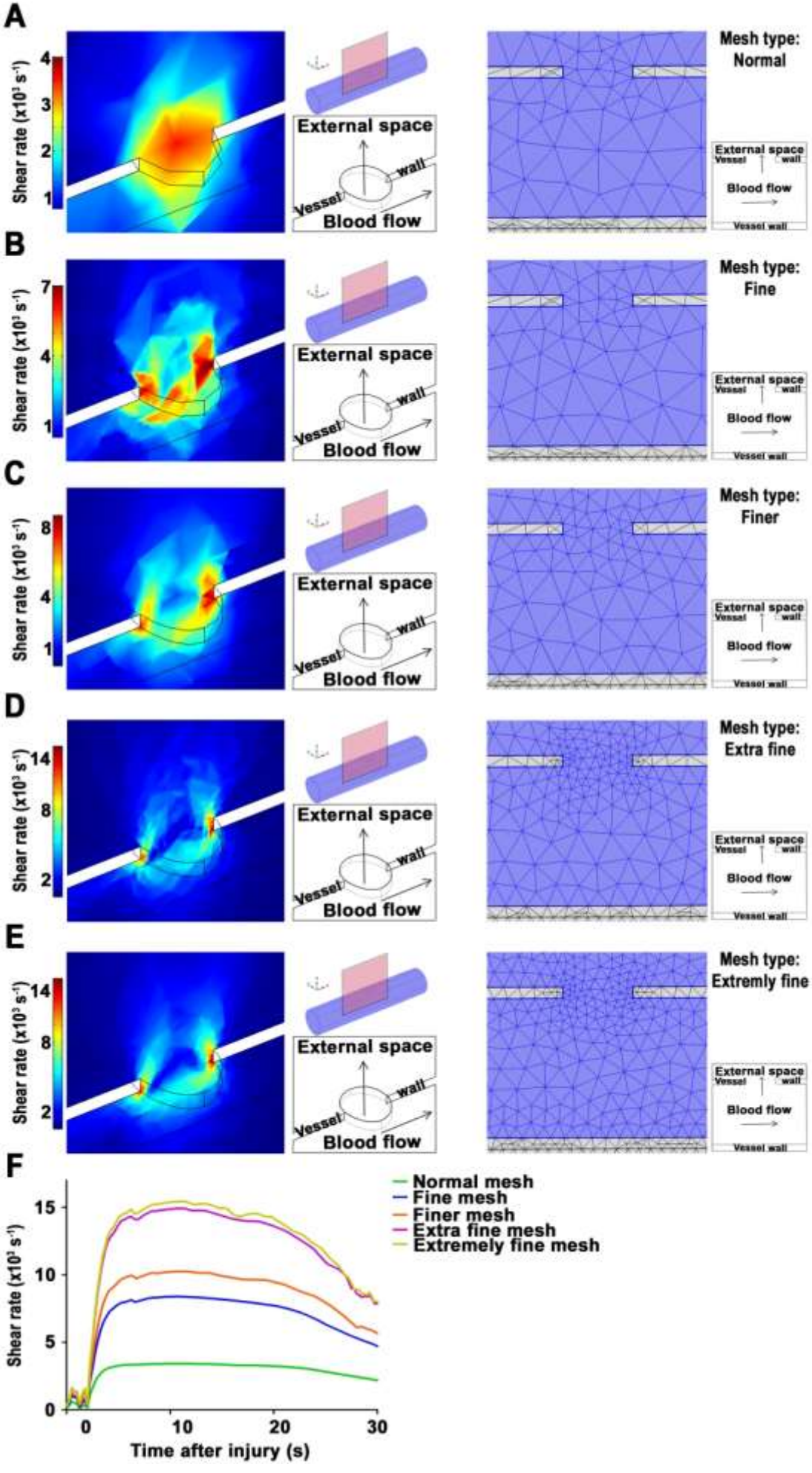

Supplementary figure 4

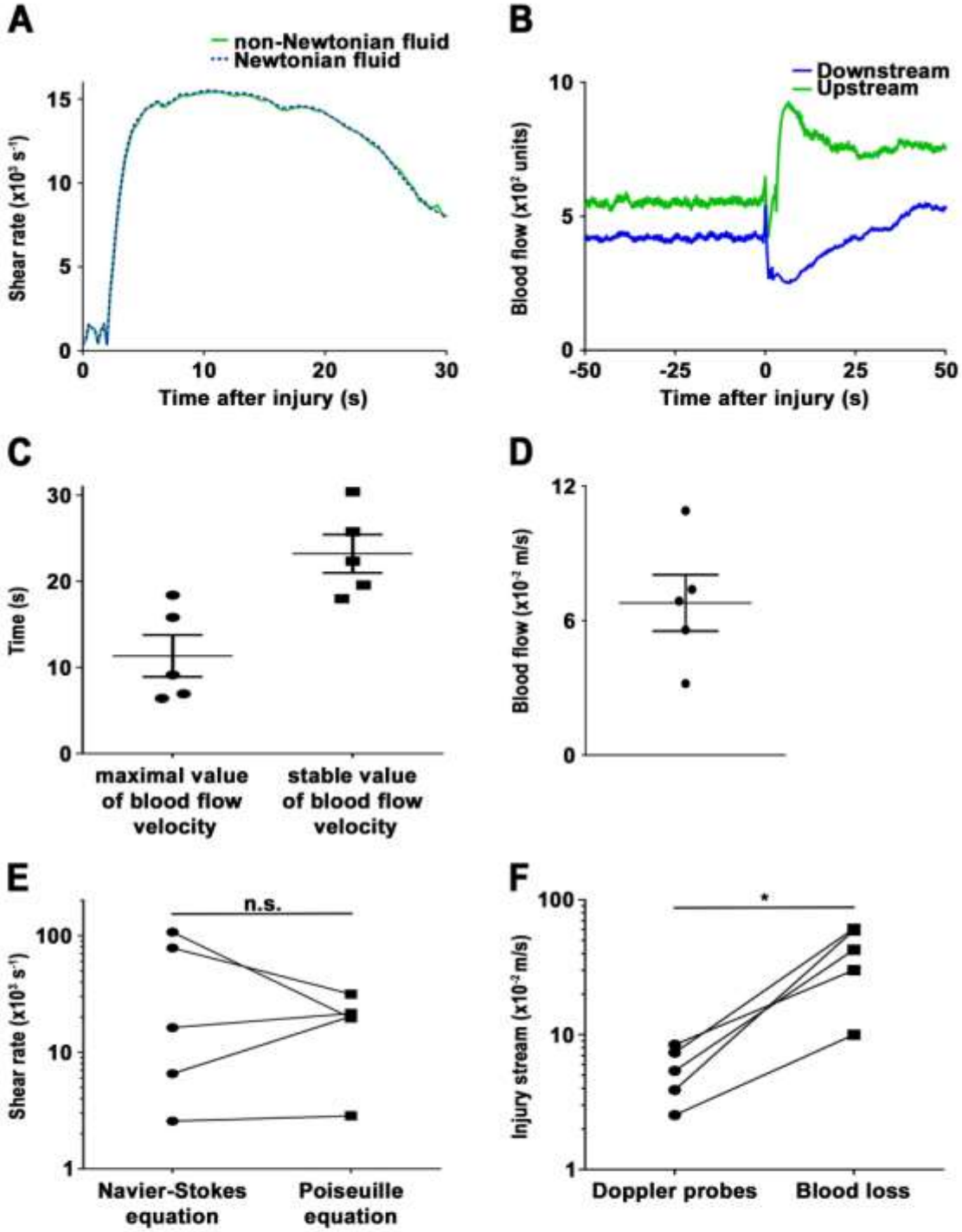

Supplementary figure 5

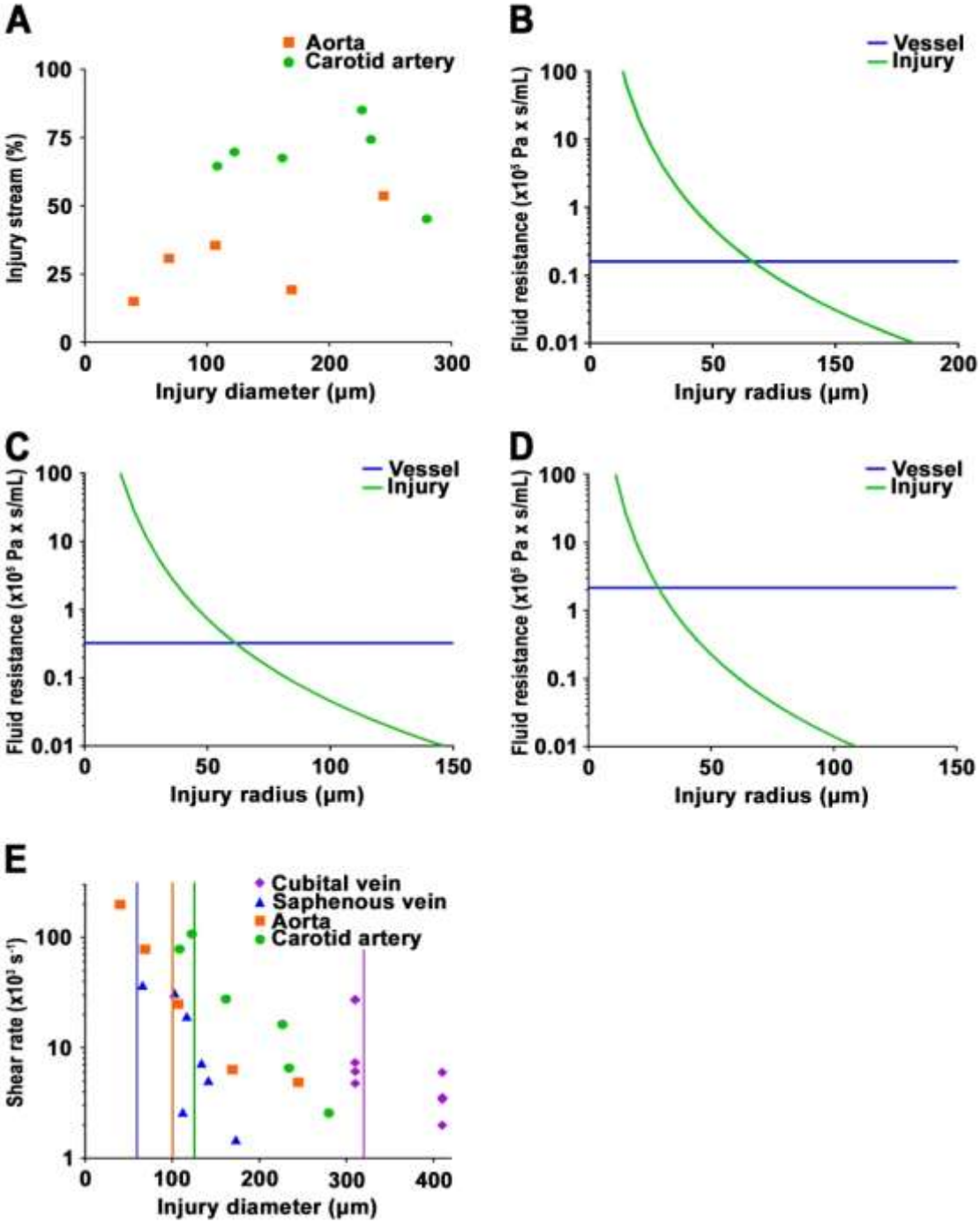

Conclusion

My study shows that after vessel puncture of the murine carotid artery, the shear rate values appear very elevated with medians of 22,000 s^{-1} at the edge of the hole where platelets start to adhere. The shear rates were increased up to 3 times as compared to a carotid with a stenosis and 20 times when compared to an intact carotid. Similar results were obtained after puncture of the aorta and saphenous vein with medians of shear rates reaching 25,000 s^{-1} and 7,000 s^{-1}, respectively. In all models, the high shear conditions were accompanied by elevated levels of elongational flow exceeding the threshold levels required for unfolding of vWF. Similar shear and elongational levels were observed after transection of the mouse spermatic artery with medians of 14,500 s^{-1} and 1,000 s^{-1}, respectively. In humans, the level of shear at the edge of a wound was highly increased after vessel damage with a catheter and reached 2,000-27,000 s^{-1}. Another interesting observation made in the puncture models in human and mice, was that the shear rates decreased steeply with increasing injury size. This phenomenon was explained by the low hydrodynamic resistance of the injuries as compared to that of the downstream vessel network.

All of these results indicate that various types of lesions in small and large mouse and human vessels can result in extremely high shear rates, which was unexpected. We propose that elevated shear rates are not specific to pathological conditions and can be equally relevant to the physiological process of hemostasis after vessel damage.

The role of integrin α5β1 in thrombus formation during hemostasis and arterial thrombosis

Publication 2:

«Characterization of the role of integrin α5β1 in platelet function, in hemostasis and experimental thrombosis»

Emily Janus-Bell[#1], Alexandra Yakusheva [#1,2], Cyril Scandola[1], Nicolas Receveur[1], Usman Muhammad Ahmed[1], Clarisse Mouriaux[1], Catherine Bourdon[1], Cécile Loubière[1], Anita Eckly[1], Yotis A Senis[1], Mikhail A Panteleev[2], Christian Gachet[1], Pierre H Mangin[1]

[1]Université de Strasbourg, INSERM, EFS Grand-Est, BPPS UMR-S1255, FMTS, F-67065 Strasbourg, France;

[2]Center for Theoretical Problems of Physicochemical Pharmacology, Moscow 119991, Russia

[#]These authors contributed equally to this work.

Thromb Haemost. 2021 Oct 1. doi: 10.1055/a-1659-6214

Introduction

Platelets express at their surface five different integrins of the β1 and β3 families: The β1 integrins comprising α2β1, α5β1 and α6β1, and the β3 integrins including αvβ3 and αIIbβ3. Among the β1 integrin family, α2β1 and α6β1 are involved in the initial step of platelet adhesion and activation to adhesive proteins of the subendothelium, and their roles in hemostasis and thrombosis have also been well studied (He et al., 2003; Schaff et al., 2013). While the role of integrin α5β1 in platelet adhesion, activation and aggregation on fibrillar fibronectin has been identified (Maurer et al., 2015), the importance of this integrin in hemostasis and in experimental thrombosis remained unknown when we started this work.

The objective of this project was to evaluate the role of integrin α5β1 in hemostasis and experimental thrombosis. For this purpose, mice invalidated for the α5β1 integrin in the platelet lineage (PF4Cre-α5-/-) were generated. We first characterized these mice and their platelets by evaluating the expression of surface receptors, in order to ensure the absence of major abnormalities. Then, we studied *in vitro* platelet functions by performing aggregometry, determining platelet activation state in response to soluble agonists by flow cytometry and by perfusing murine whole blood on different adhesive proteins. Further, we evaluated the role of integrin α5β1 in arterial thrombosis *in vivo* in three different experimental animal models of arterial thrombosis for which the rheological conditions as well as the exposed adhesive proteins were different. Finally, we examined the role of integrin α5β1 in hemostasis by using a tail bleeding time model. This work has been published in *Thrombosis and Haemostasis* in October 2021.

Accepted Manuscript online: 2021-10-01 Article published online: 2021-11-10

Characterization of the Role of Integrin α5β1 in Platelet Function, Hemostasis, and Experimental Thrombosis

Emily Janus-Bell[1,*] Alexandra Yakusheva[1,2,*] Cyril Scandola[1] Nicolas Receveur[1] Usman Muhammad Ahmed[1] Clarisse Mouriaux[1] Catherine Bourdon[1] Cécile Loubière[1] Anita Eckly[1] Yotis A. Senis[1] Mikhail A. Panteleev[2] Christian Gachet[1] Pierre H. Mangin[1]

[1]Université de Strasbourg, INSERM, EFS Grand-Est, BPPS UMR-S1255, FMTS, Strasbourg, France
[2]Center for Theoretical Problems of Physicochemical Pharmacology, Cellular Hemostasis Lab, Moscow, Russia

Address for correspondence Pierre H. Mangin, PhD, Université de Strasbourg, INSERM, EFS Grand-Est, BPPS UMR-S1255, FMTS, 10 rue Spielmann, F-67065 Strasbourg, France (e-mail: pierre.mangin@efs.sante.fr).

Thromb Haemost 2022;122:767–776.

Abstract

Objective Integrins are key regulators of various platelet functions. The pathophysiological importance of most platelet integrins has been investigated, with the exception of α5β1, a receptor for fibronectin. The aim of this study was to characterize the role of α5β1 in megakaryopoiesis, platelet function, and to determine its importance in hemostasis and arterial thrombosis.

Approach and Results We generated a mouse strain deficient for integrin α5β1 on megakaryocytes and platelets (PF4Cre-α5$^{-/-}$). PF4Cre-α5$^{-/-}$ mice were viable, fertile, and presented no apparent signs of abnormality. Megakaryopoiesis appears unaltered as evidence by a normal megakaryocyte morphology and development, which is in agreement with a normal platelet count. Expression of the main platelet receptors and the response of PF4Cre-α5$^{-/-}$ platelets to a series of agonists were all completely normal. Adhesion and aggregation of PF4Cre-α5$^{-/-}$ platelets under shear flow on fibrinogen, laminin, or von Willebrand factor were unimpaired. In contrast, PF4Cre-α5$^{-/-}$ platelets displayed a marked decrease in adhesion, activation, and aggregation on fibrillar cellular fibronectin and collagen. PF4Cre-α5$^{-/-}$ mice presented no defect in a tail-bleeding time assay and no increase in inflammatory bleeding in a reverse passive Arthus model and a lipopolysaccharide pulmonary inflammation model. Finally, no defects were observed in three distinct experimental models of arterial thrombosis based on ferric chloride-induced injury of the carotid artery, mechanical injury of the abdominal aorta, or laser-induced injury of mesenteric vessels.

Conclusion In summary, this study shows that platelet integrin α5β1 is a key receptor for fibrillar cellular fibronectin but is dispensable in hemostasis and arterial thrombosis.

Keywords
- platelets
- arterial thrombosis
- integrin α5β1
- fibronectin

* *These authors contributed equally to this work.*

received
May 4, 2021
accepted after revision
August 3, 2021
published online
October 1, 2021

DOI https://doi.org/10.1055/a-1659-6214.
ISSN 0340-6245.

Georg Thieme Verlag KG, Rüdigerstraße 14, 70469 Stuttgart, Germany

Introduction

Platelets adhere, become activated, and aggregate at a site of vessel injury to form a hemostatic plug which stops bleeding. They are also involved in maintaining vascular integrity and in the arrest of inflammatory bleeding in various organs.[1] On the other hand, platelets play an instrumental role in arterial thrombosis by inducing the formation of an occlusive thrombus in a diseased artery, which results in life-threatening ischemic pathologies such as myocardial infarction or ischemic stroke.[2] The molecular mechanisms involved in the interactions of platelets with an injured vessel wall have been extensively investigated. The initial step of attachment of circulating platelets is ensured by binding of the glycoprotein (GP) Ib–IX complex to subendothelial von Willebrand factor (vWF) at elevated shear rates.[3,4] When the flow is slower, β1 and β3 integrins assist the GPIb–IX complex to allow further platelet recruitment as well as stable adhesion to various extracellular matrix proteins.[3,4] This enables the interaction of GPVI with its ligands, including collagen, which initiates platelet activation.[5] Aggregation results through interactions of integrin αIIbβ3 with plasma fibrinogen, forming a plug that seals the breach in healthy vessels[6] or a pathological thrombus in diseased arteries.[2]

Platelets express at their surface five different integrins of the β1 and β3 families, namely α2β1, α5β1, α6β1, αvβ3, and αIIbβ3 whose main ligands are collagen, fibronectin, laminins, vitronectin, and fibrinogen, respectively. αIIbβ3, the most abundant integrin at the platelet surface,[7] enables platelet adhesion and aggregation through its binding to fibrinogen. This receptor plays a major role in hemostasis as evidenced by the hemorrhagic disorder known as Glanzmann's thrombasthenia, where αIIbβ3 is absent or nonfunctional.[8] It is also the target of a class of potent antiplatelet agents, illustrating its key involvement in arterial thrombosis.[9] The role of the other integrins, notably the β1 integrins, appears to be limited to the initial step of platelet adhesion and activation through interactions with extracellular matrix proteins. Concerning their importance, it has been shown that the absence of either α2β1 or α6β1 has no major impact on the tail-bleeding time in mice,[10,11] but reduces thrombosis in several experimental models.[11–13] In contrast, the importance of α5β1 in hemostasis and arterial thrombosis has never been studied.

Integrin α5β1 is a well-known receptor for fibronectin, which is broadly expressed on various cell types and plays an important role in migration and differentiation, especially during fetal development. As a consequence, knocking out the α5 gene results in death at the embryonic stage due to a defect in the mesoderm.[14] Concerning platelets, it has been shown that α5β1 together with αIIbβ3 plays a central role in platelet adhesion to fibronectin under shear flow.[15,16] Plasma fibronectin is very weak in supporting platelet adhesion and activation when compared to cellular fibronectin, which is probably explained by the presence of additional binding domains in the latter. In addition, both forms of fibronectin increase markedly their reactivity after polymerization and fiber formation, especially for cellular fibronectin.[17] However, although the role of α5β1 as a platelet receptor for fibronectin is recognized, its importance in hemostasis and arterial thrombosis remains unknown.

To study the role of integrin α5β1 in hemostasis and arterial thrombosis, we generated a new mouse strain which does not express this integrin on megakaryocytes or platelets (PF4Cre-α5$^{-/-}$) by crossing PF4Cre^{+} mice with animals expressing the α5 gene flanked by loxP sites. The PF4Cre-α5$^{-/-}$ megakaryocyte ultrastructure and maturation were characterized using transmission electron microscopy (TEM). The functions of platelets from PF4Cre-α5$^{-/-}$ mice were characterized using flow cytometry, aggregometry, and flow-based in vitro assays. We also employed a tail-bleeding time assay, a reverse passive Arthus (rpA) model, a lipopolysaccharide (LPS) pulmonary inflammation model, and experimental thrombosis models to evaluate the participation of integrin α5β1 in hemostasis and arterial thrombosis.

Methods

Materials

Materials and antibodies are described in the **Supplementary Material** (available in the online version).

Mice

Mice lacking integrin α5 in platelets were generated by crossing mice having a pure C57BL/6J background containing the *Itga5* gene flanked by loxP sites (α5$^{fl/fl}$) with pure C57BL/6J transgenic animals selectively expressing Cre recombinase in the megakaryocyte lineage under control of the platelet factor 4 (PF4) gene promoter (PF4-Cre^{+}; Jackson Laboratories, Bar Harbor, United States). The offspring were intercrossed to produce littermate animals homozygous for the floxed allele (PF4-Cre^{+}/α5$^{fl/fl}$, hereafter called PF4Cre-α5$^{-/-}$). C57BL/6J PF4-Cre^{+} mice served as controls (Ctrl), unless specified otherwise. Male and female mice were used.

Megakaryocyte Ultrastructure

Bone marrow samples were fixed in 2.5% glutaraldehyde and prepared for TEM as described previously.[18] Transversal thin sections of the entire bone marrow were cut, stained with uranyl acetate and lead citrate, and examined under a Jeol JEM 2100-Plus (Japan). The number of cells was expressed as the density per unit area (defined as one square of the grid, i.e., 16,000 µm^2). Megakaryocytes at stages I, II, and III were identified according to Eckly et al using distinct ultrastructural characteristics.[18] Stage I corresponded to a cell 10 to 15 µm in diameter with a large nucleus; stage II, to a cell 15 to 20 µm in diameter containing platelet-specific granules; and stage III, to mature megakaryocytes having a well-developed demarcation membrane system with clearly defined platelet territories and a peripheral zone. Megakaryocytes from three different mice were analyzed for both the control and the PF4Cre-α5$^{-/-}$ strain.

Platelet Count, Volume, and Glycoprotein Expression

Whole blood was collected into ethylenediaminetetraacetic acid (EDTA) (6 mM) after severing the tail of anesthetized

mice. Platelet count and volume were analyzed in an automatic cell counter (Scil Animal Care Company, Altorf, France) and surface GP expression was determined by flow cytometry. Expression of the α5 subunit was quantified in platelet lysates using automated capillary-based immunoassay (ProteinSimple Wes, San Jose, United States), as previously described.[19]

Platelet-Rich Plasma Aggregations

Mouse platelet-rich plasma (PRP) was prepared by centrifugation of blood collected on hirudin (100 U/mL) and adjusted to 300,000 platelets/μL with platelet-poor plasma from the same mouse. Platelet aggregation was measured as reported previously.[20]

Preparation and Properties of Washed Mouse Platelets

Washed mouse platelets were prepared as reported previously.[20] Agonist-induced binding of soluble fibrinogen and exposure of P-selectin were determined as previously described,[11] while phosphatidylserine exposure was quantified by Alexa Fluor 488-annexin V binding.

In Vitro Flow-Based Adhesion Assay

PDMS flow chambers (0.1 × 1 mm) were coated with vWF-binding protein (DDR2, 100 μg/mL), fibrinogen (100 μg/mL), laminins (100 μg/mL), collagen (200 μg/mL), or soluble cellular fibronectin (300 μg/mL) overnight at 4°C. Mechanical stretching of soluble cellular fibronectin was performed to form fibrillar cellular fibronectin as described previously.[17] To prevent nonspecific adhesion, the channels were blocked with phosphate-buffered saline containing human serum albumin (10 mg/mL) for 30 minutes at room temperature. Hirudinated (100 U/mL) whole blood was drawn from the abdominal aorta of anesthetized mice. The hirudinated blood was perfused through the chambers at the indicated wall shear rates and platelet adhesion was observed in real time and analyzed as detailed elsewhere.[11] Thrombus formation on fibrillar cellular fibronectin was monitored as previously reported.[17]

In Vivo Thrombosis Models

Platelets were labeled by administering 3,3′-dihexyloxacarbocyanine iodide to anesthetized mice. Ferric chloride ($FeCl_3$)-mediated thrombosis was induced by applying a 3 × 3 mm Whatman filter paper saturated with 7.5% $FeCl_3$ laterally to the carotid artery for 2.5 minutes. Thrombosis was initiated mechanically by pinching the abdominal aorta with forceps for 15 seconds. Thrombus formation was monitored in real time with a fluorescence microscope (Leica Microsystems, San Westlar, Germany) and a CCD (charge-coupled device) camera (CoolSNAP HQ2, Photometrics, Roper Scientific). Laser-induced thrombosis was triggered in mesenteric arterioles using a high-intensity 440-nm pulsed nitrogen dye laser applied with a Micropoint system (Photonic Instruments, Andor Technology, Belfast, United Kingdom) causing a deep injury. Thrombus formation was monitored in real time by bright field and fluorescence microscopy (Leica DM IRB) using a CMOS ORCA Flash V2 camera (Hamamatsu Photonics, Massy, France).

Bleeding Time

The bleeding time and volume of blood lost were determined by transversally severing a 3-mm segment from mouse tails, as reported previously.[21]

Cutaneous and Pulmonary Inflammation Models

An rpA reaction was elicited in anesthetized mice by intradermal injection of an antibovine serum albumin antibody (60 μg/spot), followed by retro-orbital injection of bovine serum albumin (75 mg/kg), as previously described.[1]

A lung inflammation model was induced in anesthetized mice by intranasal inoculation of *Pseudomonas aeruginosa* LPS (1 μg/mouse) in 60 μL of saline, as previously described.[1]

Statistical Analyses

Statistical analyses were performed with GraphPad Prism software (see figure legends).

Results

Characterization and Megakaryopoiesis of PF4Cre-α5-Deficient Mice

To study the role of platelet integrin α5β1, we crossed a mouse strain floxed for the α5 gene with a strain expressing Cre recombinase under control of the PF4 promoter (PF4Cre-α5$^{-/-}$). We used a quantitative biochemical approach to provide evidence that platelets from these mice expressed almost no integrin α5 anymore as compared to PF4-Cre mice (►**Fig. 1A, B**). No obvious abnormalities were detected in PF4Cre-α5$^{-/-}$ mice that were bred and developed normally. These mice have no increase in embryonic lethality, nor variation of the litter size and they present no abnormality in survival. Physical appearance and behavior are also unchanged.

PF4Cre-α5$^{-/-}$ mice presented a normal maturation and morphology of their megakaryocytes as assessed by their observation of ultrastructure on TEM images (►**Fig. 1C**). While the number of megakaryocytes in the bone marrow appears slightly increased in PF4Cre-α5$^{-/-}$ mice, the distribution of the different maturation stages was unchanged in PF4Cre-α5$^{-/-}$ as compared to control mice, suggesting no major impact of integrin α5 in megakaryopoiesis (►**Fig. 1D, E**). In agreement, we observed that deletion of α5 had no impact on the platelet count or volume (►**Table 1**). Thus, PF4Cre-α5-deficient mice appeared to be normal and PF4Cre-α5-deficient megakaryocytes displayed no difference in development and maturation.

Characterization of PF4Cre-α5-Deficient Platelets

The surface expression of the major GPs was normal (►**Table 1**), except for that of integrin α5 (►**Fig. 1A, B**). Using light-transmission aggregometry, we found that platelets

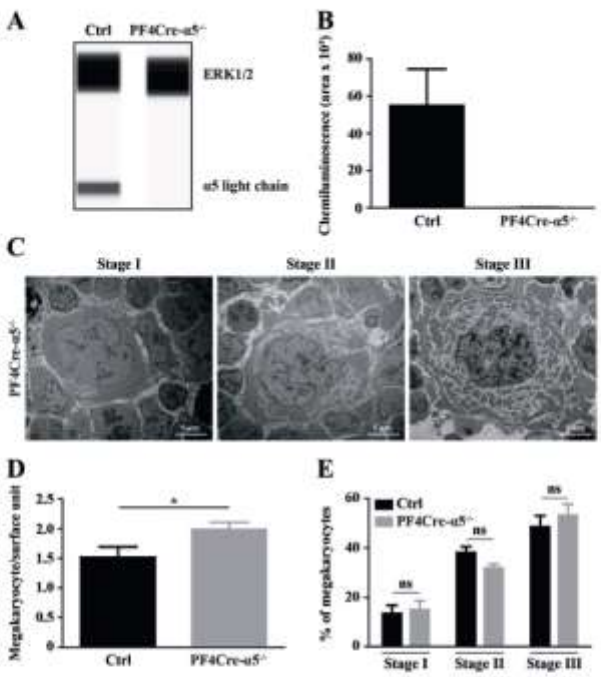

Fig. 1 Absence of platelet α5 expression and normal megakaryopoiesis in PF4Cre-α5-deficient mice. (**A**) Representative immunoblots of the α5 subunit and ERK1/2 (loading control). (**B**) Quantification of chemiluminescence peak areas of electropherograms obtained by capillary-based immunoassay of platelet lysates with anti-α5 antibody. Data expressed as mean ± standard error of the mean (SEM) from three separate experiments. (**C**) Transmission electron microscopy (TEM) images illustrating a typical ultrastructure of PF4Cre-α5$^{-/-}$ megakaryocytes at their different maturation stages. (**D**) In situ quantification of megakaryocytes in the bone marrow by TEM. Values are expressed as the mean ± SEM for three mice. (**E**) The distribution in the different maturation stages was established according to megakaryocyte morphology (see the Materials and Methods section) on TEM images. Values are expressed as the mean ± SEM for three mice. Data were compared by Student unpaired *t*-test (D) or Chi-square test (E); $^{*}p < 0.05$.

from PF4Cre-α5$^{-/-}$ mice aggregated normally in response to a series of agonists including adenosine diphosphate (ADP) (5 µmol/L), collagen (2.5 µg/mL), and U46619 (2 µmol/L) in PRP, presenting the advantage to contain plasma fibronectin (►**Fig. 2A, B**). Similar results were obtained with washed platelet aggregation to various agonists (►**Supplementary Fig. S1**, available in the online version). In addition, no differences in P-selectin exposure, fibrinogen binding or annexin V binding in response to ADP, thrombin, protein-ase-activated receptor 4 (PAR-4) peptide or convulxin were observed by flow cytometry in PF4Cre-α5$^{-/-}$ platelets as compared to controls (►**Fig. 2C–E**). This confirmed that platelets deficient in integrin α5 respond normally to a GPVI ligand and a series of soluble agonists. These results indicate that PF4Cre-α5-deficient platelets presented no defect in response to soluble agonists.

Characterization of PF4Cre-α5-Deficient Platelet Adhesion under Shear Flow

We next evaluated the ability of α5β1 to support platelet adhesion to various surfaces under flow by perfusing hir-udinated whole blood over immobilized proteins. We ob-served normal adhesion and rolling of PF4Cre-α5$^{-/-}$ platelets recruited to vWF bound to DDR2 at 1,500 s^{-1} (►**Fig. 3A**) and normal adhesion of these platelets to fibrino-gen and laminin at 300 s^{-1} (►**Fig. 3B**). In contrast, adhesion of PF4Cre-α5$^{-/-}$ platelets to immobilized fibrillar cellular fibronectin displayed a major defect as compared to controls, with a 78% reduction in the number of adherent platelets at 8 minutes (Ctrl: $7.1 \pm 0.7 \times 10^3$/mm^2; PF4Cre-α5$^{-/-}$: $1.6 \pm 0.05 \times 10^3$/mm^2) (►**Fig. 3C, D**). A detailed analysis indicated that α5β1 was important to establish the initial bond with fibronectin, as the recruitment of PF4Cre-α5$^{-/-}$ platelets to the surface was decreased by 55% as compared to controls (►**Fig. 3E**). Moreover, study of the adhesive behavior

Table 1 Platelet counts, volumes, and expression of major surface glycoproteins in Ctrl and PFC4re-α5$^{-/-}$ mice

	Ctrl	PF4Cre-α5$^{-/-}$	Number of mice
Platelet count	$1{,}095 \pm 48 \times 10^3$/µL	$1{,}119 \pm 29 \times 10^3$/µL	13
Mean platelet volume	4.98 ± 0.07 µm^3	4.68 ± 0.02 µm^3	13
αIIbβ3	5.28 ± 0.98	4.87 ± 1.20	6
α2	10.50 ± 0.07	11.03 ± 0.19	6
α5	1.23 ± 0.04	0.32 ± 0.04	9
α6	13.57 ± 0.22	13.27 ± 0.13	6
β1	4.69 ± 0.92	4.55 ± 1.01	6
GPIbα	5.01 ± 0.85	5.04 ± 0.15	6
GPV	0.99 ± 0.06	0.97 ± 0.03	6
GPIX	2.04 ± 0.12	2.06 ± 0.03	6
GPVI	1.66 ± 0.05	1.46 ± 0.04	6

Abbreviation: GP, glycoprotein.
Note: Platelet counts and volumes in Ctrl and PF4Cre-α5$^{-/-}$ mice were analyzed with an automatic cell counter; values represent the mean ± standard error of the mean (SEM). The surface expression of various glycoproteins on platelets in whole blood from Ctrl and PF4Cre-α5$^{-/-}$ mice was evaluated using selective antibodies and flow cytometry; results are expressed as the mean fluorescence intensity (MFI) ± SEM.

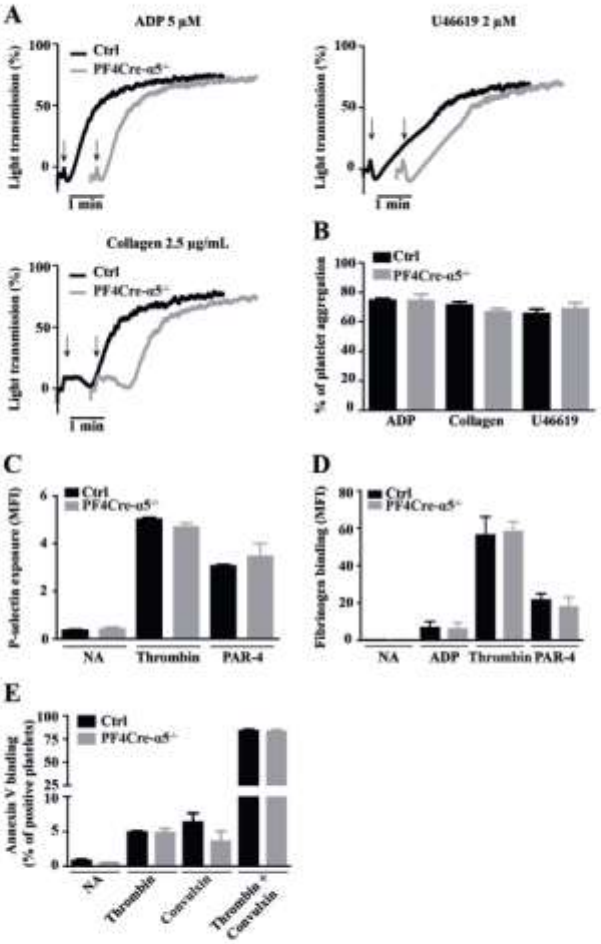

Fig. 2 Characterization of the functional properties of PF4Cre-α5$^{-/-}$ platelets. (**A, B**) Plasma-rich platelets (PRPs) (3.0×10^5 platelet/µL) from Ctrl and PF4Cre-α5$^{-/-}$ mice were stimulated with adenosine diphosphate (ADP) (5 µmol/L), U46619 (2 µmol/L), or collagen (2.5 µg/mL). *Arrows* indicate the point of agonist addition and aggregation profiles are representative of three separate experiments (A). The bar graph represents the percentage of platelet aggregation at 5 minutes ($n = 3$) (B). (**C, D**) Washed platelets (5.0×10^4/µL) from Ctrl and PF4Cre-α5$^{-/-}$ mice were stimulated for 10 minutes with ADP (2 µmol/L), thrombin (0.25 U/mL) or protease-activated receptor 4 (PAR-4) (1 mmol/L) and the binding of a fluorescein isothiocyanate (FITC)-conjugated anti-P-selectin antibody (C) or FITC-fibrinogen (D) was detected by flow cytometry. Results represent the mean fluorescence intensity (MFI) ± standard error of the mean (SEM) in three separate experiments performed in duplicate and were compared by the Mann–Whitney test. (**E**) Washed platelets (3.0×10^5/µL) from Ctrl and PF4Cre-α5$^{-/-}$ mice were stimulated with thrombin (0.25 U/mL), convulxin (15 nmol/L), or both for 15 minutes, incubated with Alexa Fluor 488-annexin V for 20 minutes and analyzed by flow cytometry. The forward light scatter and fluorescence intensity of 10,000 cells were collected with a logarithmic gain and the percentage of annexin V-positive platelets was determined in the upper quadrant of the plot. Data are expressed as the mean ± SEM in three separate experiments performed in duplicate.

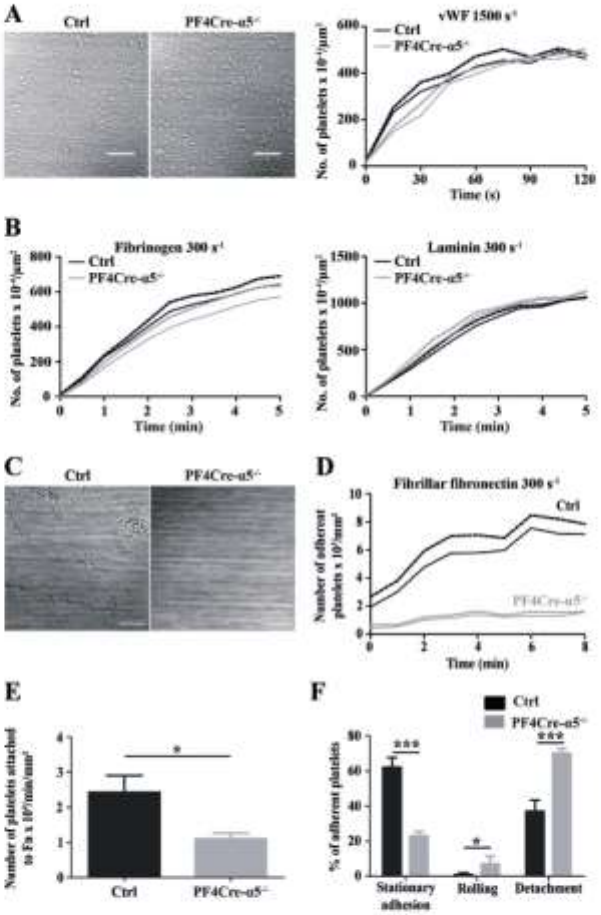

Fig. 3 PF4Cre-α5$^{-/-}$ platelets adhere normally to von Willebrand factor (vWF), fibrinogen, and laminin but not to fibronectin. (**A**) Whole blood from Ctrl ($n = 3$) and PF4Cre-α5$^{-/-}$ mice ($n = 3$) was perfused at 1,500 s^{-1} through PDMS flow chambers coated with vWF binding protein (DDR2, 100 µg/mL). Platelet adhesion was visualized in random fields by differential interference contrast (DIC) microscopy, scale bar: 20 µm. The number of adherent platelets was determined over 2 minutes. (**B**) Whole blood from Ctrl ($n = 3$) and PF4Cre-α5$^{-/-}$ mice ($n = 3$) was perfused at 300 s^{-1} through PDMS flow chambers coated with fibrinogen (100 µg/mL) or laminin 411 (100 µg/mL). Platelet adhesion was visualized in random fields by DIC microscopy and the number of adherent platelets was quantified over 5 minutes. (**C, D**) Whole blood from Ctrl ($n = 5$) and PF4Cre-α5$^{-/-}$ mice ($n = 4$) was perfused at 300 s^{-1} through PDMS flow chambers coated with cellular fibrillar fibronectin (300 µg/mL). Platelet adhesion was visualized in random fields by DIC microscopy, scale bar: 20 µm (C). The number of adherent platelets was determined over 8 minutes (D). (**E, F**) Whole blood from Ctrl ($n = 5$) and PF4Cre-α5$^{-/-}$ mice ($n = 5$) was perfused at 300 s^{-1} through PDMS flow chambers coated with fibronectin and platelet attachment was quantified over 60 seconds (E). The behavior of platelets on the fibronectin surface was recorded for 20 platelets per perfusion over a period of 90 seconds in 5 different movies (F). Results are expressed as the mean ± standard error of the mean (SEM) and in the curved graphs (A, B, and D) the *solid line* represents the mean and *dashed line* the SEM. Results were compared by two-way ANOVA (D), the Mann–Whitney test (E), or Chi-square test (F); $^*p < 0.05$.

of the recruited platelets showed a marked increase in numbers of PF4Cre-α5$^{-/-}$ platelets detaching from the surface and a clear decrease in stationary adhesion, highlighting the importance of α5β1 in stabilizing the bonds between platelets and fibronectin (►**Fig. 3F**). These results indicated that platelet integrin α5β1 is a major receptor for fibronectin supporting platelet attachment and maintaining the bonds to ensure stable adhesion.

A Major Defect of PF4Cre-α5$^{-/-}$ Platelet Activation and Aggregation on Fibrillar Cellular Fibronectin and Collagen

Platelet activation is a key step in thrombus formation. Microscopic fluorescence images showed a clear JonA-PE signal for control platelets accumulating on fibrillar cellular fibronectin under flow at 300 s^{-1}, while only a weak signal was detected for PF4Cre-α5$^{-/-}$ platelets, indicating that α5β1 is important to promote αIIbβ3 activation on fibronectin (Ctrl: 26.9 ± 8.8 × 10^4 AU; PF4Cre-α5$^{-/-}$: 3.5 ± 2.7 × 10^4 AU) (►**Fig. 4A, B**). We observed that thrombi formed in control blood but not in PF4Cre-α5$^{-/-}$ blood, highlighting a key role of α5β1 in platelet aggregation on fibrillar cellular fibronectin (►**Fig. 4C, D**). Surprisingly, a defect in thrombus formation was also observed when PF4Cre-α5$^{-/-}$ blood was perfused over fibrillar collagen, a surface which does not directly activate α5β1, suggesting that this integrin participates in thrombus build-up, probably through interactions with plasma fibronectin (►**Fig. 4E, F**). This role of mouse α5β1 in thrombus growth over fibrillar collagen was however not observed when human blood was perfused with a blocking anti-α5 antibody, suggesting a species difference (data not shown). Altogether, these findings indicated that integrin α5β1 plays an important role in thrombus growth on fibronectin.

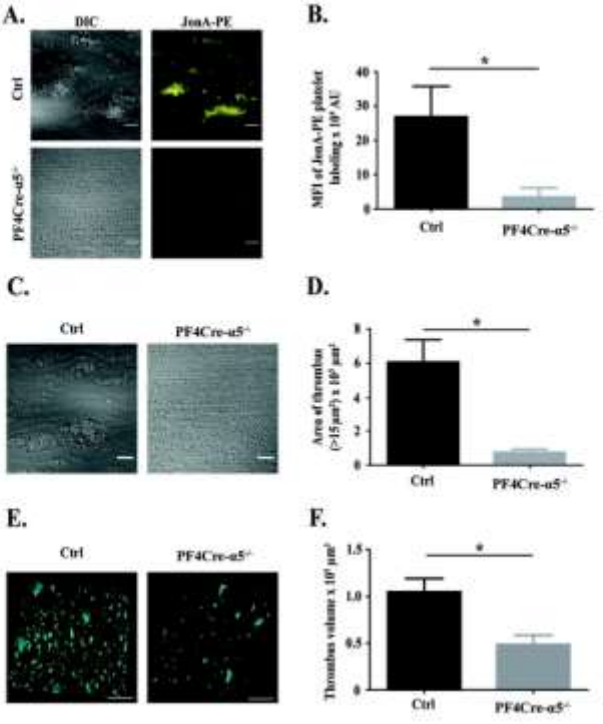

Fig. 4 Defective activation and aggregation of PF4Cre-α5$^{-/-}$ mouse platelets on fibronectin and collagen. (**A, B**) Whole blood from Ctrl ($n = 5$) and PF4Cre-α5$^{-/-}$ mice ($n = 5$) was perfused at 300 s^{-1} through PDMS flow chambers coated with cellular fibrillar fibronectin (300 µg/mL) for 15 minutes. Platelet adhesion was visualized in random fields by differential interference contrast (DIC) microscopy and JonA-PE fluorescence microscopy, scale bar: 20 µm (A). The mean fluorescence intensity of JonA-PE platelet labeling was quantified (B). (**C, D**) Whole blood from Ctrl ($n = 4$) and PF4Cre-α5$^{-/-}$ mice ($n = 4$) was perfused at 300 s^{-1} through PDMS flow chambers coated with fibronectin for 15 minutes. Thrombus formation was visualized in random fields by DIC microscopy, scale bar: 20 µm (C). The area of thrombi of more than 15 µm^2 was quantified (D). (**E, F**) Whole blood from PF4-Cre$^-$ ($n = 7$) and PF4Cre-α5$^{-/-}$ mice ($n = 7$) was perfused at 300 s^{-1} through PDMS flow chambers coated with collagen (200 µg/mL) for 10 minutes. Platelet aggregation was visualized in random fields by confocal microscopy, scale bar: 50 µm (E). The volume of the thrombi was quantified (F). Results are expressed as the mean ± standard error of the mean (SEM) and were compared by the Mann–Whitney test (B, D, and F); $^*p < 0.05$.

α5β1 Does Not Act as a Major Platelet Receptor in Experimental Thrombosis

Mice deficient in platelet integrin α5β1 were studied in three distinct models of localized vascular injury to expose the subendothelium matrix, which is known to contain fibrillar cellular fibronectin. When the common carotid artery was injured with a 7.5% solution of $FeCl_3$, PF4Cre-α5$^{-/-}$ mice ($n = 9$) presented a similar profile of thrombus formation and disaggregation as compared to controls ($n = 6$) (area under the curve, Ctrl: 6 ± 2 × 10^8 µm^2; PF4Cre-α5$^{-/-}$: 10 ± 2 × 10^8 µm^2; $p > 0.05$; ►**Fig. 5A, B**; ►**Supplementary Fig. S2A**, available in the online version). A comparable result was obtained after mechanical injury of the abdominal aorta with forceps, the thrombus area in PF4Cre-α5$^{-/-}$ mice ($n = 8$) being not significantly different from that in control mice ($n = 8$) (area under the curve, Ctrl: 12 ± 4 × 10^7 µm^2; PF4Cre-α5$^{-/-}$: 17 ± 4 × 10^7 µm^2; $p > 0.05$; ►**Fig. 5C, D**; ►**Supplementary Fig. S2B**, available in the online version). Finally, following laser-induced injury of mesenteric arteries, PF4Cre-α5$^{-/-}$ ($n = 5$ vessels on three mice) also formed thrombi in a similar manner to control mice ($n = 6$ vessels in three mice) (area under the curve, Ctrl: 7 ± 1 × 10^6 µm^2; PF4Cre-α5$^{-/-}$: 7 ± 1 × 10^6 µm^2; $p > 0.05$). (►**Fig. 5E, F**; ►**Supplementary Fig. S2C**, available in the online version). Hence mouse platelet α5β1 did not appear to be a major receptor for arterial thrombosis.

Platelets from PF4Cre-α5$^{-/-}$ Mice Display No Important Hemostatic Defect

PF4Cre-α5$^{-/-}$ mice did not present any spontaneous bleeding. In addition, PF4Cre-α5$^{-/-}$ mice showed no signs of excessive bleeding during surgery as compared to control animals, suggesting that the lack of this integrin on platelets does not critically affect hemostasis. This was further supported by a normal bleeding time ($n = 6$) (Ctrl: 302 ± 119 s; PF4Cre-α5$^{-/-}$: 121 ± 17 s) and normal volume of blood lost ($n = 6$) (Ctrl: 259 ± 130 µL; PF4Cre-α5$^{-/-}$: 130 ± 84 µL) in a tail-bleeding time assay (►**Fig. 6A, B**). Finally, we did not observe any effect on inflammatory bleeding in PF4Cre-α5$^{-/-}$ mice as compared to control mice in an rpA model of skin inflammation (►**Fig. 6C, D**) and in a LPS pulmonary inflammation model (►**Fig. 6E, F**). These results do not favor a major role of integrin α5β1 in the murine hemostatic system.

Discussion

Platelets express numerous adhesion receptors, notably integrins, to sense the proteins exposed on the

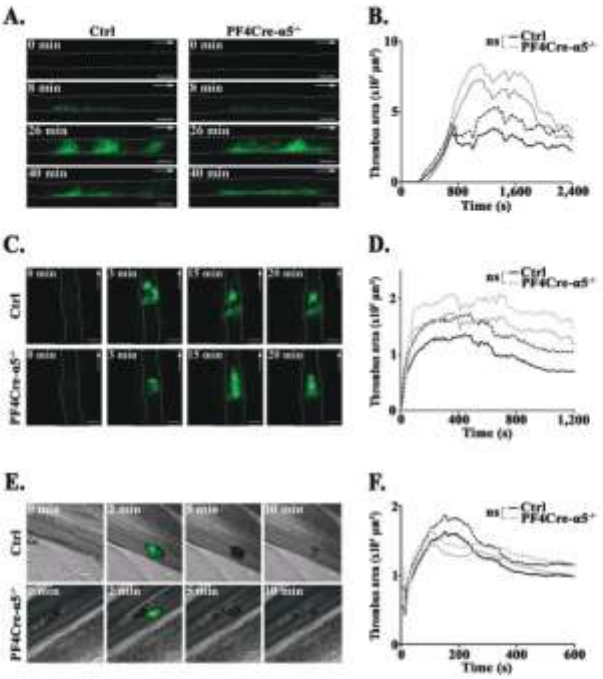

Fig. 5 Platelet integrin α5β1 does not play a major role in experimental thrombosis in mice. (**A, B**) Thrombosis was triggered in Ctrl ($n = 6$) and PF4Cre-α5$^{-/-}$ mice ($n = 9$) by application of a filter paper saturated with 7.5% $FeCl_3$ to the common carotid artery. Representative fluorescence images of the thrombus (*green*) at the indicated time points after injury, scale bar: 500 µm (A). (**C, D**) thrombosis was triggered in Ctrl ($n = 8$) and PF4Cre-α5$^{-/-}$ mice ($n = 8$) by compression of the abdominal aorta with forceps. Representative fluorescence images of the thrombus (*green*) at the indicated time points after injury, scale bar: 500 µm (C). (**E, F**) thrombosis was triggered in 6 vessels in 3 control mice and in 5 vessels in 3 PF4Cre-α5$^{-/-}$ mice by superficial laser injury of a mesenteric arteriole. Representative composite images of the thrombus (*green*) using bright field and fluorescence microscopy at the indicated time points after injury, scale bar: 50 µm (E). *Arrows* indicate the direction of blood flow and the *dotted lines* the borders of the vessels. The time course of thrombus growth is represented by its surface area (mean in solid line ± standard error of the mean (SEM) in dashed line) (B, D and F). Results were compared by two-way ANOVA.

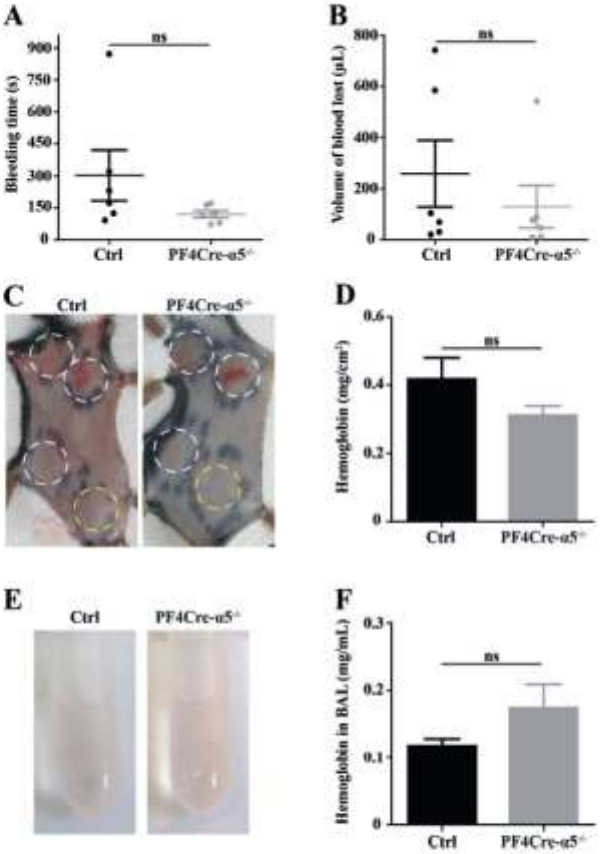

Fig. 6 PF4Cre-α5$^{-/-}$ mice display a normal bleeding time and do not present cutaneous or pulmonary bleeding under inflammatory conditions. (**A, B**) The tail of Ctrl ($n = 6$) and PF4Cre-α5$^{-/-}$ mice ($n = 6$) was sectioned. The time required for the first arrest of bleeding was recorded (A) and the volume of blood lost was measured over 30 minutes (B). The symbols correspond to individual mice. (**C**) Representative images of skin lesions 4 hours after induction of a reverse passive Arthus (rpA) reaction in Ctrl and PF4Cre-α5$^{-/-}$ mice. *White circles* represent the points of injection of an antibovine serum albumin antibody and *yellow circles* the points of injection of control IgG. (**D**) Quantification of the hemoglobin content (mg/cm²) in skin biopsies from Ctrl ($n = 4$) and PF4Cre-α5$^{-/-}$ mice ($n = 4$). (**E**) Representative images of bronchoalveolar liquid (BAL) 24 hours after LPS intranasal inoculation in Ctrl and PF4Cre-α5$^{-/-}$ mice. (**F**) Quantification of the hemoglobin content (mg/mL) in the BAL from Ctrl ($n = 8$) and PF4Cre-α5$^{-/-}$ mice ($n = 8$). Values are the mean ± standard error of the mean (SEM) and results were compared by the Mann–Whitney test. IgG, immunoglobulin G; LPS, lipopolysaccharide.

subendothelium of an injured vessel and to ensure their efficient recruitment to the site of injury. We show in this study, using tissue-specific knock-out combined with in vitro flow-based assays, that integrin α5β1 is a functionally key receptor for efficient platelet adhesion, activation, and aggregation on immobilized fibrillar cellular fibronectin, which are found in the vessel wall. Interestingly, in the absence of α5β1, the other main platelet receptor for fibronectin, αIIbβ3, was inefficient in promoting normal platelet adhesion, activation, and aggregation, highlighting the importance of α5β1 in these processes. We also identified an unexpected role of α5β1 in platelet aggregation on collagen. Despite these important functional roles identified in vitro, we found that platelet α5β1 did not play an essential role in the arrest of bleeding after trauma or under inflammatory conditions. Moreover, three distinct experimental models of thrombosis revealed no impact on thrombus formation in α5β1-deficient mice as compared to controls, suggesting that this receptor is unlikely to represent a major factor in arterial thrombosis.

We observed that α5β1-deficient platelets aggregated normally in response to a series of soluble agonists and to collagen. In addition, fibrinogen binding and P-selectin and annexin V exposure in response to soluble agonists were completely normal, indicating no role of α5β1 in the amplification step of platelet activation driven by these agonists. Adhesion under flow of α5β1-deficient platelets to many adhesive surfaces including fibrinogen, laminins, and vWF

was likewise unchanged. In contrast, we observed a marked impairment of the adhesion of these platelets to immobilized fibrillar cellular fibronectin and collagen. These results suggest that α5β1 is a highly specialized platelet receptor for probably only one adhesive protein, fibronectin. This is not a unique case, as platelets express many receptors to sense a single adhesive protein, notably the GPIb–IX complex and integrins α2β1, α6β1, and αvβ3 which bind respectively to vWF, collagen, laminins, and vitronectin.[6] The reason why platelets have maintained distinct specific receptors is probably to ensure efficient adhesion to a wide range of matrices which can be exposed by different types of vessels and at different depths of injury.[22]

It is well established that platelets express two main receptors for fibronectin, α5β1 and αIIbβ3. Our results support a major role for α5β1 as a receptor for fibronectin, since in its absence, we observed a dramatic reduction in platelet adhesion and activation on fibrillar cellular fibronectin with almost no aggregation at all. As a consequence, our observations also indicate that αIIbβ3 alone is not sufficient to compensate for the absence of α5β1 in the case of adhesion to a fibronectin surface. We further found that α5β1, in addition to its role in initiating platelet adhesion and activation on fibronectin,[15,16] contributed to thrombus growth on collagen, a process known to be mainly ensured by αIIbβ3.[23–25] However, the impairment we observed when perfusing PF4Cre-α5$^{-/-}$ blood over collagen was modest as compared to what has been reported when αIIbβ3 is blocked or absent, where no thrombus growth occurs and only a platelet monolayer forms.[4] One remaining question is the mechanism by which α5β1 participates in thrombus build-up, as this receptor does not interact with fibrinogen or vWF, two adhesive proteins found in a growing thrombus. Ni et al reported many years ago that mice deficient in both vWF and fibrinogen were still able to form thrombi at late stages and proposed a role of fibronectin in this process.[26] It is therefore reasonable to propose that fibronectin exposed after platelet activation or plasma fibronectin, through interaction with α5β1, participates in platelet aggregation. This is consistent with the role of platelet α5β1 in facilitating the assembly of soluble plasma fibronectin into fibrils on the surface of activated platelets within a growing thrombus.[27] Such a multimerization of fibronectin would increase its reactivity and prothrombotic potential. Moreover, it has been proposed that the CD40 ligand (CD40L) can interact with α5β1[28] and that it can support thrombus formation under flow over fibrillar collagen.[29] It is therefore possible that CD40L secreted from granules upon platelet activation can interact with platelet α5β1 integrin and participate in thrombus growth over collagen.

Petzold et al reported that the absence of all three platelet β1 integrins resulted in an increased tail-bleeding time, suggesting that one or more of these integrins play an important part in normal hemostasis.[30] Using a similar tail-bleeding time assay, we found that α5β1-deficient mice did not bleed longer or lose more blood as compared to controls, indicating that α5β1 is not a key platelet receptor for hemostasis in mice. This result might appear surprising, especially since the absence of either α2 or α6 likewise had no impact on the tail-bleeding time.[10,11] A possible explanation is that β1 integrins play redundant roles in hemostasis, where the absence of one integrin can be compensated by the others to ensure the interaction of platelets with the extracellular matrix components.

Platelets not only arrest bleeding after trauma, but also maintain vascular integrity and stop inflammatory bleeding.[1] The molecular mechanism relies on the immunoreceptor tyrosine-based activation motif, GPVI, and C-type lectin-like receptor II, which promote platelet activation.[31,32] An unresolved question is which receptors support platelet adhesion at sites of inflammatory bleeding, since the process appears to be independent of two major adhesion receptors, the GPIb–IX complex and integrin αIIbβ3.[1,33] We have recently identified a role of β1 integrins in this process (Janus-Bell et al, submitted manuscript). However, our results exclude a key role of α5β1, since no bleeding phenotype was observed in PF4Cre-α5$^{-/-}$ mice using a cutaneous rpA model and a LPS pulmonary inflammation model. While further studies will be required to identify the adhesion receptors important to stop inflammatory bleeding, it is tempting to speculate that compensatory mechanisms between such receptors could explain why no major bleeding occurs when only one of them is absent.

Using three distinct models of arterial thrombosis, in different vessels and under distinct rheological conditions, we did not observe any significant difference in any experimental model of thrombosis. These results indicate that α5β1 alone does not play a central role in experimental thrombosis. Moreover, α5β1 appears to be less important than the two other β1 integrins, α2β1 and α6β1, which have both been shown to contribute to experimental thrombosis in at least one of the models used in this study.[11,12,34] The apparent discrepancy we observed between an important role of α5β1 in platelet aggregation on fibronectin in vitro and the absence of a role in experimental models of thrombosis could be linked to the nature of the surface exposed to the flowing blood in vivo, which might not contain enough fibrillar cellular fibronectin. Another explanation could be the ability of other platelet adhesion receptors to compensate for the lack of α5β1 on platelets. As it has been reported that an evolved atherosclerotic plaque is particularly rich in fibrillar cellular fibronectin,[35,36] it might be interesting to test the impact of α5β1 blockade in apolipoprotein E-deficient models of atherosclerotic plaque rupture. To date, there is no information available about the role of human α5β1 integrin in arterial thrombosis in humans.

In conclusion, in vitro experiments performed with α5β1-deficient mouse platelets indicated that this integrin plays a very important role in supporting platelet adhesion, activation, and aggregation on fibrillar fibronectin and participates in thrombus growth. However, integrin α5β1 appears to be dispensable for hemostasis under normal and inflammatory conditions and is also not essential in in vivo models of experimental thrombosis.

What is known about this topic?

- Platelets express β1 and β3 integrins to allow adhesion, activation, and aggregation.
- α5β1 and αIIbβ3 are the main platelet receptors for fibronectin supporting platelet adhesion to fibronectin under flow condition.

What does this paper add?

- This study highlights the important role of α5β1 in supporting platelet adhesion, activation, and aggregation on fibrillar cellular fibronectin using PF4Cre-α5-deficient mice.
- We provide evidence that in the absence of α5β1, the other platelet receptor for fibronectin, αIIbβ3, is unable to support normal platelet adhesion to immobilized fibronectin with no platelet aggregation at all.
- Platelet α5β1 is dispensable for hemostasis under normal and inflammatory conditions and does not play a key role in experimental thrombosis.

Author Contributions
A.Y., C.S., E.J.B., and N.R. acquired, analyzed, and interpreted the data and wrote the manuscript; C.B., C.L., C.M., and U.M.A. acquired and analyzed the data; A.E., M.A.P., and Y.A.S. designed the research, interpreted the data, and wrote the manuscript; C.G. contributed to writing of the manuscript; P.H.M. conceived and designed the research, interpreted the data, wrote the manuscript, and handled funding and supervision.

Funding
This work was supported by INSERM, EFS, ARMESA (Association de Recherche et Développement en Médecine et Santé Publique), and SFH (Société Française d'Hématologie). The reported study was funded by RFBR, project number 19-34-9003 9.

Conflict of Interest
None declared.

References

1 Goerge T, Ho-Tin-Noe B, Carbo C, et al. Inflammation induces hemorrhage in thrombocytopenia. Blood 2008;111(10):4958–4964
2 Jackson SP. Arterial thrombosis–insidious, unpredictable and deadly. Nat Med 2011;17(11):1423–1436
3 Savage B, Saldívar E, Ruggeri ZM. Initiation of platelet adhesion by arrest onto fibrinogen or translocation on von Willebrand factor. Cell 1996;84(02):289–297
4 Savage B, Almus-Jacobs F, Ruggeri ZM. Specific synergy of multiple substrate-receptor interactions in platelet thrombus formation under flow. Cell 1998;94(05):657–666
5 Zahid M, Mangin P, Loyau S, et al. The future of glycoprotein VI as an antithrombotic target. J Thromb Haemost 2012;10(12):2418–2427
6 Versteeg HH, Heemskerk JWM, Levi M, Reitsma PH. New fundamentals in hemostasis. Physiol Rev 2013;93(01):327–358
7 Wagner CL, Mascelli MA, Neblock DS, Weisman HF, Coller BS, Jordan RE. Analysis of GPIIb/IIIa receptor number by quantification of 7E3 binding to human platelets. Blood 1996;88(03):907–914
8 Nurden AT. Glanzmann thrombasthenia. Orphanet J Rare Dis 2006;1:10
9 Jamasbi J, Ayabe K, Goto S, Nieswandt B, Peter K, Siess W. Platelet receptors as therapeutic targets: past, present and future. Thromb Haemost 2017;117(07):1249–1257
10 Habart D, Cheli Y, Nugent DJ, Ruggeri ZM, Kunicki TJ. Conditional knockout of integrin α2β1 in murine megakaryocytes leads to reduced mean platelet volume. PLoS One 2013;8(01):e55094
11 Schaff M, Tang C, Maurer E, et al. Integrin α6β1 is the main receptor for vascular laminins and plays a role in platelet adhesion, activation, and arterial thrombosis. Circulation 2013;128(05):541–552
12 He L, Pappan LK, Grenache DG, et al. The contributions of the alpha 2 beta 1 integrin to vascular thrombosis in vivo. Blood 2003;102(10):3652–3657
13 Kuijpers MJE, Schulte V, Bergmeier W, et al. Complementary roles of glycoprotein VI and alpha2beta1 integrin in collagen-induced thrombus formation in flowing whole blood ex vivo. FASEB J 2003;17(06):685–687
14 Yang JT, Rayburn H, Hynes RO. Embryonic mesodermal defects in alpha 5 integrin-deficient mice. Development 1993;119(04):1093–1105
15 Beumer S, IJsseldijk MJ, de Groot PG, Sixma JJ. Platelet adhesion to fibronectin in flow: dependence on surface concentration and shear rate, role of platelet membrane glycoproteins GP IIb/IIIa and VLA-5, and inhibition by heparin. Blood 1994;84(11):3724–3733
16 McCarty OJT, Zhao Y, Andrew N, et al. Evaluation of the role of platelet integrins in fibronectin-dependent spreading and adhesion. J Thromb Haemost 2004;2(10):1823–1833
17 Maurer E, Schaff M, Receveur N, et al. Fibrillar cellular fibronectin supports efficient platelet aggregation and procoagulant activity. Thromb Haemost 2015;114(06):1175–1188
18 Eckly A, Strassel C, Cazenave J-P, Lanza F, Léon C, Gachet C. Characterization of megakaryocyte development in the native bone marrow environment. Methods Mol Biol 2012;788:175–192
19 Nagy Z, Mori J, Ivanova V-S, Mazharian A, Senis YA. Interplay between the tyrosine kinases Chk and Csk and phosphatase PTPRJ is critical for regulating platelets in mice. Blood 2020;135(18):1574–1587
20 Cazenave J-P, Ohlmann P, Cassel D, Eckly A, Hechler B, Gachet C. Preparation of washed platelet suspensions from human and rodent blood. Methods Mol Biol 2004;272:13–28
21 Léon C, Eckly A, Hechler B, et al. Megakaryocyte-restricted MYH9 inactivation dramatically affects hemostasis while preserving platelet aggregation and secretion. Blood 2007;110(09):3183–3191
22 Bergmeier W, Hynes RO. Extracellular matrix proteins in hemostasis and thrombosis. Cold Spring Harb Perspect Biol 2012;4(02):4
23 Cho J, Mosher DF. Impact of fibronectin assembly on platelet thrombus formation in response to type I collagen and von Willebrand factor. Blood 2006;108(07):2229–2236
24 Matuskova J, Chauhan AK, Cambien B, et al. Decreased plasma fibronectin leads to delayed thrombus growth in injured arterioles. Arterioscler Thromb Vasc Biol 2006;26(06):1391–1396
25 Ni H, Yuen PST, Papalia JM, et al. Plasma fibronectin promotes thrombus growth and stability in injured arterioles. Proc Natl Acad Sci U S A 2003;100(05):2415–2419
26 Ni H, Denis CV, Subbarao S, et al. Persistence of platelet thrombus formation in arterioles of mice lacking both von Willebrand factor and fibrinogen. J Clin Invest 2000;106(03):385–392

27 Olorundare OE, Peyruchaud O, Albrecht RM, Mosher DF. Assembly of a fibronectin matrix by adherent platelets stimulated by lysophosphatidic acid and other agonists. Blood 2001;98(01): 117–124
28 Léveillé C, Bouillon M, Guo W, et al. CD40 ligand binds to alpha5beta1 integrin and triggers cell signaling. J Biol Chem 2007;282(08):5143–5151
29 Kuijpers MJE, Mattheij NJA, Cipolla L, et al. Platelet CD40L modulates thrombus growth via phosphatidylinositol 3-kinase β, and not via CD40 and IκB kinase α. Arterioscler Thromb Vasc Biol 2015;35(06):1374–1381
30 Petzold T, Ruppert R, Pandey D, et al. β1 integrin-mediated signals are required for platelet granule secretion and hemostasis in mouse. Blood 2013;122(15):2723–2731
31 Boulaftali Y, Hess PR, Getz TM, et al. Platelet ITAM signaling is critical for vascular integrity in inflammation. J Clin Invest 2013; 123(02):908–916
32 Gros A, Syvannarath V, Lamrani L, et al. Single platelets seal neutrophil-induced vascular breaches via GPVI during immune-complex-mediated inflammation in mice. Blood 2015;126(08):1017–1026
33 Rayes J, Jadoui S, Lax S, et al. The contribution of platelet glycoprotein receptors to inflammatory bleeding prevention is stimulus and organ dependent. Haematologica 2018;103(06): e256–e258
34 Kuijpers MJE, Pozgajova M, Cosemans JMEM, et al. Role of murine integrin alpha2beta1 in thrombus stabilization and embolization: contribution of thromboxane A2. Thromb Haemost 2007;98(05): 1072–1080
35 Bültmann A, Li Z, Wagner S, et al. Impact of glycoprotein VI and platelet adhesion on atherosclerosis–a possible role of fibronectin. J Mol Cell Cardiol 2010;49(03):532–542
36 Matter CM, Schuler PK, Alessi P, et al. Molecular imaging of atherosclerotic plaques using a human antibody against the extra-domain B of fibronectin. Circ Res 2004;95(12):1225–1233

Supplementary Materials and Methods

Materials

Glutaraldehyde was from Electron Microscopy Sciences (EMS) (Hatfield, Pennsylvania, United States), lead citrate from Leica Microsystems GmbH (Vienna, Austria), and uranyl acetate from Ladd Research Industries (Williston, Vermont, United States). Adenosine diphosphate (ADP), human cellular soluble fibronectin (F2518), fatty acid free human serum albumin (HSA), hemoglobin (Hb), fibrinogen, thrombin, U46619, and lipopolysaccharide (LPS) *Pseudomonas aeruginosa* were from Sigma-Aldrich (Lyon, France). Ethylenediaminetetraacetic acid (EDTA) was from Invitrogen (Paisley, United Kingdom), acid citrate dextrose (ACD) from Bioluz (St-Jean-de-Luz, France), and recombinant hirudin from Transgene (Illkirch-Graffenstaden, France). Apyrase was purified from potatoes as previously described.[1] Collagen was from Takeda (Horm, Linz, Austria), laminin from Biolamina (Stockholm, Sweden), and von Willebrand factor (vWF)-binding protein DDR2 was from Cambcol (Ely, United Kingdom). Alexa Fluor 488-annexin V was from Life Technologies (Bleiswijk, the Netherlands). FITC-fibrinogen and $DIOC_6$ (3,3′-dihexyloxacarbocyanine iodide) were from Molecular Probes (Paisley, United Kingdom). Ferric chloride ($FeCl_3$) was from Prolabo (Fontenay-sous-Bois, France) and bovine serum albumin (BSA) from Euromedex (Souffelweyersheim, France). Xylazine (Rompun) from Bayer, ketamine (Imalgene) from Merial, and isoflurane (Vetflurane) from Virbac were purchased from Elvetis (Domloup, France).

Antibodies

PE-conjugated anti-α2 (clone HMα2), anti-α5 (clone 5H10-27) and anti-α6 antibodies (clone GOH3), and Alexa Fluor 488-conjugated anti-β1 antibody (clone HMβ1-1) were from Biolegend (San Diego, California, United States). FITC-conjugated anti-αIIbβ3 (clone Leo.F2), anti-GPIbα (clone Xia.G7), anti-GPV (clone Gon.G6), anti-GPIX (clone Xia.B4), anti-GPVI (clone Jaq.1) and anti-β3 antibodies (clone Luc.H11), and PE-conjugated antiactivated αIIbβ3 antibody (JONA-PE) were from Emfret Analytics (Würzburg, Germany). FITC-coupled anti-P-selectin antibody (clone RB40.34) was from BD Pharmingen (San Diego, California, United States). Anti-α5 antibody (clone EPR7854) used in capillary-based immunoassay was from Abcam (Cambridge, United Kingdom). Anti-ERK1/2 antibody was from Cell Signaling Technology (Danvers, Massachusetts, United States). Anti-BSA antibody was from MP Biomedicals (Solon, Ohio, United States) and nonimmunizing immunoglobulin G (IgG)-control from Southern Biotech (Birmingham, Alabama, United States).

Platelet Glycoprotein Expression

Whole blood was collected into ETDA (6 mM) after a 1-mm severing of the tail of mice anesthetized with isoflurane inhalation. Briefly, collected blood was diluted with phosphate-buffered saline (PBS) to obtain a concentration of 100,000 platelets/μL. Labeled antibodies against murine platelet αIIbβ3, α2, α5, α6, β1, GPIbα, GPV, GPIX, and GPVI were incubated with diluted blood for 20 minutes at room temperature. After dilution with 500 μL of PBS, surface glycoprotein expression of 10,000 platelet events was determined by flow cytometry.

Platelet-Rich Plasma Preparation and Measurement of Platelet Aggregation

Blood drawn into hirudin anticoagulant from the abdominal aorta of four mice was pooled and PRP was obtained by centrifugation. PRP platelet aggregation was measured turbidimetrically in an APACT 4004 aggregometer (ELITech, Puteaux, France) in response to ADP (5 μM), collagen (2.5 μg/mL), and U46619 (2 μM).

Washed Platelet Preparation, and Measurement of Platelet Aggregation, P-selectin Exposure, Soluble Fibrinogen and Annexin V Binding

Blood drawn into ACD anticoagulant from the abdominal aorta of four to five mice was pooled and platelets were washed by sequential centrifugations and adjusted to 300,000 platelets/μL in Tyrode's albumin buffer containing 0.02 U/mL apyrase. Washed platelet aggregation was measured turbidimetrically in an APACT 4004 aggregometer (ELITech, Puteaux, France) in response to ADP (2 μM), collagen (2.5 μg/mL), thrombin (0.2 U/mL), and U46619 (1 μM). For soluble fibrinogen binding and P-selectin exposure, washed platelets adjusted to 50,000 platelets/μL were incubated with FITC-fibrinogen (20 μg/mL) or FITC-coupled anti-P-selectin antibody (25 μg/mL) and stimulated with agonists (ADP 2 μM, thrombin 0.25 U/mL or PAR4 1 mM). For phosphatidylserine exposure, washed platelets adjusted to 300,000 platelets/μL were stimulated with agonists (convulxin 15 nM, thrombin 0.25 U/mL, or both) for 15 minutes and then incubated with Alexa Fluor 488-annexin V (1/10th) for 20 minutes in the presence of 100 U/mL hirudin. Fluorescence was determined as previously published.[2]

In Vitro Flow-Based Adhesion Assay and Measurement of Thrombi Volume

Flow experiments were performed as previously described.[2] PDMS flow chambers (0.1 × 1 mm) were coated with vWF-binding protein (DDR2, 100 μg/mL), fibrinogen (100 μg/mL), laminins (100 μg/mL), or collagen (200 μg/mL) overnight and blocked with HSA (10 mg/mL in PBS) for 30 minutes. Hirudinated (100 U/mL) whole blood drawn from the abdominal aorta of adult mice was perfused through the coated PDMS chambers with a programmable syringe pump (Harvard Apparatus, Holliston, Massachusetts, United States) at indicated wall shear rates for the indicated time. Platelet adhesion was monitored by differential interference contrast (DIC) (Leica DMI4000B) using a 63x, 1.25 NA oil objective and a Hamamatsu ORCA Flash 4L.T camera (Hamamatsu Photonics, Massy, France).

For fibronectin flow-based assays, PDMS flow chambers (0.1 × 1 mm) were coated with cellular fibronectin (300 µg/mL) overnight and blocked with HSA (10 mg/mL in PBS) for 30 minutes. Mechanical stretching of cellular fibronectin was performed as described.[3] After hirudinated (100 U/mL) whole blood perfusion at 300 s^{-1} for 15 minutes, the number of adherent platelets was quantified on DIC images and the platelet adhesion behavior was analyzed on videos: platelets adherent for more than 15 s were considered stationary adherent and platelets adherent for less than 15 s were classified in the detachment class. After hirudinated (100 U/mL) whole blood perfusion in the presence of JONA-PE (1/50e) at 300 s^{-1} for 15 minutes, αIIbβ3 integrin activation was determined by quantification of fluorescence images. Fluorescent platelets were monitored by DIC or fluorescence microscopy (Leica DMI4000B) using a 40x, 1.3 NA oil objective and a CMOS ORCA Flash 4LT camera (Hamamatsu Photonics, Massy, France). Hirudinated (100 U/mL) whole blood perfusion at 300 s^{-1} for 15 minutes was used to quantify area of thrombus over fibronectin.

Ferric Chloride-Mediated Thrombosis in Carotid Artery

$FeCl_3$-mediated thrombosis was performed in 7- to 11-week-old mice as previously described.[4] Briefly, mice were anesthetized with xylazine 10 mg/kg and ketamine 100 mg/kg and received an injection of $DIOC_6$ to label platelets. The left common carotid artery was exposed and vascular injury was induced by applying a 3 × 3 mm Whatman filter paper saturated with 7.5% $FeCl_3$ laterally to the carotid artery for 2.5 minutes. Thrombus formation was monitored for 40 minutes in real time with a fluorescence microscope (Leica Microsystems, San Westlar, Germany) coupled to a CCD (charge-coupled device) camera (ORCA-Fusion C14440-20UP, Hamamatsu, Japan). Image acquisition and analysis were performed with Metamorph software (Molecular Devices, Sunnyvale, California, United States).

Mechanical-Injury-Induced Thrombus Formation in Abdominal Aorta

Thrombosis was performed in 8- to 10-week-old mice as previously described.[5] Briefly, the abdominal aorta of xylazine 10 mg/kg and ketamine 100 mg/kg anesthetized mice was isolated and $DIOC_6$ was injected to label platelets. A mechanical injury of the aorta was induced by pinching it with forceps for 15 seconds. Thrombus formation was monitored in real time with a fluorescence microscope (Leica Microsystems San Westlar, Germany) and a CCD camera (ORCA-Fusion C14440-20UP, Hamamatsu, Japan). Image acquisition and analysis were performed with Metamorph software (Molecular Devices, Sunnyvale, California, United States).

Laser-Induced Thrombus Formation in Mesenteric Arterioles

Thrombosis was performed in 3- to 4-week-old mice (10–13 g) as previously described.[6] Briefly, mice were anesthetized with xylazine 10 mg/kg and ketamine 100 mg/kg and received an injection of $DIOC_6$ to label platelets. A localized deep injury of a mesenteric arteriole (85–115 µm in diameter) was induced with a high-intensity 440-nm-pulsed nitrogen dye laser applied with a Micropoint system (Photonic Instruments, Andor Technology, Belfast, United Kingdom). Images were acquired with SlideBook 6 software (3i SAS, Paris, France).

Bleeding Time

The bleeding times and volumes of blood lost were determined by transversally severing a 3-mm segment from the distal tail of 50- to 60-day-old mice anesthetized with isoflurane inhalation, as previously reported.[7] The tail was immersed in 0.9% saline at 37°C and the time needed for the bleeding to stop was recorded. The saline tube containing blood was spun for 5 minutes, the pellet was homogenized in lysis buffer and used for blood lost quantification comparing the optical density at 540 nm with a standard curve.

Reverse Passive Arthus Reaction

An reverse passive Arthus (rpA) reaction was elicited on isoflurane anesthetized 9- to 16-week-old mice by intradermal injection of an anti-BSA antibody or nonimmunizing IgG (60 µg/spot in PBS), followed by retro-orbital injection of BSA (75 mg/kg in PBS), as previously described.[8] Mice were killed after 4 hours and 8-mm skin biopsies were homogenized in 250 µL PBS. The homogenate was spun for 5 minutes and the supernatant used for Hb analysis, comparing the optical density at 405 nm with a standard curve.

LPS Lung Inflammation Model

Here, 9- to 20-week-old mice were anesthetized with xylazine 5 mg/kg and ketamine 5 mg/kg. The lung inflammation model was induced in by intranasal inoculation of *P. aeruginosa* LPS (1 µg/mouse) in 60 µL of saline, as previously described. Mice were killed after 24 hours and bronchoalveolar lavage was performed by cannulating trachea with an 18-G feeding needle. Lungs were lavaged two times with 1 mL cold PBS. Hb was analyzed in pooled BAL from each mouse comparing the optical density at 405 nm with a standard curve.

References

1 Cazenave J-P, Ohlmann P, Cassel D, Eckly A, Hechler B, Gachet C. Preparation of washed platelet suspensions from human and rodent blood. Methods Mol Biol 2004;272:13–28
2 Schaff M, Tang C, Maurer E, et al. Integrin α6β1 is the main receptor for vascular laminins and plays a role in platelet adhesion, activation, and arterial thrombosis. Circulation 2013;128(05):541–552
3 Maurer E, Schaff M, Receveur N, et al. Fibrillar cellular fibronectin supports efficient platelet aggregation and procoagulant activity. Thromb Haemost 2015;114(06):1175–1188
4 Eckly A, Hechler B, Freund M, et al. Mechanisms underlying FeCl3-induced arterial thrombosis. J Thromb Haemost 2011;9(04):779–789
5 Mangin PH, Tang C, Bourdon C, et al. A humanized glycoprotein VI (GPVI) mouse model to assess the antithrombotic efficacies of anti-GPVI agents. J Pharmacol Exp Ther 2012;341(01):156–163

6 Hechler B, Nonne C, Eckly A, et al. Arterial thrombosis: relevance of a model with two levels of severity assessed by histologic, ultrastructural and functional characterization. J Thromb Haemost 2010;8(01):173–184
7 Léon C, Eckly A, Hechler B, et al. Megakaryocyte-restricted MYH9 inactivation dramatically affects hemostasis while preserving platelet aggregation and secretion. Blood 2007;110(09):3183–3191
8 Goerge T, Ho-Tin-Noe B, Carbo C, et al. Inflammation induces hemorrhage in thrombocytopenia. Blood 2008;111(10):4958–4964

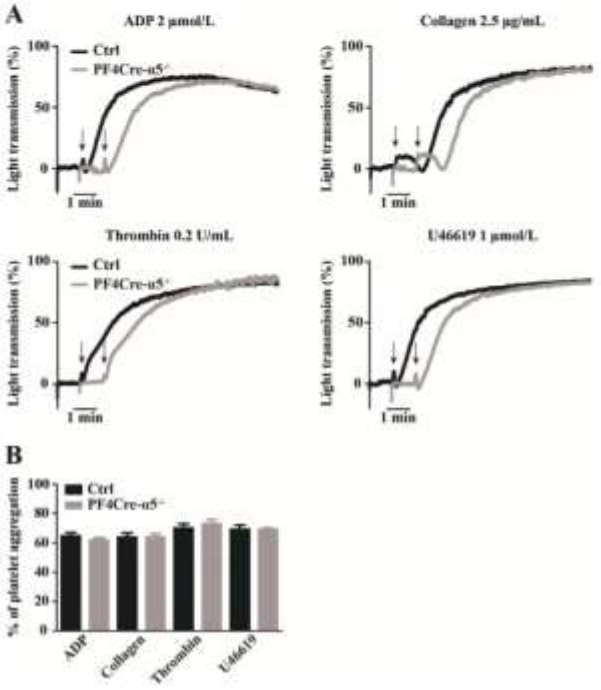

Supplementary Fig. S1 Washed platelets (3.0×10^5/µL) from Ctrl and PF4Cre-α5$^{-/-}$ mice were stimulated with adenosine diphosphate (ADP) (2 µmol/L), collagen (2.5 µg/mL), or U46619 (1 µmol/L) in the presence of fibrinogen (320 µg/mL) or with thrombin (0.2 U/mL) in the absence of fibrinogen. (**A**) *Arrows* indicate the point of agonist addition and aggregation profiles are representative of three separate experiments. (**B**) The bar graph represents the percentage of platelet aggregation at 5 minutes ($n = 3$). Values are the mean ± standard error of the mean (SEM).

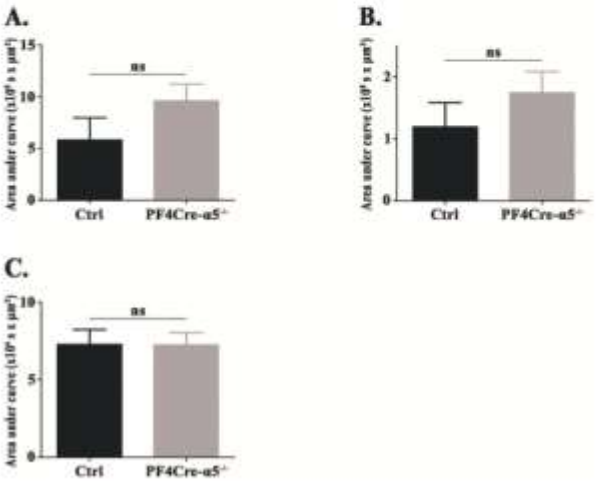

Supplementary Fig. S2 (**A**) Thrombosis was triggered in Ctrl ($n = 6$) and PF4Cre-α5$^{-/-}$ mice ($n = 9$) by application of a filter paper saturated with 7.5% $FeCl_3$ to the common carotid artery. (**B**) Thrombosis was triggered in Ctrl ($n = 8$) and PF4Cre-α5$^{-/-}$ mice ($n = 8$) by compression of the abdominal aorta with forceps. (**C**) Thrombosis was triggered in 6 vessels in 3 control mice and in 5 vessels in 3 PF4Cre-α5$^{-/-}$ mice by superficial laser injury of a mesenteric arteriole. The bar graphs represent the area under the curves of thrombus area. Results were compared by the Mann–Whitney test.

Conclusion

The results of this work show that the platelets of mice deficient for α5β1 do not show any particular defect. PF4Cre-α5$^{-/-}$ platelets have a normal count and volume, as well as a normal expression of the main surface receptors (αIIbβ3, α2, α6, β1, GPIbα, GPV, GPIX, GPVI), apart for the α5 integrin which is absent. Aggregation of PF4Cre-α5$^{-/-}$ platelets was also normal in response to series of agonists such as collagen, ADP, U46619, a thromboxane A2 analog, and thrombin. Absence of α5 integrin on platelets has no major impact on integrin αIIbβ3 activation and granule secretion. Platelets of these mice adhere normally to a surface of vWF, fibrinogen or laminins under shear flow. However, they present a major defect in adhesion, activation, and aggregation on a fibrillar fibronectin surface. In three experimental models of arterial thrombosis, mice invalidated for the α5β1 presented a normal profile of thrombus formation and disaggregation as compared to controls. Finally, the normal tail-bleeding time favors no major role of this integrin in hemostasis.

Together, the results gathered in this study suggest that α5β1 integrin plays an instrumental role in the adhesion, activation and aggregation of platelets to fibrillar fibronectin, and might also participate in thrombus growth on collagen. However, our results indicate that integrin α5β1 does not play a major role in hemostasis or arterial thrombosis in mice. It remains possible that integrin α5β1 could play a more important role in a lesion exposing a large amount of fibronectin, but this remains to be demonstrated. We conclude that it is unlikely that integrin α5β1 represents an interesting anti-thrombotic target.

The central role of fibrin in arrest of the hemostatic response

Publication 3:

« Fibrin on the thrombus surface turns off the hemostatic response»

Alexandra Yakusheva[1,2], Muhammad Usman Ahmed[1], Catherine Bourdon[1] et al.

[1]Université de Strasbourg, INSERM, EFS Grand-Est, BPPS UMR-S1255, FMTS, F-67065 Strasbourg, France;

[2]Center for Theoretical Problems of Physicochemical Pharmacology, Moscow 119991, Russia

In preparation

Introduction

Following an injury of a healthy vessel, tissue factor and adhesive proteins of the subendothelium are exposed to the flowing blood and initiate the hemostatic response. Thanks to the use of intravital microscopy in various experimental models of vessel injury in mice, the dynamic process of platelet aggregation has been unraveled. First, platelets accumulate to form a large, sometimes subocclusive aggregate, which then disaggregates to leave a platelet rich plug to cover the site of injury. This plug is stabilized by fibrin which forms as the result of fibrinogen cleavage by thrombin generated locally upon tissue factor exposure. The bi-phasic nature of plug formation is essential to avoid unwanted occlusion and ischemia in surrounding tissues. While the mechanism allowing platelet aggregation is very well characterized, the one limiting this process and switching off the hemostatic response is still unclear.

The objective of my third project was to evaluate the role of fibrin in the dynamics of the formation of a hemostatic plug, beyond its stabilizing role. For this purpose, we characterized the dynamic of thrombus and fibrin formation and the plug composition in $FeCl_3$ injury and needle puncture models by using histology, fluorescence microscopy, and electron microscopy approaches. Then, we studied *in vitro* the ability of platelets to form aggregates on fibrin-poor and fibrin-rich aggregates by using a blood flow assay. Further, we evaluated *in vivo* the role of fibrin in thrombus formation by mechanically or pharmacologically removing the aggregate before fibrin was predominant in the clot. Finally, we examined *in vivo* the dynamic of thrombus growth using $FeCl_3$-induced model, in transgenic FibAEK mice presenting a mutation of the Aa chain of fibrinogen which cannot form a fibrin network. A manuscript related to this work is in preparation.

Fibrin covering the thrombus surface turns off the hemostatic response

Alexandra Yakusheva[1,2], Muhammad Usman Ahmed[1], Catherine Bourdon[1], *et al*.,

[1]Université de Strasbourg, INSERM, EFS Grand-Est, BPPS UMR-S1255, FMTS, F-67065 Strasbourg, France; [2]Center for Theoretical Problems of Physicochemical Pharmacology, Moscow 119991, Russia;

Corresponding authors: Pierre H. Mangin, Université de Strasbourg, INSERM, EFS Grand-Est, BPPS UMR-S1255, FMTS, 10 rue Spielmann, F-67065 Strasbourg, France; Phone : (+33) 3 88 21 25 25 ; Fax: (+33) 3 88 21 25 21; E-mail: pierre.mangin@efs.sante.fr;

Running head: Fibrin arrests thrombus regrowth

Key Points:

Fibrin plays a central role in the arrest of the hemostatic response, beyond its stabilizing role.

Fibrin turns off the physiological response of plug formation by preventing further platelet incorporation.

Text word count in abstract: 245

Text word count:

Figure/Table count: 5

Reference count: 32

Scientific Categories: Thrombosis and Hemostasis; Vascular Biology

ABSTRACT

Following an injury of a healthy vessel, the subendothelium proteins are exposed to the flowing blood and initiate the hemostatic response. While the mechanism allowing platelet aggregation is very well characterized, the one switching off the hemostatic response is still unclear. The aim of this work was to evaluate the role of fibrin in the dynamics of the formation of a hemostatic plug, beyond its stabilizing role. Using a flow-based assay, we observed that the presence of a fibrin layer on top of an aggregate prevents its growth. Mechanical removal of the thrombus after vessel flicking resulted in continuous regrowth which stopped only when fibrin reached its maximal level within the thrombus surface and covered it. *In vivo* experiments with pharmacological agents removing fibrin during thrombus growth lead to thrombus embolization, which allowed the aggregate to grow again, and this regrowth process could be repeated many times. Finally, the dynamic of thrombus formation in FibAEK mice was profoundly altered with as expected a lack of thrombus stabilization, but additionally we observed that the hemostatic process was prolonged compared to a control with successive growth and embolization phases. In conclusion, these findings identify a central role of fibrin in the arrest of the hemostatic response, by limiting platelet adhesion to the plug. In addition to its very well-established role in stabilizing the clot, fibrin is also instrumental in regulating the hemostatic response by turning off the physiological response of plug formation and preventing further platelet incorporation.

INTRODUCTION

Hemostasis is a finely tuned physiological process initiated after vessel injury and which aims at repairing the vessel to rapidly stop blood loss and to restore a normal blood intake to supply downstream tissues and organs[1]. It is composed of three interconnected steps and starts with primary hemostasis, which is initiated thanks to the unique ability of blood platelets to be recruited to thrombogenic subendothelial proteins exposed at sites of injury[2]. Platelets then activate and form an aggregate through their ability to bind plasma proteins such as von Willebrand factor (vWF) and fibrinogen, allowing platelet aggregation to form the hemostatic plug[3,4]. In parallel, the tissue factor (TF) exposed in the vessel wall initiates secondary hemostasis or coagulation, which is a cascade of enzymatic reactions amplified at the surface of negatively charged surfaces of platelets and endothelial cells[5]. This leads to the generation of thrombin, a key serine protease, which cleaves fibrinogen into an insoluble fibrin network which stabilizes the clot[6]. At later stages, fibrinolysis is activated and removes the remaining part of the clot to restore normal blood flow and full vessel wall repair[7].

Platelet plug formation is central for a relevant hemostatic response and to ensure the arrest of bleeding. One of its unique feature is that it is very rapidly initiated following vessel injury to form the aggregate as quickly as possible, thereby limiting blood loss. Plug formation requires to be finely regulated to allow a suitable response, *i.e.* occlusive clot formation in case of vessel rupture or a non-occlusive plug for weaker injuries[8]. This is essential to avoid an excessive response which could result in unnecessary occlusion in vessels presenting modest injuries, thereby avoiding reduction of blood supply to downstream tissues. While the process of platelet adhesion, activation and aggregation at site of injury is very well understood, the

process limiting extensive platelet aggregation and switching off the hemostatic response remains fully unknown. In this manuscript, we studied the dynamics of platelet plug formation using *in vivo* mouse models to investigate the regulation of the hemostatic process. We identified a central role of fibrin, which in addition to its very well-established role in stabilizing the clot, is instrumental in regulating the hemostatic response by turning off the physiological response of plug formation.

MATERIALS AND METHODS

FibAEK mice

Mice carrying a mutant form of fibrinogen were generated by backcrossing FibAEK progeny mice (Matthew J. Flick Laboratory) with C57Bl/6J (Jackson Labs) as was described[9]. In all animal studies, gender and age matched (6-8 weeks) mice were used

Mouse model of hemostasis based on vessel puncture

WT mice with a pure C57BL/6 background were maintained in the animal facilities of the EFS Grand-Est. Ethical approval for the experiments was obtained from the French Ministry of Research. Fluorescent agents (3,3'-dihexyloxacarbocyanine iodide ($DIOC_6$) (Thermo Fisher Scientific, MA, USA); DyLight650-coupled anti-fibrin antibody 59d8 (Inserm UMR_S11076, Marseille, France)) were injected into the jugular vein of 7-28 week-old mice, 5 min before the experiment, to label platelets. The common carotid artery was exposed surgically and was then punctured with a 25-gauge needle. Thrombus formation was monitored in real time with fluorescent microscope coupled to a CCD camera. At the end of the experiment, the thrombus was fixed and processed for histology or electron microscopy[10].

In vivo models of arterial thrombosis

Fluorescent agents were injected into the jugular vein 5 min before initiation of thrombus formation. The abdominal aorta of anesthetized WT mice (8-10 weeks old) was exposed and mechanically injured by pinching with forceps (type 11063-07, F.S.T., Heidelberg, Germany), as previously described[11]. FeCl3-injury was performed as in[10]. Briefly, the common carotid arteries of anesthetized WT mice (7 to 10 weeks old) were exposed and the left carotid artery was injured by applying a 1 mm long patch of filter paper (1M Whatmann) saturated with 7.5% FeCl3 for 2.5 min.

Drug administration

Mice were infused through the jugular vein with either saline (control), rt-PA (10 mg/kg) or hirudin (20 mg/kg) at the indicated times.

Histology of the carotid artery

Before injury, the ligature was prepared in both ends of the carotid artery. At the end of experiment, the vessel was fixed with 300 ul 4% paraformaldehyde was placed on the vessel as previously described[12]. After 15 minutes, the ligature was put and the carotid artery was excised, placed in 4% paraformaldehyde overnight and rinsed with phosphate buffer saline. Then it was placed in increasing concentrations of saccharose and was frozen in optimal cutting temperature compound. The sample was sectioned at 8-um thickness by microtome-cryostat. The sample was labelled with DAPI. Imaging was performed with a Leica confocal microsystem SP5 DMI 6000.

Scanning electron microscopy

Before injury, the ligature was prepared in both ends of the carotid artery. At the end of experiment, the vessel was fixed with 2% glutaraldehyde and 2% paraformaldehyde by transcardiac perfusion. The carotid artery was then excised and post-fixed in 2% glutaraldehyde and 2% paraformaldehyde overnight. The isolated vessel segment was sectioned in the middle by razor and it was dehydrated in increasing concentrations of ethanol followed by hexamethyldisilazine and glued onto a cover slip with the lumen uppermost. The cover slips were sputtered with gold prior to observation at 5 kV under an FEG Sirion SEM (FEI). The chemical distribution of elements was studied by energy dispersive X-ray emission microanalysis (EDX) of selected sections using an ESEM (FEI) at 20 kV, spot size 4.

In vitro flow-based adhesion assay

Microfluidic flow chambers were prepared as previously described[13]. Briefly, the chambers were coated with a solution of fibrillary Horm collagen (200 µg/mL) overnight at 4℃ and blocked with phosphate buffered saline (PBS) 10 mg/mL human serum albumin for 30 minutes at room temperature. For fibrin-poor thrombus formation, hirudinated (100 U/mL) whole blood from healthy human volunteers was labelled with DiOC6 (3,3'-dihexyloxacarbocyanine iodide;1 µmol/L) and was perfused through the coated microfluidic flow chambers with a syringe pump (Harvard Apparatus, Holliston, MA, USA) at 37℃ at 1500 s−1. For fibrin-reach thrombus formation, citrated (3.2%) human whole blood was labelled with a DyLight 647-coupled anti-fibrin antibody (10 µg/mL) and DiOC6 (3,3'-dihexyloxacarbocyanine iodide;1 µmol/L) and was recalcified by adding CaCl2 (12.5 mmol/L) and MgCl2 (3.5 mmol/L) just before perfusing it through microfluidic flow chambers at 1500 s−1. Once platelet rich thrombi were formed, a brief washing step was performed to rinse the thrombi before perfusing hirudinated blood

stained with RAM.1-A567 (2 µg/mL) from the same donor. Fluorescence emission was measured using a confocal Leica SP8 inverted microscope with a resonant scanner and a 40× oil objective. Series of optical sections in xyz were taken from the base to the peak of the thrombi (Leica LAS X software). Images were then stacked and the volume of the thrombi was determined with ImageJ software (National Institutes of Health, Bethesda, MD, USA).

Statistical analyses

All statistical analyses were performed using a GraphPad Prism program, version 6.0 (Prism, GraphPad, La Jolla, CA, USA). All values are reported as the mean ± standard error of the mean for a normal distribution, or median for a non-normal distribution. The data of two groups were compared by the two-tailed paired test.

RESULTS

Insight into the dynamics of the formation of a hemostatic plug. To gain insight into the process stopping the hemostatic response after a localized vessel injury, we used *in vivo* mouse models of vascular injury. We first observed that puncturing the carotid artery of adult mice with a needle resulted in bleeding followed by the formation of a platelet and fibrin-rich plug which stops blood loss. Real-time video microscopy showed that the plug formation is reversible presenting a bell-shaped curve with a phase of growth, embolization to finally stabilize. The thrombus embolization occurs at 250 ± 50 sec after thrombus onset, after which no platelets accumulated anymore (**Figure 1A**). Fibrin appeared with a delay of 60 ± 20 sec after the first platelets adhered at site of injury, and grew progressively occupying 40 ± 20 % of thrombus area at the

time of embolization. By 450 sec after thrombosis initiation fibrin occupied 60 ± 15 % of thrombus area coinciding with no more platelet accumulation (**Figure 1B**). Interestingly, when $FeCl_3$ was applied to the carotid, a similar kinetic of platelet aggregation and fibrin formation was evidenced, with the only distinction of the formation of a mural thrombus (**Figure 1C**). In this model, there was no more platelets accumulation after thrombus embolization, which starts at 1,030 ± 80 sec, when fibrin occupied 52 ± 9 % of its maximum area and its amount was 70 ± 9% of fibrin maximum area 300 sec after embolization (**Figure 1D**). Similar observations were also obtained after a mechanical injury with forceps of the aorta, even though the overall process was more rapid compared to the two other models (**Figure 1E-F**). Together, a common feature of three distinct models of vascular injury indicate that the arrest of thrombus growth, *i.e.* of the hemostatic response, appeared after thrombus embolization and coincides with the time at which fibrin occupied most of the area of the plug.

Fibrin covers the hemostatic plug. To better appreciate the spatiotemporal localization of fibrin within a plug, the carotid artery of adult mice was injured with $FeCl_3$ and fibrin distribution in the thrombus was studied by different approaches. Fluorescence images using a macroscope to have a large field of view, indicated that after 1500 sec, when the most part of the thrombus was embolized, fibrin occupied 32 ± 8 % of the area of the residual platelet rich plug (**Figure 2A**). Histological analysis of these thrombi revealed that fibrin staining reached the top of the thrombus, suggesting its exposure to the flowing blood (**Figure 2B**). This result was confirmed using scanning electron microscopy (SEM) which showed that a large area of the plug contained fibrin on its top that covers the thrombus surface (**Figure 2C**). Similar observations were made for plugs forming after puncture of the carotid artery and pinching of aorta.

Fluorescence images confirmed that after 400 sec and 1,100 sec, fibrin occupied 63 ± 20 % and 70 ± 20 % of the area of the residual platelet plug and covered his surface for puncture (**Figure 2D-E**) and pinching models (**Figure 2F-G**), respectively. Together, these imaging approaches indicate that the residual platelet plug is very rich in fibrin, which reaches its top to form a layer. This observation questions whether such a layer exhibits a protective function and could stop further platelet adhesion and aggregation to stop the hemostatic response.

A fibrin layer prevents thrombus growth *in vitro*. To test the hypothesis of fibrin being involved in arresting the hemostatic response, we used an *in vitro* approach. Using a flow-based assay, we formed fibrin-poor and fibrin-rich thrombi by perfusing hirudinated and recalcified citrated blood over collagen at 1,500 s^{-1}, respectively (**Figure 3A**). The mean thrombus volumes of fibrin-poor and fibrin-rich thrombi were 10±2 x 10^4 μm^3 and 9±3 x 10^4 μm^3 (mean ± SEM, n=5), respectively (**Figure 3B, C**). We next perfused human hirudinated whole blood over the pre-formed thrombi to evaluate their thrombogenic potential. We observed thrombus build-up on fibrin poor aggregates (3±1 x 10^4 μm^3), while this process was reduced by more than 10 times on fibrin-rich thrombi (0.3±0.1 x 10^4 μm^3 (mean ± SEM, n=5) (**Figure 3B, D**). This *in vitro* observation indicates a negative role of fibrin in thrombus growth and allows to hypothesize that a fibrin layer could exhibit a protective function and efficiently limit platelet adhesion and aggregation.

Fibrin stops the process of platelet recruitment and aggregation *in vivo*. To test the hypothesis that fibrin limits thrombus growth *in vivo* after thrombus embolization,

we injured the carotid artery of an adult mouse with a solution of $FeCl_3$, and once the thrombus reached its maximal size and fibrin only started to appear in the core (fibrin poor thrombus), we mechanically removed the thrombus by flicking the vessel. Interestingly, under such conditions where fibrin is largely absent from the aggregate, the thrombus was able to repeatedly form again and stopped only when fibrin reached its maximal level *i.e.*, the thrombus surface (**Figure 4A-B**). This result was confirmed by using a pharmacological approach based on rtPA injection to lyse the fibrin content within the aggregate when the thrombus reached its maximal size (**Figure 4C**). As expected rtPA in contrast to saline and even hirudin efficiently reduced the level of fibrin within the thrombus and destabilized the aggregate to induce embolization that was not observed to other solutions (**Figure 4D, E; Sup. Figure 1A**). Interestingly, this did not lead to the arrest of the hemostatic process but led to a regrowth process which far exceeded the time at which aggregation stops in the control and with hirudin (**Figure 4F**). In addition, this regrowth could be repeated several times, further highlighting a role of fibrin in the arrest of the hemostatic response (**Figure 4F**).

A genetically modified mouse defective in fibrin formation a marked impairment in the arrest of the hemostatic response. To confirm the hypothesis that fibrin limits thrombus growth and exclude side effects of mechanical and pharmacological approaches, we studied the thrombus formation after $FeCl_3$-induced thrombosis in transgenic FibAEK mice presenting a mutation of the Aa chain of fibrinogen. These mice present a normal level of circulating fibrinogen, but do not have the ability to form an insoluble fibrin network. The dynamic of thrombus formation in FibAEK mice consists of a repeated series of growths and embolizations during all experimental time (**Figure 5A, B**). In addition, the amount of regrowth processes during thrombus

formation was significantly higher in FibAEK mice compared to WT mice (**Figure 5C**). More importantly, we could not detect a time at which the process stopped and had to terminate the experiments after 60 min, which far exceeds the time at which aggregation stops in controls (**Figure 5D**). In conclusion, these findings identified a central role of fibrin, which in addition to its very well-established role in stabilizing the clot, is also instrumental in regulating the hemostatic response by turning off the physiological response of plug formation and preventing further platelet incorporation.

DISCUSSION

The results of this work show that the process of thrombus growth leads to the formation of a stable platelet rich plug which ended up covered by fibrin in three distinct experimental models of vascular injury in large vessels. Using a flow-based assay, we observed that the presence of a fibrin layer on top of an aggregate prevents its growth. In agreement, we observed that mechanical removal of a thrombus formed *in vivo*, after vessel flicking, resulted in continuous regrowth which stopped when fibrin reached the top of the thrombus. Moreover, *in vivo* experiments with pharmacological agents removing the fibrin during the thrombus growth phase, leads to thrombus embolization, which allowed the aggregate to grow again. Interestingly this regrowth process could be repeated many times. Finally, the dynamic of thrombus formation in FibAEK mice was profoundly altered with an expected defect in thrombus stabilization, and an additional prolongation of the hemostatic process composed of successive growth and embolization phases. This study identified a novel instrumental role for fibrin in turning off the physiological response of plug formation by limiting further incorporation of circulating platelets.

Vessel injury in various mouse models of localized vascular injury results in a very similar dynamic of thrombosis, with an initial growth of a very large thrombus, followed by a stage of embolization leaving a patch covering the lesion. The main focus of our study was to understand why following embolization of the large aggregate, the patch composed of highly activated platelets remained inert and did not grow again. This study is purely focused on understanding the physiological process of hemostasis, and is not considering a situation of arterial thrombosis. It is also important to highlight that we did not study the process of embolization *per se*, neither the process of occlusive thrombus formation. Our study was clearly focused on the first couple of minutes after vessel injury and the profile of the thrombus that forms is common to various vessels and mode of injury including a mechanical injury of the aorta, photochemical injury of the carotid, electrolytic injury of the femoral vein, laser-injury of the cremaster vessels and mesenteric arterioles, puncture injury of femoral vein and aorta and $FeCl_3$-induced injury of the aorta and mesenteric arterioles [10,11,14-19].

We observed that the surface of the residual patch formed in three different experimental models was covered by a layer of fibrin. These results correlate with the thrombus structure obtained after laser-induced injury in mouse mesenteric vessels which was reported to be mainly composed of platelets and covered by fibrin [20]. Such a fibrin biofilm was also detected on human intracoronary thrombi which were aspirated in patients with acute myocardial infarction [21]. Similar observations were made on thrombi responsible for large vessel occlusion in the setting of acute ischemic stroke [22]. Together, these results indicate that various thrombi from animal models or from patients share in common the presence of a fibrin layer on the luminal side. While the group of Robert Ariëns proposed that such fibrin biofilms play an antimicrobial function, its role in hemostasis had never been addressed [23]. We propose here that the fibrin

layer plays an important role in the passivation of the thrombus and promotes thereby the arrest of the hemostatic response.

While the main result of this study indicates that the fibrin layer covering the thrombus switches off the process of thrombus growth, the precise mechanism remains to be determined. An obvious explanation of the arrest of thrombus growth is that the fibrin layer is poorly adhesive as shown in *in vitro* based experiments with a fibrin layer not efficiently promoting platelet activation and aggregation, and do therefore not represent a nucleation site for further growth [24]. In addition, it is well established that fibrin traps thrombin limiting its diffusion and pro-thrombotic effects [25,26]. This is best illustrated when we compared the effect rtPA versus rtPA combined to the direct thrombin inhibitor hirudin. While rtPA started to lyse fibrin and free thrombin a regrowth was observed which was due to thrombin as this effect disappeared in the presence of hirudin (**Figure 4, Sup. Figure 1**). Whether there are additional ways by which fibrin arrests thrombus growth cannot be excluded. One potential explanation could be that fibrin decreases the permeability-porosity of thrombus, thereby limits the transport velocity of soluble agonists released by platelets in thrombus core [27,28]. It is also possible that the fibrin layer on the residual thrombus surface restricts the distribution of granule content, for example, the exposure of vWF from α-granules as this molecule could remained trapped in fibrin fibers and not reach the thrombus surface to allow platelet recruitment [29,30].

From a hemostatic standpoint, the platelet plug should be formed as quickly as possible to limit blood loss after vessel injury. While an occlusive aggregate is required after rupture of a vessel wall, a non-occlusive plug should be formed in case of non-penetrating injuries. This is essential to avoid an unnecessary vessel occlusion, which would impair blood supply to downstream tissues. Our study proposes that the arrest

of the hemostatic process is finely tuned by fibrin. Based on this data, it could be assumed that fibrin would be present in elevated quantities to form a non-occlusive thrombus and low quantities to allow the formation of an occlusive clot when a dramatically injured vessel has to be closed to avoid excessive blood loss. This hypothesis is in agreement with the literature, as murine thrombi formed after perforating laser injury have lower mounts of fibrin compared to thrombi forming after non-penetrating injury induced by laser ablation [31,32]. Because of a lack of sufficient amount of experimental evidence, the difference in occlusive and non-occlusive thrombi composition and the role of fibrin in it, requires further investigations.

In conclusion, our findings identify a central role of fibrin in the arrest of the hemostatic response, by passivating the surface of the thrombus and thereby limiting platelet adhesion to the plug. We propose that, in addition to its very well-established role in stabilizing the clot, fibrin is also instrumental in regulating the hemostatic response by turning off the physiological response of plug formation and preventing further platelet incorporation.

ACKNOWLEDGEMENTS

We thank J.N. Mulvihill for reviewing the English of the manuscript and J.Y. Rinckel and F. Proamer for help in preparing the samples for SEM. This work was supported by the Ministry of Education and Science of Russia (075-15-2022-242).

AUTHORSHIP

AY acquired and analyzed the data; MUA performed in vitro experiments; AY and CB performed in vivo experiments; PM conceived and designed the research and handled funding and supervision.

DISCLOSURES

The authors declare no conflicts of interest.

REFERENCES

1. Sierra C, Moreno M, Garcia-Ruiz JC. The physiology of hemostasis. *Blood Coagul Fibrinolysis*. 2022;33(Suppl 1):S1-S2.
2. Broos K, Feys HB, De Meyer SF, Vanhoorelbeke K, Deckmyn H. Platelets at work in primary hemostasis. *Blood Rev*. 2011;25(4):155-167.
3. Savage B, Saldivar E, Ruggeri ZM. Initiation of platelet adhesion by arrest onto fibrinogen or translocation on von Willebrand factor. *Cell*. 1996;84(2):289-297.
4. Bergmeier W, Hynes RO. Extracellular matrix proteins in hemostasis and thrombosis. *Cold Spring Harb Perspect Biol*. 2012;4(2).
5. Palta S, Saroa R, Palta A. Overview of the coagulation system. *Indian J Anaesth*. 2014;58(5):515-523.
6. Norris LA. Blood coagulation. *Best Pract Res Clin Obstet Gynaecol*. 2003;17(3):369-383.
7. Gale AJ. Continuing education course #2: current understanding of hemostasis. *Toxicol Pathol*. 2011;39(1):273-280.
8. Holinstat M. Normal platelet function. *Cancer Metastasis Rev*. 2017;36(2):195-198.
9. Prasad JM, Gorkun OV, Raghu H, et al. Mice expressing a mutant form of fibrinogen that cannot support fibrin formation exhibit compromised antimicrobial host defense. *Blood*. 2015;126(17):2047-2058.
10. Eckly A, Hechler B, Freund M, et al. Mechanisms underlying FeCl3-induced arterial thrombosis. *J Thromb Haemost*. 2011;9(4):779-789.
11. Tang C, Wang Y, Lei D, et al. Standardization of a well-controlled in vivo mouse model of thrombus formation induced by mechanical injury. *Thromb Res*. 2016;141:49-57.
12. Nechipurenko DY, Receveur N, Yakimenko AO, et al. Clot Contraction Drives the Translocation of Procoagulant Platelets to Thrombus Surface. *Arterioscler Thromb Vasc Biol*. 2019;39(1):37-47.

13. Ahmed MU, Receveur N, Janus-Bell E, et al. Respective roles of Glycoprotein VI and FcgammaRIIA in the regulation of alphaIIbbeta3-mediated platelet activation to fibrinogen, thrombus buildup, and stability. *Res Pract Thromb Haemost*. 2021;5(5):e12551.

14. Nonne C, Lenain N, Hechler B, et al. Importance of platelet phospholipase Cgamma2 signaling in arterial thrombosis as a function of lesion severity. *Arterioscler Thromb Vasc Biol*. 2005;25(6):1293-1298.

15. Wang Y, Gao H, Shi C, et al. Leukocyte integrin Mac-1 regulates thrombosis via interaction with platelet GPIbalpha. *Nat Commun*. 2017;8:15559.

16. Smith SA, Choi SH, Collins JN, Travers RJ, Cooley BC, Morrissey JH. Inhibition of polyphosphate as a novel strategy for preventing thrombosis and inflammation. *Blood*. 2012;120(26):5103-5110.

17. Denis CV, Wagner DD. Platelet adhesion receptors and their ligands in mouse models of thrombosis. *Arterioscler Thromb Vasc Biol*. 2007;27(4):728-739.

18. Kolyada A, Porter A, Beglova N. Inhibition of thrombotic properties of persistent autoimmune anti-beta2GPI antibodies in the mouse model of antiphospholipid syndrome. *Blood*. 2014;123(7):1090-1097.

19. Yakusheva AA, Butov KR, Bykov GA, et al. Traumatic vessel injuries initiating hemostasis generate high shear conditions. *Blood Adv*. 2022.

20. Kamocka MM, Mu J, Liu X, et al. Two-photon intravital imaging of thrombus development. *J Biomed Opt*. 2010;15(1):016020.

21. Zabczyk M, Natorska J, Zalewski J, Undas A. Fibrin biofilm can be detected on intracoronary thrombi aspirated from patients with acute myocardial infarction. *Cardiovasc Res*. 2019;115(6):1026-1028.

22. Di Meglio L, Desilles JP, Ollivier V, et al. Acute ischemic stroke thrombi have an outer shell that impairs fibrinolysis. *Neurology*. 2019;93(18):e1686-e1698.

23. Macrae FL, Duval C, Papareddy P, et al. A fibrin biofilm covers blood clots and protects from microbial invasion. *J Clin Invest*. 2018;128(8):3356-3368.

24. Perrella G, Huang J, Provenzale I, et al. Nonredundant Roles of Platelet Glycoprotein VI and Integrin alphaIIbbeta3 in Fibrin-Mediated Microthrombus Formation. *Arterioscler Thromb Vasc Biol*. 2021;41(2):e97-e111.

25. Muthard RW, Welsh JD, Brass LF, Diamond SL. Fibrin, gamma'-fibrinogen, and transclot pressure gradient control hemostatic clot growth during human blood flow

over a collagen/tissue factor wound. *Arterioscler Thromb Vasc Biol*. 2015;35(3):645-654.
26. Tosenberger A, Ataullakhanov F, Bessonov N, Panteleev M, Tokarev A, Volpert V. Modelling of platelet-fibrin clot formation in flow with a DPD-PDE method. *J Math Biol*. 2016;72(3):649-681.
27. Du J, Kim D, Alhawael G, Ku DN, Fogelson AL. Clot Permeability, Agonist Transport, and Platelet Binding Kinetics in Arterial Thrombosis. *Biophys J*. 2020;119(10):2102-2115.
28. Tomaiuolo M, Stalker TJ, Welsh JD, Diamond SL, Sinno T, Brass LF. A systems approach to hemostasis: 2. Computational analysis of molecular transport in the thrombus microenvironment. *Blood*. 2014;124(11):1816-1823.
29. Kim DA, Ashworth KJ, Di Paola J, Ku DN. Platelet alpha-granules are required for occlusive high-shear-rate thrombosis. *Blood Adv*. 2020;4(14):3258-3267.
30. Masalceva AA, Kaneva VN, Panteleev MA, et al. Analysis of microvascular thrombus mechanobiology with a novel particle-based model. *J Biomech*. 2022;130:110801.
31. Hechler B, Nonne C, Eckly A, et al. Arterial thrombosis: relevance of a model with two levels of severity assessed by histologic, ultrastructural and functional characterization. *J Thromb Haemost*. 2010;8(1):173-184.
32. Getz TM, Piatt R, Petrich BG, Monroe D, Mackman N, Bergmeier W. Novel mouse hemostasis model for real-time determination of bleeding time and hemostatic plug composition. *J Thromb Haemost*. 2015;13(3):417-425.

FIGURE LEGEND

Figure 1. The dynamics of the thrombus formation after vessel wall injury. A-B, Thrombus formation was induced by needle puncture of the left common carotid artery of wild-type mice. **A,** Representative fluorescence images of the thrombus (platelets labeled in green, fibrin labeled in red) at the indicated time points after injury with a 25G needle. Scale bar: 500 μm. The arrows represent the direction of blood flow and

the dotted lines the borders of the vessel. **B,** The curve shows the area of the platelets aggregate and fibrin as a function of the time after injury. **C-D**, Thrombus formation was induced by FeCl3 (7.5%)-injury of the left common carotid artery of wild type mice. **C**, Representative fluorescence images of the thrombus (platelets labeled in green, fibrin labeled in red) were taken at the indicated time points after injury. Scale bar: 500 µm. The arrow represents the direction of the blood flow and the dotted line the borders of the vessel. **D**, The curve shows the area of the platelets aggregate and fibrin as a function of the time after injury. **E-F**, Thrombus formation was induced by pinching the mouse aorta with forceps. **E**, Representative fluorescence images of the thrombus (platelets labeled in green, fibrin labeled in red) were taken at the indicated time points after injury. Scale bar: 250 µm. The arrow represents the direction of the blood flow and the dotted line the borders of the vessel. **F,** The curve shows the area of the platelets aggregate and fibrin as a function of the time after injury.

Figure 2. Fibrin covers the hemostatic plug. A-C, Thrombus formation was induced by FeCl3 (7.5%)-injury of the left common carotid artery of wild type mice and fixed at the last time point. **A,** The dot plot (left) shows the fibrin area of the residual plug expressed as the percentage of the thrombus area measured by intravital microscopy. Data are presented as the mean ± SEM and individual symbols represent individual mice. Representative fluorescence image (right) of the thrombus 40 min after initiation of the experiment. Platelets are shown in green and fibrin in red. Scale bar: 500 µm. The arrow represents the direction of the blood flow and the dotted line the borders of the vessel. **B**, Representative histology image of the residual plug 1,610 sec after $FeCl_3$-injury. **C,** Representative scanning electron microscopy images of the residual plug X min after $FeCl_3$-injury. The thrombus is composed of tightly packed platelets, fibrous strands whose ultrastructure resembles to fibrin colored on the enlarged image

of the area in the red square in gray and green, respectively. **D-E**, Thrombus formation was induced by needle puncture with a 25G needle of the left common carotid artery of wild-type mice. **D,** The dot plot (left) shows the fibrin area of the intraluminal residual plug expressed as the percentage of the thrombus area measured by intravital microscopy. Data are presented as the mean ± SEM and individual symbols represent individual mice. Representative fluorescence image (right) of the thrombus 71 sec after initiation of the experiment. Platelets are shown in green and fibrin in red. Scale bar: 500 µm. The arrow represents the direction of the blood flow and the dotted line the borders of the vessel. **E**, Representative scanning electron microscopy images of the intraluminal residual plug 10 min after puncture. The thrombus is composed of tightly packed platelets, fibrous strands whose ultrastructure resembles to fibrin colored on the enlarged image of the area in the red square in gray and green, respectively. **F-G**, Thrombus formation was induced by pinching the mouse aorta with forceps. **F,** The dot plot (left) shows the fibrin area of the intraluminal residual plug expressed as the percentage of the thrombus area measured by intravital microscopy. Data are presented as the mean ± SEM and individual symbols represent individual mice. Representative fluorescence image (right) of the thrombus 1,140 sec after initiation of the experiment. Platelets are shown in green and fibrin in red. Scale bar: 500 µm. The arrow represents the direction of the blood flow and the dotted line the borders of the vessel. **E**, Representative scanning electron microscopy images of the intraluminal residual plug 1,200 sec after pinching. The thrombus is composed of tightly packed platelets, fibrous strands whose ultrastructure resembles to fibrin colored on the enlarged image of the area in the red square in gray and green, respectively.

Figure 3. Comparison of thrombus growth between fibrin-poor and fibrin-rich clots *in vitro*. A-C, Thrombus formation (1st population) was induced by perfusing citrated (for fibrin-rich aggregate) or hirudinated (for fibrin-poor aggregate) human whole blood through collagen coated microfluidic flow chambers at 1500 s^{-1}. Once platelet thrombi were formed, a brief washing step was performed to rinse the thrombi before perfusing hirudinated blood from the same donor to form thrombi (2nd population). **A**, Representative 3D reconstructed confocal microscopy images of first population (in grey), second population (in green) and overlay of fibrin-poor or fibrin-rich aggregates (fibrin in red). **B**, Bar graphs shows the thrombus volume of 1st and 2nd population of fibrin-rich and fibrin-poor aggregates. Data are presented as the mean ± SEM (n=5) and individual symbols represent individual mice. **C**, The dot plot shows the thrombus volume of 1st population of fibrin-poor or fibrin-rich aggregates. Data are presented as the mean ± SEM (n=5) and individual symbols represent individual donor. Result was compared by unpaired t-test. Ns $p > 0.05$. **D**, The dot plot shows the thrombus volume of 2nd population of fibrin-poor or fibrin-rich aggregates. Data are presented as the mean ± SEM (n=5) and individual symbols represent individual donor. Result was compared by unpaired t-test. ** – $p \leq 0.01$.

Figure 4. The role of fibrin in thrombus formation after vessel wall injury *in vivo*. A-B, Thrombus formation was induced by FeCl3 (7.5%)-injury of the left common carotid artery of wild type mice and the thrombus was destroyed by flicking the vessel at the indicated time points. **A**, Representative fluorescence images of the thrombus (platelets labeled in green, fibrin labeled in red) were taken at the indicated time points after injury. Scale bar: 500 µm. The arrow represents the direction of the blood flow and the dotted line the borders of the vessel. **B**, The curve shows the area of the platelets aggregate and fibrin as a function of the time after injury. **C-F,** Thrombus

formation was induced by FeCl3 (7.5%)-injury of the left common carotid artery of wild type mice and was followed by injection of 10 mg/kg rtPA (**C, D, F**) or saline (**E, F**) 20 min after thrombus initiation. The time represents the time of the injection. **C**, Representative fluorescence images of the thrombus (platelets labeled in green, fibrin labeled in red) were taken at the indicated time points after rtPA injection. Scale bar: 500 µm. The arrow represents the direction of the blood flow and the dotted line the borders of the vessel. **D**, The curve shows the area of the platelets aggregate and fibrin as a function of the time after rtPA injection. **E**, The curve shows the area of the platelets aggregate and fibrin as a function of the time after saline injection. **F**, The dot plot shows the amount of thrombus regrowth after rtPA and saline injection. Data are presented as the mean ± SEM (n=4) and individual symbols represent individual mice. Result was compared by unpaired t-test. * – p≤ 0.05.

Figure 5. The thrombus formation after vessel wall injury in FibAEK mice. A-B, Thrombus formation was induced by FeCl3 (7.5%)-injury of the left common carotid artery of FibAEK mice. **A**, Representative fluorescence images of the thrombus (platelets labeled in green, fibrin labeled in red) were taken at the indicated time points after injury. Scale bar: 500 µm. The arrow represents the direction of the blood flow and the dotted line the borders of the vessel. **B**, The curve shows the area of the platelets aggregate and fibrin as a function of the time after injury. **C**, The dot plot shows the amount of thrombus regrowth in WT and FibAEK mice. Data are presented as the mean ± SEM (n=6) and individual symbols represent individual mice. Result was compared by unpaired t-test. ** – p≤ 0.01. **D**, The dot plot shows the time at which platelets stop to adhere to the thrombus in WT and FibAEK mice. Data are presented as the mean ± SEM (n=6) and individual symbols represent individual mice. Result was compared by unpaired t-test. ** – p≤ 0.01.

Supplementary Figure 1. The role of fibrin in thrombus formation after vessel wall injury *in vivo*. A, Thrombus formation was induced by FeCl3 (7.5%)-injury of the left common carotid artery of wild type mice and was followed by injection of 20 mg/kg hirudin 20 min after thrombus initiation. The time represents the time of the injection. The curve shows the area of the platelets aggregate and fibrin as a function of the time after injection.

Figure 1

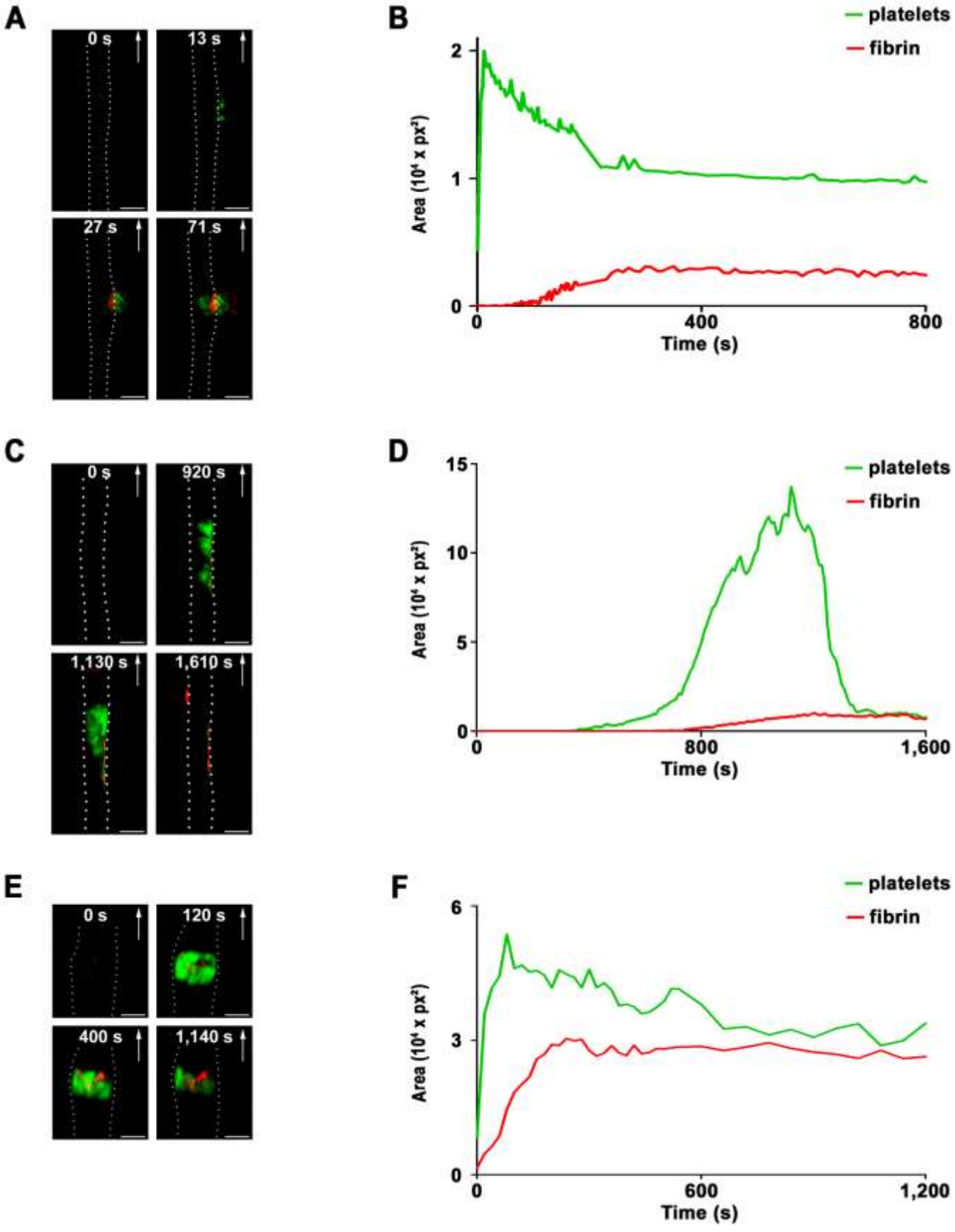
A
0 s
13 s
27 s
71 s
B
platelets
fibrin
Area (10⁴ x px²)
2
1
0
0
400
800
Time (s)
C
0 s
920 s
1,130 s
1,610 s
D
platelets
fibrin
Area (10⁴ x px²)
15
10
5
0
0
800
1,600
Time (s)
E
0 s
120 s
400 s
1,140 s
F
platelets
fibrin
Area (10⁴ x px²)
6
3
0
0
600
1,200
Time (s)

Figure 2

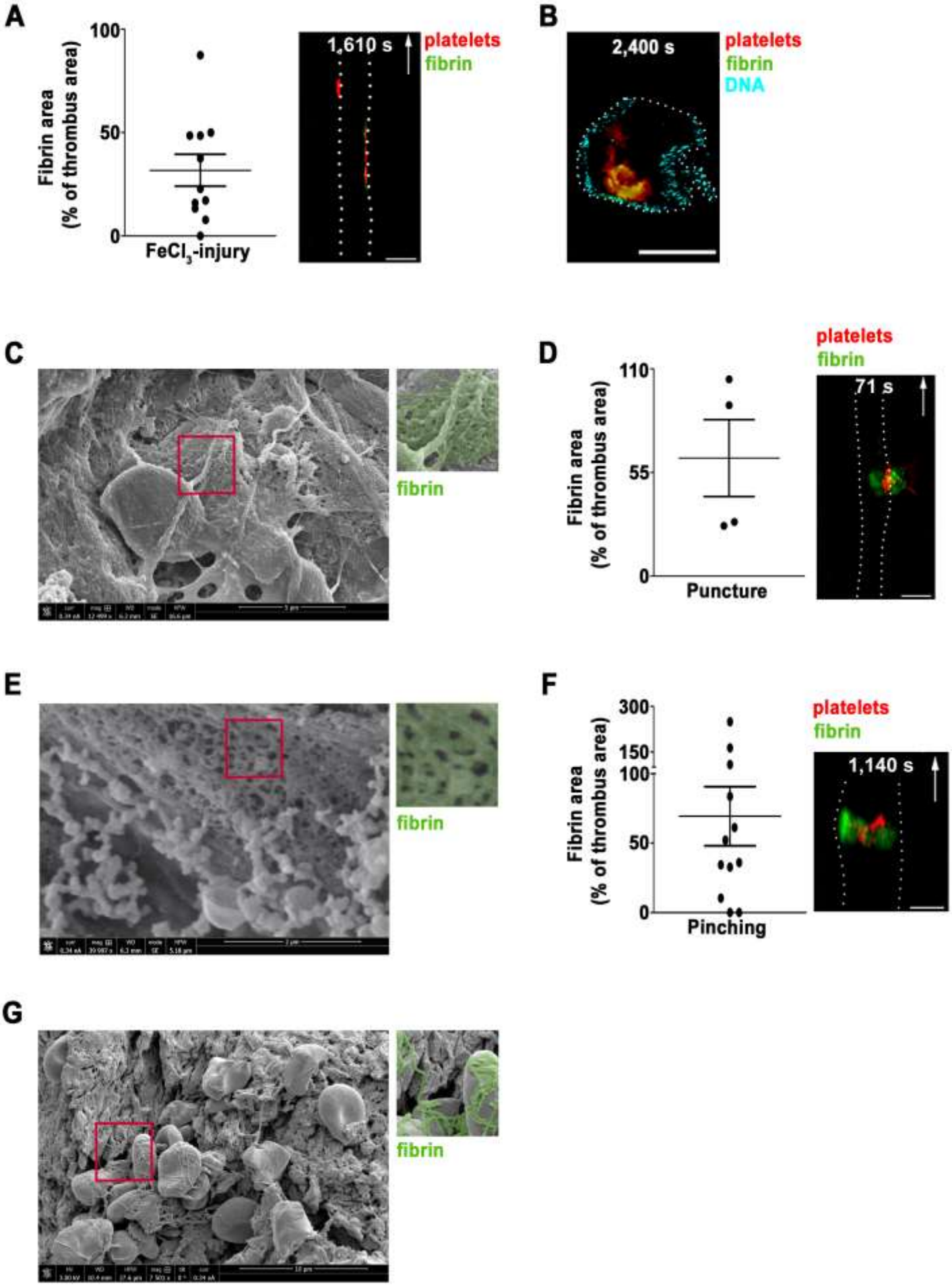
A
Fibrin area (% of thrombus area)
100
50
0
FeCl3-injury
1,610 s
platelets
fibrin
B
2,400 s
platelets
fibrin
DNA
C
fibrin
D
Fibrin area (% of thrombus area)
110
55
0
Puncture
platelets
fibrin
71 s
E
fibrin
F
Fibrin area (% of thrombus area)
300
150
100
50
0
Pinching
platelets
fibrin
1,140 s
G
fibrin

Figure 3

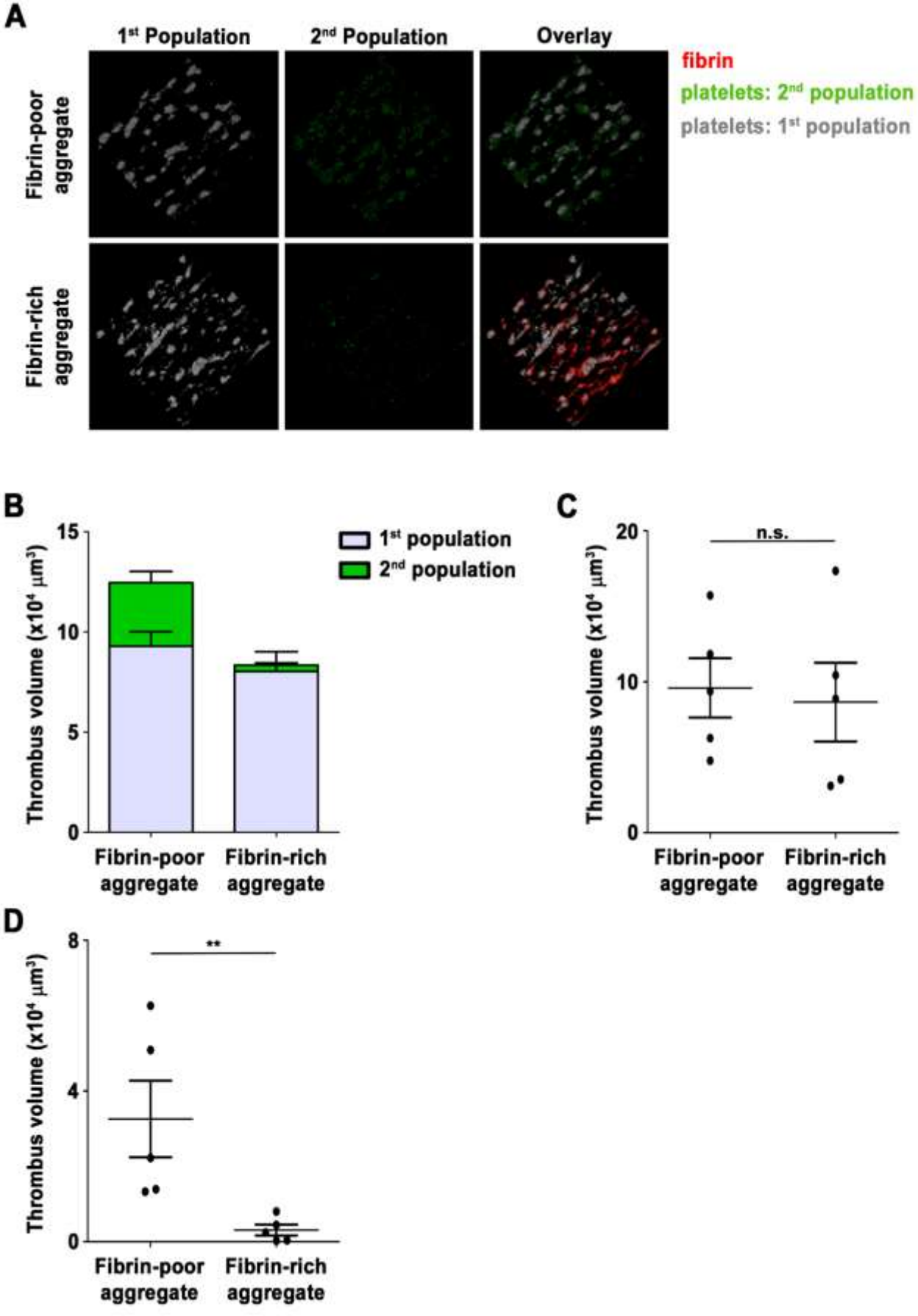
A
1st Population
2nd Population
Overlay
fibrin
platelets: 2nd population
platelets: 1st population
Fibrin-poor aggregate
Fibrin-rich aggregate
B
Thrombus volume (x10⁴ μm³)
1st population
2nd population
Fibrin-poor aggregate
Fibrin-rich aggregate
C
n.s.
Thrombus volume (x10⁴ μm³)
Fibrin-poor aggregate
Fibrin-rich aggregate
D
**
Thrombus volume (x10⁴ μm³)
Fibrin-poor aggregate
Fibrin-rich aggregate

Figure 4

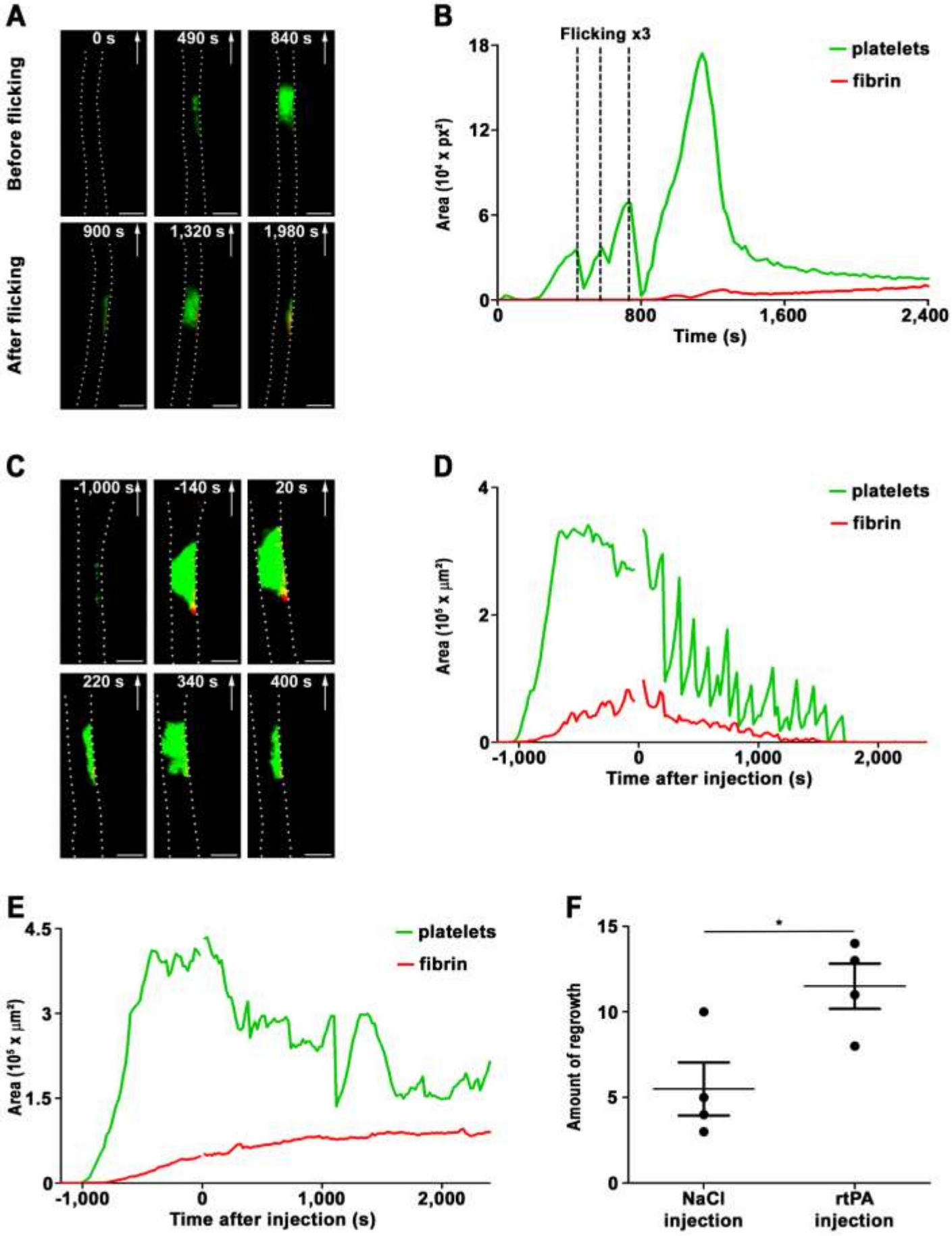
A
Before flicking
After flicking
0 s
490 s
840 s
900 s
1,320 s
1,980 s
B
Flicking x3
platelets
fibrin
Area (10⁴ x px²)
Time (s)
C
-1,000 s
-140 s
20 s
220 s
340 s
400 s
D
platelets
fibrin
Area (10⁵ x µm²)
Time after injection (s)
E
platelets
fibrin
Area (10⁵ x µm²)
Time after injection (s)
F
Amount of regrowth
NaCl injection
rtPA injection
*

Figure 5

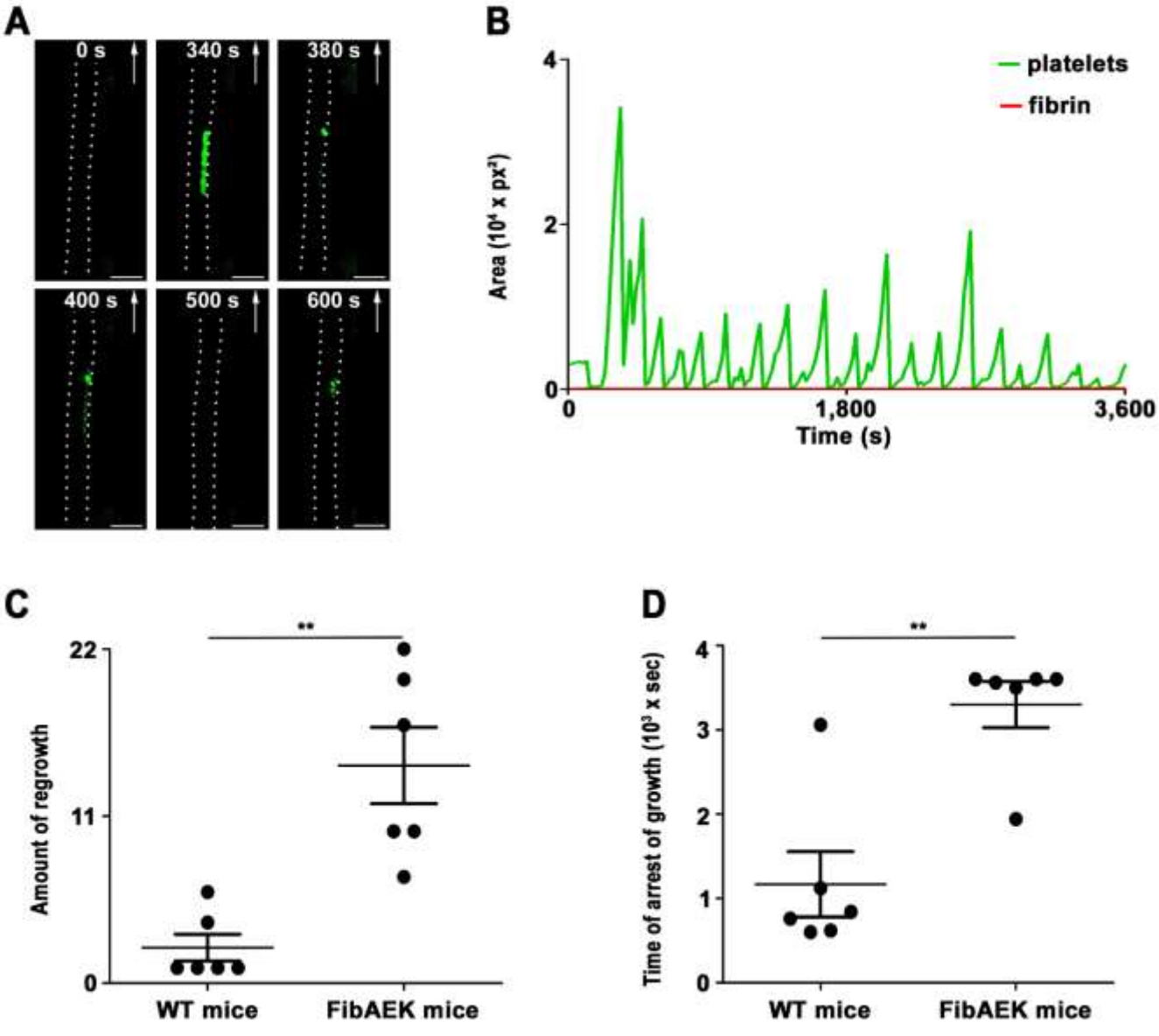
A
0 s
340 s
380 s
400 s
500 s
600 s
B
platelets
fibrin
Area (10⁴ x px²)
4
2
0
0
1,800
3,600
Time (s)
C
**
22
11
0
Amount of regrowth
WT mice
FibAEK mice
D
**
4
3
2
1
0
Time of arrest of growth (10³ x sec)
WT mice
FibAEK mice

Supplementary Figure 1

A

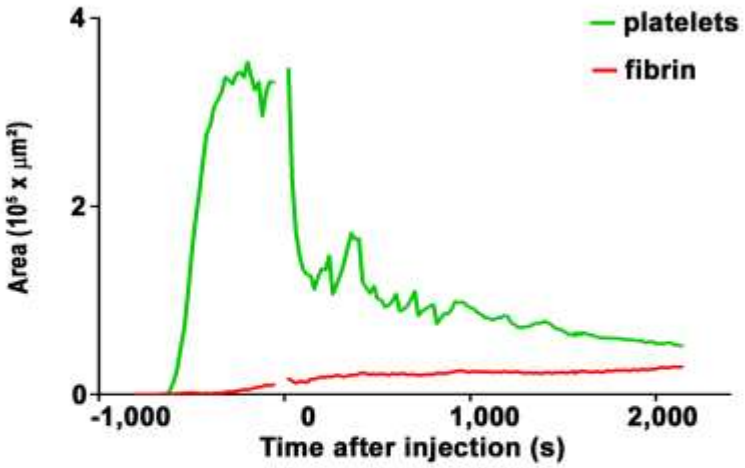

Conclusion

The results of this work show that the process of thrombus growth leads to the formation of a stable platelet rich plug which was covered by fibrin in three distinct experimental models of vascular injury in large vessels. Using a flow-based assay, we observed that the presence of a fibrin layer on top of an aggregate prevents its growth. Mechanical removal of the thrombus after vessel flicking resulted in continuous regrowth which stopped only when fibrin reached its maximal level within the thrombus surface and covered it. *In vivo* experiments with pharmacological agents removing the fibrin during thrombus growth lead to thrombus embolization, which allowed the aggregate to grow again, and this regrowth process was repeated many times. Finally, the dynamic of thrombus formation in FibAEK mice was profoundly altered with as expected a lack of thrombus stabilization, but additionally we also observed that the hemostatic process was prolonged compared to a control with successive growth and embolization phases.

In conclusion, these findings identified a central role of fibrin in the arrest of the hemostatic response, by limiting platelet adhesion to the plug. We propose that, in addition to its very well-established role in stabilizing the clot, fibrin is also instrumental in regulating the hemostatic response by turning off the physiological response of plug formation and preventing further platelet incorporation.

General Discussion and Perspectives

After vascular injury, platelets adhere, activate and aggregate at the injury site to form a hemostatic plug that limits bleeding. They are also involved in arterial thrombosis, which is the cause of serious pathologies such as myocardial infarction or ischemic stroke. Arterial thrombosis is treated by antiplatelet drugs which have shown their effectiveness in markedly reducing the mortality rates of thrombotic pathologies. However, the main limitation of these treatments is the increased risk of bleeding limiting their use in some clinical situations, such as ischemic stroke, for which the risk of hemorrhagic transformation is high and can have deleterious consequences for the patient. Identifying the specific features of hemostasis and arterial thrombosis in terms of molecular mechanisms or rheological conditions could provide valuable information to reduce the risk of bleeding while maintaining the antithrombotic effect.

To address this question, the objective of my thesis project consisted in: i) the characterization of flow conditions occurring after lesion of a healthy vessel; ii) the identification of the importance of platelet integrin α5β1 in hemostasis and arterial thrombosis; iii) the evaluation of the role of fibrin in the termination of the hemostatic response.

In the 1,800s the physician Rudolf Virchow described three key features of intravascular venous thrombosis, *i.e*, endothelial injury, stasis of blood flow and hypercoagulability, which later were expanded to recognize the importance of blood flow in the regulation of hemostasis and arterial thrombosis. The parameter most commonly used to characterize blood flow is the shear rate. In intact vessels, the wall shear rate (WSR), which is the velocity gradient near the vessel wall, ranging from about 100 s^{-1} in veins up to 2,000 s^{-1} in small arterioles. In diseased vessels, in which an atherosclerotic plaque forms a severe stenosis, the WSR can reach several 10,000 s^{-1}. Since the high shear found at the apex of a plaque is recognized as a specific feature

of thrombosis, targeting high shear has been proposed as an innovative strategy to selectively block thrombosis with a minor impact on hemostasis, thereby potentially avoiding bleeding complications. A major caveat of this paradigm and the anti-thrombotic strategy derived from it, is that the current knowledge of blood flow parameters occurring *in vivo*, are based on intact vessels in homeostatic conditions, and the rheological conditions taking place in the wound after vessel wall rupture have never been measured experimentally. The main finding of my first project is that various types of lesions in small and large mouse and human blood vessels result in extremely high shear rates at the edge of the wound where hemostasis occurs. The data demonstrate that shear rates reached during hemostasis are much greater than those occurring in intact vessels and currently proposed as being relevant for hemostasis. These results challenge the belief in the field that hemostasis is a process that depends on low and intermediate shears ($< 2{,}000\ s^{-1}$), while occlusive thrombosis in regions of plaque occurs under high shear. This paradigm shift in the field questions the postulate that targeting thrombus formation at high shear is a specific anti-thrombotic approach.

Hemostasis is taking place in many distinct settings including after injuries resulting in internal bleeding and resulting in bruising, or after open injuries responsible for external bleeding with blood leaving into the external environment. Any type of bleeding is induced by a pressure drop between two points of flow, *i.e.* inside the circulation and outside the vessel. My first project was focused on traumatic injuries resulting in external bleeding. In this situation the bleeding is induced by pressure drop occurring between the blood circulation system and the atmosphere, with a drop evaluated at about 600 mmHg ($\Delta P \approx 600$ mmHg). By comparison, internal bleeding is induced by a pressure drop appearing between the surrounding tissues and the circulation system that should be much lower due to tissue compression ($\Delta P \approx 10\text{-}74$ mmHg) (Ashton, 1975). Our study reports the occurrence of high shear rates in the case of external

bleeding, while blood flow levels taking place during internal bleeding are still unknown and require further investigation. It would have been very interesting to obtain results by using, for example, a laser-induced model adapted to induce a perforating injury of small vessels resulting in internal bleeding and study the effect of active closure of small arterioles under vasomotor tone and passive collapse of soft-walled capillaries.

In our study, we proposed that external bleeding occurs under two different flow regimes: "constant pressure" for small injuries (< 30 µm) and "constant flow" for big injuries (> 150 µm). The occurrence of a "constant flow" regime was determined experimentally as it was possible to generate a large wound in the vessel wall by using a needle. However, a limitation of my study is that it was not possible to provide experimental evidence that for small injuries the shear rate relies on pressure drop – the "constant pressure" regime. We could unfortunately not perform smaller injuries due to technical limitations and generate such data. Other studies faced similar issues, notably a publication using an experimental hemostasis model based on laser injury of the saphenous vein where the injury diameter was 48 µm, demonstrating the high challenge to perform injuries smaller than 30 µm in diameter which is necessary to switch to another flow regime for this vessel (Getz et al., 2015). A detailed analysis of fluid dynamics for tiny injuries would be definitely interesting and important but requires development of new technical approaches.

Based on observation of the presence of elevated shear at the edge of a wound in healthy vessels, we can now hypothesize that targeting high shear will probably not be devoid of bleeding complications after traumatic injuries (falls, trauma, surgery, *etc*) and, therefore, would not represent a specific antithrombotic strategy. However, whether there is a rheological

parameter which could be used as a specific antithrombotic target remains an open and attractive question. One of them could be an excessive elongation flow which is known to be thrombogenic due to its efficiency in unfolding vWF and promoting platelet adhesion and activation. In our study, we also observed occurrence of increased elongational flows in injured healthy vessels when compared to values in intact vessels. Upcoming studies should identify the levels of elongational flows occurring in hemostatic and thrombotic settings and define the threshold of elongational flows precipitating vWF unfolding to determine whether this parameter can discriminate such situations. Another potential flow parameter discriminating hemostasis from thrombosis is turbulence which does not occur in the setting of hemostasis but could take place in the post-stenotic areas in diseased arteries. A detailed analysis of fluid dynamics in the setting of thrombosis would be definitely interesting and important to define turbulent conditions an elongational flow conditions found in regions where thrombosis is exacerbated.

Antiplatelet agents used in the clinic mainly target the platelet activation and aggregation stages, which is the case of aspirin, P2Y12 inhibitors and integrin αIIbβ3 blockers. Another option of antiplatelet treatment would be to develop drugs targeting the interaction of platelets with the extracellular matrix in order to interrupt the initial step of the thrombotic process. These platelet-extracellular matrix interactions notably involve integrins of the β1 family (Bergmeier and Hynes, 2012). Among these are the integrins α2β1 and α6β1 which have already been proposed to participate in experimental thrombosis, and whose involvement in hemostasis appears modest, making them potentially interesting new antiplatelet targets (He et al., 2003; Schaff et al., 2013). At the beginning of my PhD, the importance of integrin α5β1 in hemostasis and experimental thrombosis had never been evaluated, and became the aim of my second project.

The bleeding time of mice not expressing the α5β1 integrin specifically at the platelet level was not modified. The same results were published for mice deficient for α2β1 and α6β1 in which bleeding times were normal (He et al., 2003; Schaff et al., 2013). Interestingly, the mice deficient for the three β1 integrins were described to present an increased bleeding time which suggested that these three receptors are important to ensure hemostasis, but present an important functional compensation. It also suggested that blocking only one of these receptors in the setting of a pharmacological antithrombotic approach might reduce arterial thrombosis for some of them and potentially be devoid of bleeding risk (Petzold et al., 2013).

Our findings indicate that the platelet integrin α5β1 plays a key role in the adhesion, activation and aggregation of platelets *in vitro* on a surface of fibrillar cellular fibronectin. However, our study did not show any major role of this integrin in models of experimental thrombosis *in vivo*. A potential explanation for this apparent discrepancy between the results obtained *in vitro* and *in vivo*, could rely in different rheological conditions. Indeed, while the blood perfusion *in vitro* over fibronectin was performed at 300 s^{-1}, it is well known that WSR found in mouse arteries are 5 to 10-times higher (Panteleev et al., 2021). Unfortunately, using such elevated WSR *in vitro* was not achievable as adhesion no longer occurred onto fibrillar fibronectin above 1,000 s^{-1}, which is in agreement with previously published studies (Maurer et al., 2015). At the molecular level, this lack of adhesion is most likely explained by the fact that immobilized fibronectin very inefficiently adsorbs plasma vWF compared to collagen. It would have been very interesting to obtain results at high wall shear rates *in vitro* by using, for example, a mixed matrix of vWF and cellular fibrillar fibronectin or by covering the flow chamber surface with cell-derived extracellular matrix. This matrix could be produced by

immortalized fibroblasts and it is rich in fibrillar fibronectin which supports platelet adhesion even under high shear rates (Maurer et al., 2015).

Our results indicate that α5β1 alone does not play a central role in experimental thrombosis, and one could be tempted to conclude that α5β1 is less important than the two other β1 integrins, α2β1 and α6β1, which have both been shown to contribute to experimental thrombosis (He et al., 2003; Schaff et al., 2013). This hypothesis is also supported by the fact that we have studied PF4Cre-α6-deficient mice in the same experimental thrombosis models as PF4Cre-α5-deficient mice and only observed a defect in the former strain (Schaff et al., 2013). We should nevertheless remain cautious as the injuries applied in the different experimental models might not expose sufficient amounts of fibronectin and therefore not favor the observation of a defect in PF4Cre-α5-deficient mice. Moreover, in patients, arterial thrombosis generally occurs in a diseased vessel after rupture of an atherosclerotic plaque which is rich in fibronectin (Rohwedder et al., 2012). Therefore, an analysis of thrombus formation in a plaque rupture model in mice deficient for α5β1 integrin would have been definitely interesting and important to fully estimate the role of this integrin *in vivo*. To reproduce atherosclerosis, α5β1 deficient mice could be crossed with mice deficient in apolipoprotein E (ApoE) and the plaque could be ruptured by a needle or ultrasound to induce thrombosis (Hechler and Gachet, 2011a). Finally, our observations result from mouse studies, and it remains possible that the role of α5β1 might be more important in humans.

Platelet plug formation is a dynamic process which could be divided into three stages: the transient build-up of a sub-occlusive thrombus, which is followed by disaggregation and ends up in the stabilization of a residual patch. Such a profile has been observed in numerous

in vivo studies in large and small vessels under different types of injuries (Denis and Wagner, 2007; Nonne et al., 2005; Smith et al., 2012; Tang et al., 2016; Wang et al., 2017). While the process of platelet adhesion, activation and aggregation at the site of injury is very well understood, the mechanism limiting extensive platelet aggregation to switch off the process remains fully unknown, which became the aim of my third project.

Using intravital microscopy of laser-induced cremaster muscle arteriole thrombosis, the group of Lawrence Brass has reported that a thrombus is heterogeneous in composition with a core of highly activated platelets close to the site of injury, surrounded by a shell of less activated platelets (Stalker et al., 2013). The core region is composed of tightly packed platelets and is the primary site of thrombin activity and fibrin deposition. A limitation of this view is that it is a snapshot at one given time point and does not take into account the dynamic aspect of thrombus formation which is very important. Our findings took into account the dynamics of thrombus formation and focused on the end stage when the plug formation ends. Our results indicate that the arrest of thrombus growth appeared after embolization of the shell, when only a fibrin-rich core was exposed to the blood. We propose that this core is covered with a fibrin layer, which exhibits a protective function, plays an important role in the passivation of the thrombus and promotes thereby the arrest of the hemostatic response.

In our study, we provided evidence for the formation of a fibrin layer on the thrombus surface in needle- and $FeCl_3$-injury models in the carotid artery formed under arterial blood flow conditions. The limitation of our study is the lack of evidence of fibrin layer formation under venous blood flow conditions. The group of Rosen E. demonstrated that fibrin was a main component of the stabilized thrombus area by using a fibrin(ogen) antibody in a laser-induced

injury model of the mesenteric venule (Kamocka et al., 2010). However, there is no other study of stabilized (after embolization) thrombus composition under venous conditions. Therefore, an analysis of fibrin distribution in a remaining thrombus after vein injury would have been definitely interesting and important to fully estimate the role of fibrin in the arrest of thrombus growth.

Our results indicate that the fibrin layer covering the thrombus switches off the process of thrombus growth. However, we did not fully investigate the mechanism of this process. An obvious explanation of the arrest of thrombus growth is that the fibrin layer is poorly adhesive and reactive so that when platelets adhere to it, they do not become fully activated and do therefore not represent a nucleation site for further growth. Another explanation could be that fibrin physically or chemically traps thrombin within the thrombus limiting its diffusion and avoiding it to sustain platelet activation and enhance coagulation. Therefore, *in vivo* analysis of thrombin diffusion within the thrombus during its growth could be interesting for further investigation of the mechanism of the arrest of the hemostatic response.

Under hemostatic conditions, the platelet plug should be formed as quickly as possible to limit blood loss after injury. Depending on the injury severity the plug geometry has to be different. Indeed, an occlusive aggregate is required after the rupture of small vessels while a non-occlusive plug has to be formed in case of smaller injuries, when the circulation still persists, but blood is pouring out of the vessel. This is essential to avoid an excessive response which could result in unnecessary occlusion in vessels presenting modest injuries, thereby avoiding reduction of blood supply to downstream tissues. Our study hypothesized that this process of arrest of hemostasis is finely tuned by fibrin. If fibrin indeed stops the hemostatic

process one could wonder how a plug can become occlusive in the case of a vessel transection. Interestingly, we observed that in such a case, the thrombus forming is very rich in platelets but does not contain significant amounts of fibrin, which explains its ability to fully grow in the lumen. It remains to be determined why after vessel transection, no significant levels of fibrin are formed, which will require further investigations.

To conclude, my work is part of a global perspective of characterizing the role of fibrin and platelet receptors in hemostasis and thrombosis, which could not only help to better appreciate and discriminate hemostasis from thrombosis, but also open new avenues for specific antithrombotic strategies. My work indicates that targeting high shear rates is not a specific antithrombotic strategy since high shear also occurs in injured healthy vessels. In my second study focused on integrin α5β1, I could show that this integrin plays an important role in platelet accumulation on fibronectin, but not in experimental thrombosis in mice, which suggests that this receptor might not be a relevant antiplatelet target. Finally, I identified of a role for fibrin in turning off the physiological response of plug formation and preventing further platelet incorporation.

Bibliography

Aarts, P.A., van den Broek, S.A., Prins, G.W., Kuiken, G.D., Sixma, J.J., and Heethaar, R.M. (1988). Blood platelets are concentrated near the wall and red blood cells, in the center in flowing blood. Arteriosclerosis *8*, 819-824.

Abbonante, V., Di Buduo, C.A., Gruppi, C., De Maria, C., Spedden, E., De Acutis, A., Staii, C., Raspanti, M., Vozzi, G., Kaplan, D.L., *et al.* (2017). A new path to platelet production through matrix sensing. Haematologica *102*, 1150-1160.

Abbracchio, M.P., Burnstock, G., Boeynaems, J.M., Barnard, E.A., Boyer, J.L., Kennedy, C., Knight, G.E., Fumagalli, M., Gachet, C., Jacobson, K.A., *et al.* (2006). International Union of Pharmacology LVIII: update on the P2Y G protein-coupled nucleotide receptors: from molecular mechanisms and pathophysiology to therapy. Pharmacological reviews *58*, 281-341.

Adair, B.D., Xiong, J.P., Maddock, C., Goodman, S.L., Arnaout, M.A., and Yeager, M. (2005). Three-dimensional EM structure of the ectodomain of integrin {alpha}V{beta}3 in a complex with fibronectin. The Journal of cell biology *168*, 1109-1118.

Afosah, D.K., Ofori, E., Mottamal, M., and Al-Horani, R.A. (2022). Factor IX(a) inhibitors: an updated patent review (2003-present). Expert opinion on therapeutic patents *32*, 381-400.

Ahmed, M.U., Kaneva, V., Loyau, S., Nechipurenko, D., Receveur, N., Le Bris, M., Janus-Bell, E., Didelot, M., Rauch, A., Susen, S., *et al.* (2020). Pharmacological Blockade of Glycoprotein VI Promotes Thrombus Disaggregation in the Absence of Thrombin. Arteriosclerosis, thrombosis, and vascular biology *40*, 2127-2142.

Akuta, K., Kiyomizu, K., Kashiwagi, H., Kunishima, S., Nishiura, N., Banno, F., Kokame, K., Kato, H., Kanakura, Y., Miyata, T., *et al.* (2020). Knock-in mice bearing constitutively active alphaIIb(R990W) mutation develop macrothrombocytopenia with severe platelet dysfunction. Journal of thrombosis and haemostasis : JTH *18*, 497-509.

Alberts, M.J., Shang, T., and Magadan, A. (2015). Endovascular Therapy for Acute Ischemic Stroke: Dawn of a New Era. JAMA neurology *72*, 1101-1103.

Aleman, M.M., Walton, B.L., Byrnes, J.R., Wang, J.G., Heisler, M.J., Machlus, K.R., Cooley, B.C., and Wolberg, A.S. (2013). Elevated prothrombin promotes venous, but not arterial, thrombosis in mice. Arteriosclerosis, thrombosis, and vascular biology *33*, 1829-1836.

Alexander-Katz, A., Schneider, M.F., Schneider, S.W., Wixforth, A., and Netz, R.R. (2006). Shear-flow-induced unfolding of polymeric globules. Physical review letters *97*, 138101.

Alshehri, O.M., Hughes, C.E., Montague, S., Watson, S.K., Frampton, J., Bender, M., and Watson, S.P. (2015). Fibrin activates GPVI in human and mouse platelets. Blood *126*, 1601-1608.

Alvarez, V., Rossetti, A.O., Papavasileiou, V., and Michel, P. (2013). Acute seizures in acute ischemic stroke: does thrombolysis have a role to play? Journal of neurology *260*, 55-61.

Amane, H.S., and Burte, N.P. (2011). A comparative study of dalteparin and unfractionated heparin in patients with unstable angina pectoris. Indian journal of pharmacology *43*, 703-706.

Ambrosio, A.L., and Di Pietro, S.M. (2017). Storage pool diseases illuminate platelet dense granule biogenesis. Platelets *28*, 138-146.

Andersen, H., Greenberg, D.L., Fujikawa, K., Xu, W., Chung, D.W., and Davie, E.W. (1999). Protease-activated receptor 1 is the primary mediator of thrombin-stimulated platelet procoagulant activity. Proceedings of the National Academy of Sciences of the United States of America *96*, 11189-11193.

Ando, T., Xuan, W., Xu, T., Dai, T., Sharma, S.K., Kharkwal, G.B., Huang, Y.Y., Wu, Q., Whalen, M.J., Sato, S., *et al.* (2011). Comparison of therapeutic effects between pulsed and continuous wave 810-nm wavelength laser irradiation for traumatic brain injury in mice. PloS one *6*, e26212.

Andre, P., Delaney, S.M., LaRocca, T., Vincent, D., DeGuzman, F., Jurek, M., Koller, B., Phillips, D.R., and Conley, P.B. (2003). P2Y12 regulates platelet adhesion/activation, thrombus

growth, and thrombus stability in injured arteries. The Journal of clinical investigation *112*, 398-406.

Andrews, R.K., Arthur, J.F., and Gardiner, E.E. (2014). Targeting GPVI as a novel antithrombotic strategy. Journal of blood medicine *5*, 59-68.

Andrews, R.K., Gardiner, E.E., Shen, Y., Whisstock, J.C., and Berndt, M.C. (2003). Glycoprotein Ib-IX-V. The international journal of biochemistry & cell biology *35*, 1170-1174.

Anfray, A., Brodin, C., Drieu, A., Potzeha, F., Dalarun, B., Agin, V., Vivien, D., and Orset, C. (2021). Single- and two- chain tissue type plasminogen activator treatments differentially influence cerebral recovery after stroke. Experimental neurology *338*, 113606.

Antonijevic, N.M., Zivkovic, I.D., Jovanovic, L.M., Matic, D.M., Kocica, M.J., Mrdovic, I.B., Kanjuh, V.I., and Culafic, M.D. (2017). Dabigatran - Metabolism, Pharmacologic Properties and Drug Interactions. Current drug metabolism *18*, 622-635.

Ashton, H. (1975). The effect of increased tissue pressure on blood flow. Clinical orthopaedics and related research, 15-26.

Astarita, J.L., Acton, S.E., and Turley, S.J. (2012). Podoplanin: emerging functions in development, the immune system, and cancer. Frontiers in immunology *3*, 283.

Ataullakhanov, F.I., and Guriia, G.T. (1994). [Spatial aspects of the dynamics of blood coagulation. I. Hypothesis]. Biofizika *39*, 89-96.

Atkinson, B.T., Jasuja, R., Chen, V.M., Nandivada, P., Furie, B., and Furie, B.C. (2010). Laser-induced endothelial cell activation supports fibrin formation. Blood *116*, 4675-4683.

Awtry, E.H., and Loscalzo, J. (2000). Aspirin. Circulation *101*, 1206-1218.

Bagot, C.N., and Arya, R. (2008). Virchow and his triad: a question of attribution. British journal of haematology *143*, 180-190.

Bailey, K., Bettelheim, F.R., Lorand, L., and Middlebrook, W.R. (1951). Action of thrombin in the clotting of fibrinogen. Nature *167*, 233-234.

Banner, D.W., D'Arcy, A., Chene, C., Winkler, F.K., Guha, A., Konigsberg, W.H., Nemerson, Y., and Kirchhofer, D. (1996). The crystal structure of the complex of blood coagulation factor VIIa with soluble tissue factor. Nature *380*, 41-46.

Baqi, Y., and Muller, C.E. (2019). Antithrombotic P2Y12 receptor antagonists: recent developments in drug discovery. Drug discovery today *24*, 325-333.

Bark, D.L., Jr., and Ku, D.N. (2010). Wall shear over high degree stenoses pertinent to atherothrombosis. Journal of biomechanics *43*, 2970-2977.

Barr, J.D., Chauhan, A.K., Schaeffer, G.V., Hansen, J.K., and Motto, D.G. (2013). Red blood cells mediate the onset of thrombosis in the ferric chloride murine model. Blood *121*, 3733-3741.

Basmadjian, D. (1990). The effect of flow and mass transport in thrombogenesis. Annals of biomedical engineering *18*, 685-709.

Bauer, M., Retzer, M., Wilde, J.I., Maschberger, P., Essler, M., Aepfelbacher, M., Watson, S.P., and Siess, W. (1999). Dichotomous regulation of myosin phosphorylation and shape change by Rho-kinase and calcium in intact human platelets. Blood *94*, 1665-1672.

Baumgartner, H.R. (1973). The role of blood flow in platelet adhesion, fibrin deposition, and formation of mural thrombi. Microvascular research *5*, 167-179.

Bearer, E.L., Prakash, J.M., and Li, Z. (2002). Actin dynamics in platelets. International review of cytology *217*, 137-182.

Ben Addi, A., Cammarata, D., Conley, P.B., Boeynaems, J.M., and Robaye, B. (2010). Role of the P2Y12 receptor in the modulation of murine dendritic cell function by ADP. Journal of immunology *185*, 5900-5906.

Bender, M., Hagedorn, I., and Nieswandt, B. (2011). Genetic and antibody-induced glycoprotein VI deficiency equally protects mice from mechanically and FeCl(3) -induced thrombosis. Journal of thrombosis and haemostasis : JTH *9*, 1423-1426.

Bender, M., May, F., Lorenz, V., Thielmann, I., Hagedorn, I., Finney, B.A., Vogtle, T., Remer, K., Braun, A., Bosl, M., *et al.* (2013). Combined in vivo depletion of glycoprotein VI and C-type lectin-like receptor 2 severely compromises hemostasis and abrogates arterial thrombosis in mice. Arteriosclerosis, thrombosis, and vascular biology *33*, 926-934.

Benis, A.M., Usami, S., and Chien, S. (1971). Determination of the shear stress-shear rate relation for blood by Couette viscometry. Biorheology *8*, 65-69.

Bennett, J.S., Chan, C., Vilaire, G., Mousa, S.A., and DeGrado, W.F. (1997). Agonist-activated alphavbeta3 on platelets and lymphocytes binds to the matrix protein osteopontin. The Journal of biological chemistry *272*, 8137-8140.

Bergmeier, W., and Hynes, R.O. (2012). Extracellular matrix proteins in hemostasis and thrombosis. Cold Spring Harbor perspectives in biology *4*.

Bergmeier, W., Piffath, C.L., Goerge, T., Cifuni, S.M., Ruggeri, Z.M., Ware, J., and Wagner, D.D. (2006). The role of platelet adhesion receptor GPIbalpha far exceeds that of its main ligand, von Willebrand factor, in arterial thrombosis. Proceedings of the National Academy of Sciences of the United States of America *103*, 16900-16905.

Best, D., Senis, Y.A., Jarvis, G.E., Eagleton, H.J., Roberts, D.J., Saito, T., Jung, S.M., Moroi, M., Harrison, P., Green, F.R., *et al.* (2003). GPVI levels in platelets: relationship to platelet function at high shear. Blood *102*, 2811-2818.

Beumer, S., MJ, I.J., de Groot, P.G., and Sixma, J.J. (1994). Platelet adhesion to fibronectin in flow: dependence on surface concentration and shear rate, role of platelet membrane glycoproteins GP IIb/IIIa and VLA-5, and inhibition by heparin. Blood *84*, 3724-3733.

Bhatt, D.L., Steg, P.G., Ohman, E.M., Hirsch, A.T., Ikeda, Y., Mas, J.L., Goto, S., Liau, C.S., Richard, A.J., Rother, J., *et al.* (2006). International prevalence, recognition, and treatment of cardiovascular risk factors in outpatients with atherothrombosis. Jama *295*, 180-189.

Bix, G., Fu, J., Gonzalez, E.M., Macro, L., Barker, A., Campbell, S., Zutter, M.M., Santoro, S.A., Kim, J.K., Hook, M., *et al.* (2004). Endorepellin causes endothelial cell disassembly of actin cytoskeleton and focal adhesions through alpha2beta1 integrin. The Journal of cell biology *166*, 97-109.

Boettner, B., and Van Aelst, L. (2009). Control of cell adhesion dynamics by Rap1 signaling. Current opinion in cell biology *21*, 684-693.

Bohnsack, J.F. (1992). CD11/CD18-independent neutrophil adherence to laminin is mediated by the integrin VLA-6. Blood *79*, 1545-1552.

Bolton-Maggs, P.H. (1996). Factor XI deficiency. Bailliere's clinical haematology *9*, 355-368.

Bos, J.L. (2005). Linking Rap to cell adhesion. Current opinion in cell biology *17*, 123-128.

Boukerche, H., Berthier-Vergnes, O., Tabone, E., Dore, J.F., Leung, L.L., and McGregor, J.L. (1989). Platelet-melanoma cell interaction is mediated by the glycoprotein IIb-IIIa complex. Blood *74*, 658-663.

Bradford, H.N., Dela Cadena, R.A., Kunapuli, S.P., Dong, J.F., Lopez, J.A., and Colman, R.W. (1997). Human kininogens regulate thrombin binding to platelets through the glycoprotein Ib-IX-V complex. Blood *90*, 1508-1515.

Bradford, H.N., Pixley, R.A., and Colman, R.W. (2000). Human factor XII binding to the glycoprotein Ib-IX-V complex inhibits thrombin-induced platelet aggregation. The Journal of biological chemistry *275*, 22756-22763.

Brehm, M.A. (2017). Von Willebrand factor processing. Hamostaseologie *37*, 59-72.

Brisson, C., Azorsa, D.O., Jennings, L.K., Moog, S., Cazenave, J.P., and Lanza, F. (1997). Co-localization of CD9 and GPIIb-IIIa (alpha IIb beta 3 integrin) on activated platelet pseudopods and alpha-granule membranes. Histochem J *29*, 153-165.

Bromberger, T., Klapproth, S., Rohwedder, I., Zhu, L., Mittmann, L., Reichel, C.A., Sperandio, M., Qin, J., and Moser, M. (2018). Direct Rap1/Talin1 interaction regulates platelet and neutrophil integrin activity in mice. Blood *132*, 2754-2762.

Broos, K., Feys, H.B., De Meyer, S.F., Vanhoorelbeke, K., and Deckmyn, H. (2011). Platelets at work in primary hemostasis. Blood reviews *25*, 155-167.

Brummel-Ziedins, K.E., Branda, R.F., Butenas, S., and Mann, K.G. (2009). Discordant fibrin formation in hemophilia. Journal of thrombosis and haemostasis : JTH *7*, 825-832.

Bryckaert, M., Rosa, J.P., Denis, C.V., and Lenting, P.J. (2015). Of von Willebrand factor and platelets. Cellular and molecular life sciences : CMLS *72*, 307-326.

Buchanan, G.R., and Handin, R.I. (1976). Platelet function in the Chediak-Higashi syndrome. Blood *47*, 941-948.

Burke, R.D. (1999). Invertebrate integrins: structure, function, and evolution. International review of cytology *191*, 257-284.

Burkhart, J.M., Vaudel, M., Gambaryan, S., Radau, S., Walter, U., Martens, L., Geiger, J., Sickmann, A., and Zahedi, R.P. (2012). The first comprehensive and quantitative analysis of human platelet protein composition allows the comparative analysis of structural and functional pathways. Blood *120*, e73-82.

Butenas, S. (2012). Tissue factor structure and function. Scientifica *2012*, 964862.

Byon, W., Garonzik, S., Boyd, R.A., and Frost, C.E. (2019). Apixaban: A Clinical Pharmacokinetic and Pharmacodynamic Review. Clinical pharmacokinetics *58*, 1265-1279.

Capra, V., Back, M., Angiolillo, D.J., Cattaneo, M., and Sakariassen, K.S. (2014). Impact of vascular thromboxane prostanoid receptor activation on hemostasis, thrombosis, oxidative stress, and inflammation. Journal of thrombosis and haemostasis : JTH *12*, 126-137.

Carman, C.V., and Springer, T.A. (2003). Integrin avidity regulation: are changes in affinity and conformation underemphasized? Current opinion in cell biology *15*, 547-556.

Cathcart, M.C., Tamosiuniene, R., Chen, G., Neilan, T.G., Bradford, A., O'Byrne, K.J., Fitzgerald, D.J., and Pidgeon, G.P. (2008). Cyclooxygenase-2-linked attenuation of hypoxia-induced pulmonary hypertension and intravascular thrombosis. The Journal of pharmacology and experimental therapeutics *326*, 51-58.

Cattaneo, M. (2007). Platelet P2 receptors: old and new targets for antithrombotic drugs. Expert review of cardiovascular therapy *5*, 45-55.

Cattaneo, M., Zighetti, M.L., Lombardi, R., Martinez, C., Lecchi, A., Conley, P.B., Ware, J., and Ruggeri, Z.M. (2003). Molecular bases of defective signal transduction in the platelet P2Y12 receptor of a patient with congenital bleeding. Proceedings of the National Academy of Sciences of the United States of America *100*, 1978-1983.

Cawthern, K.M., van 't Veer, C., Lock, J.B., DiLorenzo, M.E., Branda, R.F., and Mann, K.G. (1998). Blood coagulation in hemophilia A and hemophilia C. Blood *91*, 4581-4592.

Cesarman-Maus, G., and Hajjar, K.A. (2005). Molecular mechanisms of fibrinolysis. British journal of haematology *129*, 307-321.

Chan, B.M., and Hemler, M.E. (1993). Multiple functional forms of the integrin VLA-2 can be derived from a single alpha 2 cDNA clone: interconversion of forms induced by an anti-beta 1 antibody. The Journal of cell biology *120*, 537-543.

Chapin, J.C., and Hajjar, K.A. (2015). Fibrinolysis and the control of blood coagulation. Blood reviews *29*, 17-24.

Chaudhry, R., Usama, S.M., and Babiker, H.M. (2022). Physiology, Coagulation Pathways. In StatPearls (Treasure Island (FL)).

Chauhan, A.K., Kisucka, J., Lamb, C.B., Bergmeier, W., and Wagner, D.D. (2007). von Willebrand factor and factor VIII are independently required to form stable occlusive thrombi in injured veins. Blood *109*, 2424-2429.

Chen, J., Diacovo, T.G., Grenache, D.G., Santoro, S.A., and Zutter, M.M. (2002). The alpha(2) integrin subunit-deficient mouse: a multifaceted phenotype including defects of branching morphogenesis and hemostasis. The American journal of pathology *161*, 337-344.

Chen, Y., Ju, L.A., Zhou, F., Liao, J., Xue, L., Su, Q.P., Jin, D., Yuan, Y., Lu, H., Jackson, S.P., *et al.* (2019). An integrin alphaIIbbeta3 intermediate affinity state mediates biomechanical platelet aggregation. Nature materials *18*, 760-769.

Cheng, Y., Austin, S.C., Rocca, B., Koller, B.H., Coffman, T.M., Grosser, T., Lawson, J.A., and FitzGerald, G.A. (2002). Role of prostacyclin in the cardiovascular response to thromboxane A2. Science *296*, 539-541.

Chintala, M., Strony, J., Yang, B., Kurowski, S., and Li, Q. (2010). SCH 602539, a protease-activated receptor-1 antagonist, inhibits thrombosis alone and in combination with cangrelor in a Folts model of arterial thrombosis in cynomolgus monkeys. Arteriosclerosis, thrombosis, and vascular biology *30*, 2143-2149.

Christofori, G. (2007). Cancer: division of labour. Nature *446*, 735-736.

Cirincione, B., Kowalski, K., Nielsen, J., Roy, A., Thanneer, N., Byon, W., Boyd, R., Wang, X., Leil, T., LaCreta, F., *et al.* (2018). Population Pharmacokinetics of Apixaban in Subjects With Nonvalvular Atrial Fibrillation. CPT: pharmacometrics & systems pharmacology *7*, 728-738.

Cohen, A.T., Dobromirski, M., and Gurwith, M.M. (2014). Managing pulmonary embolism from presentation to extended treatment. Thrombosis research *133*, 139-148.

Conley, P.B., and Delaney, S.M. (2003). Scientific and therapeutic insights into the role of the platelet P2Y12 receptor in thrombosis. Current opinion in hematology *10*, 333-338.

Connolly, S.J., Ezekowitz, M.D., Yusuf, S., Eikelboom, J., Oldgren, J., Parekh, A., Pogue, J., Reilly, P.A., Themeles, E., Varrone, J., *et al.* (2009). Dabigatran versus warfarin in patients with atrial fibrillation. The New England journal of medicine *361*, 1139-1151.

Cooley, B.C. (2012). Murine models of thrombosis. Thrombosis research *129 Suppl 2*, S62-64.

Cornelissen, I., Palmer, D., David, T., Wilsbacher, L., Concengco, C., Conley, P., Pandey, A., and Coughlin, S.R. (2010). Roles and interactions among protease-activated receptors and P2ry12 in hemostasis and thrombosis. Proceedings of the National Academy of Sciences of the United States of America *107*, 18605-18610.

Corral, J., Rivera, J., Gonzalez-Conejero, R., and Vicente, V. (1999). The number of platelet glycoprotein Ia molecules is associated with the genetically linked 807 C/T and HPA-5 polymorphisms. Transfusion *39*, 372-378.

Cosemans, J.M., Kuijpers, M.J., Lecut, C., Loubele, S.T., Heeneman, S., Jandrot-Perrus, M., and Heemskerk, J.W. (2005). Contribution of platelet glycoprotein VI to the thrombogenic effect of collagens in fibrous atherosclerotic lesions. Atherosclerosis *181*, 19-27.

Cosemans, J.M., Munnix, I.C., Wetzker, R., Heller, R., Jackson, S.P., and Heemskerk, J.W. (2006). Continuous signaling via PI3K isoforms beta and gamma is required for platelet ADP receptor function in dynamic thrombus stabilization. Blood *108*, 3045-3052.

Cosmi, B., Fredenburgh, J.C., Rischke, J., Hirsh, J., Young, E., and Weitz, J.I. (1997). Effect of nonspecific binding to plasma proteins on the antithrombin activities of unfractionated heparin, low-molecular-weight heparin, and dermatan sulfate. Circulation *95*, 118-124.

Costa, J.L., Fauci, A.S., and Wolff, S.M. (1976). A platelet abnormality in the Chediak-Higashi syndrome of man. Blood *48*, 517-520.

Coughlin, S.R. (2005). Protease-activated receptors in hemostasis, thrombosis and vascular biology. Journal of thrombosis and haemostasis : JTH *3*, 1800-1814.

Czaja, B., Gutierrez, M., Zavodszky, G., de Kanter, D., Hoekstra, A., and Eniola-Adefeso, O. (2020). The influence of red blood cell deformability on hematocrit profiles and platelet margination. PLoS computational biology *16*, e1007716.

Dashkevich, N.M., Ovanesov, M.V., Balandina, A.N., Karamzin, S.S., Shestakov, P.I., Soshitova, N.P., Tokarev, A.A., Panteleev, M.A., and Ataullakhanov, F.I. (2012). Thrombin activity propagates in space during blood coagulation as an excitation wave. Biophysical journal *103*, 2233-2240.

Davi, G., Santilli, F., and Vazzana, N. (2012). Thromboxane receptors antagonists and/or synthase inhibitors. Handbook of experimental pharmacology, 261-286.

David-Ferreira, J.F. (1964). The blood platelet: electron microscopic studies. International review of cytology *17*, 99-148.

De Luca, M., Facey, D.A., Favaloro, E.J., Hertzberg, M.S., Whisstock, J.C., McNally, T., Andrews, R.K., and Berndt, M.C. (2000). Structure and function of the von Willebrand factor A1 domain: analysis with monoclonal antibodies reveals distinct binding sites involved in recognition of the platelet membrane glycoprotein Ib-IX-V complex and ristocetin-dependent activation. Blood *95*, 164-172.

de Moerloose, P., Boehlen, F., and Neerman-Arbez, M. (2010). Fibrinogen and the risk of thrombosis. Seminars in thrombosis and hemostasis *36*, 7-17.

Defreyn, G., Machin, S.J., Carreras, L.O., Dauden, M.V., Chamone, D.A., and Vermylen, J. (1981). Familial bleeding tendency with partial platelet thromboxane synthetase deficiency: reorientation of cyclic endoperoxide metabolism. British journal of haematology *49*, 29-41.

Denis, C., Methia, N., Frenette, P.S., Rayburn, H., Ullman-Cullere, M., Hynes, R.O., and Wagner, D.D. (1998). A mouse model of severe von Willebrand disease: defects in hemostasis and thrombosis. Proceedings of the National Academy of Sciences of the United States of America *95*, 9524-9529.

Denis, C.V., and Wagner, D.D. (2007). Platelet adhesion receptors and their ligands in mouse models of thrombosis. Arteriosclerosis, thrombosis, and vascular biology *27*, 728-739.

DeWald, T.A., Washam, J.B., and Becker, R.C. (2018). Anticoagulants: Pharmacokinetics, Mechanisms of Action, and Indications. Neurosurgery clinics of North America *29*, 503-515.

Di Paola, J., Jugessur, A., Goldman, T., Reiland, J., Tallman, D., Sayago, C., and Murray, J.C. (2005). Platelet glycoprotein I(b)alpha and integrin alpha2 beta1 polymorphisms: gene frequencies and linkage disequilibrium in a population diversity panel. Journal of thrombosis and haemostasis : JTH *3*, 1511-1521.

Di Stasio, E., and De Cristofaro, R. (2010). The effect of shear stress on protein conformation: Physical forces operating on biochemical systems: The case of von Willebrand factor. Biophysical chemistry *153*, 1-8.

Dormann, D., Clemetson, J.M., Navdaev, A., Kehrel, B.E., and Clemetson, K.J. (2001). Alboaggregin A activates platelets by a mechanism involving glycoprotein VI as well as glycoprotein Ib. Blood *97*, 929-936.

Dowd, P., Ham, S.W., Naganathan, S., and Hershline, R. (1995). The mechanism of action of vitamin K. Annual review of nutrition *15*, 419-440.

Drake, T.A., Morrissey, J.H., and Edgington, T.S. (1989). Selective cellular expression of tissue factor in human tissues. Implications for disorders of hemostasis and thrombosis. The American journal of pathology *134*, 1087-1097.

Drury, D.R., and McMaster, P.D. (1929). The Liver as the Source of Fibrinogen. The Journal of experimental medicine *50*, 569-578.

Du, X.-Y., Magnenat, E., Wells, T.N., and Clemetson, K.J. (2002a). Alboluxin, a snake C-type lectin from Trimeresurus albolabris venom is a potent platelet agonist acting via GPIb and GPVI. Thrombosis and haemostasis *87*, 692-698.

Du, X.Y., Clemetson, J.M., Navdaev, A., Magnenat, E.M., Wells, T.N., and Clemetson, K.J. (2002b). Ophioluxin, a convulxin-like C-type lectin from Ophiophagus hannah (King cobra) is

a powerful platelet activator via glycoprotein VI. The Journal of biological chemistry *277*, 35124-35132.

Dubois, C., Panicot-Dubois, L., Gainor, J.F., Furie, B.C., and Furie, B. (2007). Thrombin-initiated platelet activation in vivo is vWF independent during thrombus formation in a laser injury model. The Journal of clinical investigation *117*, 953-960.

Dubois, C., Panicot-Dubois, L., Merrill-Skoloff, G., Furie, B., and Furie, B.C. (2006). Glycoprotein VI-dependent and -independent pathways of thrombus formation in vivo. Blood *107*, 3902-3906.

Dupuy, E., Soria, C., Molho, P., Zini, J.M., Rosenstingl, S., Laurian, C., Bruneval, P., and Tobelem, G. (2001). Embolized ischemic lesions of toes in an afibrinogenemic patient: possible relevance to in vivo circulating thrombin. Thrombosis research *102*, 211-219.

Eckly, A., Hechler, B., Freund, M., Zerr, M., Cazenave, J.P., Lanza, F., Mangin, P.H., and Gachet, C. (2011). Mechanisms underlying FeCl3-induced arterial thrombosis. Journal of thrombosis and haemostasis : JTH *9*, 779-789.

Eckly, A., Rinckel, J.Y., Proamer, F., Ulas, N., Joshi, S., Whiteheart, S.W., and Gachet, C. (2016). Respective contributions of single and compound granule fusion to secretion by activated platelets. Blood *128*, 2538-2549.

Eckstein, E.C., Tilles, A.W., and Millero, F.J., 3rd (1988). Conditions for the occurrence of large near-wall excesses of small particles during blood flow. Microvascular research *36*, 31-39.

Eikelboom, J.W., Wallentin, L., Connolly, S.J., Ezekowitz, M., Healey, J.S., Oldgren, J., Yang, S., Alings, M., Kaatz, S., Hohnloser, S.H., *et al.* (2011). Risk of bleeding with 2 doses of dabigatran compared with warfarin in older and younger patients with atrial fibrillation: an analysis of the randomized evaluation of long-term anticoagulant therapy (RE-LY) trial. Circulation *123*, 2363-2372.

Emini Veseli, B., Perrotta, P., De Meyer, G.R.A., Roth, L., Van der Donckt, C., Martinet, W., and De Meyer, G.R.Y. (2017). Animal models of atherosclerosis. European journal of pharmacology *816*, 3-13.

Erhardt, J.A., Toomey, J.R., Douglas, S.A., and Johns, D.G. (2006). P2X1 stimulation promotes thrombin receptor-mediated platelet aggregation. Journal of thrombosis and haemostasis : JTH *4*, 882-890.

Esmon, N.L., and Esmon, C.T. (1988). Protein C and the endothelium. Seminars in thrombosis and hemostasis *14*, 210-215.

Ezumi, Y., Shindoh, K., Tsuji, M., and Takayama, H. (1998). Physical and functional association of the Src family kinases Fyn and Lyn with the collagen receptor glycoprotein VI-Fc receptor gamma chain complex on human platelets. The Journal of experimental medicine *188*, 267-276.

Fabre, J.E., Nguyen, M., Latour, A., Keifer, J.A., Audoly, L.P., Coffman, T.M., and Koller, B.H. (1999). Decreased platelet aggregation, increased bleeding time and resistance to thromboembolism in P2Y1-deficient mice. Nature medicine *5*, 1199-1202.

Falati, S., Gross, P., Merrill-Skoloff, G., Furie, B.C., and Furie, B. (2002). Real-time in vivo imaging of platelets, tissue factor and fibrin during arterial thrombus formation in the mouse. Nature medicine *8*, 1175-1181.

Falati, S., Gross, P.L., Merrill-Skoloff, G., Sim, D., Flaumenhaft, R., Celi, A., Furie, B.C., and Furie, B. (2004). In vivo models of platelet function and thrombosis: study of real-time thrombus formation. Methods in molecular biology *272*, 187-197.

Fay, W.P., Parker, A.C., Ansari, M.N., Zheng, X., and Ginsburg, D. (1999). Vitronectin inhibits the thrombotic response to arterial injury in mice. Blood *93*, 1825-1830.

Feng, J., Garrity, D., Call, M.E., Moffett, H., and Wucherpfennig, K.W. (2005). Convergence on a distinctive assembly mechanism by unrelated families of activating immune receptors. Immunity *22*, 427-438.

Finamore, F., Reny, J.L., Malacarne, S., Fontana, P., and Sanchez, J.C. (2019). A high glucose level is associated with decreased aspirin-mediated acetylation of platelet cyclooxygenase (COX)-1 at serine 529: A pilot study. Journal of proteomics *192*, 258-266.

Finn, A.V., Nakano, M., Narula, J., Kolodgie, F.D., and Virmani, R. (2010). Concept of vulnerable/unstable plaque. Arteriosclerosis, thrombosis, and vascular biology *30*, 1282-1292.

Fisher, C., and Rossmann, J.S. (2009). Effect of non-newtonian behavior on hemodynamics of cerebral aneurysms. Journal of biomechanical engineering *131*, 091004.

Fitch-Tewfik, J.L., and Flaumenhaft, R. (2013). Platelet granule exocytosis: a comparison with chromaffin cells. Frontiers in endocrinology *4*, 77.

Fleck, R.A., Rao, L.V., Rapaport, S.I., and Varki, N. (1990). Localization of human tissue factor antigen by immunostaining with monospecific, polyclonal anti-human tissue factor antibody. Thrombosis research *59*, 421-437.

Francis, S.E., Goh, K.L., Hodivala-Dilke, K., Bader, B.L., Stark, M., Davidson, D., and Hynes, R.O. (2002). Central roles of alpha5beta1 integrin and fibronectin in vascular development in mouse embryos and embryoid bodies. Arteriosclerosis, thrombosis, and vascular biology *22*, 927-933.

Fredrickson, B.J., Dong, J.F., McIntire, L.V., and Lopez, J.A. (1998). Shear-dependent rolling on von Willebrand factor of mammalian cells expressing the platelet glycoprotein Ib-IX-V complex. Blood *92*, 3684-3693.

Fredriksson, R., Lagerstrom, M.C., Lundin, L.G., and Schioth, H.B. (2003). The G-protein-coupled receptors in the human genome form five main families. Phylogenetic analysis, paralogon groups, and fingerprints. Molecular pharmacology *63*, 1256-1272.

Fressinaud, E., Baruch, D., Girma, J.P., Sakariassen, K.S., Baumgartner, H.R., and Meyer, D. (1988). von Willebrand factor-mediated platelet adhesion to collagen involves platelet membrane glycoprotein IIb-IIIa as well as glycoprotein Ib. The Journal of laboratory and clinical medicine *112*, 58-67.

Frey, J.L. (2005). Recombinant tissue plasminogen activator (rtPA) for stroke. The perspective at 8 years. The neurologist *11*, 123-133.

Frojmovic, M.M., and Milton, J.G. (1982). Human platelet size, shape, and related functions in health and disease. Physiological reviews *62*, 185-261.

Fuller, G.L., Williams, J.A., Tomlinson, M.G., Eble, J.A., Hanna, S.L., Pohlmann, S., Suzuki-Inoue, K., Ozaki, Y., Watson, S.P., and Pearce, A.C. (2007). The C-type lectin receptors CLEC-2 and Dectin-1, but not DC-SIGN, signal via a novel YXXL-dependent signaling cascade. The Journal of biological chemistry *282*, 12397-12409.

Fung, C.Y., Cendana, C., Farndale, R.W., and Mahaut-Smith, M.P. (2007). Primary and secondary agonists can use P2X(1) receptors as a major pathway to increase intracellular Ca(2+) in the human platelet. Journal of thrombosis and haemostasis : JTH *5*, 910-917.

Fuster, J.J., Castillo, A.I., Zaragoza, C., Ibanez, B., and Andres, V. (2012). Animal models of atherosclerosis. Progress in molecular biology and translational science *105*, 1-23.

Gachet, C. (2006). Regulation of platelet functions by P2 receptors. Annual review of pharmacology and toxicology *46*, 277-300.

Gachet, C. (2008). P2 receptors, platelet function and pharmacological implications. Thrombosis and haemostasis *99*, 466-472.

Gachet, C. (2015). Antiplatelet drugs: which targets for which treatments? Journal of thrombosis and haemostasis : JTH *13 Suppl 1*, S313-322.

Gachet, C., Leon, C., and Hechler, B. (2006). The platelet P2 receptors in arterial thrombosis. Blood cells, molecules & diseases *36*, 223-227.

Gale, A.J. (2011). Continuing education course #2: current understanding of hemostasis. Toxicologic pathology *39*, 273-280.

Galkina, E., and Ley, K. (2007). Vascular adhesion molecules in atherosclerosis. Arteriosclerosis, thrombosis, and vascular biology *27*, 2292-2301.

Gammie, J.S., Zenati, M., Kormos, R.L., Hattler, B.G., Wei, L.M., Pellegrini, R.V., Griffith, B.P., and Dyke, C.M. (1998). Abciximab and excessive bleeding in patients undergoing emergency cardiac operations. The Annals of thoracic surgery *65*, 465-469.

Garcia, D.A., Baglin, T.P., Weitz, J.I., and Samama, M.M. (2012). Parenteral anticoagulants: Antithrombotic Therapy and Prevention of Thrombosis, 9th ed: American College of Chest Physicians Evidence-Based Clinical Practice Guidelines. Chest *141*, e24S-e43S.

Geberhiwot, T., Ingerpuu, S., Pedraza, C., Neira, M., Lehto, U., Virtanen, I., Kortesmaa, J., Tryggvason, K., Engvall, E., and Patarroyo, M. (1999). Blood platelets contain and secrete laminin-8 (alpha4beta1gamma1) and adhere to laminin-8 via alpha6beta1 integrin. Experimental cell research *253*, 723-732.

Georas, S.N., McIntyre, B.W., Ebisawa, M., Bednarczyk, J.L., Sterbinsky, S.A., Schleimer, R.P., and Bochner, B.S. (1993). Expression of a functional laminin receptor (alpha 6 beta 1, very late activation antigen-6) on human eosinophils. Blood *82*, 2872-2879.

Getz, T.M., Dangelmaier, C.A., Jin, J., Daniel, J.L., and Kunapuli, S.P. (2010). Differential phosphorylation of myosin light chain (Thr)18 and (Ser)19 and functional implications in platelets. Journal of thrombosis and haemostasis : JTH *8*, 2283-2293.

Getz, T.M., Piatt, R., Petrich, B.G., Monroe, D., Mackman, N., and Bergmeier, W. (2015). Novel mouse hemostasis model for real-time determination of bleeding time and hemostatic plug composition. Journal of thrombosis and haemostasis : JTH *13*, 417-425.

Gijsen, F.J., Allanic, E., van de Vosse, F.N., and Janssen, J.D. (1999). The influence of the non-Newtonian properties of blood on the flow in large arteries: unsteady flow in a 90 degrees curved tube. Journal of biomechanics *32*, 705-713.

Gimbrone, M.A., Jr., and Garcia-Cardena, G. (2016). Endothelial Cell Dysfunction and the Pathobiology of Atherosclerosis. Circulation research *118*, 620-636.

Giordano, A., Musumeci, G., D'Angelillo, A., Rossini, R., Zoccai, G.B., Messina, S., Coscioni, E., Romano, S., and Romano, M.F. (2016). Effects Of Glycoprotein IIb/IIIa Antagonists: Anti Platelet Aggregation And Beyond. Current drug metabolism *17*, 194-203.

Girolami, A., Ruzzon, E., Tezza, F., Scandellari, R., Vettore, S., and Girolami, B. (2006). Arterial and venous thrombosis in rare congenital bleeding disorders: a critical review. Haemophilia : the official journal of the World Federation of Hemophilia *12*, 345-351.

Gitz, E., Pollitt, A.Y., Gitz-Francois, J.J., Alshehri, O., Mori, J., Montague, S., Nash, G.B., Douglas, M.R., Gardiner, E.E., Andrews, R.K., *et al.* (2014). CLEC-2 expression is maintained on activated platelets and on platelet microparticles. Blood *124*, 2262-2270.

Giuliano, S., Nesbitt, W.S., Rooney, M., and Jackson, S.P. (2003). Bidirectional integrin alphaIIbbeta3 signalling regulating platelet adhesion under flow: contribution of protein kinase C. The Biochemical journal *372*, 163-172.

Glagov, S., Zarins, C., Giddens, D.P., and Ku, D.N. (1988). Hemodynamics and atherosclerosis. Insights and perspectives gained from studies of human arteries. Archives of pathology & laboratory medicine *112*, 1018-1031.

Goldsmith, H.L., and Turitto, V.T. (1986). Rheological aspects of thrombosis and haemostasis: basic principles and applications. ICTH-Report--Subcommittee on Rheology of the International Committee on Thrombosis and Haemostasis. Thrombosis and haemostasis *55*, 415-435.

Gomez-Outes, A., Terleira-Fernandez, A.I., Calvo-Rojas, G., Suarez-Gea, M.L., and Vargas-Castrillon, E. (2013). Dabigatran, Rivaroxaban, or Apixaban versus Warfarin in Patients with Nonvalvular Atrial Fibrillation: A Systematic Review and Meta-Analysis of Subgroups. Thrombosis *2013*, 640723.

Gorog, D.A., and Jeong, Y.H. (2015). Platelet function tests: why they fail to guide personalized antithrombotic medication. Journal of the American Heart Association *4*.

Goschnick, M.W., Lau, L.M., Wee, J.L., Liu, Y.S., Hogarth, P.M., Robb, L.M., Hickey, M.J., Wright, M.D., and Jackson, D.E. (2006). Impaired "outside-in" integrin alphaIIbbeta3 signaling and thrombus stability in TSSC6-deficient mice. Blood *108*, 1911-1918.

Grad, E., Pachino, R.M., FitzGerald, G.A., and Danenberg, H.D. (2012). Role of thromboxane receptor in C-reactive protein-induced thrombosis. Arteriosclerosis, thrombosis, and vascular biology *32*, 2468-2474.

Grambow, E., Klee, G., Klar, E., and Vollmar, B. (2020). The slow releasing hydrogen sulfide donor GYY4137 reduces neointima formation upon FeCl3 injury of the carotid artery in mice. Clinical hemorheology and microcirculation *75*, 409-417.

Gremmel, T., Frelinger, A.L., 3rd, and Michelson, A.D. (2016). Platelet Physiology. Seminars in thrombosis and hemostasis *42*, 191-204.

Gresham, C., Levine, M., and Ruha, A.M. (2009). Case files of the Medical Toxicology Fellowship at Banner Good Samaritan Medical Center in Phoenix, AZ: a non-warfarin anticoagulant overdose. Journal of medical toxicology : official journal of the American College of Medical Toxicology *5*, 242-249.

Grossi, I.M., Hatfield, J.S., Fitzgerald, L.A., Newcombe, M., Taylor, J.D., and Honn, K.V. (1988). Role of tumor cell glycoproteins immunologically related to glycoproteins Ib and IIb/IIIa in tumor cell-platelet and tumor cell-matrix interactions. FASEB journal : official publication of the Federation of American Societies for Experimental Biology *2*, 2385-2395.

Grover, S.P., and Mackman, N. (2018). Tissue Factor: An Essential Mediator of Hemostasis and Trigger of Thrombosis. Arteriosclerosis, thrombosis, and vascular biology *38*, 709-725.

Gruner, S., Prostredna, M., Koch, M., Miura, Y., Schulte, V., Jung, S.M., Moroi, M., and Nieswandt, B. (2005). Relative antithrombotic effect of soluble GPVI dimer compared with anti-GPVI antibodies in mice. Blood *105*, 1492-1499.

Gu, S.X., and Lentz, S.R. (2018). Fibrin films: overlooked hemostatic barriers against microbial infiltration. The Journal of clinical investigation *128*, 3243-3245.

Guidetti, G., Bertoni, A., Viola, M., Tira, E., Balduini, C., and Torti, M. (2002). The small proteoglycan decorin supports adhesion and activation of human platelets. Blood *100*, 1707-1714.

Guidetti, G.F., Lova, P., Bernardi, B., Campus, F., Baldanzi, G., Graziani, A., Balduini, C., and Torti, M. (2008). The Gi-coupled P2Y12 receptor regulates diacylglycerol-mediated signaling in human platelets. The Journal of biological chemistry *283*, 28795-28805.

Gupta, R., Lin, M., Mehta, A., Aedma, S.K., Shah, R., Ranchal, P., Vyas, A.V., Singh, S., Kluck, B., Combs, W.G., *et al.* (2021). Protease-Activated Receptor Antagonist for Reducing Cardiovascular Events - A Review on Vorapaxar. Current problems in cardiology, 101035.

Gurbel, P.A., Kuliopulos, A., and Tantry, U.S. (2015). G-protein-coupled receptors signaling pathways in new antiplatelet drug development. Arteriosclerosis, thrombosis, and vascular biology *35*, 500-512.

Habart, D., Cheli, Y., Nugent, D.J., Ruggeri, Z.M., and Kunicki, T.J. (2013). Conditional knockout of integrin alpha2beta1 in murine megakaryocytes leads to reduced mean platelet volume. PloS one *8*, e55094.

Haining, E.J., Cherpokova, D., Wolf, K., Becker, I.C., Beck, S., Eble, J.A., Stegner, D., Watson, S.P., and Nieswandt, B. (2017). CLEC-2 contributes to hemostasis independently of classical hemITAM signaling in mice. Blood *130*, 2224-2228.

Haining, E.J., Lowe, K.L., Wichaiyo, S., Kataru, R.P., Nagy, Z., Kavanagh, D.P., Lax, S., Di, Y., Nieswandt, B., Ho-Tin-Noe, B., *et al.* (2021). Lymphatic blood filling in CLEC-2-deficient mouse models. Platelets *32*, 352-367.

Halushka, P.V., Mais, D.E., and Garvin, M. (1986). Binding of a thromboxane A2/prostaglandin H2 receptor antagonist to guinea-pig platelets. European journal of pharmacology *131*, 49-54.

Halvorsen, S., Atar, D., Yang, H., De Caterina, R., Erol, C., Garcia, D., Granger, C.B., Hanna, M., Held, C., Husted, S., *et al.* (2014). Efficacy and safety of apixaban compared with warfarin according to age for stroke prevention in atrial fibrillation: observations from the ARISTOTLE trial. European heart journal *35*, 1864-1872.

Hamberg, M., Svensson, J., and Samuelsson, B. (1975). Thromboxanes: a new group of biologically active compounds derived from prostaglandin endoperoxides. Proceedings of the National Academy of Sciences of the United States of America *72*, 2994-2998.

Hamilton, J.R., Cornelissen, I., and Coughlin, S.R. (2004). Impaired hemostasis and protection against thrombosis in protease-activated receptor 4-deficient mice is due to lack of thrombin signaling in platelets. Journal of thrombosis and haemostasis : JTH *2*, 1429-1435.

Han, J., Lim, C.J., Watanabe, N., Soriani, A., Ratnikov, B., Calderwood, D.A., Puzon-McLaughlin, W., Lafuente, E.M., Boussiotis, V.A., Shattil, S.J., *et al.* (2006). Reconstructing and deconstructing agonist-induced activation of integrin alphaIIbbeta3. Current biology : CB *16*, 1796-1806.

Harrison, P.M., Keays, R., Bray, G.P., Alexander, G.J., and Williams, R. (1990). Improved outcome of paracetamol-induced fulminant hepatic failure by late administration of acetylcysteine. Lancet *335*, 1572-1573.

Harter, K., Levine, M., and Henderson, S.O. (2015). Anticoagulation drug therapy: a review. The western journal of emergency medicine *16*, 11-17.

Hartman, G.D., Egbertson, M.S., Halczenko, W., Laswell, W.L., Duggan, M.E., Smith, R.L., Naylor, A.M., Manno, P.D., Lynch, R.J., Zhang, G., *et al.* (1992). Non-peptide fibrinogen receptor antagonists. 1. Discovery and design of exosite inhibitors. Journal of medicinal chemistry *35*, 4640-4642.

Hartwig, J.H., Barkalow, K., Azim, A., and Italiano, J. (1999). The elegant platelet: signals controlling actin assembly. Thrombosis and haemostasis *82*, 392-398.

Hathcock, J.J. (2006). Flow effects on coagulation and thrombosis. Arteriosclerosis, thrombosis, and vascular biology *26*, 1729-1737.

Haydari, Z., Shams, H., Jahed, Z., and Mofrad, M.R.K. (2020). Kindlin Assists Talin to Promote Integrin Activation. Biophysical journal *118*, 1977-1991.

He, L., Pappan, L.K., Grenache, D.G., Li, Z., Tollefsen, D.M., Santoro, S.A., and Zutter, M.M. (2003). The contributions of the alpha 2 beta 1 integrin to vascular thrombosis in vivo. Blood *102*, 3652-3657.

Hechler, B., and Gachet, C. (2011a). Comparison of two murine models of thrombosis induced by atherosclerotic plaque injury. Thrombosis and haemostasis *105 Suppl 1*, S3-12.

Hechler, B., and Gachet, C. (2011b). P2 receptors and platelet function. Purinergic signalling *7*, 293-303.

Hechler, B., Lenain, N., Marchese, P., Vial, C., Heim, V., Freund, M., Cazenave, J.P., Cattaneo, M., Ruggeri, Z.M., Evans, R., *et al.* (2003). A role of the fast ATP-gated P2X1 cation channel in thrombosis of small arteries in vivo. The Journal of experimental medicine *198*, 661-667.

Hechler, B., Leon, C., Vial, C., Vigne, P., Frelin, C., Cazenave, J.P., and Gachet, C. (1998). The P2Y1 receptor is necessary for adenosine 5'-diphosphate-induced platelet aggregation. Blood *92*, 152-159.

Hechler, B., Magnenat, S., Zighetti, M.L., Kassack, M.U., Ullmann, H., Cazenave, J.P., Evans, R., Cattaneo, M., and Gachet, C. (2005). Inhibition of platelet functions and thrombosis through

selective or nonselective inhibition of the platelet P2 receptors with increasing doses of NF449 [4,4',4",4"'-(carbonylbis(imino-5,1,3-benzenetriylbis-(carbonylimino)))tetrakis -benzene-1,3-disulfonic acid octasodium salt]. The Journal of pharmacology and experimental therapeutics *314*, 232-243.

Hechler, B., Nonne, C., Eckly, A., Magnenat, S., Rinckel, J.Y., Denis, C.V., Freund, M., Cazenave, J.P., Lanza, F., and Gachet, C. (2010). Arterial thrombosis: relevance of a model with two levels of severity assessed by histologic, ultrastructural and functional characterization. Journal of thrombosis and haemostasis : JTH *8*, 173-184.

Hechler, B., Nonne, C., Roh, E.J., Cattaneo, M., Cazenave, J.P., Lanza, F., Jacobson, K.A., and Gachet, C. (2006). MRS2500 [2-iodo-N6-methyl-(N)-methanocarba-2'-deoxyadenosine-3',5'-bisphosphate], a potent, selective, and stable antagonist of the platelet P2Y1 receptor with strong antithrombotic activity in mice. The Journal of pharmacology and experimental therapeutics *316*, 556-563.

Heijnen, H., and van der Sluijs, P. (2015). Platelet secretory behaviour: as diverse as the granules ... or not? Journal of thrombosis and haemostasis : JTH *13*, 2141-2151.

Henriksen, R.A., and Hanks, V.K. (2002). PAR-4 agonist AYPGKF stimulates thromboxane production by human platelets. Arteriosclerosis, thrombosis, and vascular biology *22*, 861-866.

Hickey, M.J., Williams, S.A., and Roth, G.J. (1989). Human platelet glycoprotein IX: an adhesive prototype of leucine-rich glycoproteins with flank-center-flank structures. Proceedings of the National Academy of Sciences of the United States of America *86*, 6773-6777.

Hindriks, G., Ijsseldijk, M.J., Sonnenberg, A., Sixma, J.J., and de Groot, P.G. (1992). Platelet adhesion to laminin: role of Ca2+ and Mg2+ ions, shear rate, and platelet membrane glycoproteins. Blood *79*, 928-935.

Hinze, A.V., Mayer, P., Harst, A., and von Kugelgen, I. (2013). P2X1 receptor-mediated inhibition of the proliferation of human coronary smooth muscle cells involving the transcription factor NR4A1. Purinergic signalling *9*, 677-686.

Hirsh, J., Raschke, R., Warkentin, T.E., Dalen, J.E., Deykin, D., and Poller, L. (1995). Heparin: mechanism of action, pharmacokinetics, dosing considerations, monitoring, efficacy, and safety. Chest *108*, 258S-275S.

Hitchcock, J.R., Cook, C.N., Bobat, S., Ross, E.A., Flores-Langarica, A., Lowe, K.L., Khan, M., Dominguez-Medina, C.C., Lax, S., Carvalho-Gaspar, M., *et al.* (2015). Inflammation drives thrombosis after Salmonella infection via CLEC-2 on platelets. The Journal of clinical investigation *125*, 4429-4446.

Hodivala-Dilke, K.M., McHugh, K.P., Tsakiris, D.A., Rayburn, H., Crowley, D., Ullman-Cullere, M., Ross, F.P., Coller, B.S., Teitelbaum, S., and Hynes, R.O. (1999). Beta3-integrin-deficient mice are a model for Glanzmann thrombasthenia showing placental defects and reduced survival. The Journal of clinical investigation *103*, 229-238.

Hoefer, T., Rana, A., Niego, B., Jagdale, S., Albers, H.J., Gardiner, E.E., Andrews, R.K., Van der Meer, A.D., Hagemeyer, C.E., and Westein, E. (2021). Targeting shear gradient activated von Willebrand factor by the novel single-chain antibody A1 reduces occlusive thrombus formation in vitro. Haematologica *106*, 2874-2884.

Hoffman, M., Colina, C.M., McDonald, A.G., Arepally, G.M., Pedersen, L., and Monroe, D.M. (2007). Tissue factor around dermal vessels has bound factor VII in the absence of injury. Journal of thrombosis and haemostasis : JTH *5*, 1403-1408.

Hohmann, J.D., Wang, X., Krajewski, S., Selan, C., Haller, C.A., Straub, A., Chaikof, E.L., Nandurkar, H.H., Hagemeyer, C.E., and Peter, K. (2013). Delayed targeting of CD39 to activated platelet GPIIb/IIIa via a single-chain antibody: breaking the link between antithrombotic potency and bleeding? Blood *121*, 3067-3075.

Hollopeter, G., Jantzen, H.M., Vincent, D., Li, G., England, L., Ramakrishnan, V., Yang, R.B., Nurden, P., Nurden, A., Julius, D., *et al.* (2001). Identification of the platelet ADP receptor targeted by antithrombotic drugs. Nature *409*, 202-207.

Holme, M.N., Fedotenko, I.A., Abegg, D., Althaus, J., Babel, L., Favarger, F., Reiter, R., Tanasescu, R., Zaffalon, P.L., Ziegler, A., *et al.* (2012). Shear-stress sensitive lenticular vesicles for targeted drug delivery. Nature nanotechnology *7*, 536-543.

Holmsen, H. (1989). Physiological functions of platelets. Annals of medicine *21*, 23-30.

Holmsen, H., and Dangelmaier, C.A. (1989). Measurement of secretion of lysosomal acid glycosidases. Methods in enzymology *169*, 336-342.

Holtkotter, O., Nieswandt, B., Smyth, N., Muller, W., Hafner, M., Schulte, V., Krieg, T., and Eckes, B. (2002). Integrin alpha 2-deficient mice develop normally, are fertile, but display partially defective platelet interaction with collagen. The Journal of biological chemistry *277*, 10789-10794.

Honn, K.V., Chen, Y.Q., Timar, J., Onoda, J.M., Hatfield, J.S., Fligiel, S.E., Steinert, B.W., Diglio, C.A., Grossi, I.M., Nelson, K.K., *et al.* (1992a). Alpha IIb beta 3 integrin expression and function in subpopulations of murine tumors. Experimental cell research *201*, 23-32.

Honn, K.V., Tang, D.G., and Crissman, J.D. (1992b). Platelets and cancer metastasis: a causal relationship? Cancer metastasis reviews *11*, 325-351.

Hu, P., and Luo, B.H. (2013). Integrin bi-directional signaling across the plasma membrane. Journal of cellular physiology *228*, 306-312.

Huang, J., Driscoll, E.M., Gonzales, M.L., Park, A.M., and Lucchesi, B.R. (2000). Prevention of arterial thrombosis by intravenously administered platelet P2T receptor antagonist AR-C69931MX in a canine model. The Journal of pharmacology and experimental therapeutics *295*, 492-499.

Huang, J., Li, X., Shi, X., Zhu, M., Wang, J., Huang, S., Huang, X., Wang, H., Li, L., Deng, H., *et al.* (2019). Platelet integrin alphaIIbbeta3: signal transduction, regulation, and its therapeutic targeting. Journal of hematology & oncology *12*, 26.

Huang, J., Shi, X., Xi, W., Liu, P., Long, Z., and Xi, X. (2015). Evaluation of targeting c-Src by the RGT-containing peptide as a novel antithrombotic strategy. Journal of hematology & oncology *8*, 62.

Hughan, S.C., Spring, C.M., Schoenwaelder, S.M., Sturgeon, S., Alwis, I., Yuan, Y., McFadyen, J.D., Westein, E., Goddard, D., Ono, A., *et al.* (2014). Dok-2 adaptor protein regulates the shear-dependent adhesive function of platelet integrin alphaIIbbeta3 in mice. The Journal of biological chemistry *289*, 5051-5060.

Hughes, C.E., Pollitt, A.Y., Mori, J., Eble, J.A., Tomlinson, M.G., Hartwig, J.H., O'Callaghan, C.A., Futterer, K., and Watson, S.P. (2010). CLEC-2 activates Syk through dimerization. Blood *115*, 2947-2955.

Humphries, J.D., Byron, A., and Humphries, M.J. (2006). Integrin ligands at a glance. Journal of cell science *119*, 3901-3903.

Hynes, R.O. (2002). Integrins: bidirectional, allosteric signaling machines. Cell *110*, 673-687.

Ilich, A., Bokarev, I., and Key, N.S. (2017). Global assays of fibrinolysis. International journal of laboratory hematology *39*, 441-447.

Ilkan, Z., Watson, S., Watson, S.P., and Mahaut-Smith, M.P. (2018). P2X1 Receptors Amplify FcgammaRIIa-Induced Ca2+ Increases and Functional Responses in Human Platelets. Thrombosis and haemostasis *118*, 369-380.

Induruwa, I., Moroi, M., Bonna, A., Malcor, J.D., Howes, J.M., Warburton, E.A., Farndale, R.W., and Jung, S.M. (2018). Platelet collagen receptor Glycoprotein VI-dimer recognizes fibrinogen and fibrin through their D-domains, contributing to platelet adhesion and activation during thrombus formation. Journal of thrombosis and haemostasis : JTH *16*, 389-404.

Inoue, O., Hokamura, K., Shirai, T., Osada, M., Tsukiji, N., Hatakeyama, K., Umemura, K., Asada, Y., Suzuki-Inoue, K., and Ozaki, Y. (2015). Vascular Smooth Muscle Cells Stimulate Platelets and Facilitate Thrombus Formation through Platelet CLEC-2: Implications in Atherothrombosis. PloS one *10*, e0139357.

Inoue, O., Suzuki-Inoue, K., Dean, W.L., Frampton, J., and Watson, S.P. (2003). Integrin alpha2beta1 mediates outside-in regulation of platelet spreading on collagen through activation of Src kinases and PLCgamma2. The Journal of cell biology *160*, 769-780.

Inoue, O., Suzuki-Inoue, K., McCarty, O.J., Moroi, M., Ruggeri, Z.M., Kunicki, T.J., Ozaki, Y., and Watson, S.P. (2006). Laminin stimulates spreading of platelets through integrin alpha6beta1-dependent activation of GPVI. Blood *107*, 1405-1412.

Isenberg, W.M., McEver, R.P., Phillips, D.R., Shuman, M.A., and Bainton, D.F. (1987). The platelet fibrinogen receptor: an immunogold-surface replica study of agonist-induced ligand binding and receptor clustering. The Journal of cell biology *104*, 1655-1663.

Jackson, S.P., Nesbitt, W.S., and Westein, E. (2009). Dynamics of platelet thrombus formation. Journal of thrombosis and haemostasis : JTH *7 Suppl 1*, 17-20.

Jaffe, E.A., Hoyer, L.W., and Nachman, R.L. (1974). Synthesis of von Willebrand factor by cultured human endothelial cells. Proceedings of the National Academy of Sciences of the United States of America *71*, 1906-1909.

Jamasbi, J., Ayabe, K., Goto, S., Nieswandt, B., Peter, K., and Siess, W. (2017). Platelet receptors as therapeutic targets: Past, present and future. Thrombosis and haemostasis *117*, 1249-1257.

Jandrot-Perrus, M., Hermans, C., and Mezzano, D. (2019). Platelet glycoprotein VI genetic quantitative and qualitative defects. Platelets *30*, 708-713.

Jarvis, G.E., Raynal, N., Langford, J.P., Onley, D.J., Andrews, A., Smethurst, P.A., and Farndale, R.W. (2008). Identification of a major GpVI-binding locus in human type III collagen. Blood *111*, 4986-4996.

Jennings, L.K., and Phillips, D.R. (1982). Purification of glycoproteins IIb and III from human platelet plasma membranes and characterization of a calcium-dependent glycoprotein IIb-III complex. The Journal of biological chemistry *257*, 10458-10466.

Johnston, S.C., Amarenco, P., Denison, H., Evans, S.R., Himmelmann, A., James, S., Knutsson, M., Ladenvall, P., Molina, C.A., Wang, Y., *et al.* (2020). Ticagrelor and Aspirin or Aspirin Alone in Acute Ischemic Stroke or TIA. The New England journal of medicine *383*, 207-217.

Jones, D.A., Wright, P., Alizadeh, M.A., Fhadil, S., Rathod, K.S., Guttmann, O., Knight, C., Timmis, A., Baumbach, A., Wragg, A., *et al.* (2021). The use of novel oral anticoagulants compared to vitamin K antagonists (warfarin) in patients with left ventricular thrombus after acute myocardial infarction. European heart journal Cardiovascular pharmacotherapy *7*, 398-404.

Jones, S., Evans, R.J., and Mahaut-Smith, M.P. (2014). Ca2+ influx through P2X1 receptors amplifies P2Y1 receptor-evoked Ca2+ signaling and ADP-evoked platelet aggregation. Molecular pharmacology *86*, 243-251.

Jung, S.M., Moroi, M., Soejima, K., Nakagaki, T., Miura, Y., Berndt, M.C., Gardiner, E.E., Howes, J.M., Pugh, N., Bihan, D., *et al.* (2012). Constitutive dimerization of glycoprotein VI (GPVI) in resting platelets is essential for binding to collagen and activation in flowing blood. The Journal of biological chemistry *287*, 30000-30013.

Junghans, U., Seitz, R.J., Aulich, A., Freund, H.J., and Siebler, M. (2001). Bleeding risk of tirofiban, a nonpeptide GPIIb/IIIa platelet receptor antagonist in progressive stroke: an open pilot study. Cerebrovascular diseases *12*, 308-312.

Jurk, K., Clemetson, K.J., de Groot, P.G., Brodde, M.F., Steiner, M., Savion, N., Varon, D., Sixma, J.J., Van Aken, H., and Kehrel, B.E. (2003). Thrombospondin-1 mediates platelet adhesion at high shear via glycoprotein Ib (GPIb): an alternative/backup mechanism to von Willebrand factor. FASEB journal : official publication of the Federation of American Societies for Experimental Biology *17*, 1490-1492.

Kahn, M.L., Nakanishi-Matsui, M., Shapiro, M.J., Ishihara, H., and Coughlin, S.R. (1999). Protease-activated receptors 1 and 4 mediate activation of human platelets by thrombin. The Journal of clinical investigation *103*, 879-887.

Kahn, M.L., Zheng, Y.W., Huang, W., Bigornia, V., Zeng, D., Moff, S., Farese, R.V., Jr., Tam, C., and Coughlin, S.R. (1998). A dual thrombin receptor system for platelet activation. Nature *394*, 690-694.

Kamocka, M.M., Mu, J., Liu, X., Chen, N., Zollman, A., Sturonas-Brown, B., Dunn, K., Xu, Z., Chen, D.Z., Alber, M.S., *et al.* (2010). Two-photon intravital imaging of thrombus development. Journal of biomedical optics *15*, 016020.

Kamran, H., Jneid, H., Kayani, W.T., Virani, S.S., Levine, G.N., Nambi, V., and Khalid, U. (2021). Oral Antiplatelet Therapy After Acute Coronary Syndrome: A Review. Jama *325*, 1545-1555.

Kappert, K., Blaschke, F., Meehan, W.P., Kawano, H., Grill, M., Fleck, E., Hsueh, W.A., Law, R.E., and Graf, K. (2001). Integrins alphavbeta3 and alphavbeta5 mediate VSMC migration and are elevated during neointima formation in the rat aorta. Basic research in cardiology *96*, 42-49.

Katagiri, K., and Kinashi, T. (2012). Rap1 and integrin inside-out signaling. Methods in molecular biology *757*, 279-296.

Kato, K., Kanaji, T., Russell, S., Kunicki, T.J., Furihata, K., Kanaji, S., Marchese, P., Reininger, A., Ruggeri, Z.M., and Ware, J. (2003). The contribution of glycoprotein VI to stable platelet adhesion and thrombus formation illustrated by targeted gene deletion. Blood *102*, 1701-1707.

Kattula, S., Byrnes, J.R., and Wolberg, A.S. (2017). Fibrinogen and Fibrin in Hemostasis and Thrombosis. Arteriosclerosis, thrombosis, and vascular biology *37*, e13-e21.

Kehrel, B., Balleisen, L., Kokott, R., Mesters, R., Stenzinger, W., Clemetson, K.J., and van de Loo, J. (1988). Deficiency of intact thrombospondin and membrane glycoprotein Ia in platelets with defective collagen-induced aggregation and spontaneous loss of disorder. Blood *71*, 1074-1078.

Keragala, C.B., and Medcalf, R.L. (2021). Plasminogen: an enigmatic zymogen. Blood *137*, 2881-2889.

Kerzmann, A., Haumann, A., Boesmans, E., Detry, O., and Defraigne, J.O. (2018). [Acute mesenteric ischemia]. Revue medicale de Liege *73*, 300-303.

Kim, S., Foster, C., Lecchi, A., Quinton, T.M., Prosser, D.M., Jin, J., Cattaneo, M., and Kunapuli, S.P. (2002). Protease-activated receptors 1 and 4 do not stimulate G(i) signaling pathways in the absence of secreted ADP and cause human platelet aggregation independently of G(i) signaling. Blood *99*, 3629-3636.

Kim, S., Jin, J., and Kunapuli, S.P. (2004). Akt activation in platelets depends on Gi signaling pathways. The Journal of biological chemistry *279*, 4186-4195.

Kinashi, T. (2005). Intracellular signalling controlling integrin activation in lymphocytes. Nature reviews Immunology *5*, 546-559.

Kita, D., Takino, T., Nakada, M., Takahashi, T., Yamashita, J., and Sato, H. (2001). Expression of dominant-negative form of Ets-1 suppresses fibronectin-stimulated cell adhesion and migration through down-regulation of integrin alpha5 expression in U251 glioma cell line. Cancer research *61*, 7985-7991.

Klages, B., Brandt, U., Simon, M.I., Schultz, G., and Offermanns, S. (1999). Activation of G12/G13 results in shape change and Rho/Rho-kinase-mediated myosin light chain phosphorylation in mouse platelets. The Journal of cell biology *144*, 745-754.

Knight, C.G., Morton, L.F., Peachey, A.R., Tuckwell, D.S., Farndale, R.W., and Barnes, M.J. (2000). The collagen-binding A-domains of integrins alpha(1)beta(1) and alpha(2)beta(1) recognize the same specific amino acid sequence, GFOGER, in native (triple-helical) collagens. The Journal of biological chemistry *275*, 35-40.

Kohler, S., Schmid, F., and Settanni, G. (2015). The Internal Dynamics of Fibrinogen and Its Implications for Coagulation and Adsorption. PLoS computational biology *11*, e1004346.

Kohnken, R., Porcu, P., and Mishra, A. (2017). Overview of the Use of Murine Models in Leukemia and Lymphoma Research. Frontiers in oncology *7*, 22.

Kolesnikov, M., Farache, J., and Shakhar, G. (2015). Intravital two-photon imaging of the gastrointestinal tract. Journal of immunological methods *421*, 73-80.

Konstantinides, S., Ware, J., Marchese, P., Almus-Jacobs, F., Loskutoff, D.J., and Ruggeri, Z.M. (2006). Distinct antithrombotic consequences of platelet glycoprotein Ibalpha and VI deficiency in a mouse model of arterial thrombosis. Journal of thrombosis and haemostasis : JTH *4*, 2014-2021.

Korin, N., Kanapathipillai, M., Matthews, B.D., Crescente, M., Brill, A., Mammoto, T., Ghosh, K., Jurek, S., Bencherif, S.A., Bhatta, D., *et al.* (2012). Shear-activated nanotherapeutics for drug targeting to obstructed blood vessels. Science *337*, 738-742.

Kraft, W.K., Gilmartin, J.H., Chappell, D.L., Gheyas, F., Walker, B.M., Nagalla, S., Naik, U.P., Horrow, J.C., Wrishko, R.E., Zhang, S., *et al.* (2016). Effect of Vorapaxar Alone and in Combination with Aspirin on Bleeding Time and Platelet Aggregation in Healthy Adult Subjects. Clinical and translational science *9*, 221-227.

Kritzik, M., Savage, B., Nugent, D.J., Santoso, S., Ruggeri, Z.M., and Kunicki, T.J. (1998). Nucleotide polymorphisms in the alpha2 gene define multiple alleles that are associated with differences in platelet alpha2 beta1 density. Blood *92*, 2382-2388.

Kroll, M.H., Hellums, J.D., McIntire, L.V., Schafer, A.I., and Moake, J.L. (1996). Platelets and shear stress. Blood *88*, 1525-1541.

Kuijpers, M.J., Gilio, K., Reitsma, S., Nergiz-Unal, R., Prinzen, L., Heeneman, S., Lutgens, E., van Zandvoort, M.A., Nieswandt, B., Egbrink, M.G., *et al.* (2009). Complementary roles of platelets and coagulation in thrombus formation on plaques acutely ruptured by targeted ultrasound treatment: a novel intravital model. Journal of thrombosis and haemostasis : JTH *7*, 152-161.

Kuijpers, M.J., Pozgajova, M., Cosemans, J.M., Munnix, I.C., Eckes, B., Nieswandt, B., and Heemskerk, J.W. (2007). Role of murine integrin alpha2beta1 in thrombus stabilization and embolization: contribution of thromboxane A2. Thrombosis and haemostasis *98*, 1072-1080.

Kujovich, J.L. (2011). Factor V Leiden thrombophilia. Genetics in medicine : official journal of the American College of Medical Genetics *13*, 1-16.

Kulkarni, R., and Soucie, J.M. (2011). Pediatric hemophilia: a review. Seminars in thrombosis and hemostasis *37*, 737-744.

Kurian, C.J., Drelich, D.A., and Rizk, S. (2020). Successful liver transplant from a hemophilia A donor with no development of hemophilia A in recipient. Journal of thrombosis and haemostasis : JTH *18*, 853-856.

Kurihara, O., Takano, M., Soeda, T., Fracassi, F., Araki, M., Nakajima, A., McNulty, I., Lee, H., Mizuno, K., and Jang, I.K. (2021). Degree of luminal narrowing and composition of thrombus in plaque erosion. Journal of thrombosis and thrombolysis *51*, 143-150.

Kurokawa, K., Nakamura, T., Aoki, K., and Matsuda, M. (2005). Mechanism and role of localized activation of Rho-family GTPases in growth factor-stimulated fibroblasts and neuronal cells. Biochemical Society transactions *33*, 631-634.

Kurz, K.D., Main, B.W., and Sandusky, G.E. (1990). Rat model of arterial thrombosis induced by ferric chloride. Thrombosis research *60*, 269-280.

Kusada, A., Isogai, N., and Cooley, B.C. (2007). Electric injury model of murine arterial thrombosis. Thrombosis research *121*, 103-106.

Lages, B., Malmsten, C., Weiss, H.J., and Samuelsson, B. (1981). Impaired platelet response to thromboxane-A2 and defective calcium mobilization in a patient with a bleeding disorder. Blood *57*, 545-552.

Lak, M., Keihani, M., Elahi, F., Peyvandi, F., and Mannucci, P.M. (1999). Bleeding and thrombosis in 55 patients with inherited afibrinogenaemia. British journal of haematology *107*, 204-206.

Lam, L.H., Silbert, J.E., and Rosenberg, R.D. (1976). The separation of active and inactive forms of heparin. Biochemical and biophysical research communications *69*, 570-577.

Lanas, A., Dumonceau, J.M., Hunt, R.H., Fujishiro, M., Scheiman, J.M., Gralnek, I.M., Campbell, H.E., Rostom, A., Villanueva, C., and Sung, J.J.Y. (2018). Non-variceal upper gastrointestinal bleeding. Nature reviews Disease primers *4*, 18020.

Lane, D.A., Preston, F.E., VanRoss, M.E., and Kakkar, V.V. (1978). Characterization of serum fibrinogen and fibrin fragments produced during disseminated intravascular coagulation. British journal of haematology *40*, 609-615.

Larrieu-Lahargue, F., Welm, A.L., Thomas, K.R., and Li, D.Y. (2011). Netrin-4 activates endothelial integrin {alpha}6{beta}1. Circulation research *109*, 770-774.

Larsson, P., Tarlac, V., Wang, T.Y., Bonnard, T., Hagemeyer, C.E., Hamilton, J.R., Medcalf, R.L., Cody, S.H., and Boknas, N. (2022). Scanning laser-induced endothelial injury: a

standardized and reproducible thrombosis model for intravital microscopy. Scientific reports *12*, 3955.

Lasica, R., Djukanovic, L., Popovic, D., Savic, L., Mrdovic, I., Radovanovic, N., Radovanovic, M.R., Polovina, M., Stojanovic, R., Matic, D., *et al.* (2022). Use of Anticoagulant Therapy in Patients with Acute Myocardial Infarction and Atrial Fibrillation. Medicina *58*.

Laurens, N., Koolwijk, P., and de Maat, M.P. (2006). Fibrin structure and wound healing. Journal of thrombosis and haemostasis : JTH *4*, 932-939.

Leadley, R.J., Jr., Chi, L., Rebello, S.S., and Gagnon, A. (2000). Contribution of in vivo models of thrombosis to the discovery and development of novel antithrombotic agents. Journal of pharmacological and toxicological methods *43*, 101-116.

Lecchi, A., Razzari, C., Paoletta, S., Dupuis, A., Nakamura, L., Ohlmann, P., Gachet, C., Jacobson, K.A., Zieger, B., and Cattaneo, M. (2015). Identification of a new dysfunctional platelet P2Y12 receptor variant associated with bleeding diathesis. Blood *125*, 1006-1013.

Lecut, C., Frederix, K., Johnson, D.M., Deroanne, C., Thiry, M., Faccinetto, C., Maree, R., Evans, R.J., Volders, P.G., Bours, V., *et al.* (2009). P2X1 ion channels promote neutrophil chemotaxis through Rho kinase activation. Journal of immunology *183*, 2801-2809.

Lefort, C.T., Rossaint, J., Moser, M., Petrich, B.G., Zarbock, A., Monkley, S.J., Critchley, D.R., Ginsberg, M.H., Fassler, R., and Ley, K. (2012). Distinct roles for talin-1 and kindlin-3 in LFA-1 extension and affinity regulation. Blood *119*, 4275-4282.

Leger, A.J., Jacques, S.L., Badar, J., Kaneider, N.C., Derian, C.K., Andrade-Gordon, P., Covic, L., and Kuliopulos, A. (2006). Blocking the protease-activated receptor 1-4 heterodimer in platelet-mediated thrombosis. Circulation *113*, 1244-1254.

Lenain, N., Freund, M., Leon, C., Cazenave, J.P., and Gachet, C. (2003). Inhibition of localized thrombosis in P2Y1-deficient mice and rodents treated with MRS2179, a P2Y1 receptor antagonist. Journal of thrombosis and haemostasis : JTH *1*, 1144-1149.

Leon, C., Alex, M., Klocke, A., Morgenstern, E., Moosbauer, C., Eckly, A., Spannagl, M., Gachet, C., and Engelmann, B. (2004). Platelet ADP receptors contribute to the initiation of intravascular coagulation. Blood *103*, 594-600.

Leon, C., Freund, M., Ravanat, C., Baurand, A., Cazenave, J.P., and Gachet, C. (2001). Key role of the P2Y(1) receptor in tissue factor-induced thrombin-dependent acute thromboembolism: studies in P2Y(1)-knockout mice and mice treated with a P2Y(1) antagonist. Circulation *103*, 718-723.

Leon, C., Hechler, B., Freund, M., Eckly, A., Vial, C., Ohlmann, P., Dierich, A., LeMeur, M., Cazenave, J.P., and Gachet, C. (1999). Defective platelet aggregation and increased resistance to thrombosis in purinergic P2Y(1) receptor-null mice. The Journal of clinical investigation *104*, 1731-1737.

Leon, C., Hechler, B., Vial, C., Leray, C., Cazenave, J.P., and Gachet, C. (1997). The P2Y1 receptor is an ADP receptor antagonized by ATP and expressed in platelets and megakaryoblastic cells. FEBS letters *403*, 26-30.

Leon, C., Ravanat, C., Freund, M., Cazenave, J.P., and Gachet, C. (2003). Differential involvement of the P2Y1 and P2Y12 receptors in platelet procoagulant activity. Arteriosclerosis, thrombosis, and vascular biology *23*, 1941-1947.

Li, J., Vootukuri, S., Shang, Y., Negri, A., Jiang, J.K., Nedelman, M., Diacovo, T.G., Filizola, M., Thomas, C.J., and Coller, B.S. (2014). RUC-4: a novel alphaIIbbeta3 antagonist for prehospital therapy of myocardial infarction. Arteriosclerosis, thrombosis, and vascular biology *34*, 2321-2329.

Li, S.S., Gao, S., Chen, Y., Bao, H., Li, Z.T., Yao, Q.P., Liu, J.T., Wang, Y., and Qi, Y.X. (2021). Platelet-derived microvesicles induce calcium oscillations and promote VSMC migration via TRPV4. Theranostics *11*, 2410-2423.

Li, Y., Choi, H., Zhou, Z., Nolasco, L., Pownall, H.J., Voorberg, J., Moake, J.L., and Dong, J.F. (2008). Covalent regulation of ULVWF string formation and elongation on endothelial cells under flow conditions. Journal of thrombosis and haemostasis : JTH *6*, 1135-1143.

Liang, H.P., Morel-Kopp, M.C., Clemetson, J.M., Clemetson, K.J., Kekomaki, R., Kroll, H., Michaelides, K., Tuddenham, E.G., Vanhoorelbeke, K., and Ward, C.M. (2005). A common ancestral glycoprotein (GP) 9 1828A>G (Asn45Ser) gene mutation occurring in European families from Australia and Northern Europe with Bernard-Soulier Syndrome (BSS). Thrombosis and haemostasis *94*, 599-605.

Libby, P., Buring, J.E., Badimon, L., Hansson, G.K., Deanfield, J., Bittencourt, M.S., Tokgozoglu, L., and Lewis, E.F. (2019). Atherosclerosis. Nature reviews Disease primers *5*, 56.

Libby, P., Ridker, P.M., and Hansson, G.K. (2011). Progress and challenges in translating the biology of atherosclerosis. Nature *473*, 317-325.

Lippi, G., Franchini, M., and Targher, G. (2011). Arterial thrombus formation in cardiovascular disease. Nature reviews Cardiology *8*, 502-512.

Litvinov, R.I., Gorkun, O.V., Owen, S.F., Shuman, H., and Weisel, J.W. (2005). Polymerization of fibrin: specificity, strength, and stability of knob-hole interactions studied at the single-molecule level. Blood *106*, 2944-2951.

Liu, B., and Tang, D. (2011). Influence of non-Newtonian properties of blood on the wall shear stress in human atherosclerotic right coronary arteries. Molecular & cellular biomechanics : MCB *8*, 73-90.

Lockyer, S., Okuyama, K., Begum, S., Le, S., Sun, B., Watanabe, T., Matsumoto, Y., Yoshitake, M., Kambayashi, J., and Tandon, N.N. (2006). GPVI-deficient mice lack collagen responses and are protected against experimentally induced pulmonary thromboembolism. Thrombosis research *118*, 371-380.

Lombard, S.E., Pollitt, A.Y., Hughes, C.E., Di, Y., McKinnon, T., O'Callaghan C, A., and Watson, S.P. (2018). Mouse podoplanin supports adhesion and aggregation of platelets under arterial shear: A novel mechanism of haemostasis. Platelets *29*, 716-722.

Lopez, J.A., Chung, D.W., Fujikawa, K., Hagen, F.S., Davie, E.W., and Roth, G.J. (1988). The alpha and beta chains of human platelet glycoprotein Ib are both transmembrane proteins containing a leucine-rich amino acid sequence. Proceedings of the National Academy of Sciences of the United States of America *85*, 2135-2139.

Lou, Z., and Yang, W.J. (1993). A computer simulation of the non-Newtonian blood flow at the aortic bifurcation. Journal of biomechanics *26*, 37-49.

Lowe, G.D., Lee, A.J., Rumley, A., Price, J.F., and Fowkes, F.G. (1997). Blood viscosity and risk of cardiovascular events: the Edinburgh Artery Study. British journal of haematology *96*, 168-173.

Lowe, K.L., Navarro-Nunez, L., Benezech, C., Nayar, S., Kingston, B.L., Nieswandt, B., Barone, F., Watson, S.P., Buckley, C.D., and Desanti, G.E. (2015). The expression of mouse CLEC-2 on leucocyte subsets varies according to their anatomical location and inflammatory state. European journal of immunology *45*, 2484-2493.

Luo, B.H., Carman, C.V., and Springer, T.A. (2007a). Structural basis of integrin regulation and signaling. Annual review of immunology *25*, 619-647.

Luo, S.Z., Mo, X., Afshar-Kharghan, V., Srinivasan, S., Lopez, J.A., and Li, R. (2007b). Glycoprotein Ibalpha forms disulfide bonds with 2 glycoprotein Ibbeta subunits in the resting platelet. Blood *109*, 603-609.

Lusis, A.J. (2000). Atherosclerosis. Nature *407*, 233-241.

Lutz, R.J., Hsu, L., Menawat, A., Zrubek, J., and Edwards, K. (1983). Comparison of steady and pulsatile flow in a double branching arterial model. Journal of biomechanics *16*, 753-766.

Machacek, M., Hodgson, L., Welch, C., Elliott, H., Pertz, O., Nalbant, P., Abell, A., Johnson, G.L., Hahn, K.M., and Danuser, G. (2009). Coordination of Rho GTPase activities during cell protrusion. Nature *461*, 99-103.

MacKenzie, A.B., Mahaut-Smith, M.P., and Sage, S.O. (1996). Activation of receptor-operated cation channels via P2X1 not P2T purinoceptors in human platelets. The Journal of biological chemistry *271*, 2879-2881.

Mackie, I.J., and Bull, H.A. (1989). Normal haemostasis and its regulation. Blood reviews *3*, 237-250.

Mackman, N. (2008). Triggers, targets and treatments for thrombosis. Nature *451*, 914-918.

Mackman, N., Tilley, R.E., and Key, N.S. (2007). Role of the extrinsic pathway of blood coagulation in hemostasis and thrombosis. Arteriosclerosis, thrombosis, and vascular biology *27*, 1687-1693.

Magnusson, M.K., and Mosher, D.F. (1998). Fibronectin: structure, assembly, and cardiovascular implications. Arteriosclerosis, thrombosis, and vascular biology *18*, 1363-1370.

Mahaut-Smith, M.P. (2012). The unique contribution of ion channels to platelet and megakaryocyte function. Journal of thrombosis and haemostasis : JTH *10*, 1722-1732.

Mammadova-Bach, E., Ollivier, V., Loyau, S., Schaff, M., Dumont, B., Favier, R., Freyburger, G., Latger-Cannard, V., Nieswandt, B., Gachet, C., *et al.* (2015). Platelet glycoprotein VI binds to polymerized fibrin and promotes thrombin generation. Blood *126*, 683-691.

Mangin, P., Yap, C.L., Nonne, C., Sturgeon, S.A., Goncalves, I., Yuan, Y., Schoenwaelder, S.M., Wright, C.E., Lanza, F., and Jackson, S.P. (2006). Thrombin overcomes the thrombosis defect associated with platelet GPVI/FcRgamma deficiency. Blood *107*, 4346-4353.

Mangin, P., Yuan, Y., Goncalves, I., Eckly, A., Freund, M., Cazenave, J.P., Gachet, C., Jackson, S.P., and Lanza, F. (2003). Signaling role for phospholipase C gamma 2 in platelet glycoprotein

Ib alpha calcium flux and cytoskeletal reorganization. Involvement of a pathway distinct from FcR gamma chain and Fc gamma RIIA. The Journal of biological chemistry *278*, 32880-32891.

Mangin, P.H., Onselaer, M.B., Receveur, N., Le Lay, N., Hardy, A.T., Wilson, C., Sanchez, X., Loyau, S., Dupuis, A., Babar, A.K., *et al.* (2018). Immobilized fibrinogen activates human platelets through glycoprotein VI. Haematologica *103*, 898-907.

Mangin, P.H., Tang, C., Bourdon, C., Loyau, S., Freund, M., Hechler, B., Gachet, C., and Jandrot-Perrus, M. (2012). A humanized glycoprotein VI (GPVI) mouse model to assess the antithrombotic efficacies of anti-GPVI agents. The Journal of pharmacology and experimental therapeutics *341*, 156-163.

Mann, K.G., Nesheim, M.E., Church, W.R., Haley, P., and Krishnaswamy, S. (1990). Surface-dependent reactions of the vitamin K-dependent enzyme complexes. Blood *76*, 1-16.

Mant, J., Hobbs, F.D., Fletcher, K., Roalfe, A., Fitzmaurice, D., Lip, G.Y., Murray, E., investigators, B., and Midland Research Practices, N. (2007). Warfarin versus aspirin for stroke prevention in an elderly community population with atrial fibrillation (the Birmingham Atrial Fibrillation Treatment of the Aged Study, BAFTA): a randomised controlled trial. Lancet *370*, 493-503.

Marcucci, R., Berteotti, M., Gori, A.M., Giusti, B., Rogolino, A.A., Sticchi, E., Liotta, A.A., Ageno, W., De Candia, E., Gresele, P., *et al.* (2021). Heparin induced thrombocytopenia: position paper from the Italian Society on Thrombosis and Haemostasis (SISET). Blood transfusion = Trasfusione del sangue *19*, 14-23.

Marguerie, G.A., Plow, E.F., and Edgington, T.S. (1979). Human platelets possess an inducible and saturable receptor specific for fibrinogen. The Journal of biological chemistry *254*, 5357-5363.

Marosfoi, M.G., Korin, N., Gounis, M.J., Uzun, O., Vedantham, S., Langan, E.T., Papa, A.L., Brooks, O.W., Johnson, C., Puri, A.S., *et al.* (2015). Shear-Activated Nanoparticle Aggregates

Combined With Temporary Endovascular Bypass to Treat Large Vessel Occlusion. Stroke *46*, 3507-3513.

Martin-Salces, M., Jimenez-Yuste, V., Alvarez, M.T., Quintana, M., and Hernandez-Navarro, F. (2010). Review: Factor XI deficiency: review and management in pregnant women. Clinical and applied thrombosis/hemostasis : official journal of the International Academy of Clinical and Applied Thrombosis/Hemostasis *16*, 209-213.

Martin, E.M., Zuidscherwoude, M., Moran, L.A., Di, Y., Garcia, A., and Watson, S.P. (2021). The structure of CLEC-2: mechanisms of dimerization and higher-order clustering. Platelets *32*, 733-743.

Martyanov, A.A., Balabin, F.A., Dunster, J.L., Panteleev, M.A., Gibbins, J.M., and Sveshnikova, A.N. (2020). Control of Platelet CLEC-2-Mediated Activation by Receptor Clustering and Tyrosine Kinase Signaling. Biophysical journal *118*, 2641-2655.

Martyanov, A.A., Kaneva, V.N., Panteleev, M.A., and Sveshnikova, A.N. (2018). [CLEC-2 induced signalling in blood platelets]. Biomeditsinskaia khimiia *64*, 387-396.

Massberg, S., Gawaz, M., Gruner, S., Schulte, V., Konrad, I., Zohlnhofer, D., Heinzmann, U., and Nieswandt, B. (2003). A crucial role of glycoprotein VI for platelet recruitment to the injured arterial wall in vivo. The Journal of experimental medicine *197*, 41-49.

Matsubara, Y., Murata, M., Maruyama, T., Handa, M., Yamagata, N., Watanabe, G., Saruta, T., and Ikeda, Y. (2000). Association between diabetic retinopathy and genetic variations in alpha2beta1 integrin, a platelet receptor for collagen. Blood *95*, 1560-1564.

Maurer, E., Schaff, M., Receveur, N., Bourdon, C., Mercier, L., Nieswandt, B., Dubois, C., Jandrot-Perrus, M., Goetz, J.G., Lanza, F., *et al.* (2015). Fibrillar cellular fibronectin supports efficient platelet aggregation and procoagulant activity. Thrombosis and haemostasis *114*, 1175-1188.

Maurer, E., Tang, C., Schaff, M., Bourdon, C., Receveur, N., Ravanat, C., Eckly, A., Hechler, B., Gachet, C., Lanza, F., *et al.* (2013). Targeting platelet GPIbbeta reduces platelet adhesion, GPIb signaling and thrombin generation and prevents arterial thrombosis. Arteriosclerosis, thrombosis, and vascular biology *33*, 1221-1229.

Maxwell, M.J., Westein, E., Nesbitt, W.S., Giuliano, S., Dopheide, S.M., and Jackson, S.P. (2007). Identification of a 2-stage platelet aggregation process mediating shear-dependent thrombus formation. Blood *109*, 566-576.

May, F., Hagedorn, I., Pleines, I., Bender, M., Vogtle, T., Eble, J., Elvers, M., and Nieswandt, B. (2009). CLEC-2 is an essential platelet-activating receptor in hemostasis and thrombosis. Blood *114*, 3464-3472.

Mazzucato, M., Pradella, P., Cozzi, M.R., De Marco, L., and Ruggeri, Z.M. (2002). Sequential cytoplasmic calcium signals in a 2-stage platelet activation process induced by the glycoprotein Ibalpha mechanoreceptor. Blood *100*, 2793-2800.

McCarty, O.J., Zhao, Y., Andrew, N., Machesky, L.M., Staunton, D., Frampton, J., and Watson, S.P. (2004). Evaluation of the role of platelet integrins in fibronectin-dependent spreading and adhesion. Journal of thrombosis and haemostasis : JTH *2*, 1823-1833.

Mehta, L.S., Beckie, T.M., DeVon, H.A., Grines, C.L., Krumholz, H.M., Johnson, M.N., Lindley, K.J., Vaccarino, V., Wang, T.Y., Watson, K.E., *et al.* (2016). Acute Myocardial Infarction in Women: A Scientific Statement From the American Heart Association. Circulation *133*, 916-947.

Meltzer, M.E., Doggen, C.J., de Groot, P.G., Rosendaal, F.R., and Lisman, T. (2009). The impact of the fibrinolytic system on the risk of venous and arterial thrombosis. Seminars in thrombosis and hemostasis *35*, 468-477.

Merrill, E.W., Cokelet, G.C., Britten, A., and Wells, R.E., Jr. (1963). Non-Newtonian Rheology of Human Blood--Effect of Fibrinogen Deduced by "Subtraction". Circulation research *13*, 48-55.

Mo, X., Liu, L., Lopez, J.A., and Li, R. (2012). Transmembrane domains are critical to the interaction between platelet glycoprotein V and glycoprotein Ib-IX complex. Journal of thrombosis and haemostasis : JTH *10*, 1875-1886.

Moake, J.L., Turner, N.A., Stathopoulos, N.A., Nolasco, L., and Hellums, J.D. (1988). Shear-induced platelet aggregation can be mediated by vWF released from platelets, as well as by exogenous large or unusually large vWF multimers, requires adenosine diphosphate, and is resistant to aspirin. Blood *71*, 1366-1374.

Moake, J.L., Turner, N.A., Stathopoulos, N.A., Nolasco, L.H., and Hellums, J.D. (1986). Involvement of large plasma von Willebrand factor (vWF) multimers and unusually large vWF forms derived from endothelial cells in shear stress-induced platelet aggregation. The Journal of clinical investigation *78*, 1456-1461.

Modderman, P.W., Admiraal, L.G., Sonnenberg, A., and von dem Borne, A.E. (1992). Glycoproteins V and Ib-IX form a noncovalent complex in the platelet membrane. The Journal of biological chemistry *267*, 364-369.

Molloy, C.P., Yao, Y., Kammoun, H., Bonnard, T., Hoefer, T., Alt, K., Tovar-Lopez, F., Rosengarten, G., Ramsland, P.A., van der Meer, A.D., *et al.* (2017). Shear-sensitive nanocapsule drug release for site-specific inhibition of occlusive thrombus formation. Journal of thrombosis and haemostasis : JTH *15*, 972-982.

Mor-Cohen, R. (2016). Disulfide Bonds as Regulators of Integrin Function in Thrombosis and Hemostasis. Antioxidants & redox signaling *24*, 16-31.

Mosesson, M.W. (2005). Fibrinogen and fibrin structure and functions. Journal of thrombosis and haemostasis : JTH *3*, 1894-1904.

Mumford, A.D., Frelinger, A.L., 3rd, Gachet, C., Gresele, P., Noris, P., Harrison, P., and Mezzano, D. (2015). A review of platelet secretion assays for the diagnosis of inherited platelet secretion disorders. Thrombosis and haemostasis *114*, 14-25.

Munnix, I.C., Strehl, A., Kuijpers, M.J., Auger, J.M., van der Meijden, P.E., van Zandvoort, M.A., oude Egbrink, M.G., Nieswandt, B., and Heemskerk, J.W. (2005). The glycoprotein VI-phospholipase Cgamma2 signaling pathway controls thrombus formation induced by collagen and tissue factor in vitro and in vivo. Arteriosclerosis, thrombosis, and vascular biology *25*, 2673-2678.

Murakami, M.T., Zela, S.P., Gava, L.M., Michelan-Duarte, S., Cintra, A.C., and Arni, R.K. (2003). Crystal structure of the platelet activator convulxin, a disulfide-linked alpha4beta4 cyclic tetramer from the venom of Crotalus durissus terrificus. Biochemical and biophysical research communications *310*, 478-482.

Mutch, N.J., Moore, N.R., Wang, E., and Booth, N.A. (2003). Thrombus lysis by uPA, scuPA and tPA is regulated by plasma TAFI. Journal of thrombosis and haemostasis : JTH *1*, 2000-2007.

Nader, E., Skinner, S., Romana, M., Fort, R., Lemonne, N., Guillot, N., Gauthier, A., Antoine-Jonville, S., Renoux, C., Hardy-Dessources, M.D., *et al.* (2019). Blood Rheology: Key Parameters, Impact on Blood Flow, Role in Sickle Cell Disease and Effects of Exercise. Frontiers in physiology *10*, 1329.

National Institute of Neurological, D., and Stroke rt, P.A.S.S.G. (1995). Tissue plasminogen activator for acute ischemic stroke. The New England journal of medicine *333*, 1581-1587.

Nesbitt, S., Nesbit, A., Helfrich, M., and Horton, M. (1993). Biochemical characterization of human osteoclast integrins. Osteoclasts express alpha v beta 3, alpha 2 beta 1, and alpha v beta 1 integrins. The Journal of biological chemistry *268*, 16737-16745.

Ni, H., Denis, C.V., Subbarao, S., Degen, J.L., Sato, T.N., Hynes, R.O., and Wagner, D.D. (2000). Persistence of platelet thrombus formation in arterioles of mice lacking both von Willebrand factor and fibrinogen. The Journal of clinical investigation *106*, 385-392.

Ni, H., and Freedman, J. (2003). Platelets in hemostasis and thrombosis: role of integrins and their ligands. Transfusion and apheresis science : official journal of the World Apheresis Association : official journal of the European Society for Haemapheresis *28*, 257-264.

Nichols, C., Khoury, J., Brott, T., and Broderick, J. (2008). Intravenous recombinant tissue plasminogen activator improves arterial recanalization rates and reduces infarct volumes in patients with hyperdense artery sign on baseline computed tomography. Journal of stroke and cerebrovascular diseases : the official journal of National Stroke Association *17*, 64-68.

Nicole, O., Docagne, F., Ali, C., Margaill, I., Carmeliet, P., MacKenzie, E.T., Vivien, D., and Buisson, A. (2001). The proteolytic activity of tissue-plasminogen activator enhances NMDA receptor-mediated signaling. Nature medicine *7*, 59-64.

Nieswandt, B., Brakebusch, C., Bergmeier, W., Schulte, V., Bouvard, D., Mokhtari-Nejad, R., Lindhout, T., Heemskerk, J.W., Zirngibl, H., and Fassler, R. (2001). Glycoprotein VI but not alpha2beta1 integrin is essential for platelet interaction with collagen. The EMBO journal *20*, 2120-2130.

Nieswandt, B., Varga-Szabo, D., and Elvers, M. (2009). Integrins in platelet activation. Journal of thrombosis and haemostasis : JTH *7 Suppl 1*, 206-209.

Nieswandt, B., and Watson, S.P. (2003). Platelet-collagen interaction: is GPVI the central receptor? Blood *102*, 449-461.

Nieuwenhuis, H.K., Akkerman, J.W., Houdijk, W.P., and Sixma, J.J. (1985). Human blood platelets showing no response to collagen fail to express surface glycoprotein Ia. Nature *318*, 470-472.

Nigatu, A., Sime, W., Gorfu, G., Geberhiwot, T., Anduren, I., Ingerpuu, S., Doi, M., Tryggvason, K., Hjemdahl, P., and Patarroyo, M. (2006). Megakaryocytic cells synthesize and platelets secrete alpha5-laminins, and the endothelial laminin isoform laminin 10 (alpha5beta1gamma1) strongly promotes adhesion but not activation of platelets. Thrombosis and haemostasis *95*, 85-93.

Nonne, C., Lenain, N., Hechler, B., Mangin, P., Cazenave, J.P., Gachet, C., and Lanza, F. (2005). Importance of platelet phospholipase Cgamma2 signaling in arterial thrombosis as a function of lesion severity. Arteriosclerosis, thrombosis, and vascular biology *25*, 1293-1298.

Norris, L.A. (2003). Blood coagulation. Best practice & research Clinical obstetrics & gynaecology *17*, 369-383.

Nurden, A.T. (2006). Glanzmann thrombasthenia. Orphanet journal of rare diseases *1*, 10.

Nurden, P., Savi, P., Heilmann, E., Bihour, C., Herbert, J.M., Maffrand, J.P., and Nurden, A. (1995). An inherited bleeding disorder linked to a defective interaction between ADP and its receptor on platelets. Its influence on glycoprotein IIb-IIIa complex function. The Journal of clinical investigation *95*, 1612-1622.

O'Donnell, V.B., Murphy, R.C., and Watson, S.P. (2014). Platelet lipidomics: modern day perspective on lipid discovery and characterization in platelets. Circulation research *114*, 1185-1203.

Offermanns, S. (2006). Activation of platelet function through G protein-coupled receptors. Circulation research *99*, 1293-1304.

Offermanns, S., Laugwitz, K.L., Spicher, K., and Schultz, G. (1994). G proteins of the G12 family are activated via thromboxane A2 and thrombin receptors in human platelets. Proceedings of the National Academy of Sciences of the United States of America *91*, 504-508.

Ohlmann, P., Lecchi, A., El-Tayeb, A., Muller, C.E., Cattaneo, M., and Gachet, C. (2013). The platelet P2Y(12) receptor under normal and pathological conditions. Assessment with the radiolabeled selective antagonist [(3)H]PSB-0413. Purinergic signalling *9*, 59-66.

Ojalill, M., Parikainen, M., Rappu, P., Aalto, E., Jokinen, J., Virtanen, N., Siljamaki, E., and Heino, J. (2018). Integrin alpha2beta1 decelerates proliferation, but promotes survival and invasion of prostate cancer cells. Oncotarget *9*, 32435-32447.

Onishi, A., St Ange, K., Dordick, J.S., and Linhardt, R.J. (2016). Heparin and anticoagulation. Front Biosci (Landmark Ed) *21*, 1372-1392.

Opal, S.M., Kessler, C.M., Roemisch, J., and Knaub, S. (2002). Antithrombin, heparin, and heparan sulfate. Critical care medicine *30*, S325-331.

Ornelas, A., Zacharias-Millward, N., Menter, D.G., Davis, J.S., Lichtenberger, L., Hawke, D., Hawk, E., Vilar, E., Bhattacharya, P., and Millward, S. (2017). Beyond COX-1: the effects of aspirin on platelet biology and potential mechanisms of chemoprevention. Cancer metastasis reviews *36*, 289-303.

Ossovskaya, V.S., and Bunnett, N.W. (2004). Protease-activated receptors: contribution to physiology and disease. Physiological reviews *84*, 579-621.

Oury, C., Kuijpers, M.J., Toth-Zsamboki, E., Bonnefoy, A., Danloy, S., Vreys, I., Feijge, M.A., De Vos, R., Vermylen, J., Heemskerk, J.W., *et al.* (2003). Overexpression of the platelet P2X1 ion channel in transgenic mice generates a novel prothrombotic phenotype. Blood *101*, 3969-3976.

Oury, C., Sticker, E., Cornelissen, H., De Vos, R., Vermylen, J., and Hoylaerts, M.F. (2004). ATP augments von Willebrand factor-dependent shear-induced platelet aggregation through Ca2+-calmodulin and myosin light chain kinase activation. The Journal of biological chemistry *279*, 26266-26273.

Oury, C., Toth-Zsamboki, E., Thys, C., Tytgat, J., Vermylen, J., and Hoylaerts, M.F. (2001). The ATP-gated P2X1 ion channel acts as a positive regulator of platelet responses to collagen. Thrombosis and haemostasis *86*, 1264-1271.

Owens, A.P., 3rd, and Mackman, N. (2010). Tissue factor and thrombosis: The clot starts here. Thrombosis and haemostasis *104*, 432-439.

Ozaki, Y., Asazuma, N., Suzuki-Inoue, K., and Berndt, M.C. (2005). Platelet GPIb-IX-V-dependent signaling. Journal of thrombosis and haemostasis : JTH *3*, 1745-1751.

Palta, S., Saroa, R., and Palta, A. (2014). Overview of the coagulation system. Indian journal of anaesthesia *58*, 515-523.

Panteleev, M.A., Korin, N., Reesink, K.D., Bark, D.L., Cosemans, J., Gardiner, E.E., and Mangin, P.H. (2021). Wall shear rates in human and mouse arteries: Standardization of hemodynamics for in vitro blood flow assays: Communication from the ISTH SSC subcommittee on biorheology. Journal of thrombosis and haemostasis : JTH *19*, 588-595.

Panteleev, M.A., Ovanesov, M.V., Kireev, D.A., Shibeko, A.M., Sinauridze, E.I., Ananyeva, N.M., Butylin, A.A., Saenko, E.L., and Ataullakhanov, F.I. (2006). Spatial propagation and localization of blood coagulation are regulated by intrinsic and protein C pathways, respectively. Biophysical journal *90*, 1489-1500.

Parastatidis, I., Thomson, L., Burke, A., Chernysh, I., Nagaswami, C., Visser, J., Stamer, S., Liebler, D.C., Koliakos, G., Heijnen, H.F., *et al.* (2008). Fibrinogen beta-chain tyrosine nitration is a prothrombotic risk factor. The Journal of biological chemistry *283*, 33846-33853.

Pasquet, J.M., Gross, B., Quek, L., Asazuma, N., Zhang, W., Sommers, C.L., Schweighoffer, E., Tybulewicz, V., Judd, B., Lee, J.R., *et al.* (1999). LAT is required for tyrosine phosphorylation of phospholipase cgamma2 and platelet activation by the collagen receptor GPVI. Molecular and cellular biology *19*, 8326-8334.

Patti, G., Micieli, G., Cimminiello, C., and Bolognese, L. (2020). The Role of Clopidogrel in 2020: A Reappraisal. Cardiovascular therapeutics *2020*, 8703627.

Paul, B.Z., Vilaire, G., Kunapuli, S.P., and Bennett, J.S. (2003). Concurrent signaling from Galphaq- and Galphai-coupled pathways is essential for agonist-induced alphavbeta3 activation on human platelets. Journal of thrombosis and haemostasis : JTH *1*, 814-820.

Perry, D.J. (2003). Factor VII deficiency. Blood coagulation & fibrinolysis : an international journal in haemostasis and thrombosis *14 Suppl 1*, S47-54.

Petitou, M., Herault, J.P., Bernat, A., Driguez, P.A., Duchaussoy, P., Lormeau, J.C., and Herbert, J.M. (1999). Synthesis of thrombin-inhibiting heparin mimetics without side effects. Nature *398*, 417-422.

Petzold, T., Ruppert, R., Pandey, D., Barocke, V., Meyer, H., Lorenz, M., Zhang, L., Siess, W., Massberg, S., and Moser, M. (2013). beta1 integrin-mediated signals are required for platelet granule secretion and hemostasis in mouse. Blood *122*, 2723-2731.

Phillips, D.R., and Agin, P.P. (1977). Platelet plasma membrane glycoproteins. Evidence for the presence of nonequivalent disulfide bonds using nonreduced-reduced two-dimensional gel electrophoresis. The Journal of biological chemistry *252*, 2121-2126.

Pierangeli, S.S., Liu, X.W., Barker, J.H., Anderson, G., and Harris, E.N. (1995). Induction of thrombosis in a mouse model by IgG, IgM and IgA immunoglobulins from patients with the antiphospholipid syndrome. Thrombosis and haemostasis *74*, 1361-1367.

Pierce, K.L., Premont, R.T., and Lefkowitz, R.J. (2002). Seven-transmembrane receptors. Nature reviews Molecular cell biology *3*, 639-650.

Piotrowicz, R.S., Orchekowski, R.P., Nugent, D.J., Yamada, K.Y., and Kunicki, T.J. (1988). Glycoprotein Ic-IIa functions as an activation-independent fibronectin receptor on human platelets. The Journal of cell biology *106*, 1359-1364.

Podoplelova, N.A., Sveshnikova, A.N., Kurasawa, J.H., Sarafanov, A.G., Chambost, H., Vasil'ev, S.A., Demina, I.A., Ataullakhanov, F.I., Alessi, M.C., and Panteleev, M.A. (2016). Hysteresis-like binding of coagulation factors X/Xa to procoagulant activated platelets and phospholipids results from multistep association and membrane-dependent multimerization. Biochimica et biophysica acta *1858*, 1216-1227.

Poujol, C., Nurden, A.T., and Nurden, P. (1997). Ultrastructural analysis of the distribution of the vitronectin receptor (alpha v beta 3) in human platelets and megakaryocytes reveals an intracellular pool and labelling of the alpha-granule membrane. British journal of haematology *96*, 823-835.

Pozgajova, M., Sachs, U.J., Hein, L., and Nieswandt, B. (2006). Reduced thrombus stability in mice lacking the alpha2A-adrenergic receptor. Blood *108*, 510-514.

Prasad, J.M., Gorkun, O.V., Raghu, H., Thornton, S., Mullins, E.S., Palumbo, J.S., Ko, Y.P., Hook, M., David, T., Coughlin, S.R., *et al.* (2015). Mice expressing a mutant form of fibrinogen that cannot support fibrin formation exhibit compromised antimicrobial host defense. Blood *126*, 2047-2058.

Quek, L.S., Pasquet, J.M., Hers, I., Cornall, R., Knight, G., Barnes, M., Hibbs, M.L., Dunn, A.R., Lowell, C.A., and Watson, S.P. (2000). Fyn and Lyn phosphorylate the Fc receptor gamma chain downstream of glycoprotein VI in murine platelets, and Lyn regulates a novel feedback pathway. Blood *96*, 4246-4253.

Quinton, T.M., and Dean, W.L. (1992). Cyclic AMP-dependent phosphorylation of the inositol-1,4,5-trisphosphate receptor inhibits Ca2+ release from platelet membranes. Biochemical and biophysical research communications *184*, 893-899.

Rainger, G.E., Buckley, C.D., Simmons, D.L., and Nash, G.B. (1999). Neutrophils sense flow-generated stress and direct their migration through alphaVbeta3-integrin. The American journal of physiology *276*, H858-864.

Rasty, S., Borzak, S., and Tisdale, J.E. (2002). Bleeding associated with eptifibatide targeting higher risk patients with acute coronary syndromes: incidence and multivariate risk factors. Journal of clinical pharmacology *42*, 1366-1373.

Rau, K.R., Quinto-Su, P.A., Hellman, A.N., and Venugopalan, V. (2006). Pulsed laser microbeam-induced cell lysis: time-resolved imaging and analysis of hydrodynamic effects. Biophysical journal *91*, 317-329.

Rayes, J., Watson, S.P., and Nieswandt, B. (2019). Functional significance of the platelet immune receptors GPVI and CLEC-2. The Journal of clinical investigation *129*, 12-23.

Reiner, M.F., Akhmedov, A., Stivala, S., Keller, S., Gaul, D.S., Bonetti, N.R., Savarese, G., Glanzmann, M., Zhu, C., Ruf, W., *et al.* (2017). Ticagrelor, but not clopidogrel, reduces arterial thrombosis via endothelial tissue factor suppression. Cardiovascular research *113*, 61-69.

Remijn, J.A., MJ, I.J., Strunk, A.L., Abbes, A.P., Engel, H., Dikkeschei, B., Dompeling, E.C., de Groot, P.G., and Slingerland, R.J. (2007). Novel molecular defect in the platelet ADP receptor P2Y12 of a patient with haemorrhagic diathesis. Clinical chemistry and laboratory medicine *45*, 187-189.

Ren, Q., Wimmer, C., Chicka, M.C., Ye, S., Ren, Y., Hughson, F.M., and Whiteheart, S.W. (2010). Munc13-4 is a limiting factor in the pathway required for platelet granule release and hemostasis. Blood *116*, 869-877.

Rhode, K.S., Lambrou, T., Hawkes, D.J., and Seifalian, A.M. (2005). Novel approaches to the measurement of arterial blood flow from dynamic digital X-ray images. IEEE transactions on medical imaging *24*, 500-513.

Rijken, D.C., and Lijnen, H.R. (2009). New insights into the molecular mechanisms of the fibrinolytic system. Journal of thrombosis and haemostasis : JTH *7*, 4-13.

Risser, F., Urosev, I., Lopez-Morales, J., Sun, Y., and Nash, M.A. (2022). Engineered Molecular Therapeutics Targeting Fibrin and the Coagulation System: a Biophysical Perspective. Biophysical reviews *14*, 427-461.

Roberto, M., Radovanovic, D., Butta, C., Tersalvi, G., Krull, J., Erne, P., Rickli, H., Pedrazzini, G.B., and Moccetti, M. (2021). Dual antiplatelet therapy is under-prescribed in patients with surgically treated acute myocardial infarction. Interactive cardiovascular and thoracic surgery *33*, 687-694.

Rocha, L.A., Learmonth, D.A., Sousa, R.A., and Salgado, A.J. (2018). alphavbeta3 and alpha5beta1 integrin-specific ligands: From tumor angiogenesis inhibitors to vascularization promoters in regenerative medicine? Biotechnology advances *36*, 208-227.

Rohan, V., Baxa, J., Tupy, R., Cerna, L., Sevcik, P., Friesl, M., Polivka, J., Jr., Polivka, J., and Ferda, J. (2014). Length of occlusion predicts recanalization and outcome after intravenous thrombolysis in middle cerebral artery stroke. Stroke *45*, 2010-2017.

Rohwedder, I., Montanez, E., Beckmann, K., Bengtsson, E., Duner, P., Nilsson, J., Soehnlein, O., and Fassler, R. (2012). Plasma fibronectin deficiency impedes atherosclerosis progression and fibrous cap formation. EMBO molecular medicine *4*, 564-576.

Rolf, M.G., Brearley, C.A., and Mahaut-Smith, M.P. (2001). Platelet shape change evoked by selective activation of P2X1 purinoceptors with alpha,beta-methylene ATP. Thrombosis and haemostasis *85*, 303-308.

Rosado, J.A., and Sage, S.O. (2001). Role of the ERK pathway in the activation of store-mediated calcium entry in human platelets. The Journal of biological chemistry *276*, 15659-15665.

Ruggeri, Z.M. (2009). Platelet adhesion under flow. Microcirculation *16*, 58-83.

Sakakura, K., Nakano, M., Otsuka, F., Ladich, E., Kolodgie, F.D., and Virmani, R. (2013). Pathophysiology of atherosclerosis plaque progression. Heart, lung & circulation *22*, 399-411.

Sakariassen, K.S., Orning, L., and Turitto, V.T. (2015). The impact of blood shear rate on arterial thrombus formation. Future science OA *1*, FSO30.

Samama, M., Lecrubier, C., Conard, J., Hotchen, M., Breton-Gorius, J., Vargaftig, B., Chignard, M., Lagarde, M., and Dechavanne, M. (1981). Constitutional thrombocytopathy with subnormal response to thromboxane A2. British journal of haematology *48*, 293-303.

Sambrano, G.R., Weiss, E.J., Zheng, Y.W., Huang, W., and Coughlin, S.R. (2001). Role of thrombin signalling in platelets in haemostasis and thrombosis. Nature *413*, 74-78.

Sang, Y., Roest, M., de Laat, B., de Groot, P.G., and Huskens, D. (2021). Interplay between platelets and coagulation. Blood reviews *46*, 100733.

Santoro, S.A., Rajpara, S.M., Staatz, W.D., and Woods, V.L., Jr. (1988). Isolation and characterization of a platelet surface collagen binding complex related to VLA-2. Biochemical and biophysical research communications *153*, 217-223.

Santoso, S., Kunicki, T.J., Kroll, H., Haberbosch, W., and Gardemann, A. (1999). Association of the platelet glycoprotein Ia C807T gene polymorphism with nonfatal myocardial infarction in younger patients. Blood *93*, 2449-2453.

Sarratt, K.L., Chen, H., Zutter, M.M., Santoro, S.A., Hammer, D.A., and Kahn, M.L. (2005). GPVI and alpha2beta1 play independent critical roles during platelet adhesion and aggregate formation to collagen under flow. Blood *106*, 1268-1277.

Savage, B., Almus-Jacobs, F., and Ruggeri, Z.M. (1998). Specific synergy of multiple substrate-receptor interactions in platelet thrombus formation under flow. Cell *94*, 657-666.

Savage, B., Saldivar, E., and Ruggeri, Z.M. (1996). Initiation of platelet adhesion by arrest onto fibrinogen or translocation on von Willebrand factor. Cell *84*, 289-297.

Scarborough, R.M., Naughton, M.A., Teng, W., Rose, J.W., Phillips, D.R., Nannizzi, L., Arfsten, A., Campbell, A.M., and Charo, I.F. (1993). Design of potent and specific integrin

antagonists. Peptide antagonists with high specificity for glycoprotein IIb-IIIa. The Journal of biological chemistry *268*, 1066-1073.

Schaff, M., Tang, C., Maurer, E., Bourdon, C., Receveur, N., Eckly, A., Hechler, B., Arnold, C., de Arcangelis, A., Nieswandt, B., *et al.* (2013). Integrin alpha6beta1 is the main receptor for vascular laminins and plays a role in platelet adhesion, activation, and arterial thrombosis. Circulation *128*, 541-552.

Schmid-Schonbein, H., Born, G.V., Richardson, P.D., Cusack, N., Rieger, H., Forst, R., Rohling-Winkel, I., Blasberg, P., and Wehmeyer, A. (1981). Rheology of thrombotic processes in flow: the interaction of erythrocytes and thrombocytes subjected to high flow forces. Biorheology *18*, 415-444.

Schneider, D.J., Seecheran, N., Raza, S.S., Keating, F.K., and Gogo, P. (2015). Pharmacodynamic effects during the transition between cangrelor and prasugrel. Coronary artery disease *26*, 42-48.

Schoenwaelder, S.M., Darbousset, R., Cranmer, S.L., Ramshaw, H.S., Orive, S.L., Sturgeon, S., Yuan, Y., Yao, Y., Krycer, J.R., Woodcock, J., *et al.* (2017). Corrigendum: 14-3-3zeta regulates the mitochondrial respiratory reserve linked to platelet phosphatidylserine exposure and procoagulant function. Nature communications *8*, 16125.

Schoenwaelder, S.M., Ono, A., Sturgeon, S., Chan, S.M., Mangin, P., Maxwell, M.J., Turnbull, S., Mulchandani, M., Anderson, K., Kauffenstein, G., *et al.* (2007). Identification of a unique co-operative phosphoinositide 3-kinase signaling mechanism regulating integrin alpha IIb beta 3 adhesive function in platelets. The Journal of biological chemistry *282*, 28648-28658.

Scott, D.J., Prasad, P., Philippou, H., Rashid, S.T., Sohrabi, S., Whalley, D., Kordowicz, A., Tang, Q., West, R.M., Johnson, A., *et al.* (2011). Clot architecture is altered in abdominal aortic aneurysms and correlates with aneurysm size. Arteriosclerosis, thrombosis, and vascular biology *31*, 3004-3010.

Secco, G.G., Parisi, R., Mirabella, F., Fattori, R., Genoni, G., Agostoni, P., De Luca, G., Marino, P.N., Lupi, A., and Rognoni, A. (2013). P2Y12 inhibitors: pharmacologic mechanism and clinical relevance. Cardiovascular & hematological agents in medicinal chemistry *11*, 101-105.

Sekiguchi, T., Takemoto, A., Takagi, S., Takatori, K., Sato, S., Takami, M., and Fujita, N. (2016). Targeting a novel domain in podoplanin for inhibiting platelet-mediated tumor metastasis. Oncotarget *7*, 3934-3946.

Shankaran, H., Alexandridis, P., and Neelamegham, S. (2003). Aspects of hydrodynamic shear regulating shear-induced platelet activation and self-association of von Willebrand factor in suspension. Blood *101*, 2637-2645.

Sharma, R., Kumar, P., Prashanth, S.P., and Belagali, Y. (2020). Dual Antiplatelet Therapy in Coronary Artery Disease. Cardiology and therapy *9*, 349-361.

Shen, B., Zhao, X., O'Brien, K.A., Stojanovic-Terpo, A., Delaney, M.K., Kim, K., Cho, J., Lam, S.C., and Du, X. (2013). A directional switch of integrin signalling and a new anti-thrombotic strategy. Nature *503*, 131-135.

Shim, Y., Kwon, I., Park, Y., Lee, H.W., Kim, J., Kim, Y.D., Nam, H.S., Park, S., and Heo, J.H. (2021). Characterization of Ferric Chloride-Induced Arterial Thrombosis Model of Mice and the Role of Red Blood Cells in Thrombosis Acceleration. Yonsei medical journal *62*, 1032-1041.

Shiraga, M., Miyata, S., Kato, H., Kashiwagi, H., Honda, S., Kurata, Y., Tomiyama, Y., and Kanakura, Y. (2005). Impaired platelet function in a patient with P2Y12 deficiency caused by a mutation in the translation initiation codon. Journal of thrombosis and haemostasis : JTH *3*, 2315-2323.

Shirai, T., Inoue, O., Tamura, S., Tsukiji, N., Sasaki, T., Endo, H., Satoh, K., Osada, M., Sato-Uchida, H., Fujii, H., *et al.* (2017). C-type lectin-like receptor 2 promotes hematogenous tumor

metastasis and prothrombotic state in tumor-bearing mice. Journal of thrombosis and haemostasis : JTH *15*, 513-525.

Shobha, N., Buchan, A.M., Hill, M.D., and Canadian Alteplase for Stroke Effectiveness, S. (2011). Thrombolysis at 3-4.5 hours after acute ischemic stroke onset--evidence from the Canadian Alteplase for Stroke Effectiveness Study (CASES) registry. Cerebrovascular diseases *31*, 223-228.

Sillen, M., and Declerck, P.J. (2021). Thrombin Activatable Fibrinolysis Inhibitor (TAFI): An Updated Narrative Review. International journal of molecular sciences *22*.

Sim, J.A., Park, C.K., Oh, S.B., Evans, R.J., and North, R.A. (2007). P2X1 and P2X4 receptor currents in mouse macrophages. British journal of pharmacology *152*, 1283-1290.

Simon, D.I., Chen, Z., Xu, H., Li, C.Q., Dong, J., McIntire, L.V., Ballantyne, C.M., Zhang, L., Furman, M.I., Berndt, M.C., *et al.* (2000). Platelet glycoprotein ibalpha is a counterreceptor for the leukocyte integrin Mac-1 (CD11b/CD18). The Journal of experimental medicine *192*, 193-204.

Simpson, D., Siddiqui, M.A., Scott, L.J., and Hilleman, D.E. (2006). Reteplase: a review of its use in the management of thrombotic occlusive disorders. American journal of cardiovascular drugs : drugs, devices, and other interventions *6*, 265-285.

Sing, C.E., and Alexander-Katz, A. (2010). Elongational flow induces the unfolding of von Willebrand factor at physiological flow rates. Biophysical journal *98*, L35-37.

Sinnaeve, P.R., and Adriaenssens, T. (2021). Dual Antiplatelet Therapy De-escalation Strategies. The American journal of cardiology *144 Suppl 1*, S23-S31.

Slater, A., Perrella, G., Onselaer, M.B., Martin, E.M., Gauer, J.S., Xu, R.G., Heemskerk, J.W., Ariens, R.A.S., and Watson, S.P. (2019). Does fibrin(ogen) bind to monomeric or dimeric GPVI, or not at all? Platelets *30*, 281-289.

Smith, S.A., Choi, S.H., Collins, J.N., Travers, R.J., Cooley, B.C., and Morrissey, J.H. (2012). Inhibition of polyphosphate as a novel strategy for preventing thrombosis and inflammation. Blood *120*, 5103-5110.

Smith, S.A., and Morrissey, J.H. (2008). Polyphosphate enhances fibrin clot structure. Blood *112*, 2810-2816.

Smith, S.A., Travers, R.J., and Morrissey, J.H. (2015). How it all starts: Initiation of the clotting cascade. Critical reviews in biochemistry and molecular biology *50*, 326-336.

Smyth, S.S., Woulfe, D.S., Weitz, J.I., Gachet, C., Conley, P.B., Goodman, S.G., Roe, M.T., Kuliopulos, A., Moliterno, D.J., French, P.A., *et al.* (2009). G-protein-coupled receptors as signaling targets for antiplatelet therapy. Arteriosclerosis, thrombosis, and vascular biology *29*, 449-457.

Solh, T., Botsford, A., and Solh, M. (2015). Glanzmann's thrombasthenia: pathogenesis, diagnosis, and current and emerging treatment options. Journal of blood medicine *6*, 219-227.

Sonnenberg, A., Modderman, P.W., and Hogervorst, F. (1988). Laminin receptor on platelets is the integrin VLA-6. Nature *336*, 487-489.

Sorini Dini, C., Nardi, G., Ristalli, F., Mattesini, A., Hamiti, B., and Di Mario, C. (2019). Contemporary Approach to Heavily Calcified Coronary Lesions. Interventional cardiology *14*, 154-163.

Spalton, J.C., Mori, J., Pollitt, A.Y., Hughes, C.E., Eble, J.A., and Watson, S.P. (2009). The novel Syk inhibitor R406 reveals mechanistic differences in the initiation of GPVI and CLEC-2 signaling in platelets. Journal of thrombosis and haemostasis : JTH *7*, 1192-1199.

Sporn, L.A., Chavin, S.I., Marder, V.J., and Wagner, D.D. (1985). Biosynthesis of von Willebrand protein by human megakaryocytes. The Journal of clinical investigation *76*, 1102-1106.

Springer, T.A. (2014). von Willebrand factor, Jedi knight of the bloodstream. Blood *124*, 1412-1425.

Springer, T.A., Zhu, J., and Xiao, T. (2008). Structural basis for distinctive recognition of fibrinogen gammaC peptide by the platelet integrin alphaIIbbeta3. The Journal of cell biology *182*, 791-800.

Sriramarao, P., Mendler, M., and Bourdon, M.A. (1993). Endothelial cell attachment and spreading on human tenascin is mediated by alpha 2 beta 1 and alpha v beta 3 integrins. Journal of cell science *105 (Pt 4)*, 1001-1012.

Staatz, W.D., Rajpara, S.M., Wayner, E.A., Carter, W.G., and Santoro, S.A. (1989). The membrane glycoprotein Ia-IIa (VLA-2) complex mediates the Mg++-dependent adhesion of platelets to collagen. The Journal of cell biology *108*, 1917-1924.

Stabenfeldt, S.E., Gourley, M., Krishnan, L., Hoying, J.B., and Barker, T.H. (2012). Engineering fibrin polymers through engagement of alternative polymerization mechanisms. Biomaterials *33*, 535-544.

Stalker, T.J. (2020). Mouse laser injury models: variations on a theme. Platelets *31*, 423-431.

Stalker, T.J., Traxler, E.A., Wu, J., Wannemacher, K.M., Cermignano, S.L., Voronov, R., Diamond, S.L., and Brass, L.F. (2013). Hierarchical organization in the hemostatic response and its relationship to the platelet-signaling network. Blood *121*, 1875-1885.

Stalker, T.J., Welsh, J.D., Tomaiuolo, M., Wu, J., Colace, T.V., Diamond, S.L., and Brass, L.F. (2014). A systems approach to hemostasis: 3. Thrombus consolidation regulates intrathrombus solute transport and local thrombin activity. Blood *124*, 1824-1831.

Stefanini, L., and Bergmeier, W. (2018). Negative regulators of platelet activation and adhesion. Journal of thrombosis and haemostasis : JTH *16*, 220-230.

Stefanini, L., Paul, D.S., Robledo, R.F., Chan, E.R., Getz, T.M., Campbell, R.A., Kechele, D.O., Casari, C., Piatt, R., Caron, K.M., *et al.* (2015). RASA3 is a critical inhibitor of RAP1-dependent platelet activation. The Journal of clinical investigation *125*, 1419-1432.

Stirling, Y. (1995). Warfarin-induced changes in procoagulant and anticoagulant proteins. Blood coagulation & fibrinolysis : an international journal in haemostasis and thrombosis *6*, 361-373.

Storch, A.S., Rocha, H.N.M., Garcia, V.P., Batista, G., Mattos, J.D., Campos, M.O., Fuly, A.L., Nobrega, A., Fernandes, I.A., and Rocha, N.G. (2018). Oscillatory shear stress induces hemostatic imbalance in healthy men. Thrombosis research *170*, 119-125.

Strassel, C., Eckly, A., Leon, C., Petitjean, C., Freund, M., Cazenave, J.P., Gachet, C., and Lanza, F. (2009). Intrinsic impaired proplatelet formation and microtubule coil assembly of megakaryocytes in a mouse model of Bernard-Soulier syndrome. Haematologica *94*, 800-810.

Sturgeon, S.A., Jones, C., Angus, J.A., and Wright, C.E. (2006). Adaptation of the Folts and electrolytic methods of arterial thrombosis for the study of anti-thrombotic molecules in small animals. Journal of pharmacological and toxicological methods *53*, 20-29.

Su, E.J., Fredriksson, L., Geyer, M., Folestad, E., Cale, J., Andrae, J., Gao, Y., Pietras, K., Mann, K., Yepes, M., *et al.* (2008). Activation of PDGF-CC by tissue plasminogen activator impairs blood-brain barrier integrity during ischemic stroke. Nature medicine *14*, 731-737.

Sugimoto, Y., Watanabe, M., Oh-hara, T., Sato, S., Isoe, T., and Tsuruo, T. (1991). Suppression of experimental lung colonization of a metastatic variant of murine colon adenocarcinoma 26 by a monoclonal antibody 8F11 inhibiting tumor cell-induced platelet aggregation. Cancer research *51*, 921-925.

Sun, B., Li, J., Okahara, K., and Kambayashi, J. (1998). P2X1 purinoceptor in human platelets. Molecular cloning and functional characterization after heterologous expression. The Journal of biological chemistry *273*, 11544-11547.

Suzuki-Inoue, K. (2019). Platelets and cancer-associated thrombosis: focusing on the platelet activation receptor CLEC-2 and podoplanin. Blood *134*, 1912-1918.

Suzuki-Inoue, K., Fuller, G.L., Garcia, A., Eble, J.A., Pohlmann, S., Inoue, O., Gartner, T.K., Hughan, S.C., Pearce, A.C., Laing, G.D., *et al.* (2006). A novel Syk-dependent mechanism of platelet activation by the C-type lectin receptor CLEC-2. Blood *107*, 542-549.

Suzuki-Inoue, K., Inoue, O., Ding, G., Nishimura, S., Hokamura, K., Eto, K., Kashiwagi, H., Tomiyama, Y., Yatomi, Y., Umemura, K., *et al.* (2010). Essential in vivo roles of the C-type lectin receptor CLEC-2: embryonic/neonatal lethality of CLEC-2-deficient mice by blood/lymphatic misconnections and impaired thrombus formation of CLEC-2-deficient platelets. The Journal of biological chemistry *285*, 24494-24507.

Suzuki-Inoue, K., Tulasne, D., Shen, Y., Bori-Sanz, T., Inoue, O., Jung, S.M., Moroi, M., Andrews, R.K., Berndt, M.C., and Watson, S.P. (2002). Association of Fyn and Lyn with the proline-rich domain of glycoprotein VI regulates intracellular signaling. The Journal of biological chemistry *277*, 21561-21566.

Sweeney, J.D. (2008). The blood bank physician as a hemostasis consultant. Transfusion and apheresis science : official journal of the World Apheresis Association : official journal of the European Society for Haemapheresis *39*, 145-150.

Tabas, I., Garcia-Cardena, G., and Owens, G.K. (2015). Recent insights into the cellular biology of atherosclerosis. The Journal of cell biology *209*, 13-22.

Takagi, J., Petre, B.M., Walz, T., and Springer, T.A. (2002). Global conformational rearrangements in integrin extracellular domains in outside-in and inside-out signaling. Cell *110*, 599-511.

Tang, C., Wang, Y., Lei, D., Huang, L., Wang, G., Chi, Q., Zheng, Y., Gachet, C., Mangin, P.H., and Zhu, L. (2016). Standardization of a well-controlled in vivo mouse model of thrombus formation induced by mechanical injury. Thrombosis research *141*, 49-57.

Tertyshnikova, S., and Fein, A. (1998). Inhibition of inositol 1,4,5-trisphosphate-induced Ca2+ release by cAMP-dependent protein kinase in a living cell. Proceedings of the National Academy of Sciences of the United States of America *95*, 1613-1617.

Thomas, D.W., Mannon, R.B., Mannon, P.J., Latour, A., Oliver, J.A., Hoffman, M., Smithies, O., Koller, B.H., and Coffman, T.M. (1998). Coagulation defects and altered hemodynamic responses in mice lacking receptors for thromboxane A2. The Journal of clinical investigation *102*, 1994-2001.

Thurston, G.B. (1972). Viscoelasticity of human blood. Biophysical journal *12*, 1205-1217.

Tigen, M.K., Ozdil, M.H., Cincin, A., Gurel, E., Sunbul, M., Sahin, A., Guctekin, T., Dogan, Z., Sayar, N., and Ozben, B. (2021). Bleeding risk with concomitant use of tirofiban and third-generation P2Y12 receptor antagonists in patients with acute myocardial infarction: A real-life data. Anatolian journal of cardiology *25*, 699-705.

Timar, J., Trikha, M., Szekeres, K., Bazaz, R., and Honn, K. (1998). Expression and function of the high affinity alphaIIbbeta3 integrin in murine melanoma cells. Clinical & experimental metastasis *16*, 437-445.

Tomaniak, M., Katagiri, Y., Modolo, R., de Silva, R., Khamis, R.Y., Bourantas, C.V., Torii, R., Wentzel, J.J., Gijsen, F.J.H., van Soest, G., *et al.* (2020). Vulnerable plaques and patients: state-of-the-art. European heart journal *41*, 2997-3004.

Toro, C., Nicoli, E.R., Malicdan, M.C., Adams, D.R., and Introne, W.J. (1993). Chediak-Higashi Syndrome. In GeneReviews((R)), M.P. Adam, G.M. Mirzaa, R.A. Pagon, S.E. Wallace, L.J.H. Bean, K.W. Gripp, and A. Amemiya, eds. (Seattle (WA)).

Toschi, V., Gallo, R., Lettino, M., Fallon, J.T., Gertz, S.D., Fernandez-Ortiz, A., Chesebro, J.H., Badimon, L., Nemerson, Y., Fuster, V., *et al.* (1997). Tissue factor modulates the thrombogenicity of human atherosclerotic plaques. Circulation *95*, 594-599.

Toth-Zsamboki, E., Oury, C., Cornelissen, H., De Vos, R., Vermylen, J., and Hoylaerts, M.F. (2003). P2X1-mediated ERK2 activation amplifies the collagen-induced platelet secretion by enhancing myosin light chain kinase activation. The Journal of biological chemistry *278*, 46661-46667.

Travis, J., and Salvesen, G.S. (1983). Human plasma proteinase inhibitors. Annual review of biochemistry *52*, 655-709.

Tripodi, A. (2011). D-dimer testing in laboratory practice. Clinical chemistry *57*, 1256-1262.

Tronik-Le Roux, D., Roullot, V., Poujol, C., Kortulewski, T., Nurden, P., and Marguerie, G. (2000). Thrombasthenic mice generated by replacement of the integrin alpha(IIb) gene: demonstration that transcriptional activation of this megakaryocytic locus precedes lineage commitment. Blood *96*, 1399-1408.

Tseng, M.T., Dozier, A., Haribabu, B., and Graham, U.M. (2006). Transendothelial migration of ferric ion in FeCl3 injured murine common carotid artery. Thrombosis research *118*, 275-280.

Tsirka, S.E., Gualandris, A., Amaral, D.G., and Strickland, S. (1995). Excitotoxin-induced neuronal degeneration and seizure are mediated by tissue plasminogen activator. Nature *377*, 340-344.

Tsivgoulis, G., Saqqur, M., Sharma, V.K., Brunser, A., Eggers, J., Mikulik, R., Katsanos, A.H., Sergentanis, T.N., Vadikolias, K., Perren, F., *et al.* (2020). Timing of Recanalization and Functional Recovery in Acute Ischemic Stroke. Journal of stroke *22*, 130-140.

Turitto, V.T., Weiss, H.J., and Baumgartner, H.R. (1984). Platelet interaction with rabbit subendothelium in von Willebrand's disease: altered thrombus formation distinct from defective platelet adhesion. The Journal of clinical investigation *74*, 1730-1741.

Ulrichts, H., Vanhoorelbeke, K., Girma, J.P., Lenting, P.J., Vauterin, S., and Deckmyn, H. (2005). The von Willebrand factor self-association is modulated by a multiple domain interaction. Journal of thrombosis and haemostasis : JTH *3*, 552-561.

Undas, A., Podolec, P., Zawilska, K., Pieculewicz, M., Jedlinski, I., Stepien, E., Konarska-Kuszewska, E., Weglarz, P., Duszynska, M., Hanschke, E., *et al.* (2009a). Altered fibrin clot structure/function in patients with cryptogenic ischemic stroke. Stroke *40*, 1499-1501.

Undas, A., Szuldrzynski, K., Brummel-Ziedins, K.E., Tracz, W., Zmudka, K., and Mann, K.G. (2009b). Systemic blood coagulation activation in acute coronary syndromes. Blood *113*, 2070-2078.

Undas, A., Zawilska, K., Ciesla-Dul, M., Lehmann-Kopydlowska, A., Skubiszak, A., Ciepluch, K., and Tracz, W. (2009c). Altered fibrin clot structure/function in patients with idiopathic venous thromboembolism and in their relatives. Blood *114*, 4272-4278.

van der Graaf, F., Keus, F.J., Vlooswijk, R.A., and Bouma, B.N. (1982). The contact activation mechanism in human plasma: activation induced by dextran sulfate. Blood *59*, 1225-1233.

van Geffen, J.P., Swieringa, F., and Heemskerk, J.W. (2016). Platelets and coagulation in thrombus formation: aberrations in the Scott syndrome. Thrombosis research *141 Suppl 2*, S12-16.

van Langevelde, K., Flinterman, L.E., van Hylckama Vlieg, A., Rosendaal, F.R., and Cannegieter, S.C. (2012). Broadening the factor V Leiden paradox: pulmonary embolism and deep-vein thrombosis as 2 sides of the spectrum. Blood *120*, 933-946.

van Zanten, G.H., de Graaf, S., Slootweg, P.J., Heijnen, H.F., Connolly, T.M., de Groot, P.G., and Sixma, J.J. (1994). Increased platelet deposition on atherosclerotic coronary arteries. The Journal of clinical investigation *93*, 615-632.

Vandenberg, P., Kern, A., Ries, A., Luckenbill-Edds, L., Mann, K., and Kuhn, K. (1991). Characterization of a type IV collagen major cell binding site with affinity to the alpha 1 beta 1 and the alpha 2 beta 1 integrins. The Journal of cell biology *113*, 1475-1483.

Vandendries, E.R., Hamilton, J.R., Coughlin, S.R., Furie, B., and Furie, B.C. (2007). Par4 is required for platelet thrombus propagation but not fibrin generation in a mouse model of thrombosis. Proceedings of the National Academy of Sciences of the United States of America *104*, 288-292.

Vassilatis, D.K., Hohmann, J.G., Zeng, H., Li, F., Ranchalis, J.E., Mortrud, M.T., Brown, A., Rodriguez, S.S., Weller, J.R., Wright, A.C., *et al.* (2003). The G protein-coupled receptor repertoires of human and mouse. Proceedings of the National Academy of Sciences of the United States of America *100*, 4903-4908.

Verheugt, F.W.A., Damman, P., Damen, S.A.J., Wykrzykowska, J.J., Woelders, E.C.I., and van Geuns, R.M. (2021). P2Y12 blocker monotherapy after percutaneous coronary intervention. Netherlands heart journal : monthly journal of the Netherlands Society of Cardiology and the Netherlands Heart Foundation *29*, 566-576.

Versteeg, H.H., Heemskerk, J.W., Levi, M., and Reitsma, P.H. (2013). New fundamentals in hemostasis. Physiological reviews *93*, 327-358.

Vial, C., Hechler, B., Leon, C., Cazenave, J.P., and Gachet, C. (1997). Presence of P2X1 purinoceptors in human platelets and megakaryoblastic cell lines. Thrombosis and haemostasis *78*, 1500-1504.

Vial, C., Rolf, M.G., Mahaut-Smith, M.P., and Evans, R.J. (2002). A study of P2X1 receptor function in murine megakaryocytes and human platelets reveals synergy with P2Y receptors. British journal of pharmacology *135*, 363-372.

Virani, S.S., Alonso, A., Aparicio, H.J., Benjamin, E.J., Bittencourt, M.S., Callaway, C.W., Carson, A.P., Chamberlain, A.M., Cheng, S., Delling, F.N., *et al.* (2021). Heart Disease and

Stroke Statistics-2021 Update: A Report From the American Heart Association. Circulation *143*, e254-e743.

Vivien, D. (2017). Can the benefits of rtPA treatment for stroke be improved? Revue neurologique *173*, 566-571.

Vogel, A., and Venugopalan, V. (2003). Mechanisms of pulsed laser ablation of biological tissues. Chemical reviews *103*, 577-644.

Voss, B., McLaughlin, J.N., Holinstat, M., Zent, R., and Hamm, H.E. (2007). PAR1, but not PAR4, activates human platelets through a Gi/o/phosphoinositide-3 kinase signaling axis. Molecular pharmacology *71*, 1399-1406.

Vu, T.K., Hung, D.T., Wheaton, V.I., and Coughlin, S.R. (1991). Molecular cloning of a functional thrombin receptor reveals a novel proteolytic mechanism of receptor activation. Cell *64*, 1057-1068.

Wagner, C.L., Mascelli, M.A., Neblock, D.S., Weisman, H.F., Coller, B.S., and Jordan, R.E. (1996). Analysis of GPIIb/IIIa receptor number by quantification of 7E3 binding to human platelets. Blood *88*, 907-914.

Wallentin, L. (2009). P2Y(12) inhibitors: differences in properties and mechanisms of action and potential consequences for clinical use. European heart journal *30*, 1964-1977.

Wallentin, L., Becker, R.C., Budaj, A., Cannon, C.P., Emanuelsson, H., Held, C., Horrow, J., Husted, S., James, S., Katus, H., *et al.* (2009). Ticagrelor versus clopidogrel in patients with acute coronary syndromes. The New England journal of medicine *361*, 1045-1057.

Wang, L., Jacobsen, S.E., Bengtsson, A., and Erlinge, D. (2004). P2 receptor mRNA expression profiles in human lymphocytes, monocytes and CD34+ stem and progenitor cells. BMC immunology *5*, 16.

Wang, Y., Gao, H., Shi, C., Erhardt, P.W., Pavlovsky, A., D, A.S., Bledzka, K., Ustinov, V., Zhu, L., Qin, J., *et al.* (2017). Leukocyte integrin Mac-1 regulates thrombosis via interaction with platelet GPIbalpha. Nature communications *8*, 15559.

Watson, A.A., Brown, J., Harlos, K., Eble, J.A., Walter, T.S., and O'Callaghan, C.A. (2007). The crystal structure and mutational binding analysis of the extracellular domain of the platelet-activating receptor CLEC-2. The Journal of biological chemistry *282*, 3165-3172.

Watson, A.A., Christou, C.M., James, J.R., Fenton-May, A.E., Moncayo, G.E., Mistry, A.R., Davis, S.J., Gilbert, R.J., Chakera, A., and O'Callaghan, C.A. (2009). The platelet receptor CLEC-2 is active as a dimer. Biochemistry *48*, 10988-10996.

Watson, J.W., and Doolittle, R.F. (2011). Peptide-derivatized albumins that inhibit fibrin polymerization. Biochemistry *50*, 9923-9927.

Watson, S.P., Auger, J.M., McCarty, O.J., and Pearce, A.C. (2005). GPVI and integrin alphaIIb beta3 signaling in platelets. Journal of thrombosis and haemostasis : JTH *3*, 1752-1762.

Watson, S.P., Herbert, J.M., and Pollitt, A.Y. (2010). GPVI and CLEC-2 in hemostasis and vascular integrity. Journal of thrombosis and haemostasis : JTH *8*, 1456-1467.

Wayner, E.A., Carter, W.G., Piotrowicz, R.S., and Kunicki, T.J. (1988). The function of multiple extracellular matrix receptors in mediating cell adhesion to extracellular matrix: preparation of monoclonal antibodies to the fibronectin receptor that specifically inhibit cell adhesion to fibronectin and react with platelet glycoproteins Ic-IIa. The Journal of cell biology *107*, 1881-1891.

Weisel, J.W. (2007). Structure of fibrin: impact on clot stability. Journal of thrombosis and haemostasis : JTH *5 Suppl 1*, 116-124.

Weisel, J.W., and Litvinov, R.I. (2013). Mechanisms of fibrin polymerization and clinical implications. Blood *121*, 1712-1719.

Weiss, E.J., Hamilton, J.R., Lease, K.E., and Coughlin, S.R. (2002). Protection against thrombosis in mice lacking PAR3. Blood *100*, 3240-3244.

Weiss, H.J., Turitto, V.T., and Baumgartner, H.R. (1978). Effect of shear rate on platelet interaction with subendothelium in citrated and native blood. I. Shear rate--dependent decrease of adhesion in von Willebrand's disease and the Bernard-Soulier syndrome. The Journal of laboratory and clinical medicine *92*, 750-764.

Wells, P.S., Holbrook, A.M., Crowther, N.R., and Hirsh, J. (1994). Interactions of warfarin with drugs and food. Annals of internal medicine *121*, 676-683.

Wencel-Drake, J.D., Painter, R.G., Zimmerman, T.S., and Ginsberg, M.H. (1985). Ultrastructural localization of human platelet thrombospondin, fibrinogen, fibronectin, and von Willebrand factor in frozen thin section. Blood *65*, 929-938.

Westrick, R.J., Winn, M.E., and Eitzman, D.T. (2007). Murine models of vascular thrombosis (Eitzman series). Arteriosclerosis, thrombosis, and vascular biology *27*, 2079-2093.

Wewer, U.M., Shaw, L.M., Albrechtsen, R., and Mercurio, A.M. (1997). The integrin alpha 6 beta 1 promotes the survival of metastatic human breast carcinoma cells in mice. The American journal of pathology *151*, 1191-1198.

Whinna, H.C. (2008). Overview of murine thrombosis models. Thrombosis research *122 Suppl 1*, S64-69.

White, J.G. (1969). The submembrane filaments of blood platelets. The American journal of pathology *56*, 267-277.

White, J.G. (1998). Use of the electron microscope for diagnosis of platelet disorders. Seminars in thrombosis and hemostasis *24*, 163-168.

Wiggins, R.C., and Cochrane, C.C. (1979). The autoactivation of rabbit Hageman factor. The Journal of experimental medicine *150*, 1122-1133.

Wihlborg, A.K., Wang, L., Braun, O.O., Eyjolfsson, A., Gustafsson, R., Gudbjartsson, T., and Erlinge, D. (2004). ADP receptor P2Y12 is expressed in vascular smooth muscle cells and stimulates contraction in human blood vessels. Arteriosclerosis, thrombosis, and vascular biology *24*, 1810-1815.

Williams, J.C., and Mackman, N. (2012). Tissue factor in health and disease. Frontiers in bioscience *4*, 358-372.

Wiviott, S.D., Braunwald, E., McCabe, C.H., Montalescot, G., Ruzyllo, W., Gottlieb, S., Neumann, F.J., Ardissino, D., De Servi, S., Murphy, S.A., *et al.* (2007). Prasugrel versus clopidogrel in patients with acute coronary syndromes. The New England journal of medicine *357*, 2001-2015.

Wolberg, A.S. (2007). Thrombin generation and fibrin clot structure. Blood reviews *21*, 131-142.

Wong, P.C., Watson, C., and Crain, E.J. (2016). The P2Y1 receptor antagonist MRS2500 prevents carotid artery thrombosis in cynomolgus monkeys. Journal of thrombosis and thrombolysis *41*, 514-521.

Woollard, K.J., Sturgeon, S., Chin-Dusting, J.P., Salem, H.H., and Jackson, S.P. (2009). Erythrocyte hemolysis and hemoglobin oxidation promote ferric chloride-induced vascular injury. The Journal of biological chemistry *284*, 13110-13118.

Woulfe, D., Jiang, H., Morgans, A., Monks, R., Birnbaum, M., and Brass, L.F. (2004). Defects in secretion, aggregation, and thrombus formation in platelets from mice lacking Akt2. The Journal of clinical investigation *113*, 441-450.

Woulfe, D., Jiang, H., Mortensen, R., Yang, J., and Brass, L.F. (2002). Activation of Rap1B by G(i) family members in platelets. The Journal of biological chemistry *277*, 23382-23390.

Woulfe, D.S. (2005). Platelet G protein-coupled receptors in hemostasis and thrombosis. Journal of thrombosis and haemostasis : JTH *3*, 2193-2200.

Wu, K.K., Le Breton, G.C., Tai, H.H., and Chen, Y.C. (1981). Abnormal platelet response to thromboxane A2. The Journal of clinical investigation *67*, 1801-1804.

Xu, W.F., Andersen, H., Whitmore, T.E., Presnell, S.R., Yee, D.P., Ching, A., Gilbert, T., Davie, E.W., and Foster, D.C. (1998). Cloning and characterization of human protease-activated receptor 4. Proceedings of the National Academy of Sciences of the United States of America *95*, 6642-6646.

Yang, J.T., Rayburn, H., and Hynes, R.O. (1993). Embryonic mesodermal defects in alpha 5 integrin-deficient mice. Development *119*, 1093-1105.

Yepes, M., and Lawrence, D.A. (2004). Tissue-type plasminogen activator and neuroserpin: a well-balanced act in the nervous system? Trends in cardiovascular medicine *14*, 173-180.

Young, D.F., and Tsai, F.Y. (1973). Flow characteristics in models of arterial stenoses. II. Unsteady flow. Journal of biomechanics *6*, 547-559.

Yu, I.S., Lin, S.R., Huang, C.C., Tseng, H.Y., Huang, P.H., Shi, G.Y., Wu, H.L., Tang, C.L., Chu, P.H., Wang, L.H., *et al.* (2004). TXAS-deleted mice exhibit normal thrombopoiesis, defective hemostasis, and resistance to arachidonate-induced death. Blood *104*, 135-142.

Zahid, M., Mangin, P., Loyau, S., Hechler, B., Billiald, P., Gachet, C., and Jandrot-Perrus, M. (2012). The future of glycoprotein VI as an antithrombotic target. Journal of thrombosis and haemostasis : JTH *10*, 2418-2427.

Zeerleder, S. (2018). Factor VII-Activating Protease: Hemostatic Protein or Immune Regulator? Seminars in thrombosis and hemostasis *44*, 151-158.

Zeiler, M., Moser, M., and Mann, M. (2014). Copy number analysis of the murine platelet proteome spanning the complete abundance range. Molecular & cellular proteomics : MCP *13*, 3435-3445.

Zhang, Y., Daubel, N., Stritt, S., and Makinen, T. (2018). Transient loss of venous integrity during developmental vascular remodeling leads to red blood cell extravasation and clearance by lymphatic vessels. Development *145*.

Zhao, W., Wei, Z., Xin, G., Li, Y., Yuan, J., Ming, Y., Ji, C., Sun, Q., Li, S., Chen, X., *et al.* (2021). Piezo1 initiates platelet hyperreactivity and accelerates thrombosis in hypertension. Journal of thrombosis and haemostasis : JTH *19*, 3113-3125.

Zheng, K., Brandt, L.J., and LeFrancois, D. (2021). Homozygous Factor V Leiden presenting as irreversible chronic colon ischemia resulting from inferior mesenteric vein thrombosis. Clinical journal of gastroenterology *14*, 1142-1146.

Zheng, Y.M., Liu, C., Chen, H., Locke, D., Ryan, J.C., and Kahn, M.L. (2001). Expression of the platelet receptor GPVI confers signaling via the Fc receptor gamma -chain in response to the snake venom convulxin but not to collagen. The Journal of biological chemistry *276*, 12999-13006.

Zhou, J., Wu, Y., Wang, L., Rauova, L., Hayes, V.M., Poncz, M., and Essex, D.W. (2015). The C-terminal CGHC motif of protein disulfide isomerase supports thrombosis. The Journal of clinical investigation *125*, 4391-4406.

Zutter, M.M., and Santoro, S.A. (1990). Widespread histologic distribution of the alpha 2 beta 1 integrin cell-surface collagen receptor. The American journal of pathology *137*, 113-120.

Alexandra YAKUSHEVA

Le rôle des plaquettes, de la fibrine et de l'hémodynamique dans l'hémostase et la thrombose artérielle

L'adhérence, l'activation et l'agrégation des plaquettes assurent l'hémostase, mais sont également à l'origine de la thrombose artérielle responsable de pathologies ischémiques graves. Toutes les étapes des deux processus sont contrôlées par le flux sanguin dont les paramètres diffèrent selon le contexte (patho)physiologique. L'objectif de ce travail a été de mieux comprendre les mécanismes impliquant les plaquettes et la fibrine en hémostase et en thrombose artérielle et de caractériser les conditions rhéologiques de l'hémostase. L'identification de taux de cisaillement élevés au niveau d'un site de lésion a élargi la gamme de paramètres rhéologiques physiologiques trouvés dans un contexte hémostatique. L'utilisation de souris déficientes en intégrine α5β1 montre le caractère modeste de cette intégrine dans l'hémostase et la thrombose artérielle. Enfin, l'identification du rôle de la fibrine dans l'arrêt de la croissance du clou hémostatique a montré sa capacité à désactiver la réponse physiologique et à limiter le recrutement de plaquettes.

Mots clés : taux de cisaillement, hémostase, intégrines, plaquettes, fibrine, thrombose artérielle

The role of platelets, fibrin and hemodynamics in hemostasis and arterial thrombosis

Platelet adhesion, activation and aggregation ensure hemostasis but can also lead to arterial thrombosis inducing serious ischemic pathologies. All steps of both processes are controlled by blood flow whose parameters differ depending on the (patho)physiological context. The aim of this work was to improve our understanding of the mechanisms implicating platelets and fibrin in hemostasis and arterial thrombosis and to characterize the rheological conditions occurring during hemostasis. Identification of elevated shear rates after vessel lesion expanded the range of physiological rheological parameters relevant to hemostasis. The use of α5β1 integrin deficient mice shows the modest role of this integrin in hemostasis and arterial thrombosis. Identification of a role for fibrin in the arrest of platelet plug formation confirmed its ability to turn off the physiological response by preventing further platelet incorporation.

Keywords: shear rate, rheology, hemostasis, integrins, platelet, fibrin, arterial thrombosis